DESIGN AND PERFORMANCE ANALYSIS OF NONLINEAR AND HYBRID CONTROL SCHEMES FOR PRESSURE REGULATION IN HYPERSONIC WIND TUNNEL

A THESIS

Submitted by

RAJANI S H

for the award of the degree

of

DOCTOR OF PHILOSOPHY

ELECTRICAL ENGINEERING DIVISION
SCHOOL OF ENGINEERING
COCHIN UNIVERSITY OF SCIENCE AND TECHNOLOGY, KOCHI

MARCH 2018

THESIS CERTIFCATE

This is to certify that the thesis entitled **DESIGN AND PERFORMANCE ANALYSIS OF NONLINEAR AND HYBRID CONTROL SCHEMES FOR PRESSURE REGULATION IN HYPERSONIC WIND TUNNEL** submitted by **RAJANI S H** to the Cochin University of Science and Technology, Kochi for the award of the degree of Doctor of Philosophy is a bonafide record of research work carried out by her under my supervision and guidance at the Division of Electrical Engineering, School of Engineering, Cochin University of Science and Technology. The contents of this thesis, in full or in parts, have not been submitted to any other University or Institute for the award of any degree or diploma. All the relevant corrections and modifications suggested by the audience during the pre-synopsis seminar and recommended by the Doctoral committee have been incorporated in this thesis.

Research Guide

Kochi-682022
Date

Dr USHA NAIR
Professor
Division of Electrical Engineering
School of Engineering
CUSAT

DECLARATION

I hereby declare that the work presented in the thesis entitled **DESIGN AND PERFORMANCE ANALYSIS OF NONLINEAR AND HYBRID CONTROL SCHEMES FOR PRESSURE REGULATION IN HYPERSONIC WIND TUNNEL** is based on the research work carried out by me under the supervision and guidance of Dr. Usha Nair for the award of degree of Doctor of Philosophy with Cochin University of Science and Technology. I further declare that the contents of this thesis, in full or in parts, have not been submitted to any other University or Institute for the award of any degree or diploma.

Kochi – 682 022   **RAJANI S H**
Date   Research Scholar

विएसएससी/एयरो/डब्लयुटीऐडी/ 07/17   दिनांक/Dt. 02.06.2017
VSSC/AERO/WTID/ 07/17

      This is to certify that Smt. Rajani S H and her guide Dr. Usha Nair visited 1m Hypersonic Wind Tunnel Facility on 26.5.2015 and had a discussion with undersigned and his team members regarding the pressure regulating system used in the facility and its control schemes for getting the inputs for modeling and controller design for her research purpose.

वर्गीस जेकब/ **Varghese Jacob**
प्रधान, डब्लयुटीऐडी/**Head, WTID**

ACKNOWLEDGEMENTS

ABSTRACT

KEYWORDS: Hypersonic Wind Tunnel; Settling chamber pressure; Optimized H-infinity controller; Hybrid controllers; Modified Adaptive Controller.

Wind tunnels are test facilities that acquires the characteristic properties of specific objects by subjecting them to controlled flow fields. This helps in investigating their dynamics before real time implementation. They find applications in varied fields, viz: testing of architectural structures like buildings and bridges, aero and space vehicles, land carriers, characterization of automobile parts etc. Hypersonic wind tunnels are ground based facilities specially operated at high speeds intended for the characteristic study of aerodynamic performance of space vehicles thereby ensuring real time flight conditions during their mission. This is achieved by testing the object or specimen to meet the performance requirements by placing them in the test section of the hypersonic wind tunnel. However, the test duration lasts for a maximum time period of 40 seconds. The air from a high storage tank is straightened and regulated in the settling chamber before reaching the test section. The valve opening to the settling chamber of the wind tunnel system is controlled for maintaining a steady air flow through the test section which is achieved using a precise controller. Thus, our research work focusses on designing a suitable controller for regulation of settling chamber pressure inside the Hypersonic wind tunnel. For this purpose, appropriate controllers are designed to regulate the flow through the pressure regulator valve. Initially, the system is modelled incorporating the important nonlinearities and its stability is ensured using different methods. Sensitivity analysis is conducted to find out the variation in pressure with variation in stem movement.

Linear, Robust, Hybrid and Adaptive control schemes are designed and analyzed for the control of settling chamber pressure in the Hypersonic wind tunnel system. A comparison based on the transient performance in terms of its rise time, settling time and percentage overshoot is carried out using Linear Quadratic Regulator, H-infinity, Optimised H-infinity, Backstepping, Sliding mode controllers, Hybrid controllers like Backstepping Sliding mode and Sliding mode Fuzzy controllers and Adaptive controllers like Model reference adaptive controller and Modified adaptive controllers. The performances are evaluated for a range of set points from 1×10^5 Pa to 300×10^5 Pa. From the analysis, it is observed that Modified Adaptive controller which is a modification of Model Reference Adaptive controller gives settling time of 0.56 s, rise time of 0.11 s without any overshoot and chatter effect. From these results, it can be concluded that Modified Adaptive Control scheme is best suited for the regulation of pressure in the settling chamber of Hypersonic wind tunnel system. Verification of the suggested algorithm adds credibility to the system performance and determines the accuracy of the performance characteristics. The design of Modified Adaptive control scheme is verified using a validated model of the existing INCAS Supersonic wind tunnel. This Modified Adaptive control exhibited the performance in the tolerable range as that of the INCAS Supersonic wind tunnel with Adaptive Fuzzy PI control algorithm. The effectiveness of the Modified Adaptive control scheme is thus verified and can be proposed for regulation of settling chamber pressure inside the Hypersonic wind tunnel system.

The limitations and future scope are also discussed in detail.

TABLE OF CONTENTS

LIST OF TABLES

LIST OF FIGURES

x

ABBREVIATIONS

AFPI   Adaptive fuzzy Proportional + Integral

BS   Backstepping

BSMC   Backstepping sliding mode controller

CLF   Control Lyapunov function

CMRAC   Model reference adaptive control

DIF   Diffuser

EDL   Entry and landing

FLC   Fuzzy logic controller

FS   Fuzzy set

H1   Heater

HI   H-Infinity

HIO   H-Infinity Optimisation

HP   High pressure system

HSP   Human space flight project

HSTDV   Hypersonic Testing Demonstrator Vehicle

IAE   Integral of absolute error

ISE   Integral of square of errors

ITAE   Integral of time absolute errors

KH   Krill Herd

LaRC   Langley Research center

LQR   Linear Quadratic Regulator

MAC   Modified Adaptive controller

MF   Membership function

MIMO   Multiple-input multiple-output

MIT   Massachusetts Institute of Technology

MRAC   Model reference adaptive control

NOZ   Nozzle

ODE	Ordinary Differential Equation
PI	Proportional + Integral
PID	Proportional + Integral + Derivative
PO	Percentage overshoot.
PRV	Pressure regulator valve
RLV	Reusable launch vehicle air breathing vehicles
RS	Rise time
SC	Settling chamber
SFC	Sliding mode Fuzzy controller
SMC	Sliding mode controller
SRP	Supersonic retropropulsion
ST	Settling time
STR	Self tuning regulator
T & E	Test and Evaluation
TS	Test Section
TSTO	Two stage to orbit
V	Vacuum chamber
VMFN	Variable Mach number Flexible Nozzle

NOTATIONS

English Symbols

C_V	Valve coefficient
N_8	Constant for engineering units
F_P	Pipe geometry constant
M	Molecular weight
Z	Compressibility factor
X_T	Critical pressure drop ratio factor
Q_C	Controllable matrix
Q_O	Observable matrix
G_d	Transfer function corresponding to input disturbance
G	Plant transfer function
M	Molecular Weight of air

Greek Symbols

β_f	Sum of effect due to the presence of food and the effect due to the current krill's best fitness value recorded
δ	Random directional vector
β	Equivalent control law
$\propto_{s1}$	Virtual control
θ	Adjustment parameter
γ	Adaptation gain of the controller
γ'	Updated adaptation gain of the controller

Miscellaneous Symbols

$P(t)$	Solution of the Riccati equation
N_i	Motion induced on i^{th} krill individual due to the other krill individuals

F_i	Foraging motion
N^{max}	Maximum induced speed
ω_n	Inertia weight
N_i^{old}	Previous motion induced.
V_f	Foraging speed,
ω_f	Inertia weight of the foraging motion
F_i^{old}	Last foraging motion value.
D^{max}	maximum diffusion speed
$V(x)$	Lyapunov function
J	Cost function

CHAPTER 1

INTRODUCTION

Whenever relative motion occurs between a solid object and atmospheric air, the molecules present in the atmosphere and that of the object gets disturbed thus generating aerodynamic forces which influences the relative motion critically depending on the shape, mass and speed of the object as well as the viscosity and compressibility of the air (Lee *et al.*, 2014; Savino *et al.*, 2009). Hence an in depth and detailed study of the aerodynamic processes occurring during such relative motion need to be conducted using an experimental setup with the objects or their scaled models especially when the relative motion falls in high speed ranges. Wind tunnels are such large scale test facilities used for acquiring the characteristic properties of specific objects by subjecting their full or scaled models to the desired conditions of air velocity, pressure and temperature. Wind tunnels find applications in varied fields like testing of aero vehicles, space crafts, land carriers like high speed trains, sports vehicles and architectural structures like buildings and bridges.

This chapter, first outlines the basics of Wind tunnel, its classifications, following which hypersonic wind tunnel is introduced and reviewed its applications. This is followed by objectives and methodology behind the contributions of the thesis. Following this, the structure of the thesis, highlighting the research to be presented is discussed.

Wind tunnels were invented at the end of the 19th century for the purpose of aerodynamic research like measuring the force and pressure distribution under controlled flow field. The first wind tunnel was setup by British aero engineer Frank

Wenham (1824–1908) in 1871. Later, large scale wind tunnels were invented during the Second World War to test the flight characteristics of supersonic aircrafts and missiles (Jones *et al.*, 2014; Baals and Corliss, 1981]. With the advancement of aerodynamic research, wind tunnels also developed and flourished to encompass varied fields of applications like, the study of flow conditions around large structures such as bridges and buildings for strengthening against workloads, characterization of automobile parts to identify suitable methods for reduction of power requirement, applications like investigation of submarine flow characteristics and the like (D'Souza *et al.*, 2015; Libii, 2011; Lohan , 2002; Flay, 2015; Rini *et al.*, 2011a; Jacob and Binu, 2009; Jones *et al.*, 2011b).

Wind tunnel is a facility which provides controlled air flow used for testing aerospace vehicle. The main advantage of the wind tunnel system is that testing can be carried out under controlled flow field than open ended experimentation. A general schematic of a wind tunnel facility is shown in Fig. 1.1 (Wikimedia, 2016).
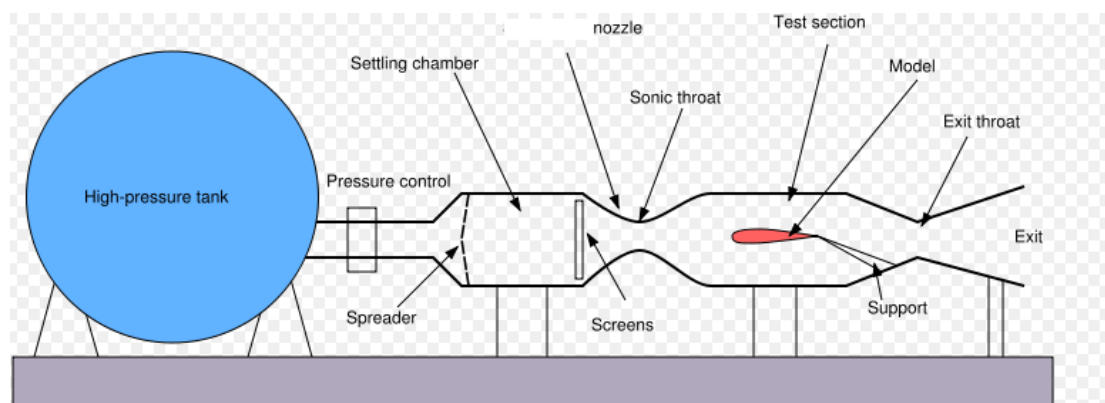
Fig. 1.1 General Schematic of wind tunnel system (Wikimedia, 2016).

Fig. 1.1 represents a Supersonic wind tunnel (Wikimedia, 2016; Nott *et al.*, 2008; Braun *et al.*, 2008) in which the main elements of the tunnel system includes high

pressure tank, pressure regulating valve, settling chamber, nozzle, test section and exit. Wind tunnel usually has a tube like appearance with which wind is allowed to flow over the testing object or a model of it. The object to be tested is fastened in the tunnel so that the air moving around the still object shows what would happen if the objects were moving through the air. To achieve uniform, high quality flow in the test section, the settling chamber and the contraction area are used to smoothen the flow. The model or space specimen to be tested is injected into the test section. The test section is generally designed based on the utility and aerodynamic considerations with uniform flow velocity (Jones *et al.*, 2011a; Jacob and Binu, 2009). The schematic of a particular space vehicle placed in the test section is shown in Fig. 1.2 (Gayon *et al.*, 2013; Bhoi and Suryanarayana, 2008).
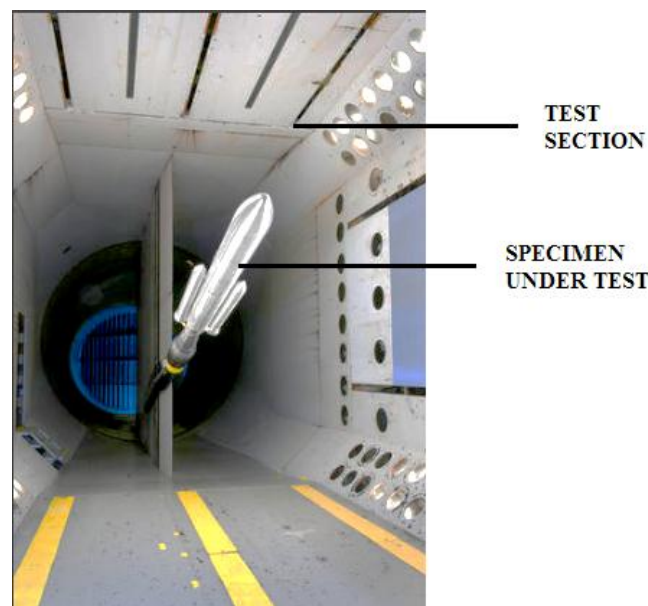
Fig. 1.2 Schematic of a specimen placed in the test section (Gayon *et al.*, 2013).

As the test duration is short, uniform regulated flow is crucial in the test section. For this purpose, we carry out a comparative study of various control scheme and propose the most suitable one to regulate the pressure which matches the desired

3

specifications of minimum overshoot and short settling time (Pope and Goin, 1965; Arbuckle, 2016; Kegelman *et al.*, 2014; Arnaiz, 1980; Kakate *et al.*, 2014). The general classification of wind tunnel is discussed in the section below.

1.1 GENERAL CLASSIFICATION OF WIND TUNNELS

Aerodynamic forces depend on Reynolds number and Mach number which are crucial parameters that must match with the flight conditions (Lee *et al.,* 2014; Savino *et al.*, 2009). Wind tunnels are basically classified according to the air flow velocity expressed in terms of Mach Number which is the ratio of speed of the object to speed of sound in air. The aerospace facilities available has different types of wind tunnels which suites many applications ranging from very slow speed to hypersonic speeds. Generally, wind tunnels fall under four major classes viz: Subsonic - with Mach number less than 0.8, Transonic - with Mach number between 0.8 and 1.2, Supersonic - with Mach number from 1.2 to 5 and Hypersonic - with Mach numbers greater than 5 (Lee *et al.*, 2014; Savino *et al.*, 2009). Based on the mode of operation, shape of the tunnel and specific applications, tunnel systems are again categorized into different groups. The high speed tunnels are classified as open loop and closed loop based on the shape of the system (Savino *et al.*, 2009; Bruce *et al.*, 2015; Botasso *et al.*, 2014). Open loop wind tunnels are open at both ends in which air is drawn from surroundings and is rejected back to the surroundings whereas in closed loop wind tunnels, the outlet. of the tunnel system is fedback to the inlet. Based on the type of operation, wind tunnels are classified as Continuous tunnels where the required test conditions are maintained for longer time span and Intermittent tunnels where the test procedure is completed within a very short duration. Thus, the Wind tunnels are generally classified based on the following (Jones *et al.*, 2014; Lohan, 2002; Pope and Goin, 1965; Arbuckle, 2016).

1. Velocity of flow.

2. Shape of the tunnel system.

3. Type of operation

4. Based on application

1. Velocity of flow:

The flow velocity of air in wind tunnels are expressed in terms of the velocity of flow in the test section with respect to velocity of sound in the free air. Mach number is defined as the ratio of speed of the object to speed of sound in gas. The variation in Mach number is based on compressibility effect which affects the design of the test section. The temperature and flow rate changes in accordance with Mach number which means the operating condition is different for different Mach number. For a fixed Mach number, in order to get. the required flow, the percentage of valve opening varies which results in minor nonlinearities in valve characteristics. Based on the flow velocity in the test section, wind tunnel classification is shown in Fig. 1.3.

Fig. 1.3 Wind tunnel classification based on Mach number.

I. Subsonic or low speed wind tunnels: This type of wind tunnels operates at low speeds usually in the range of 135m/s with Mach number less than 0.8. Here the compressibility effect is neglected to determine the Mach number and area of cross section of the test section is small. They are easy to design and cost effective. These wind tunnels are usually used in the area of fluid dynamics (Libii, 2011; Lohan, 2002; Flay, 2015).

II. Transonic wind tunnels: Transonic wind tunnels operate with Mach number between 0.8 and 1.2, with a flow velocity of 340m/s. These tunnels are used to study the aerodynamic properties since most of the aircrafts operate in this range. Transonic wind tunnel applications are extended to military aircraft & weapons, testing of space access vehicles, passenger & commercial aircraft, air turbines etc (Libii, 2011; Lohan, 2002; Flay, 2015).

III. Supersonic wind tunnels: These tunnels operate with Mach number from 1.2 to 5 which is accomplished using convergent - divergent nozzles. These tunnels are used in applications including aircraft and missile development, Inlet. performance and operability, jet. and rocket. engines, and projects including the high-speed civil transport, space shuttle, entry and landing (EDL) technology, development for parachutes and other decelerators (Nott *et al.*, 2008; Braun *et al.*, 2008; Bhoi and Suryanarayana, 2008; Pope and Goin, 1965; Arnaiz *et al.*, 1980; Hwang and Hsu, 1998; NASA).

IV. Hypersonic wind tunnels: This type of tunnels have Mach numbers greater than 5 usually in the range 5 to 15 which is achieved by convergent - divergent nozzles similar to supersonic wind tunnels. Hypersonic wind tunnels

are used for investigating the aerodynamic properties of vehicles during re-entry missions. These wind tunnels are used to facilitate hypersonic flow regime, operating at Mach numbers above 5, to characterise the aero thermal properties of the vehicle to be tested. Intermittent blow-down Hypersonic wind tunnels are more cost effective than the continuous type systems and are hence carefully calibrated for effective utilization of the limited testing time (Jones *et al.,* 2014; Baals and Corliss, 1981; D'Souza *et al.*, 2015; Libii, 2011). The technical problem in design includes maintaining high temperatures and pressures during the test run (Pope and Goin, 1965; Bruce *et al.*, 2015; Bottasso *et al.*, 2014).

2. Shape of the tunnel system.

Based on the shape of the system (Flay, 2015; Pope and Goin, 1965), wind tunnels are classified as open loop and closed loop.

I.   Open loop or Open return wind tunnel: These type of tunnels are open at both ends in which air is drawn from surroundings and is rejected back to the surroundings. Open loop type is classified into Suckdown tunnel and Blower tunnel. In Suckdown type, the inlet. is open to the atmosphere and the blower is connected at the outlet. In Blower type, the blower is connected at the inlet. which sucks air into the tunnel from the atmosphere.

II.   Closed loop (Closed return) wind tunnel: Here the outlet. of the tunnel system is fedback to the inlet. This is a good choice as the flow remains uniform compared to open loop. Moreover, in a closed circuit wind tunnel, high quality flow is assured in the test section and its power requirement is less.

3. Type of operation

Wind tunnels are classified into Continuous and Intermittent depending on the test duration (Flay, 2015; Pope and Goin, 1965).

I.   Continuous (for all speed ranges): These wind tunnels operate in Mach numbers ranging from 0.05 to 1 and are used where the test conditions are maintained constant for the entire test run. The advantage is that the test condition can be held constant over long period of time over which more accurate measurement is possible.

II. Intermittent: These types of tunnels are used for Mach numbers ranging from 0.5 to 5. The main advantage of these types of tunnels is that a single drive can run various tunnels meeting the performance requirements. Moreover, the design is simple, cost effective and model testing is very convenient with extra power availability to start the system.

Based on the operational procedures, Intermittent type are further classified into;

a) Blowdown: The Mach number for Blowdown tunnels ranges between 0.5 and 5. The advantages include high Mach capability (up to 4), easy tunnel starting, large size test section, lower construction/operating costs, superior design for propulsion experiments and smoke visualization.

b) Indraft: These tunnels use vacuum as the medium instead of pressure which helps to handle its operation easily and safely. The main advantage of these types of tunnels is that pressure regulators are not necessary to regulate the

flow. Moreover, temperature and pressure inside the tunnel system is constant, the airstream is free from contaminants and less noisy. The Indraft tunnels can operate at higher Mach numbers.

c) Intermittent pressure vacuum tunnel: These tunnels operate at Mach numbers >5 with the advantage that these tunnels are cost effective. These tunnels are applicable to variation in Mach number and Reynolds number.

4. Based on application

Wind tunnels are classified into a wide range according to their applications in varied fields such as aeronautical wind tunnel, automobile wind tunnel and aero acoustic wind tunnels.

1.2 HYPERSONIC WIND TUNNEL

With the development of space research, speed of space vehicles has been increasing over the past few decades from the speed of sound to hyper speeds. The study of aerodynamic performance of space vehicles has thus become very critical for optimizing the design of launch vehicles so as to ensure safe return of the vehicle during re-entry [Savino *et al.* (2009), Jones *et al.*, 2014; Libii, 2011; Jones *et al.*, 2011a; Jacon and Binu, 2009; Jones *et al.*, 2011b). Ground-based testing facilities like the Hypersonic wind tunnel systems are very essential for such purposes wherein real time flight conditions with specific high Mach numbers are simulated. Applications of Hypersonic wind tunnels include solving critical problems in aerodynamic and aerothermal design of launch vehicles, Human space flight project (HSP), Reusable

launch vehicle (RLV), Air breathing vehicles, Two stage to orbit (TSTO), Single stage to orbit (SSTO) and Inter planetary missions [Lee *et al.,* 2014; Savino *et al.*, 2009; D'Souza, 2015). Full scale vehicles or parts are tested using this approach thereby serving the growing demands of strategic systems. Research in this direction is progressing in organizations, viz: Defense Research and Development Organization (DRDO), Bharat Dynamics Limited for setting up wind tunnels to boost missile production (Jones *et al.*, 2011a; Jacon and Binu, 2009; Jones *et al.*, 2011b, Pope and Goin, 1965; Kakate *et al.*, 2014; Bruce *et al.*, 2015).

Hypersonic flow is defined as the flow at Mach 5 or greater at which physical properties of the flow changes rapidly and the speeds are much larger than the local speed of sound. Hypersonic wind tunnel systems consist of a high pressure storage tank (HP), Pressure regulating valve (PRV), heater (H1), settling chamber (SC), nozzle (NOZ), test section (TS), diffuser (DIF) and a vacuum vessel (V) as shown in Fig. 1.4.
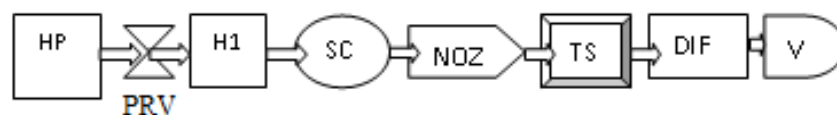
Fig.1.4 Block Schematic of Hypersonic Wind Tunnel

Hypersonic Wind Tunnel in VSSC, Trivandrum with Mach number 6 with length 1m is shown in Fig. 1.5 (Vikram Sarabhai Space Centre, VSSC).

Fig.1.5 1 m Hypersonic Wind Tunnel in VSSC, Trivandrum – Mach number 6
(Vikram Sarabhai Space Centre, VSSC)

The atmospheric air is compressed and stored in the high pressure storage tank. This compressed air from the storage tank is released through a pressure regulating valve, heater and the settling chamber to the test section. Testing is carried out by passing air at high speeds over the specimen kept in the test section. From the test section, air is released to a vacuum vessel through a diffuser which reduces the flow velocity. The heater helps to avoid liquefaction of air when it is expanded through the nozzle to achieve the required Mach number for the hypersonic flow in the test section.

A constant hypersonic flow is to be maintained in the test section throughout the test run. However, the storage tank pressure decreases continuously during a test run which will indirectly reduce the settling chamber pressure. Therefore, settling chamber pressure is to be controlled by pressure regulator valve with variable stem movement facility. The relation between the stem movement and flow rate through

the control valve generally expresses the valve characteristic. Here, PRV is an equal percentage valve wherein the stem movement versus flow rate is nonlinear. An equal percentage flow characteristic is a nonlinear curve in which the slope increases as the valve opens, while a linear flow characteristic depicts a linear relationship. A diffuser decelerates the air from test section and air is collected in the vacuum vessels. Vacuum pumps are used to evacuate the vacuum vessels. The control of the valve opening is extremely important in maintaining the settling chamber pressure in the hypersonic regime. This is achieved by properly designing a suitable controller for the regulation of settling chamber pressure.

Hypersonic wind tunnel facility focuses on testing the aerodynamic properties of parts or space vehicles as a whole which are well suited for applications during re-entry. These are also used to test systems for missiles, aircraft and re-entry vehicles flying at hypersonic speed (above Mach 5) as against the present facilities to test vehicles of speed up to Mach 5 (Savino *et al.,* 2009; Pope and Goin 1965; Bruce *et al.*, 2015; NASA).

1.3 MOTIVATION AND OBJECTIVE

One of the challenges in the aerodynamic design is to satisfy the requirements of the space vehicles during re-entry into the Earth's atmosphere like Deceleration, Heating, Accuracy of landing or Impact. During Re-entry, possible disturbances occur due to variation in velocity, atmospheric gases and aerodynamic heating leading to disaster. The most important requirements is to ensure these operating conditions of space vehicles when it crosses atmosphere to space and its return to Earth. This crucial performance parameters plays significant role during the launch, Re-entry and landing

phases of space missions and hence makes it extremely important to simulate and test these flight conditions before implementation on real launch vehicles. This is achieved by modelling of Hypersonic wind tunnel system for similar hypersonic flow conditions.

Hypersonic wind tunnel is a technological innovation in aeronautical research which pinpoints the need of continuous flow regime in the test section. Testing is to be carried out with constant settling chamber pressure in the test section. However, during the acceleration of air through the tunnel, the mass reduces continuously which leads to an unsteady pressure in the settling chamber. Therefore, the pressure in the SC has to be maintained constant using suitable control technique (Savino *et al.*, 2009; Jones *et al.*, 2014; Jones *et al.*, 2011a; Jacon and Binu, 2009; Jones *et al.*, 2011b) for obtaining stable air flow. A constant hypersonic flow is required to be maintained in the test section throughout the test run. The settling chamber pressure is to be controlled by PRV with variable stem movement facility. Therefore, the control of the valve opening is very crucial and is achieved by properly designing a suitable controller for regulating it. Thus, regulation of pressure inside the settling chamber of Hypersonic wind tunnel is maintained in the SC and thereafter in the TS throughout the test run which lasts for a duration of 40 seconds (Savino *et al.,* 2009; Jones *et al.*, 2014; Libii, 2011; Pope and Goin, 1965). The purpose of designing a control scheme for the tunnel system is to appropriately tune its dynamics so as to achieve the desired performance characteristics incorporating the important nonlinearities in the system. Numerical simulations are highly important for studying the performance of a particular control design in situations where real time experiments are expensive or dangerous considering all the input and output variables as well as possible disturbances to the system. The control scheme has to be designed based on the

information obtained from this open loop study as well as the performance parameters of the existing implemented linear control output values. Further improvement in the control design using nonlinear approach as well as possible modifications of existing control technique will definitely lead to more accurate real world lab test facility (Jones *et al.*, 2011a; Jacon and Binu, 2009; Jones *et al.*, 2011b; Pope and Goin, 1965). Discussions with the expert teams working on Hypersonic wind tunnel, it is found that the settling chamber pressure is regulated from the initial value of the pressure and is applied to an appropriate feedback controller like conventional PI, wherein this pressure is the input to the controller. As the SC pressure increases, the percentage of valve opening decreases and vice versa.

The main objective of this work is to develop an improved control algorithm for regulation of pressure inside the settling chamber of Hypersonic wind tunnel. This objective has intrinsically several tasks combined to attain the final goal. The tasks include the following.

- System modeling incorporating significant nonlinearities ensuring its stability.

- Open loop performance analysis

- Design and simulation of LQR, Linear, Robust and Nonlinear controllers.

- Identify the most suitable controller for this model.

- Verification of performance of the proposed controller.

1.4 METHODOLOGY

Basic controllers, Robust, Hybrid and Adaptive control schemes are designed for regulation of pressure inside the settling chamber of Hypersonic wind tunnel. The designed controllers are simulated, analyzed, compared and the best suitable controller is proposed. A case study on Supersonic wind tunnel plenum pressure regulation is analyzed and validated using designed Adaptive controller. Based on the above validation, the Adaptive controller design for Hypersonic wind tunnel pressure regulation is verified. The proposed algorithm is highly efficient in controlling the settling chamber pressure in terms of their transient performance parameters.

1.5 THESIS OUTLINE

In the present chapter, basics of tunnel system and its various classifications are explained. The working of the Hypersonic wind tunnel system is explained to point out the significance of the design of a highly accurate controller that is best suited for the pressure regulation.

Chapter 2 provides the background material relevant to this thesis. As this thesis focuses on regulation of pressure inside the settling chamber of Hypersonic wind tunnel, basics of wind tunnel system, various controllers and their advantages and disadvantages are reviewed in this chapter.

Chapter 3 deals with the system model incorporating the important nonlinearities. The state space model of the proposed system is discussed and stability of the system using various techniques, (1) Lyapunov stability theorem (2) phase portrait method

(3) Bode plot (4) Root locus (5) Kalman's test for controllability and observability are explained in detail.

Chapter 4 presents design and results of numerical simulation of LQR controller and three types of Robust controllers, (1) H-Infinity controllers (2) Backstepping Controller (3) Sliding mode controller.

Chapter 5 deals with design and numerical analysis of combination of different controllers, Viz: Backstepping Sliding mode controller (BSMC) and Sliding mode fuzzy controller (SFC). Appropriate combination of controllers that guarantee stability and robustness to parametric uncertainties with minimal chatter effect is also explained.

Chapter 6 describes the design and analysis of Adaptive controllers, viz: Model Reference Adaptive Control (MRAC) and Modified Adaptive control (MAC). The suitable modifications incorporated in the design of MRAC to obtain the control law of MAC is also explained in detail. A review of INCAS (National Institute for Aerospace Research "Elie Carafoli" is Romania's leading research establishment in aerospace sciences.) Supersonic wind tunnel with existing Adaptive Fuzzy PI controller and verification of results with the Modified Adaptive controller is also presented.

Chapter 7 presents performance comparison of all the controllers designed to propose the best suitable one for the pressure regulation inside the Hypersonic wind tunnel.

Chapter 8 summarizes the work presented in this thesis and provides an outlook of future work. A summary of results, discussion and conclusion of all the controller designs are also presented in the chapter.

To identify the best controller suitable for pressure regulation in Hypersonic wind tunnel, a detailed literature survey of aerodynamic research and wind tunnel systems are to be carried out. The existing controller strategies and their limitations are also very important from this point of view. A review on background knowledge of all these facts are incorporated in the forthcoming chapter 2.

CHAPTER 2

LITERATURE SURVEY

With the advancement in aerospace research, the speed of the space vehicles increases over a few decades from speed of sound to hyper speed. The space vehicles usually travel through atmosphere before reaching space and earth. The study of aerodynamic performance of space vehicles is carried out by measurement of aerodynamic forces and its dynamic analysis (D'Souza *et al.*, 2015; Libii, 2011; Pope and Goin, 1965; Kegelman *et al.*, 2014; Kakate *et al.*, 2014). Ground-based testing facilities like the wind tunnel systems are very essential for such purpose wherein flight conditions of space vehicles are simulated. Wind tunnel depicts the functions of the objects in space vehicles and promotes testing of full size versions as well as scaled models of the specimen which are expected to move in space. The aerospace facilities available in various countries have developed wind tunnels to study the movement of space vehicles in air. The approximate flight conditions are simulated inside the tunnel system to study the dynamic behavior of the space vehicles. The specimen to be tested is fastened inside the tunnel so that it is immovable [27-30].

The aerodynamic forces depend on Mach number and Reynolds number which should match with flight conditions for valid experiments (Lee *et al.*, 2014; Savino *et al.*, 2009). Mach number is a dimensionless quantity which is the ratio of flow velocity to the speed of sound in air whereas Reynold's number is also a dimensionless quantity that determines whether the type of flow pattern is laminar or turbulent. Based on Mach number, tunnels are classified as Subsonic with M < 0.8, Transonic with Mach number

0.8 < M < 1.2, Supersonic with 1.2 < M < 5.0 and Hypersonic with Mach number M > 5.0 (Lee *et al.*, 2014; Savino *et al.*, 2009; Jones *et al.*, 2014; Kakate *et al.*, 2014).

Hypersonic Wind Tunnel is a facility used to investigate the aerodynamic properties of objects by passing a stream of velocity controlled air over them. Heart of Wind Tunnel is a test section where a scale model is supported in a controlled airstream for a maximum duration of 40 seconds. Thus, regulation of pressure inside the test section is important for realizing the real time flight condition from the ground based model. This is achieved by a suitable controller capable of accurately controlling the air flow in the test section (Lee *et al.*, 2014; Savino *et al.*, 2009; Jones *et al.*, 2014; Pope and Goin, 1965; Reddy, 2007; Owen and Owen, 2007; Smith and Baxter, 1989; Cristofolini *et al.*, 2008; Hollis and Wayland, 1991; Daikert *et al.*, 1995; Lin and Wang, 2008; Alfyorov, 1995; Vargese and Binu, 2009).

In this chapter, a brief survey of literature on aerodynamic research and wind tunnel facilities is conducted. A review on background literature is carried out to assess the state of the art of designs of controllers for the purpose of settling chamber pressure regulation in hypersonic wind tunnels. The basics of various wind tunnel systems and different existing control schemes used to achieve the desired system characteristics for particular applications are also reviewed here.

2.1 WIND TUNNELS HISTORY

A rich theory was experimented in aviation in the 17th century and the first aerodynamic test device, a whirling arm apparatus was developed by Benjamin Robins for the ground based testing facility of aircraft. Sir George Cayley in early

80's used this facility to determine drag and lift of various airfoils, attaining top speeds between 10 and 20 feet per second. But whirling arm could not produce reliable, steady, controllable flow of air for testing and hence detailed analysis was found difficult. The first tunnel system setup was established in 1871 by Frank Wenham, a Council member of the Aeronautical Society of Great Britain. This tunnel was built with a length between 10 and 12 ft and driven by a fan blower steam engine. In 1880, Horatio Phillips developed a wind tunnel to carryout tests. Osborne Reynolds introduced the factor, Reynolds number as a basic parameter in the description of all fluid-flow situations like shape, turbulence and ease of heat transfer. This becomes a scientific justification for the use of models in wind tunnels to simulate real life phenomena (Jones *et al.*, 2014; Baals and Corliss, 1981; Flay, 2015; Arbuckle, 2016; Bruce *et al.*, 2015; Bottasso *et al.*, 2014).

Wind tunnels were first developed and used for aerodynamic study in 19th century (Baals and Corliss, 1981; Flay, 2015). In 1916, a wind tunnel was built at Washington Navy Yard by US Navy and another was built by France to test full size aircraft in 1929 and this was the largest tunnel system till second world war. In 1919, a Duplex wind tunnel was used for high-speed tests with a maximum speed of 110 ft per second. During World War One, National Physical Laboratory made major contributions to advances in theoretical and practical aspects of the stability of aero planes, airships, space vehicles, military applications and parachutes. Later, the use of wind tunnel was extended to second world war. For this purpose, Brits build a Supersonic tunnel in 1922 and Germans made three different Supersonic wind tunnels. Later, the use of tunnels was extended for testing bridges, buildings and so on. These days tunnel systems were used to study the effect of wind on objects or structures thereby to ensure the strength

of such buildings and tall structures. An appraisal of the advances in wind tunnel test techniques can be readily obtained by comparing the modern wind tunnel facilities with their historical predecessors till 1930. Later, the use of tunnel facility was extended to automobiles, to study the effect of forces required to move the vehicle on road. The wind tunnel test equipment facility built and used by the Wright Brothers in the early 1900's paved the way for the development of the early flying machines of this century. One of the largest wind tunnels was built in 1941 by US at Wright Field in Ohio. Later on, at the end of Second world war, US built 8 new wind tunnels which includes the largest one in Moffett Field in California. The first tunnel built specifically for human flying was designed and built by Jean St-Germain in 1978 in Montreal, Canada (Jones *et al.*, 2014).

The high-speed flow theory was developed by German scientists, in the early 1940's, following the successful operation of their Supersonic wind tunnels up to Mach number 4.4. The research in the area of hypersonics was motivated by threat of the cold war and the race for space research in the 1950s and 1960s (Lee *et al.*, 2014; Savino *et al.*, 2009; Jones *et al.*, 2014; Bhoi and Suryanarayana, 2008; Kegelman *et al.*, 2014; Arnaiz *et al.*, 1980; Owen and Owen, 2007). Hypersonic wind tunnels are used for investigating the aerodynamic properties of vehicles during re-entry missions where these vehicles need to travel from space to earth (NASA, VSSC). Hypersonic wind tunnel to study re-entry and a plasma wind tunnel to study the behaviour of materials at high speed, were set up at the Vikram Sarabhai Space Centre (VSSC) in Thiruvananthapuram in 2005 (NASA). This wind tunnel facility is used to characterize aero thermal properties and to optimize the launch vehicle design to ensure safe return of the vehicle during re-entry. A 1 metre Hypersonic Wind Tunnel with test section of

21

1m diameter and enclosed free jet with Mach number 6 was implemented. Simultaneously, a 1 metre shock tunnel with Mach numbers 8 was commissioned at the same centre. India's second largest 0.5m Hypersonic wind tunnel facility is located in Indian Institute of Science (IISC), Bangalore.

These facilities can be used for conducting tests on a larger scale, like the Hypersonic Testing Demonstrator Vehicle (HSTDV), aerospace related project testing, testing smaller planes and missiles. These facilities developed in our country would help in reducing the expenditure incurred during testing as undertaking these tests in other countries would be costly. Moreover, this would help to prevent keeping the latest capabilities under wraps due to strategic reasons as such tests outside the country can give immediate clues on what we are up to in the field of defense and in developing other such capabilities (Kegelman *et al.*, 2014; NASA, VSSC). Some of the other High speed tunnels available in the world includes, (i) NASA Langley Eight-Foot High Speed Tunnel (ii) NASA Langley Hypersonic 31 Inch Mach 10 (iii) NASA Langley Hypersonic 20 Inch Mach 6 (iv) NASA Langley Hypersonic Propulsion Integration Arc-Heated Scramjet (v) NASA Langley Hypersonic Propulsion Integration Combustion Scramjet (vi) NASA Langley Hypersonic Propulsion Integration Supersonic Combustion (viii) NASA Langley Hypersonic Propulsion Integration 15 Inch Mach 6 High-Temperature Tunnel in Hampton, Virginia, USA, NASA Glenn Hypersonic Test Facility in Sandusky, Ohio, USA, NASA Ames Hypersonic Propulsion Integration 16 Inch Shock and NASA Ames Hypersonic Propulsion Integration Direct-Connect tunnel in Mountain View, CA, USA (Baals and Corliss, 1981; Libii, 2011; Arbuckle, 2016; NASA), MARHy wind tunnel (Experimental plateform FAST) in Laboratoire ICARE, CNRS, Orleans, FRANCE.

The applications of different winds tunnels used in various fields are discussed below.

The new dynamic test rig is designed in 1995 by S V Kabin et al. to investigate the aerodynamic damping derivatives of the aircraft models in wind tunnels at high subsonic and transonic speeds (Imraan, Sharma and Flay, 2011). The dynamic test rig is equipped with the five component strain gage balance. Both direct and cross aerodynamic damping derivatives were measured. The feasibility of using luminescent coatings for surface pressure measurement in a cryogenic wind tunnel was discussed by Asai *et al.* (*National Aerospace Laboratory, Tokyo*). This technique is based on a new coating technology in which luminescent molecules are directly deposited onto the model surface by an electrochemical process. This capability allows us to measure the pressure field on the model surface in a cryogenic wind tunnel. A cryogenic wind tunnel has a capability to handle high Reynolds number air foil testing using a small air foil model in 1999 (Yamaguchi *et al.*, 1999). The Barnwell-Sewall and the Murthy methods are the readily available corrections, and were applied to the experimental pressure distributions. From the experimental study, the simple global correction to the main stream conditions works in some degree for the experimental data of low aspect ratio cases. Based on the calculation of physico-chemical processes taking place in nozzles of wind tunnel facilities it is noticed that the chemical air composition differs noticeably from the natural air composition (Klfyorov *et al.*). The algorithm was compiled using the experimental data obtained in the TsAGI MHD-gas acceleration hypersonic wind tunnel. It was able to note variation in both the initial burning stage and mole fractions of combustion products.

In 2003, an experimental analysis on the performance of the wind tunnel was conducted by Kotwani *et al.* (2003). The work focused on various losses at different sections and total pressure drop across the tunnel system estimation. It could also determine the input power required at flow velocities beyond maximum achievable flow velocity in tunnel. From the experiments, it is concluded that the efficiency of the present system goes down in the range of 25m/s. A high speed cavity ringdown scheme involving simultaneous LASER and cavity sweeping was presented by Debecker *et al.*, (2005). By performing fast measurements, it is seen that system fulfils the requirements to analyze transient flows in Hypersonic wind tunnels. Performance criteria for a full-scale open atmospheric boundary layer wind tunnel which replicates various quasi-steady and turbulent flow states on low-rise building models up to 1:25 scale was studied by Boudreau (2009). A Supersonic wind tunnel intended to use the difference between atmospheric pressure and the pressure inside the vacuum chamber to achieve desired flow velocities was developed by Butler *et al.* (2010). The tunnel was intended to achieve a test section Mach number of 3.68. The development of a wind tunnel used for wind turbine testing in a controlled environment was presented by Dolan *et al.*, (*California Polytechnic State University*). It was designed to provide wind speeds of up to 20 m/s depending on the cross-sectional area of the chamber. This system allows repeatable and controlled environmental conditions that are unavailable in the field. In 2015, a LASER-aided vision technology based high precision pose measurement in wind tunnel was performed by Wei et al. which proposed an image acquisition method for small high speed target with multi dimensional movement in wind tunnel. Simulation experiments were conducted on measuring the position and attitude of high speed

rolling targets and the accuracy was experimentally verified (Wei *et al.*, 2015). Later, NASA Langley Research center (LaRC) designed a standard package consisting of an accelerometer and vibration isolation pads to measure the pitch attitude of wind tunnel models under smooth operating conditions (Jones and Lunsford, 2005). A Supersonic wind tunnel with Mach number 2.5 was designed and fabricated by Bharath (2015). The design was based on assumptions of 2D in viscid flow and normal shock pressure recovery in the diffuser. Calibration of the system was carried out and comparison of Reservoir pressure with pressure in the test section was carried out to verify the effectiveness of this facility.

2.2 HYPERSONIC WIND TUNNEL

In earlier days, a few works were carried out in subsonic and transonic tunnels. Nowadays, works are on supersonic and more concentrated on Hypersonic wind tunnels having greater speed (Jones *et al.*, 2011a; Jacob and Binu, 2009; Jones *et al.*, 2011b). A ground based test facility which mimics the original flight parameters has to be analyzed before its real time execution. This is achieved using various wind tunnel configurations with different operating conditions like flow velocity, temperature, pressure etc (Lee *et al.*, 2014; Savino *et al.*, 2009; Jones *et al.*, 2014; Baals and Corliss, 1981; Flay, 2015; Owen and Owen, 2007; Smith and Baxter, 1989; Cristofolini *et al.*, 2008; Hollis and Wayland, 1991; Daikert *et al.*, 1995; Lin and Wang, 2008; Alfyorov, 1995; Vargese and Binu, 2009).

An experimental study of hypersonic wind tunnel diffuser was conducted by Wegener *et al.* (1953). Data on overall pressure ratios for starting and maintaining hypersonic flow for various diffuser configurations were presented. It was found that starting pressure

ratio was equal to pitot pressure ratio, thus making additional starting devices not necessary. It was also observed that air condensation in the test section at high Mach number had only minor effect on the diffuser performance. Techniques for transitional and turbulent flow measurement techniques was reviewed in 1990 (Owen *et al.*, 1990) and the status of these research in support of turbulence modeling programs are discussed. The results of experiments conducted in two Hypersonic wind tunnels are compared with previous hot wire turbulence measurements. Thus, a new concept for the measurement of the compressible shear stress terms combining both techniques are demonstrated. Laser-spectroscopic techniques was used to obtain measurements of temperature, density, and their turbulent fluctuations at Hypersonic wind tunnel conditions with uncertainties of less than 5% (McKenzie and Fletcher, 1992). Probative research is being conducted at ONERA on a new technique for measuring heat transfer measurements in wind tunnels in 1993. This method was based on the heat sensitivity of a luminescent coating applied to the model (Le Sant and Edy, 1993). The main advantage of this new technique was to provide thermographic measurements. Electron beam fluorescence technique was used to perform local and non intrusive measurements of density, vibrational and rotational temperatures and velocity in a low density flow of nitrogen or air (Mohamed *et al.*, 1995). It was applied to study the interferences between shock waves issued from two models placed in a Mach 10 flow. Velocity measurements have also been carried out. The future of Hypersonic wind Tunnel was discussed by C. Tirres in 1999, where the existing ground test capabilities, gaps in existing Test and Evaluation (T & E) infrastructure, and efforts to mitigate those shortfalls were discussed which helped to identify potential hypersonic systems that satisfy requirements for tactical missiles, aircraft and space lift systems (Tirres, 1999).

In heat transfer measurements of hypersonic wind tunnel (Simeonides, 1991), infrared thermography was used for the acquisition of high quality two-dimensional heat transfer data over aerodynamic surfaces by G Siimenides *et al.* in 1991. It is shown that the availability of an infrared scanning radiometer and a standard Digital Image Processing (DIP) system in the laboratory provides the means for the performance of highly efficient heat transfer measurements. The main advantage is providing a black and white intensity output signal than a colour wavelength output signal. At hypersonic Mach numbers, the separated boundary layer from the model base develops as a shear layer and separates the outer in-viscid hypersonic flow from low subsonic flow in the base region [58]. Suitable sensor and instrumentation are developed to characterize the base flow of blunt body at hypersonic speeds in short duration facility. The flow conditions over bodies in a free flight were compared with those realized experimentally in the test section of the hypersonic wind facility at the same flow velocities. The advantage of applying MHD-gas acceleration facilities to solve problems was demonstrated and the data on possible gas dynamic and electrodynamic parameters of these facilities and their design versions are presented (Alfyorov, *IEEE Xplore*). An experiment was conducted in the 20 inch Hypersonic wind tunnel to assess non-isentropic effects on the test section Mach number (Buck and Draper, *IEEE Xplore*). The pressures measured were then compared with a Parabolized Navier-Stokes code to define the freestream Mach number. The results indicate that there was no significant non-isentropic effects. The research program of the aerodynamics, aerothermodynamics and plasmadynamics discipline of NASA's Hypersonic Project was reviewed in 2007 (Salas, NASA). The Aerodynamic, Aerothermodynamics, and Plasmadynamics discipline of NASA's Hypersonic Project has an extensive research

27

effort to develop and validate predictive tools to enable NASA's critical missions. The critical components of this effort was described in detail including some of its modelling, computational and experimental activities. The free-jet test sections of Korea Aerospace Research Institute can reduce choking and test larger models compared with solid wall test sections. In 2014, Y J Lee et al. designed an air ejector system to simulate a test section with a Mach 3.5 test section. The existing Hypersonic wind tunnel system had an efficiency of 58%, and hence the ejector system of this was modified to conduct a Scramjet intake test with Mach 6.7 condition whose efficiency was originally 40% (Lee *et al.*, 2014). With these modification, it is found that Scramjet testing efficiency was improved from its original value. The institute designed and constructed a blow-down type, high enthalpy wind tunnel facility for hypersonic air-breathing engines like ramjet and scramjet engines.

The performance of the Hypersonic wind tunnel system depends on its regulated air flow through the test section where the specimen to be tested is kept. This regulated air flow is achieved by designing suitable controllers and the research in this direction are progressing.

2.3. CONTROLLERS

Control systems are primarily characterized by its dynamic behavior which determines the scope and quality required to regulate the system parameters. One of the conventional control schemes is PID controller. In 1942, Zeigler and Nichols developed the PID Controller tuning concept for open and closed loop system which perform well in terms of disturbance rejection. In 1953, Cohen and Coon proposed the open loop tuning method which requires limited process knowledge, but it offers

lower damping and high sensitivity to the system. Later in 1962, Wills proposed the tuning maps concept for three mode controllers. In 1967, Miller *et al.* proposed a comparison of both Ziegler Nichols and open loop controller tuning techniques which investigated the process reaction curve method. In 1972, Parker introduced the concept of the design of Proportional Integral Derivative (PID) Controllers by the optimal linear regulator theory. In 1985, based on the dominant pole design Hagglund et al. developed the auto tuning technique for the Proportional Integral Derivative (PID) Controller. In 1986 Rivera *et al.* introduced the design procedure of the Internal Model Controller to establish PID rules with a well described approach. Deshpande in 1988 introduced optimization methods to obtain the PID parameters by the optimization of the Integral Square Error (ISE), Integral Absolute Error (IAE), Integral Time Square Error (ITSE) as the performance indices. Porter and Jones in 1992, proposed the concept of the Genetic Algorithm based technique for finding the tuning parameter of the digital PID Controller. Wang and Kwok (1994) proposed the optimal design of the Proportional Integral Derivative (PID) Controller, based on the Genetic Algorithm. Later in 1995, Zibo and Naghdy proposed the concept of the application of the Genetic Algorithm for system identification. Now a number of control schemes are available (Jones *et al.*, 2014; Ogunnaike and Ray, 1994; Aslam and Kaur, 2011; Jeng and Lee, 2012).

In the PID control system analysis, design and technology (Ang and Yun Li, 2005), an overview of functionalities and tuning methods in software packages and its implementation in commercial hardware modules was presented. By including system identification and intelligent techniques in software based PID systems helps automate the entire design using tuning process. PID controllers are considered as an extreme form of a phase lead-lag compensator with one pole at the origin and the other at infinity. This

will help in future development of plug-and-play. PID controllers can operate optimally for enhanced productivity and improved quality. In 2013, Debabrata Roy et al. designed a proportional derivative (PD) feedback controller for pitch attitude control of a rocket. (Roy *et al.*, 2013).

2.3.1 Linear Quadratic Regulator Controller

Linear Quadratic Regulator (LQR) is theory of optimal control that operates the dynamic system at minimum cost. The system dynamics described by a set of linear differential equations and the cost by a quadratic functional is called the LQ problem (Ogata, 2002; Purnawan *et al.*, 2017). This involves a mathematical algorithm that minimizes a cost function with weighting factors supplied by a human. The cost function is defined as a sum of the deviations of key measurements from their desired values. Thus, this control algorithm finds those controller settings that minimize the undesired deviations, like deviations from desired altitude or process temperature. The LQR algorithm is an automated way of finding an appropriate state-feedback controller. However, the important aspect is to specify the weighting factors and compare the results with the specified design goals and this becomes the limitation with the LQR controller (Mohammad *et al.*, 2013; Mauricio *et al.*, 2012; Yin and Zhang, 2006; Huang and Zhou, 2004). A double inverted Pendulum was controlled optimally by an LQR controller by S K Yadav et al in 2012. The method is based on selecting the weighing matrices, Q and R. This optimisation based control technique was proposed considering the performance and control requirements (Yadav *et al.*, 2012).

2.3.2 H-infinity Controller

H-infinity control is a robust control technique that comes from the name of the mathematical space over which the optimization takes place. H-infinity methods are

used in control theory to synthesize controllers achieving robust performance or stabilization. H-infinity is a member of spaces introduced by the scientist, Hardy. This control is a Robust control technique which was suggested by Zames in 1981 whose design involves more analytical calculations (Mary *et al.*, 2012; Yilmaz *et al.*, 2012; Hassibi *et al.*, 2006; Vikalo *et al.*, 2005). In 1989, Doyle et al. found state space H-infinity solutions using Riccati equations (Doyle *et al.*, 1989). To use H-infinity methods, a control designer expresses the control problem as a mathematical optimization problem and then finds the controller that solves this. H-infinity techniques can be used to minimize the closed 3 loop impact of a perturbation depending on the problem formulation, the impact will either be measured in terms of stabilization or performance. In a tutorial in 1993 on robust control (Lenz, 1995), minimization of the infinity-norm of the sensitivity function of single-input-single-output linear feedback system is considered. This is limited to single-input-single-output (SISO) control systems. Minimization of the mixed sensitivity criterion results in optimal robustness. Mixed sensitivity problem is a special case of the so-called standard optimal regulation problem.

2.3.3 Optimisation Techniques

The optimization technique has three basic parameters defined, viz: objective function, unknown variables and a set of constraints about the system (Yang and Gandomi, 2012; Gümüssoy, 2004). There are three types of optimisation techniques, viz: traditional, modern and intelligent methods. The traditional optimisation technique was established by Walvekar and Lambert (1970). A number of optimisation problems were carried out from 70's and research in this area is progressing. Swisher *et al.* in 2000 provided a more

comprehensive review on various optimisation techniques (Swisher *et al.*, 2002). In order to reformulate a design problem as a mixed sensitivity problem, Robust controller is designed by H-infinity optimization by Kwakernaaak (1993). Minimization of this sensitivity problem results in optimal robustness. This method also minimizes the peak value of closed loop frequency response functions. H-infinity optimization is concerned with the minimization of system norms. Prempain and Postlethwaite (2004) extended this control technique using output loop shaping method. A number of Optimisation control algorithms are developed in recent years (Wang *et al.*, 2014; Wu *et al.*, 2011; Gandomi and Alavi, 2012; Alfi and Modares, 2011; Ali *et al.*, 2010). Robustness is of crucial importance in control system design because real engineering systems are vulnerable to external disturbances and measurement noise and there are always differences between mathematical model used for design and the actual system (Gu *et al.*, 2005), which was studied in 2005. A control system is robust if it remains stable and achieves certain performance criteria in the presence of possible uncertainties. The robust design is to find a controller for a given system, such that closed loop system becomes robust.

2.3.4 Backstepping Controller

Backstepping is a novel non-linear control method, in the control theory. Backstepping control technique was developed by Peter V. Kokotovic et al to design and stabilize controls for nonlinear dynamical systems in 1990. Because of this recursive structure, the design process starts at the known-stable system and back out new controllers that progressively stabilize each subsystems of the main system until the final external control is reached. Hence, this process is known as Backstepping (Cooper, 2005; Skjetne and Fossen, 2004; Madani and Benallegue, 2006; Joseph and Geetha, 2007;

Peng and Yang, 2008; Farrell *et al.*, 2009; Rudra and Barai, 2012; Sonneveldt *et al.*, 2007; Yang *et al.*, 2013).

Backstepping controller design was applied to the spacecraft maneuvers by Krstic & Tsiotras in 1999 and Kim & Kim in 2003 (Kim and Kim, 2003; Krstic and Tsiotras, 1999). A tracking controller for a class of underactuated mechanical systems, based on a Backstepping procedure [103] was proposed by Frazzoli *et al.* (2000). This design focused on approximation of small helicopter dynamics and the control design provides asymptotic tracking for an approximate model of small helicopters, and bounded tracking when more complete models are considered. A nonlinear approach to flight path angle control was proposed by HarkegArd and Glad (2000). Using Backstepping controller, a stabilizing control law is derived and the free parameters that spring from the Backstepping design are used to achieve a desired linear behavior around the operating point. A strategy to design a time-varying stabilizing controller of the position and the orientation of an underactuated autonomous airship was proposed by L Beji et al. in 2002 using time averaging and Backstepping approach (Beji *et al.*, 2002). The airship cannot be stabilized to a point using continuous feedback law. However, the stabilization problem is solved with an explicit homogeneous time varying control law, based on an averaging approach. The paper by Benaskeur and Desbiens (2002), addresses analysis and design issues in Adaptive PID control for linear second-order minimal phase processes using the Backstepping algorithm. This involves adding an integral action to the basic Backstepping algorithm to obtain a zero static error. An integrator is therefore added to the plant model and is then slid back to the controller equation to obtain the control law.

33

In the note by Zhou *et al.* (2004), a class of uncertain dynamic nonlinear systems preceded by unknown backlash-like hysteresis nonlinearities, where the hysteresis is modeled by a differential equation in the presence of bounded external disturbances is presented. A robust Adaptive Backstepping control algorithm was developed and is observed that the proposed controller not only can guarantee global stability, but also transient performance characteristics. Abdulgalil and Siguerdidjane (2005), developed a nonlinear Backstepping design for the control of rotary drilling system that is capable of dealing with the torsional oscillations. This work is motivated by the complex problem of the nonlinearity in drill string, which is rotated at a constant angular velocity by an electric motor. An Adaptive Backstepping controller was designed by A Ebrahim in 2005 to stabilize an inverted pendulum that is mounted on a moveable cart (Ebrahim and Murphy, 2005). The Adaptive Backstepping control synthesis technique results in the design of a controller for non-linear state differential equations with unknown parameters and generates a control law for this system with the measured states. The performance is evaluated based on the transient characteristics, complexity of implementation, and the impact of the system characteristics on the system stability. Ghommam *et al.* (2006) addressed the problem of controlling the planar position and orientation of an autonomous underactuated surface vessel. A time-invariant discontinuous feedback law based on Backstepping design is derived to guarantee global uniform asymptotic stabilization of the system to the desired configuration. To obtain high performance and good robustness for the flight simulator, an Adaptive Backstepping controller, which is robust to the parameter uncertainties and load disturbances was proposed by Wang *et al.* (2006). The parameter update law and control law are designed based on Lyapunov stability theorem. A nonlinear dynamic model for a quadrotor helicopter using Backstepping control design was presented by Madani and Benallegue (2006). Due to the under-

34

actuated property of quadrotor helicopter, the controller can set the helicopter track three Cartesian positions (x, y, z) and the yaw angle to their desired values and stabilize the pitch and roll angles. A Backstepping control based on the Lyapunov stability theory is presented to stabilize the whole system.

An Adaptive Backstepping control scheme for precise trajectory tracking of a piezoactuator-driven stage was proposed by Shieh and Hsu (2007). Based on the linear state-space model, an Adaptive Backstepping control for the trajectory tracking was developed. By using the proposed control approach to trajectory tracking of the piezoactuator-driven stage, improvements in the tracking performance, steady-state error, and robustness to disturbance was obtained. A novel decentralized PID controller design procedure based on Backstepping principles was presented by Zhang and Zhu (2007) to operate multiple-input multiple-output (MIMO) dynamic processes. First, a control Lyapunov function (CLF) and virtual control variable based on the Backstepping method was derived recursively for each loop and a multivariable controller is obtained. Sufficient stability conditions are then derived for two-input two-output and MIMO closed-loop systems, respectively. In order to achieve good handling (or flying) qualities in longitudinal axis for all flight conditions, an Adaptive Backstepping flight control law was presented by Ju and Tsai (2007). With the Backstepping technique, an adaptive controller is designed for the purpose of accomplishing desired responses under a wide range of flight envelope. In comparison with other conventional control methods, the proposed control law is much simpler and easier to implement. A new control methodology is introduced by E S Kazerooni in 2008 for nonlinear and MIMO heating, ventilating and air conditioning (HVAC) systems (Kazerooni *et al.*, 2008). A full information feedback

of states and disturbances is used for disturbance decoupling and model linearization purposes. Simulation results show that the closed-loop system has good and fast tracking, offset-free and smooth response with high disturbance decoupling and optimal energy consuming properties in the presence of time-varying loads. A robust nonlinear attitude control method for aircraft based on partitioned Backstepping and input-to-state stability theory was proposed by Bi *et al.* (2009). With this strategy the coupling of the model attitude can be dealt naturally. The control design can be applied directly to an aircraft with thrust arising from gas fuel. The state feedback control problem was addressed by C Hua et al. in 2009 for a class of nonlinear time-delay systems (Hua *et al.*, 2009). The time delays appear in all state variables of the nonlinear system, which brings a challenging issue for controller design. With the help of a Backstepping method, a memoryless state feedback controller was designed, which does not need the precise knowledge of time delays. The developed method was applied to the control design of a two-stage chemical reactor with delayed recycle streams, and the simulation results verify the effectiveness of the main results. Farivar et al. in 2011 proposed the chaos control and modified projective synchronization method for unknown heavy symmetric chaotic gyroscope systems using adaptive Backstepping control (Fariyar *et al.*, 2012). In the paper, using Neural Backstepping control technique, control laws was established which guarantees the chaos control. Here Gaussian radial basis functions are utilized to on-line estimate the system dynamic functions. The proposed method allows us to arbitrarily adjust the desired scaling by controlling the slave system. The simulation results show that the proposed method is very effective and robust against system uncertainty.

2.3.5 Sliding Mode controller

Sliding mode controller (SMC) is suitable for a large number of industrial applications because of their properties like robustness, invariance, order reduction and chattering control. Variable structure control utilizes a high speed switching control law to drive the non linear plants state trajectory onto a specified and user chosen surface in the state space and to maintain the plants state trajectory on this surface for all subsequent time. The state variables of the plant dynamics are required to satisfy and reach another set of equations which defines the switching surface. This control scheme is widely used due to its robustness against parameter variations and disturbances (Saravana Kumar *et al.*, 2009; Musmade *et al.*, 2011; Utkin, 1977; Tan *et al.*, 2005; Utkin, 1993; Shyu and Shieh, 1996; Li *et al.*, 2012; Moura *et al.*, 2007; Mondal and Mahanta, 2013; Ding *et al.*, 2013; Hong *et al.*, 2005, Iggidr *et al.*, 1996).

Chattering reduction and error convergence in Sliding mode control for a class of nonlinear systems was done by Pushkin Kachroo and Massayoshi Tomizuka (Kachroo and Tomizuka, 1996). To reduce chattering in Sliding mode control, a boundary layer around the switching surface is used and a continuous control is applied within the boundary. The above principle is used to generalize the design for the class of nonlinear systems being considered. In 1999, a survey paper (Young *et al.*, 1999) was written by Young et al. as a guide to sliding mode control for practicing control engineers. The paper incorporates an accurate assessment of chattering phenomenon perceived as motion which oscillates, providing a frame of reference for future Sliding mode control research. The important property of the control action is discontinuous nature, referred as variable structure control (VSC), where the primary function is to switch between two distinctively different system structures. The paper investigated various Sliding mode

control designs that focused on guaranteeing the robustness in the presence of practical constraints and realities. It was also concluded that introducing discontinuous SMC and restructuring the SMC design in a sampled data system framework is appropriate and positive step in SMC research.

Novel induction motor control optimizing both torque response and efficiency was proposed by Rodic and Jezernik (2002). The main contribution of the paper is a new structure of rotor flux observer aimed at the speed-sensor less operation of an induction machine servo drive at both low and high speed, where rapid speed changes can occur. In principle, the proposed method is based on driving the stator flux toward the reference stator flux vector defined by the input command and the reference rotor flux. The magnitude and orientation angle of the rotor flux of the induction motor are determined by the output of the closed-loop rotor flux observer based on Sliding mode control and Lyapunov theory. Simulations and experimental tests are provided to evaluate the consistency and performance of the proposed control technique. Sensor less Direct Field Oriented (SDFO) control of three-phase induction motors based on Sliding mode has been studied and applied to domestic washing machine drives by Xu *et al.* (2005). In this paper, three related techniques, Sliding mode flux observer, sliding mode speed controller and direct rotor speed estimator are presented for the application of SDFO Sliding mode in induction motor control system. The investigations focused on how speed regulation is improved for systems with robustness and it also concentrates on specific technical issues in washing machine drives. An experimental evaluation of a dynamical Sliding mode control for power converters was recently proposed by Cortes *et al.*, (2006). This controller is endowed with notable characteristics predicted in theory and observed in

simulations. It is observed that the system is robust under load and input voltage variations and does not require current measurements.

In 2007, A. F. Gonzalez *et al.* (Gonzalez *et al.*, 2007) presented a multi-variable DC-to-DC converter of the Boost-Boost type constituted by two cascaded Boost converters in continuous conduction mode. A Sliding mode feedback controller, based on the Generalized Proportional Integral (GPI) approach, was developed for this application. Here, robustness of the feedback scheme is tested by non-modelled sudden load resistance variations in the resistive load of the circuit. Position control of synchronous motor drive by Modified Adaptive Two-phase Sliding mode controller was designed in 2008 by Mohamed Said Sayed Ahamed, Ping Zhang and Yun-Jie Wu (Ahmed *et al.*, 2008). Chattering occurs when control signal input switches discontinuously across the boundary, which damages the electrical systems and causes vibrations in the mechanical systems. In this paper two-phase variable structure control is designed to control chattering and retain robustness of the systems. Here the first phase controls the steady states and disturbed states, whereas the second phase is used in the case of disturbed states. Important improvements have been incorporated including control of the performance of the reaching mode and reduction in chattering.

A system converting solar energy to electricity and connecting to the utility network was proposed by Jiao and Luo (2009). In order to obtain a stable output DC voltage, an improved Sliding mode controller was investigated in the paper. The reaching time was made to zero by using the designed sliding surface. The additional integral term in the improved sliding surface is used to suppress the steady-state error. In order to improve

dynamical performances with static and dynamic specifications, a systematic procedure to compute the gains of the controller based on an optimization scheme was proposed by Alaa *et al.* (2009) for a boost converter. Given a system with large variations of input voltage and load, it is necessary to guarantee good performance of the controller for large variations of operating point. A higher order Sliding mode control with self-tuning law algorithm for uncertain non-linear systems was proposed by Q Zong *et al.* (2009). The method can be viewed as the finite time stabilization based on geometric homogeneity and integral SMC. In order to reduce chattering and solve system uncertainties with unknown bound, a bipolar sigmoid function on-line adaptation and an adjustable control gain tuning approach without high frequency switching was developed. Control system stability was ensured using the Lyapunov method. The control input chattering is reduced. Two different approaches to achieve robustness with respect to the input voltage, the reference voltage and the load variations in a step-down multiphase power converter were presented in D Biel *et al.* (2010). This control algorithm regulates the output voltage to a given reference and minimizes the current ripple. An Adaptive Sliding mode speed and position observer for sensor less control of brushless DC motor (BLDCM) was proposed in 2010 by SHI Tingna *et al.*, 2010. According to the mathematical model of BLDCM, the sliding surface was defined based on the errors between actual and estimated currents. Equivalent control and Model Reference Adaptive Control (MRAC) are used to obtain position and speed signals of the rotor. The Lyapunov theory is introduced to prove the convergence of this system. The result of simulation shows that the proposed method can correctly estimate the speed and position of the rotor, and thus attaining good dynamic and static performances to the system.

Chattering reduction of Sliding mode control by low-pass filtering the control signal was done in 2010 (Tseng and Chen, 2010). In the presence of high level noise, the traditional boundary layer design is found to be ineffective in chattering reduction. In the boundary layer design, a smooth continuous function is used to approximate the discontinuous sign function in a region called boundary layer around the sliding surface. However, to achieve this, control accuracy need to be sacrificed and boundary layer width should be larger. In the proposed model, the sliding variable is estimated by a disturbance estimator and is achieved by placing an integrator in front of the system, which allows low pass filtering thereby reducing chattering. This approach has better noise immunity than conventional approach, maintaining control accuracy by a sufficiently large disturbance estimator gain. Focusing on uncertainty in singularly perturbed non-linear systems with its control performance, K J Lin (2014), discussed the use of fuzzy models, a proposal to use Neural Network based Adaptive Sliding mode control for stabilization and better convergence time. The sliding surface was determined by a Linear matrix inequality design procedure and the Lyapunov stability theorem. Simulation using an inverted pendulum model controlled by a DC motor shows the system as feasible, satisfactory, and with a comparatively better convergence time. In discussing the benefits of modified design of controllers for improving their performance against varying external factors, Jinhui Zhang and Wei Xing Zheng in 2014, use the output data as a means to develop Sliding mode controllers for more realistic (real-life) systems. This uses an iterative programming method to progressively reach the desired results for a class of linear systems with matched external disturbances. Sliding mode controllers are known to be effective and robust controllers, yet affected by uncertain systems. They gave a

singular framework design using a memory-based approach to adapt the Sliding mode controller results using output values, that showed better transient performance (Zhang and Zhang, 2014).

Contrary to existing PID and Adaptive Robust Control (ARC), Modified SMCs have shown better robustness and tracking performance. Chuansheng Tang et al. in 2014 proposed a new algorithm using a similarly Adaptive Sliding mode controller schema, considering a Permanent magnet synchronous linear motor (PMSLM) direct - drive – servo system (Tang *et al.*, 2014). This again considers the Adaptive modelling approach with the Sliding mode control approach to handle system uncertainties such as including the unknown system parameters, load disturbance, nonlinear friction. Tang et al. in 2014, established through simulation that such Adaptive SMC models provide a better response performance and smaller tracking error, when compared to more traditional models. Shen et al. in 2014, studied the sliding motion of the SMC, in detail and derived a new relationship for the same using sliding motion analysis of a discretized system for real-time modelling (Shen *et al.*, 2014). The relationship proposed use of discrete time version equations for the SMC based on two new quantities (μ^+ and μ^-) describing the sliding motion, which was in line with the Filippov's equivalent control theory (Fillipov in 1960). This modification of the system equations was done focusing on reducing the amplitude of the switching part of SMC. Shen et al. in 2014 addressed a key drawback of SMC, the chattering phenomenon, through focus on the magnitude of the controllers switching part. Most earlier studies focused on reducing/slowing down variance in the control input, whereas Shen et al. in 2014 dealt with the chattering in the other direction. The effectiveness of such an endeavor was proved through simulation results of Rossler system. An Adaptive Robust Sliding mode control for time-varying delay systems

with uncertainties was proposed by Jiangfan Ni *et al.* (2014). Initially, an Integral Sliding surface is designed so that the reaching phase has been eliminated. In this approach a new adaptive law was designed to estimate the unknown upper-bound of uncertainty and thereafter a Sliding mode controller is proposed so that system state stay on surface where the discontinuous signal function is replaced by its continuous approximation to reduce chattering. The effectiveness is proved by a numerical example.

2.3.6 Backstepping Sliding Mode Controller

In 2006, M Smaoui presented a paper on synthesis of a nonlinear controller to an electropneumatic system. The nonlinear model of the electropneumatic system is transformed to be a nonlinear affine model and a coordinate transformation is then made possible by the implementation of the nonlinear controller (Smaoui *et al.*, 2006). Two kinds of nonlinear control laws were developed to track the desired position and desired pressure. A new Adaptive Backstepping Sliding mode controller of the electronic Throttle system in modern automobiles was developed in 2014 (Bai and Tong, 2014). Electronic throttle is a DC motor driven valve with nonlinear dynamical characteristics of unknown disturbances. This valve is used to regulate air in flow into vehicles combustion system and improve the vehicle drivability, fuel economy and emissions. The proposed design scheme can not only guarantee the robust stability of the perturbed systems but also realize the output tracking to the reference input. In 2005, Baric et al. proposed a Neural Network based Sliding mode controller for an electronic throttle system in which a static Neural Network is used as an estimator of the state dependent uncertainties in the system (Barić *et al.*, 2005). During the Backstepping design process, parameter adaptive law is designed to

estimate the unknown parameter and sliding mode term is applied to compensate the unknown disturbances. A Robust Chattering Free Backstepping Sliding Mode Control Strategy for the attitude stabilization and trajectory tracking control of quadrotor helicopter with external disturbances was proposed by Basri *et al.* (2014). This combines the systematic and recursive design methodology for nonlinear feedback control strategy of Backstepping control with reliable and robust properties of Sliding mode controller. To eliminate chattering, a Fuzzy system can be utilized in the control inputs of the Backstepping Sliding Mode Controller.

2.3.7 Fuzzy Logic Controllers

Fuzzy controllers are intelligent artificial decision makers that provides a formal method for representing, manipulating, and implementing a human's heuristic knowledge to controllable form. The Fuzzy Logic set theory was first proposed by Lotfi A. Zadeh in 1965 and the concept was elaborated by Mamdani and Assilian in 1975 to apply Fuzzy Algorithm for approximation, reasoning and design of controllers in industrial applications (Yager and Filer, 1994; Mendel, 1995). In 1970s, King and Mamdani investigated applications of Fuzzy logic for the control of nonlinear industrial processes that are typically controlled by human operators. In recent years, Fuzzy logic control finds application ranging from automation of industrial process to control of electronic devices in consumer products (Jäkel *et al.*, 1990). These controllers also find application in several wind tunnels in NASA's Langley Research Center in Hampton (Jones *et al.*, 2014), VA. The intelligent controller provides the required scope for tunnels to be more efficient, safe, and economic. This approach helps to meet the desired performance of current wind

tunnels in reducing harmful emissions, maximization of run time, minimization of noise and improvement in system affordability and safety.

K. Gowrishankar et al. proposed Adaptive Fuzzy controller to control turbine speed which is capable of locating high performance areas in complex domains (Gowrishankar and Elancheralathan, 2005). Initially, an Optimised PID controller was designed and to improve the performance further, Adaptive Fuzzy controller with adjustable scale factors was designed. Performance of a Simple Tuned Fuzzy Controller and a PID Controller on a DC Motor was analyzed by Montiel *et al.* (2007). This control technique is found to be easier than PI tuning methods. An Adaptive Fuzzy PID Controller for Speed control of BLDC Motor was designed which has the ability to satisfy desired controller characteristics by Kandiban and Arulmozhiyal (2012). From the experimental verification, it is clear that for the same operating condition, the BLDC speed control using Adaptive Fuzzy PID controller has better performance than the conventional PID controller and Fuzzy PID controller when the motor was working at lower and higher speeds. In 2015, a study of Membership Functions on Mamdani-Type Fuzzy Inference System for Industrial Decision-Making was conducted by Chonghua Wang (2015). The thesis focused to control the relations between input and output variables by making the fuzzy inference system to be transparent by adjusting the membership functions. By increasing the quantity of fuzzy sets for input variables, the linearity of input-output relation and the controllability of non-linear fuzzy inference system is enhanced. Fuzzy Logic finds applications in Road Traffic and Parking Space Management, which was designed by Ahmed Tijjani Dahiru (Dahiru, 2015). In this paper, Fuzzy logic is used in developing an inference for managing traffic flow and parking

45

allocation with generalized feature that is open for modification, where the travel time to the parking space is the output variable. The rule is found to efficiently control, accurately predict and conveniently adjust the performance parameters.

2.3.8 Sliding mode Fuzzy Controllers

Combination of Sliding mode with Fuzzy controller makes the system insensitive to parametric uncertainties without chattering in the output response [162]. This approach utilizes fuzzy rules to select the sliding surface. In 1994, R Palm proposed a robust control using Fuzzy Sliding mode controller. This approach ensures good tracking in the presence of uncertainties. However, the rules increases for higher order systems. A self-learning Fuzzy Sliding mode controller based on genetic algorithms was proposed and was analyzed using mass-spring-damper system by Lin and Chen (1997). Genetic-based Sliding Mode Fuzzy Controller is designed for an inverted pendulum by Wong *et al.* (2001). Here, the fitness function is found by selecting parameters with the combination approach and is observed that system has high global performance with less hitting time and chattering.

2.3.9 Adaptive Controllers

Adaptive systems were formally introduced in 1957 by Drenick and Shahbender with the view that they are nonlinear systems derived from linear or nonlinear systems in which parameters are adjusted using input-output data. The two distinct approaches of adaptive controller are Model reference adaptive control (MRAC) and Self tuning regulator (STR). MRAC was proposed by Whitaker , Yamron and Kezer in 1958 which uses a reference model whose output represents the desired output of the system. There are a number of Adaptive control applications in aerospace, robotics, process control

46

etc. (Enbiya and Hossain, 2011; Mirkin *et al.*, 2008). In their paper, on Indirect Model reference adaptive control (MRAC), M. A. Duarte and K S Narendra in 1996 developed a method that dynamically adjusted both plant parameters and controller parameters, describing the system by a set of non-linear differential equations, as in case of direct Adaptive control methods. This helped to bypass the issues in indirect methods of Adaptive control, while retaining its benefits (Duarte and Narendra, 1996). M. Makoudi et al. in 1999, discussed discretization and presented a Model reference adaptive control (MRAC) system that is decentralized to allow for poor communication and connectivity within the discrete portions of the system under study (Makoudi and Radouane, 1999). M. A. Duarte et al. in 2002, presented a similar experimentally validated combined Model reference adaptive control (CMRAC) for complex processes like PH control of a solution in a tank reactor (Duarte *et al.*, 2002). They compared the results favorably with those from more conventional controllers like PID (Proportional − Integral - Derivative) and MRAC (Model reference adaptive control). The studies showed that knowledge of initial conditions had a great impact on controller tuning, improving performance of the controllers with respect to the performance of the PID controllers. M. T Yassen in 2003, in his work with the chua's circuit discusses how several different approaches, involving conventional linear control techniques and advanced non-linear control techniques, fail to consider the practicality of having system parameters with unknown values (Yassen, 2003). He further demonstrated how an Adaptive controller can be derived for resolving the control and synchronization problems of the modified Chua's circuit systems, handling unknown parameters. Among the approaches for control of dynamic plants with unknown parameters, direct and indirect Adaptive controls is the conventional approach till the last decade and now

focus directed towards the 2-staged Indirect Adaptive control (Liu *et al.*, 2014). This usually involved dynamically estimating plant parameters using online input-output information and using algebraic equations to calculate the related control variables or control parameters.

The study of MRAC systems was also extended to nonlinear systems extensively, to carry forward the robustness of the Adaptive controllers to variable systems affected by disturbances (Yang *et al.*, 2006). L. Yang et al. in 2006 extended this to modify the standard MRAC using three non-linear differential equations, solved through eigen-values. The modified algorithm is applied to experimental system with a non-smooth dead zone characteristic and shown to give stable and robust control. K A Wise et al. in 2006 applied Adaptive control for the control of aircraft and weapon systems (Wise *et al.*, 2006). This algorithm uses a reference model of the baseline control and adapt to make the modified variant fly close to the reference model. A class of uncertain dynamic nonlinear systems preceded by unknown backlash nonlinearity was discussed in (Zhou *et al.*, 2007) by J Zhou in 2007. The control design is achieved by introducing a smooth inverse function of the backlash and using it in the controller design of Backstepping technique. It is noted that the proposed controller not only can guarantee stability, but also transient performance. A new smooth adaptive inverse to compensate the effect of the unknown backlash was also proposed.

An optimal control modification to Model Reference Adaptive control for fast Adaptation was proposed by Nguyen and Kalmanje (2008). This control scheme exhibits high-gain control behaviours when a large adaptive gain is used to achieve fast adaptation to reduce tracking error rapidly. The fast adaptation method helps to

reduce squares of tracking error rapidly which is formulated as an optimal control problem. The optimal requirement is used to derive adaptive law using the gradient method which results in uniform boundedness of tracking error by Lyapunov's direct method. The ability for an Adaptive control algorithm to modify a pre-existing control design is considered as a strength and at the same time a weakness. It is a fact that the fast adaptation can result in high-frequency oscillations which can excite unmodeled dynamics that could affect the stability of MRAC law. Here, a new approach to fast adaptation in MRAC framework is used where the optimality condition results in introducing a damping term proportional to persistent excitation. This optimal control is observed to determine convergence and stability characteristics. The simulation results show that tracking performance is achieved at a faster rate than existing MRAC approach and that the law can tolerate a much greater time delay in the system. Simulation of Adaptive systems using MIT rule was done by C Adrian *et al.* (2008).

A Modified Adaptive control method for synchronization of some fractional chaotic systems was developed by Agarwal and Das (2013). The new algorithm introduced modification on adaptive synchronization and parameter identification method with unknown parameters based on Lyapunov stability theorem. The proposed method exhibits its simplicity and suitability for a large class of fractional order as well as integer order chaotic systems. E Kharisov et al. in 2013 compared the architecture of closed loop system in sufficient detail, showing the similarities and difference between the Adaptive controllers, viz: direct and indirect Model reference adaptive controllers (MRAC) and L_1 Adaptive controller, using frequency domain tools (Kharisov *et al.*, 2013). They show how fast adaptive gains reduces the phase margin

of an MRAC to zero showing a necessary trade off between performance and robustness. While a disturbance to external parameters may affect an MRAC adversely for a L_1 Adaptive controller, provided adaptive gains prove beneficial to both performance and robustness. Here, the trade off is resolved in the selection of a low-pass filter, which also helps to improve the disturbance − rejection tendencies within the bandwidth of the controller. A brief survey on Simple Adaptive control, a stable direct Model reference adaptive control methodology was carried out in 2013 by Itzhak Barkana (Barkana, 2013). The application of Model reference adaptive control (MRAC) methodology, however, faced practical issues. The standard Adaptive control method was the MRAC approach, which basically adapted the plant parameters to follow the control parameters starting with linear combination of the model state variables. Furthermore, in real life, plant parameters may vary under various operational and environmental conditions, which advocated the Adaptive control methodologies. Itzhak Barkana in 2013 shows the basic features of such models and presents a very detailed survey on how most of the drawbacks of the MRAC were addressed and eliminated by the Simple Adaptive control methodology (SAC). He also established how the same information used for a robust classical design, can be used to implement robust Simple Adaptive controllers. In 2014, T. Garikayi et al. developed a Model reference adaptive controller of the Plantarflexion and Dorsiflexion movements within the Sagittal plane (Garikayi *et al.*, 2014). The controller design based on dc motor actuator and empirical analysis supported with parameter estimation technique was developed. The control technique could effectively control small and precise angle movements. A survey on Adaptive systems, its history, techniques, issues and perspectives was conducted by Black *et al.* (2014). The focus was on linear plants and discussed on practical issues encountered

in making these systems stable and robust with respect to additive and multiplicative uncertainties. It was also discussed on extending these methods on nonlinear systems. A Lyapunov design based on MIT rule for Model reference adaptive control systems was presented by Chetaswi *et al.* (2015). In this method, a cost function is defined which is a function of error between output of plant and reference model, where the controller parameters are adjusted so that the cost function is minimized. This method effectively eliminates the error and thus optimal performance of the system is obtained. In 2015, Mait *et al.* proposed a new higher order Model reference adaptive control (HO-MRAC), following Direct Adaptive control that estimates the unknown time varying parameters (Maity *et al.*, 2015). This follows the Lyapunov MRAC update law, with observer type parameter predictor dynamics. This consists of stable known part, feedback of parameter error and unknown parameters which are updated using Lyapunov design and the effectiveness of the proposed approach was demonstrated using two examples.

2.4. CONTROLLERS APPLIED TO WIND TUNNELS

The performance of a controller decides the precision and accuracy at which the tunnel system operates. The function of the controller in wind tunnel system in our study is to regulate the settling chamber pressure for the nonlinear model of the Hypersonic wind tunnel system. This section presents various control approaches for Subsonic, Transonic, Supersonic and Hypersonic applications in varied fields.

2.4.1. Subsonic and Transonic Wind Tunnels

A synthetic approach for control of Intermittent wind tunnel was introduced in 1997 by Zhang et al. Due to the unpredictable variations in process dynamics and restriction of air storage volume of the wind tunnel it is difficult to control Mach number in the test section (Zhang *et al.*, 1997). This is achieved by the synthetic approach which combines Adaptive and auto-tuning with Feedforward control strategy. The Feedforward control strategy is used to compensate the loss of air storage pressure. Auto – tuning is done in open loop and to reduce the effect of noise and external disturbance, data filtering is required before identification. This approach has excellent performance of setpoint tracking and load disturbance rejection. In 2001, control design for a mathematical model of a modern arc heated Plasma wind tunnel used to test parts of space vehicles during re-entry was presented (Ambrosino *et al.*, 2001). This facility permits to study the effects of aerodynamic and thermodynamic phenomena arising on some parts of space vehicle during re-entry phase by reproducing on suitable test models. The mathematical model, based on ordinary differential equations and Neural Networks, was designed for Plasma wind tunnel system. In 2012, R. Mark Rennie et al. proposed Neural Networks to manage wind tunnel performance data (Rennie and Cain, 2012). The Neural Network is accurately trained and calibrated to simulate the behaviour of subsonic closed circuit wind tunnel. Here, Neural Networks are used to efficiently extract information from large database to organize and manipulate data for mathematical modelling and control of facility. The proposed approach trains Neural Network to estimate values of useful parameters which are not directly measured based on the control variables that are monitored frequently.

2.4.2. Supersonic wind tunnels

A PC-based pre-programmed controller was developed by J. Matsumoto in 2001 for a Supersonic blowdown wind tunnel with short run time. It starts the tunnel very quickly without any overshoot of the stagnation pressure. The control system consists of a pressure transducer, a multifunction PC board and an automatic valve (Matsumoto *et al.*, 2001). An ideal valve opening profile for a particular test was developed based on the preceding test results with the same test conditions. The profile is stored in the system memory before a test and the multifunction board sends an analog output to the automatic valve during a test. After several tests and corrective interpolations, the pressure disturbances in the plenum chamber are typically reduced to one percent of the stagnation pressure.

Performance of Supersonic wind tunnel using PI controller was evaluated by Silva and Filho (2007). It is important to estimate the best test configuration with the required stagnation pressure, geometrical configuration of nozzles and diffuser before experimental run. This method concluded that Isentropic approach could be used for preliminary project of control and that sensitivity analysis coupled with Isentropic approach could be used in the choice of measuring instrument. In 2008, American Institute of Aeronautics and Astronautics worked on controlling a Supersonic Blowdown wind tunnel in LabVIEW (Braun *et al.*, 2008). Here a PI control for the wind tunnel was developed in LabVIEW and experimental verification was carried out. In these, stagnation pressure is constant and is considered equal to plenum pressure which was controlled by one or more pressure regulators. Here the real time error between setpoint and output pressure is used by LabVIEW PI controller to output the control valve opening angle. Real time values of valve opening must be

acquired in LabVIEW from the control valve with a new value passed to it during each step of the program. The LabVIEW PI control program was designed to have maximum flexibility for the wind tunnel configuration. In this paper, LabVIEW offers ability for user to edit control program to perform variety of functions both before and during a blowdown run. PI controllers are significantly less complex to operate than Neural Network controllers, but they are susceptible to organ piping unless correct control constants can be predicted. From the experimental results, it was observed that the error in plenum chamber pressure was minimized with the developed PI algorithm in LabVIEW. In a rapid valve opening technique (Lu *et al.*, 2008) proposed by E M Braun et al. in 2008, it was a desire to bring the Supersonic tunnel to its operating condition as fast as possible. A computer-based controller was developed which is able to start a Supersonic wind tunnel very quickly without any overshoot of the stagnation pressure. An ideal valve opening profile for a particular test was developed based on test data. The profile is stored in the system memory before a test and the multifunction board sends an analog output to the automatic valve during an actual test. After several tests and corrective interpolations, the pressure disturbances in the plenum chamber are typically reduced to one percent of the stagnation pressure. Unlike a PID controller, a Pre-programmed controller is not truly a real-time system. The advantages of having a Pre-programmed controller are that it can compensate for the time delays of the inputs and slow response devices, it can shorten the starting process, and provides a unified control and monitoring system. The major disadvantage of this approach is that it takes several training test runs to optimize the performance. In 2008, design and application of simple Gain scheduled PID controller using a Neural Network model of Variable throat, Blowdown Supersonic wind tunnel was described by Nott *et al.* (2008). Thereafter with minimal assumptions, it was optimised on a Neural Network model of the tunnel

54

using Genetic algorithm to reduce the run time. Thus, the plenum pressure and test section control was done using Genetic algorithms, Neural Networks and gain scheduled PID algorithms. The above said PID control is implemented with the time variant properties of control problem by determining a functional form of integral term of the controller. The controller is optimised using Genetic algorithm on a Neural Network model of the tunnel and compared with conventional PID controller using the same Neural Network model. The process was repeated for different throat settings to find control gains for each settings. Here two Neural Networks were created to model the system to accommodate parallel training on two PCs. The results show that the Neural Network effectively modelled wind tunnel characteristics, uncertainties, sensor dynamics, and time delays. The proposed optimised controller designed is proven to work well at every throat settings for time dependent and nonlinear systems. In 2008, S R Bhoi et al. made characteristic study to predict the time histories of settling chamber pressure and storage tank pressure for a given trajectory of opening of pressure regulating valve. Minimum valve opening is predicted to maintain settling chamber pressure higher than estimated minimum at high Mach numbers (Bhoi and Suryanarayana, 2008). It is also proposed to add a Variable Mach number Flexible Nozzle (VMFN), by which it is started at low Mach numbers and required one is reached by changing the Nozzle contour.

M G Silva, in 2009, proposed two controllers, one to control stagnation pressure in the settling chamber and second based on the relation between stagnation pressure and temperature at the settling chamber which represents the Reynolds number specified for test (Silva, 2009). For a given Mach number, it is important to maximize test duration while running the tunnel at lowest stagnation pressures, considering undesirable variations of Reynolds number in the test section. Performance of the

tunnel system for different Mach numbers and Stagnation pressures were tested. Supersonic retro propulsion (SRP) has been proposed by N M Bakhtian, as a candidate enabling technology for future high-mass Mars missions (Bakhtian and Aftosmis). In AIAA meeting held on 2010, the application of Proportional-Integral-Derivative control to Supersonic wind tunnel was proposed (Busa, 2010). The existing pressure control system of wind tunnel was investigated and found to be inefficient and unreliable. However, a Programmable logic controller was used to replace the original control system and utilize EZ automation software to implement P-I-D control. The control mainly relies on the ability to maintain a constant stagnation pressure in the chamber forward of the throat. Here the PID program is controlled by EZP- Touch PLC – EDIT software, which includes common terminologies, input register, output register, discrete values, register values, tag names, and address strings. INCAS Bulletin released an Adaptive Fuzzy PI control for Blowdown wind tunnel in 2013. The main aim was to maintain the imposed experimental conditions to control the air flow using a control valve in the plant. The control scheme is validated using experimental data collected from real test cases and as part of improving the control performances, an Adaptive Fuzzy PI controller was implemented, where the entire process of INCAS Supersonic wind tunnel is completed within 15-100 seconds (Bhoi and Suryanarayana, 2008; Andrei, 2013; Butler *et al.*, 2010). The main aim in designing the proposed controller is that it should operate at different stagnation pressures and Mach numbers and has to be robust to accommodate the varying pressure and mass flow requirements safely. INCAS Supersonic Blowdown wind tunnel is pressurized aerodynamic tunnel capable of operating both at Subsonic and Supersonic speeds ensuring a high Reynolds number. The opening of the valve is made use in test run to ensure proper

parameters in the plenum chamber depending on the airflow in the tank. Validation with the PI control in LabVIEW is realized and compared with data from the real tests No. 6413 and 6414. The LabVIEW application can be used in two modes, viz: one to fine tune PI parameters, secondly to control the system using Data acquisition system in place at INCAS. After implementing with Adaptive Fuzzy PI control, there is considerable increase in performance, with less overshoot and tolerable rise time. In 2014, a mathematical model for special Blowdown Supersonic wind tunnel was developed with a set of ordinary differential and algebraic equations in software environment (Shahrbabaki *et al.*, 2014a). Later, an Intelligent Artificial Neural Network was designed to optimise the membership function of Fuzzy logic controller for aerodynamic analysis and testing on scaled models under well controlled test conditions. The main aim was to provide the test section conditions of constant Mach number, total pressure and Reynolds number for a wind tunnel run of 5 to 80 seconds duration which is achieved by controlling the valve opening progressively. The above said control algorithm helps in minimizing the error in the test section, Reynolds number during blowdown run, considering the process variables and performance of pneumatic control valve. The proposed model in the paper is helpful in process of valve sizing and choosing actuator in lowest time. The Supersonic wind tunnel performance based on plenum temperature control was enhanced by the application of Fuzzy logic controller in 2014 by A N Shahrbabaki et al. In this paper, a Proportional Derivative Fuzzy logic control was developed to control plenum stagnation temperature using a heater upstream of the plenum chamber for a Mach number 2.5 blowdown run (Shahrbabaki *et al.*, 2014b). The controller is robust to accommodate the varying pressure and mass flow requirements safely. With the simulation studies, it is noted that the reference temperature for heater controller is

57

considered to be 300 K. Experimental verification for a Mach number 25 is done to prove the accuracy of Fuzzy logic applied to Blowdown Supersonic wind tunnel and was found that for the proposed wind tunnel, the Reynolds number increases when the stagnation temperature drops. In this paper, the temperature drop is suppressed by installing heater and temperature controller. The Error in the heater performance during the run is minimized with the control program for the wind tunnel facility characteristics. The designed Intelligent control system leads to a control response with the lowest overshoot, settling time and steady state error. In 2016, Model-Based Stagnation Pressure Control is discussed in Supersonic wind tunnel and an improved mathematical model for the same is suggested (Ilić *et al.*, 2016). Hybrid Fuzzy – PID Controller for pressure regulation in Supersonic wind tunnel for Mach numbers 1.5 and 2 at 20 bar Pressure was proposed by Sunny *et al.* (2017). The controller was implemented in LabVIEW and found that it is capable of handling uncertainties and nonlinearities in the process and is superior to PID controller.

2.4.3 Hypersonic wind tunnels

Maintaining constant pressure in the settling chamber of the Hypersonic intermittent blow down type wind tunnel is an important task for its effective performance (Jones *et al.*, 2014; Jones *et al.*, 2011a; Jones *et al.*, 2011b). As the Mach number increases to hypersonic regime, more and more accurate controllers are required for the precise control of air pressure regulation in settling chamber of the Hypersonic wind tunnel system. It is clear from the available literature that only few controllers have been designed and developed for this purpose (Owen and Owen, 2002; Popov *et al.*, 2010; Kabin *et al.*, 1995; Sorensen *et al.*, 2006).

PI controllers are significantly less complex to operate than other controllers, but they are susceptible to organ piping unless correct control constants are predicted. In the thesis report by Varghese Jacob et al. in 2009 (Jacob and Binu, 2009; Jacob and Binu, 2009), the pressure in the settling chamber of wind tunnel is controlled by PI and Adaptive Fuzzy controller and a comparison was presented. The process is modelled by considering the whole system components as three pressure vessels. The continuity relation for the pressure vessel and equation for the flow through the throttling valve and nozzle is used to develop the process model in state space as well as transfer function form. A classical PI controller was designed for the linearized model of the system. The performance in terms of settling time and percentage overshoot were further improved by designing an Adaptive Fuzzy controller incorporating the varying process parameters. The design and analysis were carried out for three different setpoints and the results were verified. A Fuzzy assisted PI controller with reset wind up for the Hypersonic intermittent blow down type wind tunnel was developed by R Jones et al. in 2011 and analyzed in order to get desired Mach number and mass flow rate through the nozzle (Jones *et al.*, 2011a; Jones *et al.*, 2011b). In this paper, a controller that could adapt for different sets of pressure values, inlet pressure values, mass flow rate and temperatures was developed.

The basics of various wind tunnel systems and different control schemes used to achieve the desired characteristics for particular applications are discussed and reviewed in this chapter.

Chapter 3 details with the Hypersonic wind tunnel system model and its fundamental characteristics. Modelling and simulation play a vital role in gaining necessary and important information about the characteristics of a particular system. In general, modelling focuses on representation of interaction between the different parts or subsystem of the main system which will help in designing an appropriate control scheme for the desired performance. The purpose, block diagram description and major elements of Hypersonic wind tunnel are presented with technical details, constraints and its relevance. Thus, it provides an overall technical know - how of the system as such and suggest a good platform for design of various controllers for pressure regulation inside the settling chamber of the tunnel system.

CHAPTER 3

MODELLING AND ANALYSIS OF HYPERSONIC WIND TUNNEL SYSTEM

3.1 INTRODUCTION

The purpose of designing a control scheme for any system is to appropriately tune its dynamics so as to achieve the desired system characteristics for a particular application. In order to design a proper controller for any system, the characteristic features in open loop condition ie, without any influential feedback have to be thoroughly studied (Furian *et al.*, 2015; Murray-Smith, 2015). A model is a mathematical representation of any given system, which provides the general characteristics of the individual components of a system. The control scheme has to be designed based on these informations obtained from this open loop study considering all the performance parameters. Numerical simulations are highly important for studying the performance of a particular control design in situations where real time experiments are expensive or dangerous considering all the input and output variables as well as possible disturbances to the system. This will help in improving the control design by testing the various possible modifications with respect to performance parameters without the burden of real world or laboratory testing. Thus, in general, process modelling is performed to collect and evaluate the knowledge on a certain process as completely as possible. In the reduced process model, the boundaries of the process parameters are important whereas, simulation is a strategic tool in the field of process development and process control, which is used to present certain aspects of an existing system, or a system to be developed, as models, or to reproduce them. Physically modelling a system helps to investigate

situations that would be dangerous in real life, used in engineering and product design to investigate the effect of changes without producing a physical prototype (Jacob and Binu, 2009; Jones *et al.*, 2011b; Nott *et al.*, 2008; Braun *et al.*, 2008; Furian *et al.*, 2015; Murray-Smith, 2015). General process modelling is shown in Fig. 3.1. To model a process, initially the mathematical model of the system is obtained and suitable control technique is applied based on application. Then we validate the proposed control technique for the system under consideration. If the results of validation are unsatisfactory, then we remodel the system and if found satisfactory the control scheme can be implemented.
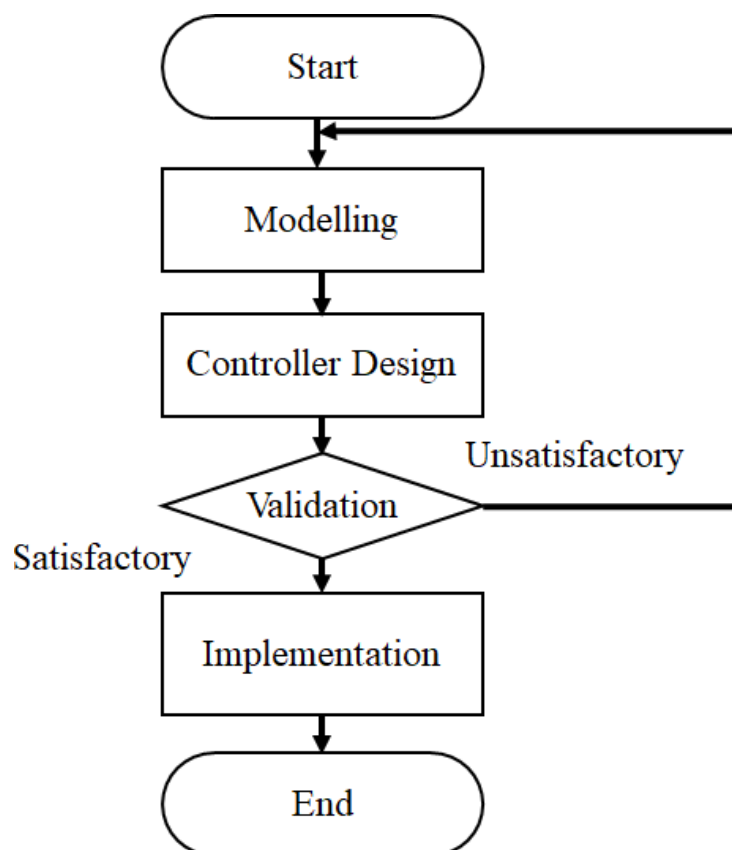
Fig. 3.1 Process Modelling

Dynamic models are sets of equations that describe the dynamic behaviour of the system in control engineering. Generally, there are 2 types of modelling techniques viz:

Physical/mathematical modelling and system identification (Furian *et al.*, 2015; Murray-Smith, 2015). Normally, the models for a dynamical system is represented using mass, energy and momentum balances. Traditionally, first principle assumptions and measurements of system parameters are used to derive nonlinear models, from which linear models are obtained. The general steps involved in modelling is represented in Fig. 3.2.
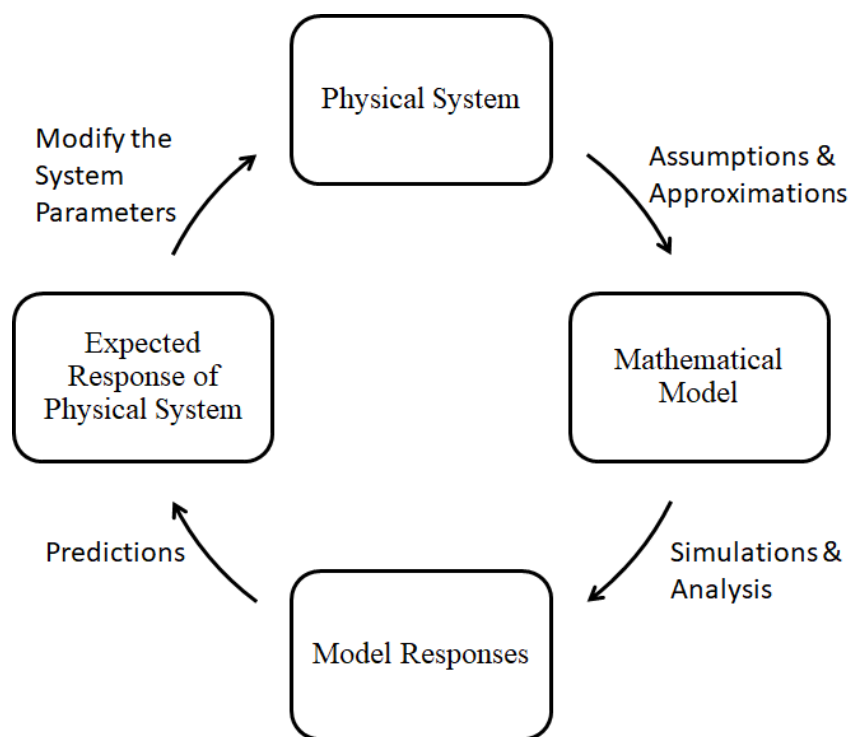
Fig. 3.2 Modelling Technique

In order to model a system, the dynamics of the physical system are analyzed, based on which assumptions and approximations are taken to represent the mathematical model. However, the system is analyzed by simulations and the response of the model is obtained from which we predict the response of the physical system. Based on the response, we modify the system parameters to physically model the system.

Physical or mathematical models, are developed based on the mathematical equations which describes the physical behaviour of the system. The relation between the system parameters, input variables and corresponding output signals are represented as mathematical expressions in the form of differential equations. The various types of mathematical models includes differential equation model, state space model and transfer function model. System identification is considered an equally important and efficient approach to derive dynamic models directly from the test data, to overcome challenges such as hardly obtained parameters of the underlying physics.

3.2 MODELLING OF HYPERSONIC WIND TUNNEL

Wind tunnels are specific research facilities developed for the study of airflow characteristics around solid objects. Wind tunnel testing finds applications in the investigation of aerodynamic properties of aero vehicles, land carriers and sports vehicles (Savino *et al.*, 2009; Pope and Goin, 1965). Wind tunnel studies are conducted for acquiring characteristic properties of specific objects by subjecting their full or scaled models to desired conditions of air velocity, pressure and temperature. Hypersonic wind tunnels are such facilities, which provide hypersonic flow regime, at Mach numbers greater than 5 for aerospace applications (Lee *et al.*, 2014; Pope and Goin, 1965). Intermittent blow-down Hypersonic wind tunnels are more cost effective than the continuous type systems and are hence carefully calibrated for effective utilization of the limited testing time (Jacob and Binu, 2009; Jones *et al.*, 2011b; Braun *et al.*, 2008; Pope and Goin, 1965).

Hypersonic wind tunnel is a self-contained facility that is used to study aerodynamic performance of space vehicles. It comprises of HP, PRV, H1, SC, NOZ and TS as

detailed in section 1.2 of Chapter 1. Air is used as working fluid in the test section. Block schematic of the Hypersonic wind tunnel systems is shown in Fig. 3.3.
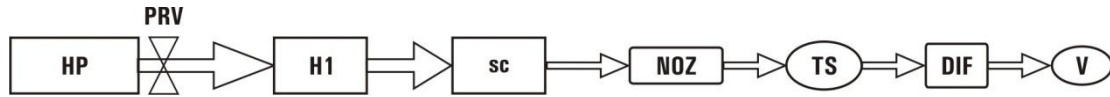
Fig.3.3 Block Diagram of Hypersonic Wind Tunnel

The object or its model is fastened in the test section and testing is carried out by passing air at high speeds over it thus mimicking real world situations, wherein the object moves with the same speed in air. For this purpose, atmospheric air is first compressed and stored in the high pressure storage tank from where it is released to TS through a pressure regulating valve, heater, settling chamber and the nozzle. PRV regulates the pressure of the air released from HP and the H1 heats up this air so as to achieve the desired operating pressure and temperature in the settling chamber. The SC and NOZ serves the purpose of smoothening the air stream so as to achieve uniform, high quality flow in the test section. While passing through the NOZ, the air gets expanded and achieves the desired Mach number for the specific hypersonic flow required in the TS. From the test section, air is released to a vacuum chamber through a diffuser, which helps in reducing the flow velocity (Jacob and Binu, 2009; Jones *et al.*, 2011b; Pope and Goin, 1965). The need for maintaining a constant hypersonic flow in the TS throughout the test run is very crucial. However, during the acceleration of air through the tunnel, the mass reduces continuously, which leads to an unsteady pressure in the settling chamber that will indirectly affect the pressure in the TS. During the test run, the pressure in the storage tank decreases gradually, which subsequently results in variation of pressure in the SC. However, a steady hypersonic flow is required to be maintained in the SC and thereafter in the TS throughout the test run which lasts for a

duration of 40 s (Jacob and Binu, 2009; Jones *et al.*, 2011b; Braun *et al.*, 2008; Pope and Goin, 1965). Therefore, the pressure in the settling chamber has to be maintained constant using PRV by adjusting the variable stem movement facility (Lee *et al.*, 2014; Savino *et al.*, 2009; Jacob and Binu, 2009; Jones *et al.*, 2011b; Pope and Goin, 1965). Thus, the control of valve opening is very crucial for maintaining the settling chamber pressure in the hypersonic flow regime, which can only be achieved by properly designing a suitable controller.

3.2.1. Assumptions and Approximations for Modelling

For mathematical modelling of Hypersonic wind tunnel system, the whole system components are considered as three pressure vessels, viz, high pressure storage tank, heater and settling chamber (Jacob and Binu, 2009; Jones *et al.*, 2011b; Pope and Goin, 1965; Furian *et al.*, 2015; Murray-Smith, 2015). We, assume the temperature variations during operations to be negligible, which makes the modelling simpler. Thus, the second pressure vessel, heater which is made of core bricks is assumed to have 100 percentage heat transfer from core brick to air so that temperature variations are negligible. Moreover, pipeline volume is accounted in the heater and the settling chamber. To model the heater, we consider the pressure drop of air and variations in Reynolds number to be negligible (Savino *et al.*, 2009; Jacob and Binu, 2009; Jones *et al.*, 2011b; Pope and Goin, 1965).

Block schematic of the Hypersonic wind tunnel systems (Jacob and Binu, 2009; Jones *et al.*, 2011b) is shown in Fig. 3.4. In order to model the system, here we consider the equations of flow rate of compressible fluid through control valve, flow rate equation

66

from empirical analysis, mass flow rate through nozzle and continuity equations (Jacob and Binu, 2009; Jones *et al.*, 2011b; Pope and Goin, 1965; Hwang and Hsu, 1998; Corneliu, 2013; Echman, D. P., 1958; Liptak, 1995).
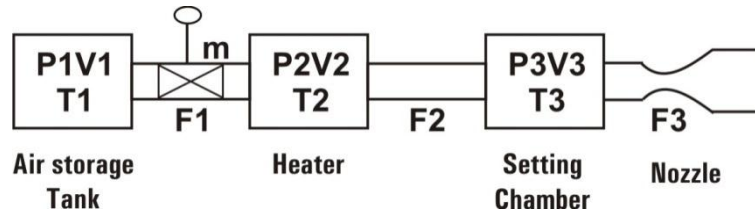
Fig. 3.4 Block diagram of the system for Modelling

The general specifications of the Hypersonic wind tunnel system includes (Jones *et al.*, 2011a, Jacob and Binu, 2009; Jones *et al.*, 2011b; Pope and Goin, 1965; Echman, D. P., 1958; Liptak, 1995):

1. Hypersonic flow	:	232Kg/sec
2. Total length of HWT	:	300m
3. Length of Settling chamber	:	65m
4. Mach Number	:	6-12
5. Operating Pressure	:	100Bar
6. Max. Operating Temperature	:	1750 K
7. Reynolds number	:	10-30
8. Run time	:	20-40sec
9. Max. Settling pressure	:	300Bar
10. Vacuum	:	10^{-2}mbar

Control valve

In general, Flow rate, F_1 of compressible fluid through control valve (Liptak, 1995) is given by

$$F_1 = mC_vN_8F_pP_1Y\sqrt{\frac{XM}{T_1Z}}$$
(3.1)

Where m is the stem movement of pressure valve, P_1 is the storage tank pressure (upstream pressure of pressure regulating valve (PRV)), C_v is the valve coefficient, N8 is the constant for engineering units, F_p is the constant for pipeline geometry, M is molecular weight of air, Z the compressibility factor (Jones *et al.*, 2011b; Liptak, 1995). X represents the ratio of difference in upstream pressure and downstream pressure to the upstream pressure of the pressure regulating valve and is given by,

$$X = \frac{P_1 - P_2}{P_1}$$
(3.2)

Where P_1 and P_2 are the upstream and downstream pressures of pressure regulating valve respectively.

Y is the expansion factor and is expressed as,

$$Y = 1 - \frac{X}{3F_KX_T}$$
(3.3)

Where, X_T is the critical pressure drop ratio factor and F_K is ratio of specific heat factor.

In short, the Flow rate is given by,

$$F_1 = f(P_1, P_2, m)$$
(3.4)

Heater

Heater is considered as the second pressure vessel. From the empirical analysis (Jones *et al.*, 2011a, Jacob and Binu, 2009; Jones *et al.*, 2011b), outflow from heater is given by,

$$F_2 = K_1 P_2 + K_2 P_3 \tag{3.5}$$

Where K_1 and K_2 are constants and P_3 is the settling chamber pressure.

Nozzle

Fixed nozzles with various cross sectional area are used for different Mach number Hypersonic wind tunnels. The speed of wind tunnel is indicated by Mach number which is defined as the ratio of speed of aircraft to speed of sound in gas. Hypersonic wind tunnel has a Mach number greater than 5. The mass flow through nozzle (Lee *et al.*, 2014; Savino *et al.*, 2009; Jones *et al.*, 2011a, Jacob and Binu, 2009; Jones *et al.*, 2011b; Pope and Goin, 1965; Liptak, 1995), F_3 is given by,

$$F_3 = \frac{K_n P_3}{\sqrt{T_3}} \tag{3.6}$$

Where K_n is the nozzle flow constant and T_3 is the settling chamber temperature. The continuity equations for the three pressure vessels (Jones *et al.*, 2011a, Jacob and Binu, 2009; Jones *et al.*, 2011b; Echman, 1958; Liptak, 1995) are,

$$C_1 \frac{dP_1}{dt} = -F_1 \tag{3.7}$$

$$C_2 \frac{dP_2}{dt} = F_1 - F_2 \tag{3.8}$$

$$C_3 \frac{dP_3}{dt} = F_2 - F_3 \tag{3.9}$$

Where

$$C_1 = \frac{V_1}{nRT_1}, \quad C_2 = \frac{V_2}{nRT_2}, \quad C_3 = \frac{V_3}{nRT_3} \tag{3.10}$$

V_1, V_2 and V_3 are volume of pressure vessel 1, 2 and 3 respectively. The model and physical parameters of the actual large scale wind tunnel obtained from (Jacob and Binu, 2009; Jones *et al.*, 2011b) is given in Table 3.1.

Table 3.1 The Physical Parameters of the system

Constants	Parameter	Values
C_V	valve coefficient	0.1305
N_8	constant for engineering units	0.000948
F_P	pipe geometry constant	1
M	molecular weight	29
Z	compressibility factor	1.077
X_T	critical pressure drop ratio factor	0.562
A	area of the pipe	$0.0130394 m^2$
$V_{1,}$	volume of the compressed air storage tank	$132\ m^3$
V_2	volume of Heater for Mach 6 operation	$18.24\ m^3$
V_3	volume of settling chamber and associated pipelines	$2.7\ m^3$

The nominal plant transfer function and state space model are derived as detailed in Appendix 1 and is given by,

$$\frac{P_3(s)}{m(s)} = \frac{7.898e007s + 4.21e005}{S^3 + 16.68S^2 + 3.367S + 0.01937} \tag{3.11}$$

For the Hypersonic wind tunnel system, there is a time delay in the response due to the presence of vessel 2 (H1) in between the PRV and the SC. Hence to account this, we incorporate transport delay to the system. The effect of delay is estimated by

70

measuring the time to respond for a particular input in closed loop condition as this delay may not necessarily be evident in the response of the system. Pade's approximation is widely used to approximate delays in continuous control systems when functions contain poles, as the use of rational functions allows them to be well-represented and its properties are good in frequency domain. This usually incorporates equal numerator and denominator degree exhibiting a jump at time, t=0. As it is difficult to determine all system poles, control systems with delays are difficult to analyze and simulate. Hence, we use Pade's approximation for the delay based on empirical analysis and analyzed the resulting system. Considering the transport delay in eq. (3.12) and valve transfer function (Lee *et al.*, 2014; Savino *et al.*, 2009; Jacob and Binu, 2009; Jones *et al.*, 2011b; Pope and Goin, 1965) in eq. (3.13), the system transfer function is given in eq. (3.14).

$$Transport\ delay\ transfer\ function = \frac{-0.03S+1}{0.03S+1} \qquad (3.12)$$

$$Valve\ transfer\ function = \frac{1}{0.5S+1} \qquad (3.13)$$

A transport delay of about 30 milliseconds is added and time constant for PRV is taken as 0.5 seconds. First order valve transfer function is also incorporated into the process and the final plant transfer function from $G_p(s)$ (Jacob and Binu, 2009; Jones *et al.*, 2011b; Pope and Goin, 1965) is given by,

$$G_p(s) = \frac{-2.369e006s^2 + 7.897e007s + 4.21e005}{0.015s^5 + 0.7802s^4 + 9.89s^3 + 18.46s^2 + 3.377s + 0.01937} \qquad (3.14)$$

3.3 SENSITIVITY ANALYSIS

Linearity and robustness are two important features of physical modelling. A robust system is one whose properties do not change explicitly if applied to a slightly different system (Jacob and Binu, 2009; Jones *et al.*, 2011b; Pope and Goin, 1965; Swain *et al.*, 2014). Sensitivity analysis is a characteristic tool to study the degree of robustness and the nonlinearities in a given system. This analysis is the study of how the variation in the output of a model can be distributed, qualitatively or quantitatively, to different sources of variation. As models are approximations of real systems, sensitivity analysis helps to ensure nonlinearity and reliability of the modelled system and determines how the input influences the output. As the valve response and characteristics are nonlinear which is accounted to the stem position or percentage of valve opening, we consider the tunnel system as nonlinear even though for the purpose of modelling, we made linearized approximations for the system as given in eq. (3.14). The real process is influenced by the significance of the transport delay and valve transfer functions and hence they are incorporated in the form of their linearized approximations. To analyze the sensitivity, the variation in heater pressure and settling chamber pressure for each 10% incremental change in stem movement is analyzed maintaining air storage pressure, P_1 constant.

With the storage tank pressure, $P_1 = 30 \times 10^6$ Pa, for each 10% increase in stem movement, the response of heater pressure and settling chamber pressure are noted and is shown in Table 3.2.

Table 3.2 Percentage of Stem movement versus Pressures, P_2 and P_3

% of stem movement	P_2(Pa)	P_3(Pa)
0%	7.7×10^6	7×10^6
10%	7.7×10^6	7×10^6
20%	7.7×10^6	7×10^6
30%	9.032×10^6	8.2242×10^6
40%	11.082×10^6	10.0915×10^6
50%	12.8158×10^6	11.67×10^6
60%	14.2355×10^6	12.964×10^6
70%	15.383×10^6	14×10^6
80%	16.3×10^6	14.845×10^6
90%	17.044×10^6	15.5165×10^6
100%	17.6455×10^6	16.05×10^6

Fig. 3. 5 shows variation in heater pressure for different valve opening ranging from 0 to 100% based on the data from Table 3.2 where heater pressure variation in accordance with the percentage of stem movement is depicted.
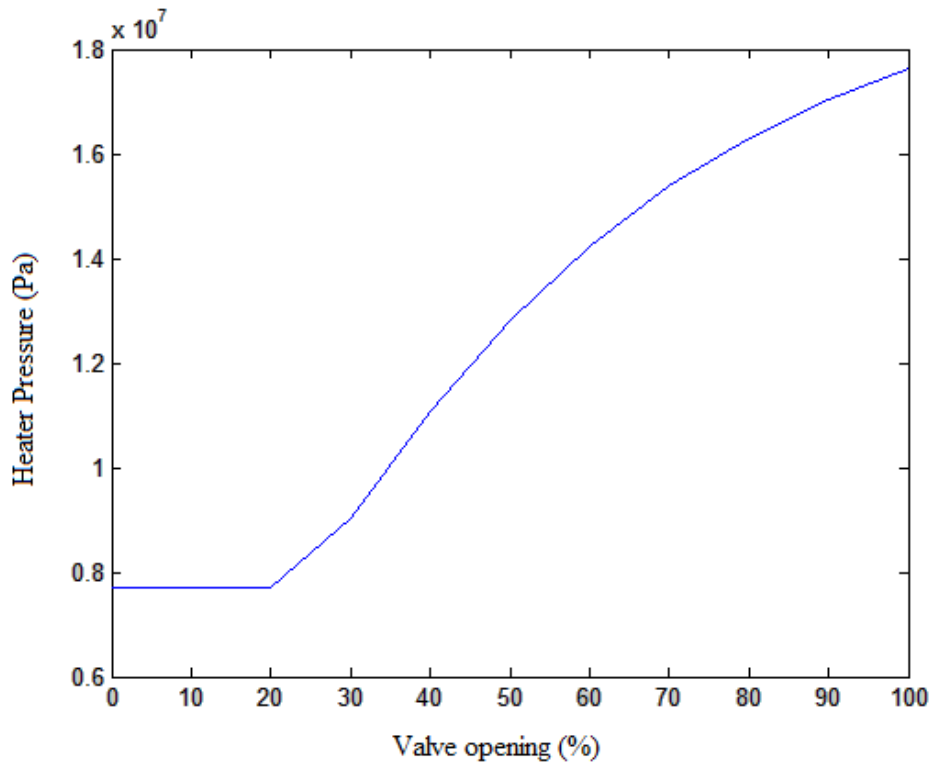
Fig. 3.5 Variation in Heater pressure for different levels of valve opening

From the figure, it is clear that for a constant initial pressure, P_1, the flow from the heater is constant for the first 20% of the valve opening and then increases at a constant rate for every 10% rise in PRV. The sensitivity for every 20% increase in stem movement is tabulated in Table 3.3.

Table 3.3 Sensitivity versus Stem movement for Heater Pressure

% of stem movement	P_2(Pa)	Sensitivity of region 1(Pa /%change in stem movement)
20%	7.7×10^6	0.1691×10^6
40%	11.082×10^6	

% of stem movement	P_2(Pa)	Sensitivity of region 2(Pa /%change in stem movement)
40%	11.082×10^6	0.1576×10^6
60%	14.2355×10^6	

% of stem movement	P_2(Pa)	Sensitivity of region 3(Pa /%change in stem movement)
60%	14.2355×10^6	0.103225×10^6
80%	16.3×10^6	

% of stem movement	P_2(Pa)	Sensitivity of region 4(Pa /%change in stem movement)
80%	16.3×10^6	0.067275×10^6
100%	17.6455×10^6	

From the above table, it is clear that the sensitivity is varying for different values of stem movement with respect to heater pressure. It is also observed that the sensitivity is varying continuously and has infinite values at infinite regions which shows the nonlinear behaviour of the system. Fig. 3.6 shows the sensitivity of heater pressure with variation in stem movement. From this figure, it is clear that the sensitivity is varying with respect to time and is a clear indication of the nonlinearity in the system.
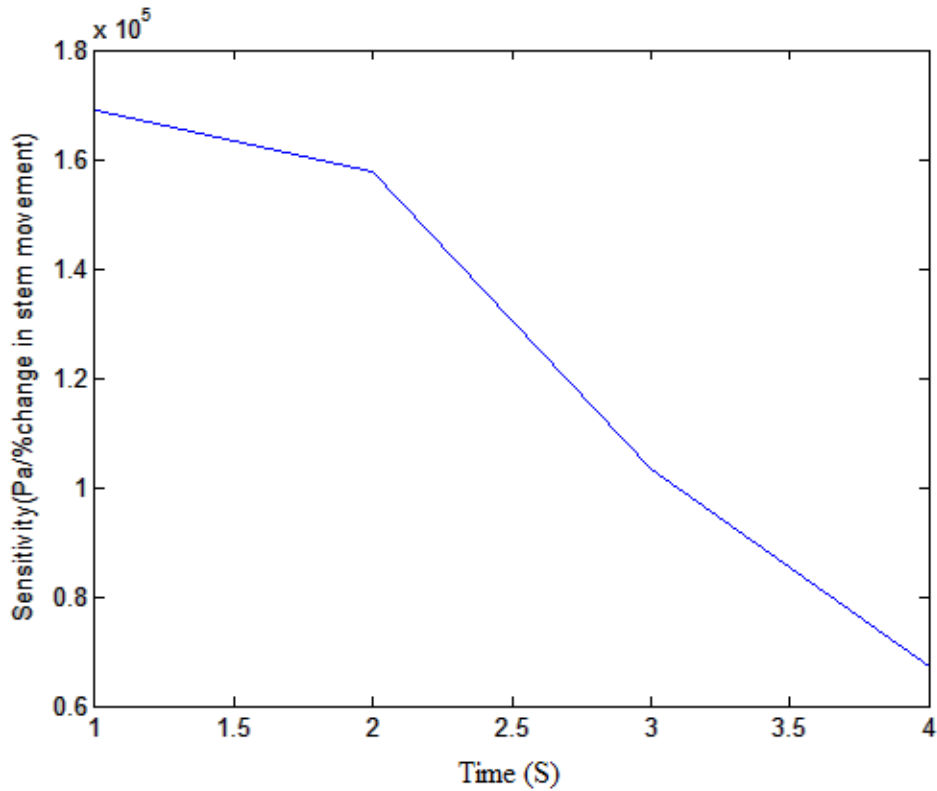
Fig. 3.6   Sensitivity of heater pressure

Similarly, the sensitivity of settling chamber pressure is analyzed maintaining the air storage tank pressure constant at 30×10^6 Pa. Fig. 3.7 shows the variation of settling chamber pressure for different values of valve opening obtained from Table. 3.4. From the figure, it is observed that the settling chamber pressure is constant for the first 20% of the valve opening and then increases at a constant rate for every 10% increase in stem movement. Table 3. 4 gives the sensitivity for each 20% increase in stem movement for settling chamber pressure. The valve response and characteristics of the tunnel system is nonlinear. In order to maintain constant settling chamber pressure in accordance with the input to the valve, practically, the system is operated first in open loop wherein we obtain the rate of valve opening for a particular pressure. This value is feed as the input during closed loop condition thereby reducing the error and hence the nonlinearity can be considered to be nominal.

75
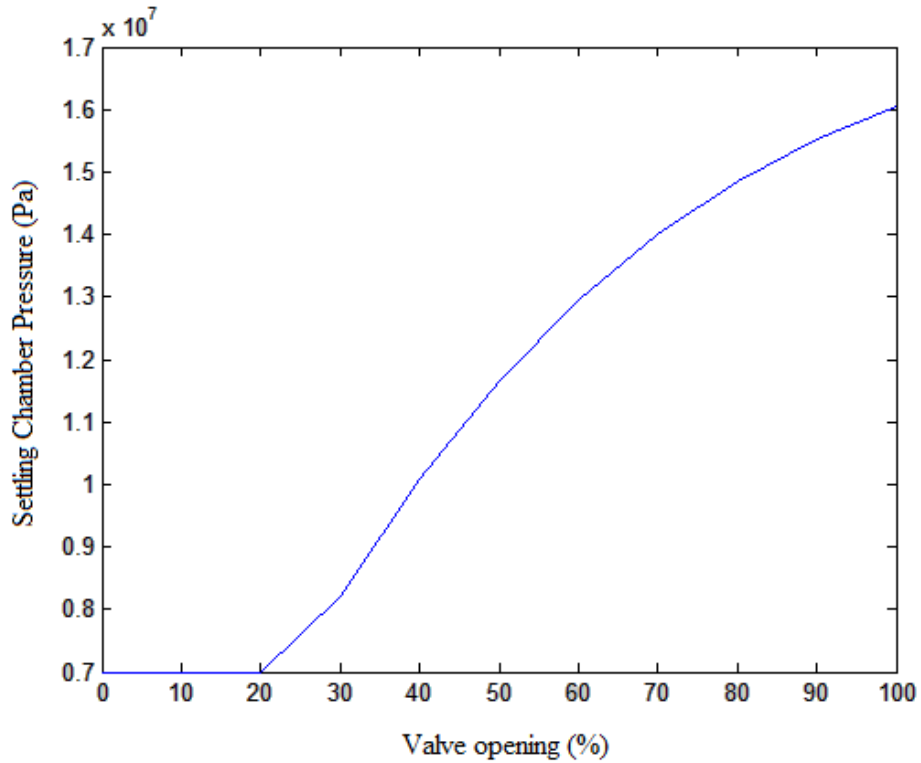
Fig. 3.7 Variation of Settling chamber pressure for different levels of valve opening.

Table 3.4 Sensitivity versus Stem movement for Settling chamber pressure

% of stem movement	$P_3(Pa)$	Sensitivity of region 1(Pa /%change in stem movement)
20%	7×10^6	0.154575×10^6
40%	10.0915×10^6	

% of stem movement	$P_3(Pa)$	Sensitivity of region 2(Pa /%change in stem movement)
40%	10.0915×10^6	0.143625×10^6
60%	12.964×10^6	

% of stem movement	$P_3(Pa)$	Sensitivity of region 3 (Pa /%change in stem movement)
60%	12.964×10^6	0.09405×10^6
80%	14.845×10^6	

% of stem movement	$P_3(Pa)$	Sensitivity of region 4(Pa /%change in stem movement)
80%	14.845×10^6	0.06025×10^6
100%	16.05×10^6	

Fig. 3.8 shows the sensitivity of settling chamber pressure with variation in stem movement and is clear that as time varies the sensitivity changes infinitely which indicates the system is nonlinear.
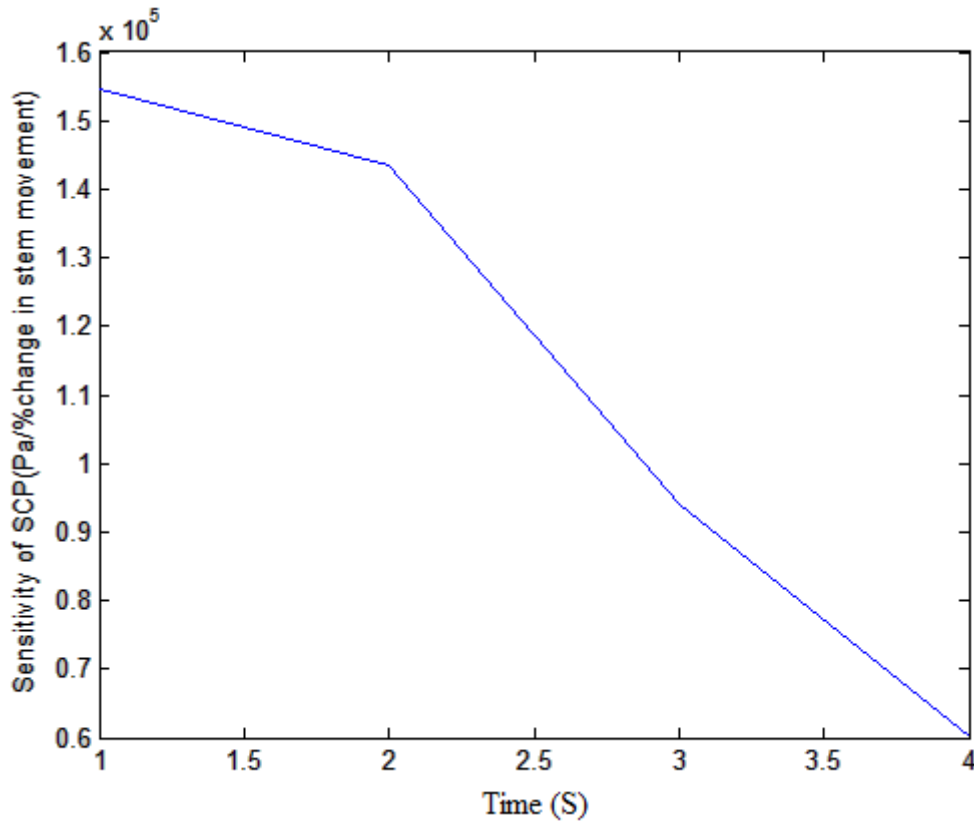
Fig. 3.8 Sensitivity of Settling chamber pressure.

From the figure, it is observed that the sensitivity of settling chamber pressure with respect to stem movement is decreasing continuously with respect to time. Therefore, it is evident that the settling chamber pressure shows nonlinear behavior. These observations obtained from Fig. 3.6 and 3.8, shows that the system is nonlinear.

3.4. PERTURBATION ANALYSIS

Perturbation studies represents the dynamic behavior and effects of the process variables which are realizations of the scaled physical models. Several perturbation

theorems are proved for nonlinear ordinary differential equations for which all subsystems of the linearized equation are integrable (Jones *et al.*, 2014). This gives a practical type of stability, expressing the property that the systems or subsystems tend to zero, and measures the effect of various types of perturbations in the systems. In studying this effect in the tunnel stem, we assume the unperturbed system to be stable. For the Hypersonic wind tunnel system, the temperature in the pressure vessel 1, T_1, Heater temperature, T_2 and temperature in vessel 3, T_3 are varying according to the operating conditions obtained from empirical analysis (Savino *et al.*, 2009; Jones *et al.*, 2011a; Jacob and Binu, 2009; Jones *et al.*, 2011b; Pope and Goin, 1965). As the specifications of Hypersonic wind tunnel is included in Section 3.2.1, it is evident that the maximum operating range for temperature is 1750 K, from which the various operating conditions based on the empirical analysis for the tunnel system within this range are selected as follows (Jones *et al.*, 2014).

Case1: $P_1 = 300 \times 10^5$ Pa, $T_1 = 300\ K$, $P_2 = 77 \times 10^5$ Pa, $T_2 = 300\ K$, $P_3 = 70 \times 10^5$ Pa, $T_3 = 539\ K$

Case2: $P_1 = 235 \times 10^5$ Pa, $T_1 = 271\ K$ $P_2 = 77 \times 10^5$ Pa, $T_2 = 650\ K$, $P_3 = 70 \times 10^5$ Pa, $T_3 = 529\ K$

Case3: $P_1 = 300 \times 10^5$ Pa, $T_1 = 300\ K$, $P_2 = 44 \times 10^5$ Pa, $T_2 = 700\ K$, $P_3 = 40 \times 10^5$ Pa, $T_3 = 518\ K$

Case4: $P_1 = 250 \times 10^5$ Pa, $T_1 = 278\ K$, $P_2 = 44 \times 10^5$ Pa, $T_2 = 650\ K$, $P_3 = 40 \times 10^5$ Pa, $T_3 = 508\ K$

Case5: $P_1 = 300 \times 10^5$ Pa, $T_1 = 300\ K$, $P_2 = 100 \times 10^5$ Pa, $T_2 = 700\ K$, $P_3 = 100 \times 10^5$ Pa, $T_3 = 554\ K$

Case6: $P_1 = 252 \times 10^5 \text{ Pa}, T_1 = 278\,K, P_2 = 100 \times 10^5 \text{ Pa}, T_2 = 650\,K, P_3 = 100 \times 10^5 \text{ Pa}, T_3 = 544\,K$

The transfer function corresponding to the above six operating conditions (Savino *et al.*, 2009; Jones *et al.*, 2011a; Jacob and Binu, 2009; Jones *et al.*, 2011b; Pope and Goin, 1965) are,

Case 1:

$$\frac{P_3(s)}{m(s)} = \frac{8.036e007s + 3.316e005}{S^3 + 16.68S^2 + 3.353S + 0.01506} \tag{3.15}$$

The generalised transfer function considering transport delay is

$$G_p(s) = \frac{-2.411e006s^2 + 8.026e007s + 3.316e005}{0.15s^5 + 3.339s^4 + 15.04s^3 + 19.61s^2 + 3.365s + 0.01506} \tag{3.16}$$

Case 2:

$$\frac{P_3(s)}{m(s)} = \frac{6.032e007s + 3.1e005}{S^3 + 16.6849S^2 + 3.105S + 0.01719} \tag{3.17}$$

The generalized transfer function considering transport delay is

$$G_p(s) = \frac{-1.81e006s^2 + 6.023e007s + 3.1e005}{0.15s^5 + 3.273s^4 + 14.66s^3 + 18.98s^2 + 3.119s + 0.01719} \tag{3.18}$$

Case 3:

$$\frac{P_3(s)}{m(s)} = \frac{7.708e007s + 1.912e005}{S^3 + 16.38S^2 + 3.255S + 0.00887} \tag{3.19}$$

The generalized transfer function considering transport delay is

$$G_p(s) = \frac{-2.312e007s^2 + 7.702e007s + 1.912e005}{0.15s^5 + 3.258s^4 + 14.6s^3 + 18.99s^2 + 3.262s + 0.00887} \tag{3.20}$$

Case 4:

$$\frac{P_3(s)}{m(s)} = \frac{6.091e007s + 1.627e005}{S^3 + 15.96S^2 + 3.001S + 0.008789} \tag{3.21}$$

The generalized transfer function considering transport delay is

$$G_p(s) = \frac{-1.827e007s^2 + 6.086e007s + 1.627e005}{0.15s^5 + 3.194s^4 + 14.22s^3 + 18.36s^2 + 3.008s + 0.008789} \tag{3.22}$$

Case 5:

$$\frac{P_3(s)}{m(s)} = \frac{8.076e007s + 4.907e005}{S^3 + 17.31S^2 + 3.436S + 0.02247} \tag{3.23}$$

The generalized transfer function considering transport delay is

$$G_p(s) = \frac{-2.423e007s^2 + 8.061e007s + 4.907e005}{0.15s^5 + 3.396s^4 + 15.36s^3 + 20.06s^2 + 3.454s + 0.02247} \tag{3.24}$$

Case 6:

$$\frac{P_3(s)}{m(s)} = \frac{6.538e007s + 4.319e005}{S^3 + 16.87S^2 + 3.179S + 0.02248} \tag{3.25}$$

The generalized transfer function considering transport delay as well as valve transfer function from eqs. (3.13) and (3.14) is

$$G_p(s) = \frac{-1.961e007s^2 + 6.525e007s + 4.319e005}{0.15s^5 + 3.331s^4 + 14.98s^3 + 19.42s^2 + 3.197s + 0.02248} \tag{3.26}$$

Sensitivity analysis is used to check the nonlinear behavior of a system. For processes that do not have a constant setpoint, but follow an infinite varying trajectory, nonlinearity measures are required for the application of the controller. The integral of time absolute error, ITAE can also be used to assess the extent of linear and nonlinear behavior with respect to variation in setpoints. Here, sensitivity analysis is

taken as a measure of nonlinearity for the application of Robust, Hybrid and Adaptive controllers as detailed in section 3.3.

3.5 STATE SPACE MODEL

The system performance in terms of settling time as well as settling accuracy are mainly influenced by factors like valve characteristics, flow rate through the three vessels, high pressure storage tank, heater and settling chamber as observed in Fig. 3.3, which are in turn decided by the choice of the control design. For modelling, the continuity equations (3.7) to (3.9) and parameter values in Table 3.1 are selected for the three vessels (Savino *et al.*, 2009; Jones *et al.*, 2011a; Jacob and Binu, 2009; Jones *et al.*, 2011b; Pope and Goin, 1965). In order to arrive at the state space model of the system, the compressed air in the air storage tank is assumed to be ideal. From the empirical analysis (Jacob and Binu, 2009; Jones *et al.*, 2011b), the nominal test conditions corresponding to temperatures in the three vessels are selected as $T_1 = 300\,K$, $T_2 = 700\,K$ and $T_3 = 539\,K$ respectively and initial pressure in air storage tank is 300×10^5 Pa. Thus, the State space model of the system is derived in Appendix 1 and is represented as follows.

$$\begin{bmatrix} \dot{P_1} \\ \dot{P_2} \\ \dot{P_3} \end{bmatrix} = \begin{bmatrix} -K_1/C_1 & 0 & 0 \\ K_1/C_1 & -K_3/C_2 & -K_4/C_2 \\ 0 & K_3/C_3 & K_4 - K_n/C_3 \end{bmatrix} \begin{bmatrix} P_1 \\ P_2 \\ P_3 \end{bmatrix} + \begin{bmatrix} -K_2/C_1 \\ K_2/C_2 \\ 0 \end{bmatrix} m\,. \quad (3.27)$$

$$Y_1 = \begin{bmatrix} 0 & 0 & 1 \end{bmatrix} \begin{bmatrix} P_1 \\ P_2 \\ P_3 \end{bmatrix}. \qquad (3.28)$$

where P_1, P_2 are the upstream and downstream pressures, P_3 is the settling chamber pressure, $u = m$ represents the displacement of the stem of PRV and K_1, K_2, K_3 and

K_4 are constants, K_n is the nozzle flow constant and, C_1, C_2, C_3 represents the gas capacitance of the three pressure vessels respectively. Here, pressure variations in each vessel is chosen as the state variables, stem movement of PRV as the input variable and settling chamber pressure as the output variable.

The flow rate through the PRV varies in accordance with the stem position, and hence it is considered as the input to the tunnel system. The parameters required for system modelling are shown in Table. 3.5 (Jacob and Binu, 2009; Jones *et al.*, 2011b).

Table 3.5 The Parameters of the system for modelling

Parameter	Value
Constant, K_1	40.74×10^{-7}
Constant, K_2	556.9
Constant, K_3	22.86×10^{-5}
Constant, K_4	-22.86×10^{-5}
Constant, K_n	$0.0404A$ where A is the area of the pipe
Constant, C_1	9.05×10^{-4}
Constant, C_2	-9.11×10^{-5}
Constant, C_3	1.78×10^{-5}

3.6. OPEN LOOP RESPONSE

Open-loop system, generally known as non-feedback system, is a type of continuous control system in which the output has no influence on the control action of the input signal. Thus, the system cannot self-correct any errors it could make when the preset value drifts, even if this results in large deviations from the preset value.

Nonlinear Model

In this chapter, we begin with a nonlinear system, linearize it at its critical points, then use linear ODE techniques to understand the approximate behavior of solutions to the linearized system, and finally apply the behavior to the nonlinear system. The system with the modelled non-linearities is simulated and the open loop response of settling chamber pressure versus time is obtained as in Fig. 3.9.
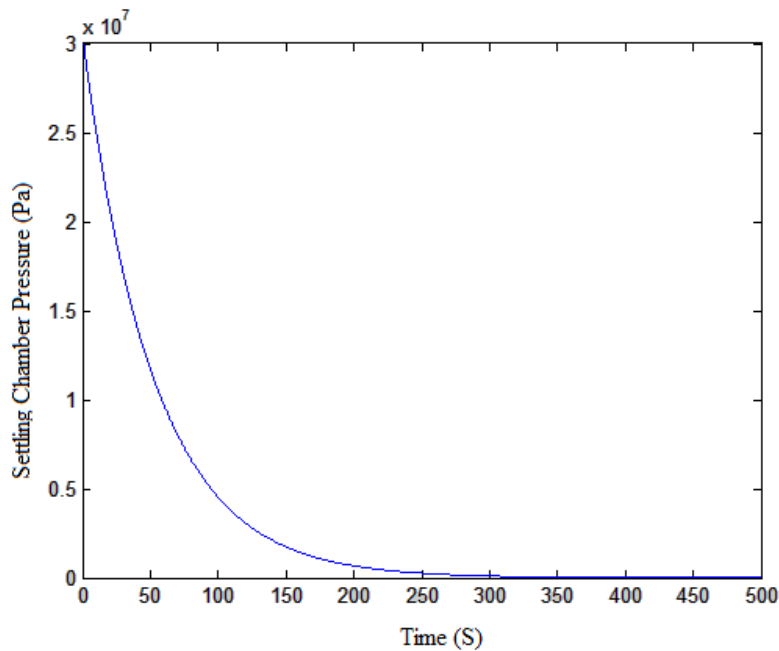
Fig. 3.9 Response of pressure, P_3 of nonlinear model.

Initially the pressure in the air storage vessel rises to 300×10^5 Pa, where the input is the stem movement. According to the stem movement, the settling chamber pressure reduces and settles to zero in 450 seconds. It can also be inferred that the settling chamber pressure P_3 attains a peak value of 300×10^5 Pa, and this pressure releases completely in 450 s. This value of 450 s for the settling time is very high for Hypersonic wind tunnels where the test duration is in the range of 40 s. Thus, the air

flow from the storage tank to the settling chamber is required to be controlled using appropriate techniques (Jacob and Binu, 2009; Jones *et al.*, 2011b).

Fig. 3.10 shows the settling chamber pressure with a sine wave as input for stem movement. Here, we provide sine wave as the input variable and it is clear from the figure that the pressure is completely released in 450 s which is same as that of the step input. It is observed from the figure that the amplitude of the signal is $1.015 \times 10^7 Pa$ and frequency is $0.55s^{-1}$.
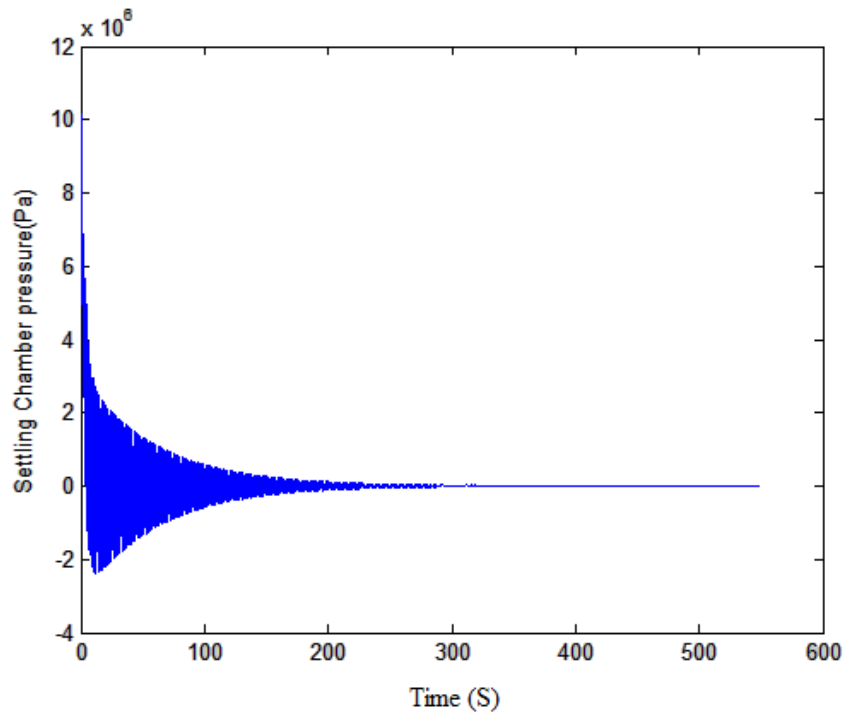
Fig. 3.10 Settling chamber pressure with sine wave input.

Fig. 3.11 represents the open loop response of pressure, P_1 of air storage tank and pressure, P_2 of heater. From these figure, it is observed that both P_1 and P_2 takes 400 s to release completely.
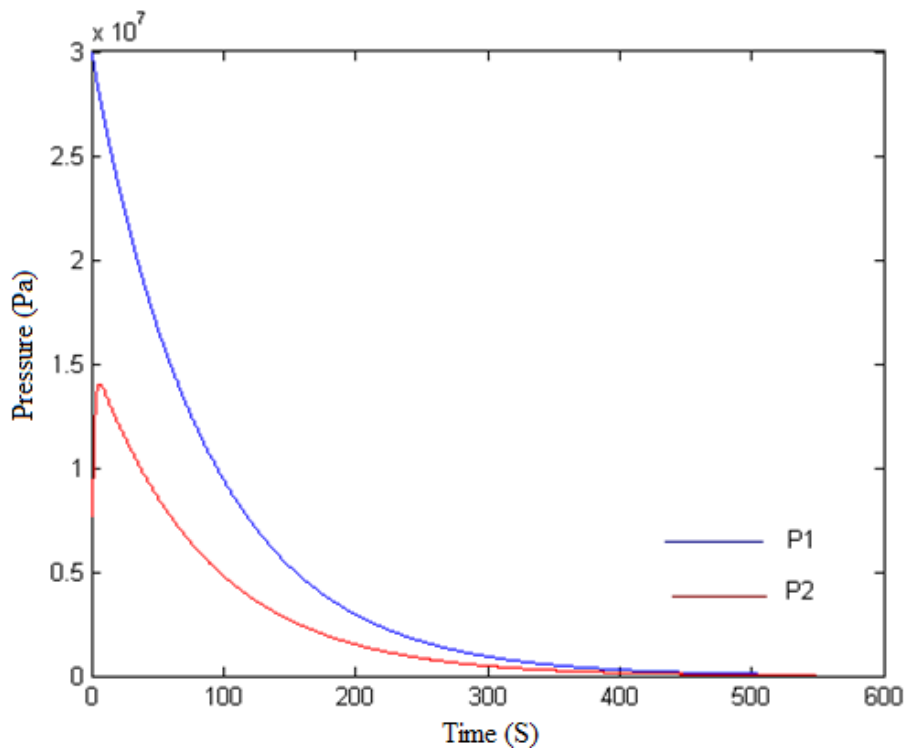
Fig. 3.11 Response of pressures, P_1 and P_2 of nonlinear model.

Linear Model

In general, majority of the real time systems are non-linear. The natural approach for analyzing a system is to solve it explicitly, and this method works well only if the system is linear. If the system is nonlinear, then solving explicitly is complicated, so we linearize the system at its equilibria and gain a qualitative understanding of the solutions by analyzing the linearized model (Jones *et al.*, 2011a; Jacob and Binu, 2009; Jones *et al.*, 2011b). Hence, the wind tunnel system is linearized and is represented in state space and its transfer function form and the response of the linearized system is shown in Fig. 3.12. From the figure, it is observed that the settling time of the chamber pressure is high as 400 s and that it needs to be reduced below 40 s. Fig.3.13 represents the settling chamber pressure of both linear and nonlinear system. From the figure, it is clear that for the

85

nonlinear model, the pressure releases completely in 450 s whereas in the linear model the time required to settle is 400 s.
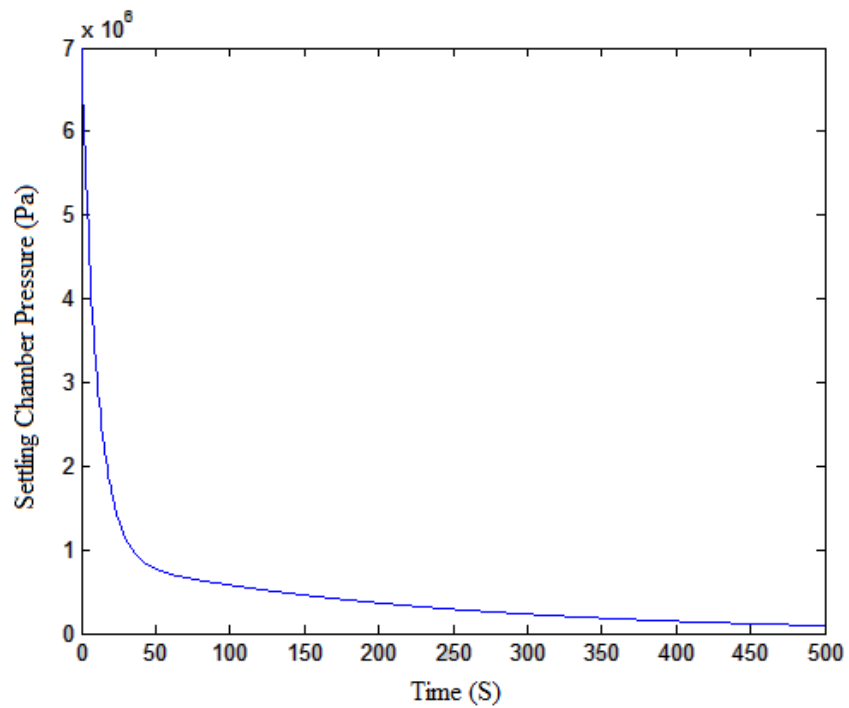
Fig. 3.12 Response of pressure, P_3 of linear model.
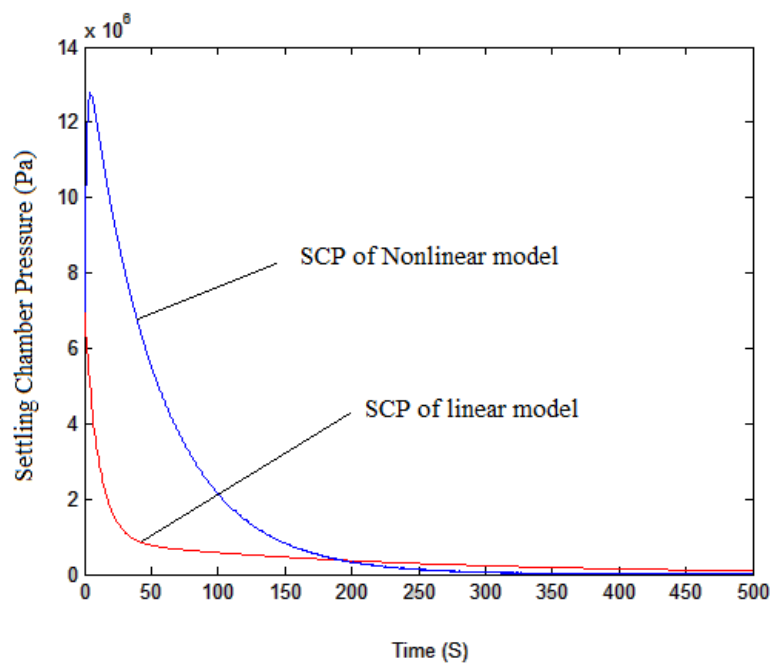
Fig. 3.13 Settling Chamber pressure, P_3 of linear and nonlinear model.

3.7 STABILITY ANALYSIS

In large complex real time systems, which incorporate new challenges in modelling and analysis have reliability issues of their components, delays and interruptions to communications between subsystems. These may result in instability of the closed-loop system, resulting in a potentially disastrous situation (Ogata, 2002; Yang *et al.*, 2013; Delfour and Mitter, 1972; Jacques and Slotine, 1991). In recent years the focus is on reliability rather than cost, which requires the need to ensure stability before designing the controller and development of fault tolerant control systems. A system is said to be stable if it produces a bounded output for a given bounded input. The stability of the system is required to be ensured before applying any type of controller to improve the performance of the system to the desired level.

Various methods used for stability analysis are Kalman's test for controllability and observability, Lyapunov stability theorem, Phase portrait method, Root locus and Bode plot methods.

1. Kalman's Test for Controllability and Observability

Stability analysis is carried out on the system model before designing the controllers. Two major concepts are available to test controllability and observability. The concept of controllability refers to the ability of a controller to arbitrarily alter the functionality of the system (Ogata, 2002; Delfour and Mitter, 1972). The term observability describes whether the internal state variables of the system are externally measurable (Gayon *et al.*, 2013; Bhoi and Suryanarayana, 2008; Arbuckle, 2016). Controllability and observability of a system are verified using the non singularity nature of the respective matrixes. By

substituting the values of the parameters K_1, K_2, K_3, K_4, Kn, C_1, C_2 and C_3 from Table 3.5 (Jones *et al.*, 2011a; Jacob and Binu, 2009; Jones *et al.*, 2011b) in eq. (3.27) and (3.28), the state matrices are obtained as,

$$[A] = \begin{bmatrix} -0.0045 & 0 & 0 \\ 0.0045 & 2.51 & 2.51 \\ 0 & 12.85 & -14.14 \end{bmatrix}$$

$$[B] = \begin{bmatrix} 617679.68 \\ 6133259.91 \\ 0 \end{bmatrix}$$

$$[C] = [0 \ 0 \ 1]$$

$$[D] = [0]$$

Kalman's test for controllability and observability (Delfour and Mitter, 1972) are carried out using eq. (3.29) and (3.30) respectively.

$$Q_C = [B \ \ AB \ \ A^2 B] \tag{3.29}$$

$$Q_O = \left[C^T \ \ A^T C^T \ \ A^{T^2} C^T \right] \tag{3.30}$$

where Q_C and Q_O represents controllability matrix and observability matrix respectively. The values of Q_C and Q_O obtained from eqs. (3.27) and (3.28) with the state matrices A, B, C are $|Q_c| = -1.26 \times 10^{22} \neq 0$ and $|Q_o| = -743.05 \times 10^{-3} \neq 0$. Thus, the rank of both the matrices are 3, indicating the nonsingular nature and thereby ensuring the complete state controllability and observability of the tunnel system (Delfour and Mitter, 1972).

2. Lyapunov Stability

Lyapunov stability theory is a standard tool for the analysis of non-linear systems which can be extended relatively to cover non-autonomous systems and also to provide a strategy for constructing stable feedback controllers. One of the methods to ensure stability is using Lyapunov stability theorem. For a dynamic system which satisfies, $\dot{x} = f(x, t),\ x(t_0) = x_0,\ x \epsilon R^n$, to ensure Lyapunov Stability criterion, we choose a continuous Lyapunov function, V(x) which is positive definite such that $\dot{V}(x, t) \leq 0$ locally in x and for all t, then the system is said to be stable.

For the tunnel system, the state variables are $X_1 = P_3$, $X_2 = P_2$, $X_3 = P_1$ (Jacob and Binu, 2009; Jones *et al.*, 2011b; Ogata, 2002; Yang *et al.*, 2013; Delfour and Mitter, 1972). The Lyapunov function, V(x) is chosen as positive definite function and is given by,

$$V(x) = x_1{}^2 + x_2{}^2 + x_3{}^2 \tag{3.31}$$

Then,

$$\dot{V}(x) = 2x_1\dot{x}_1 + 2x_2\dot{x}_2 + 2x_3\dot{x}_3 \tag{3.32}$$

By substituting the state variables and its derivatives from (Baals and Corliss, 1981; D'Souza *et al.*, 2015; Libii, 2011; Lohan, 2002; Gayon *et al.*, 2013; Bhoi and Suryanarayana, 2008; Pope and Goin, 1965), $\dot{V}(x) = -2926791$. As $\dot{V}(x)$ is negative, the tunnel system is stable according to Lyapunov stability criterion (Lohan, 2002).

3. Phase portrait method

The stability of non-linear system (Jacques and Slotine, 1991) can be analyzed by constructing its phase portrait. A system with f_1 and f_2 as the non-linear functions with states, X_1 and X_2, the state space is the plane having coordinates X_1 and X_2 (Jacob and Binu, 2009; Jones *et al.*, 2011b, Pope and Goin, 1965; Ogata, 2002; Jacques and Slotine, 1991). Here, P_1, P_2 *and* P_3 are chosen as the three state variables and the plot between $P_1 P_2$, $P_2 P_3$, $P_3 P_1$ *and* $P_3 \dot{P}_3$ are shown in Fig. 3.14 (a), (b) and 3.15 (a), (b) respectively. From the phase portraits shown in Fig. 3.14 (a), (b) and 3.15 (a), (b), it is clear that all the plots converge to zero and hence the system is found to be stable.
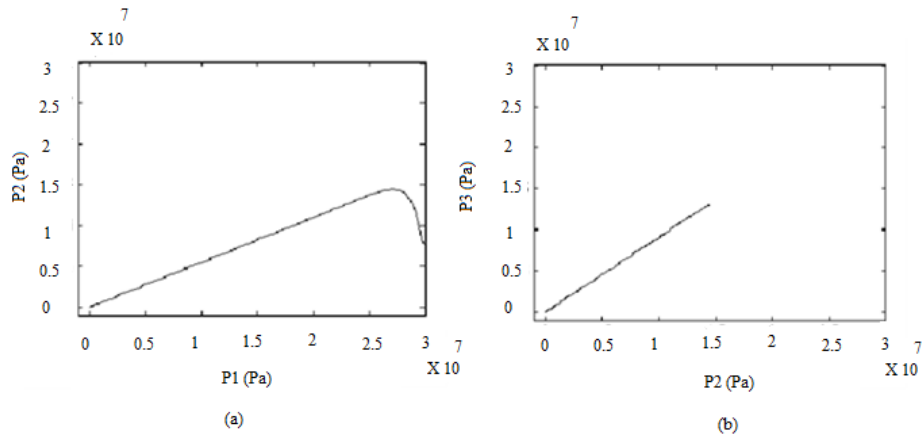
Fig. 3.14 (a) Plot of P₁P₂ (b) Plot of P₂P₃
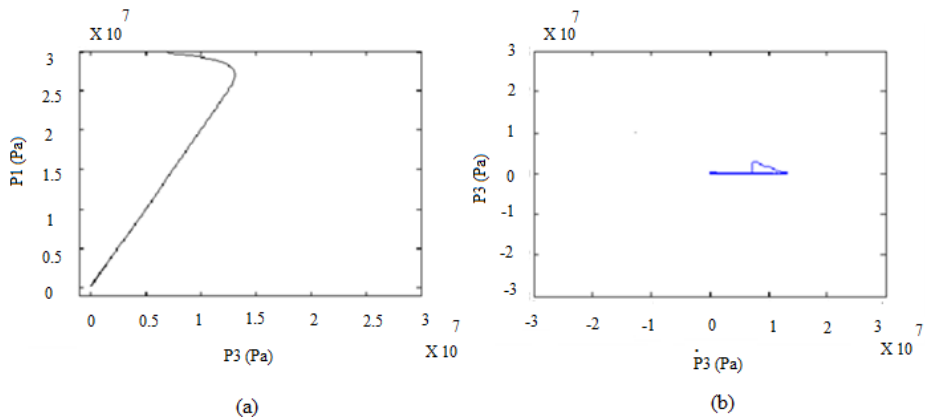
Fig. 3.15 (a) Plot of P₃P₁ (b) Plot of $P_3 \dot{P}_3$

4. Root locus

The Root locus is the locus of the roots of the characteristic equation by varying system gain K from zero to infinity. From the root locus we observe the path of the closed loop poles and can identify the nature of a given system. In order to ensure stability of the system, root locus method is applied to the transfer function in eq. (3.14). Fig. 3.16 shows the graphical method of determining stability by root locus method. From the figure, it is clear that the root locus is on the left half of the s-plane and hence the system is stable for all positive values of gain, K (Jacob and Binu, 2009; Jones *et al.*, 2011b, Pope and Goin, 1965; Ogata, 2002; Jacques and Slotine, 1991).
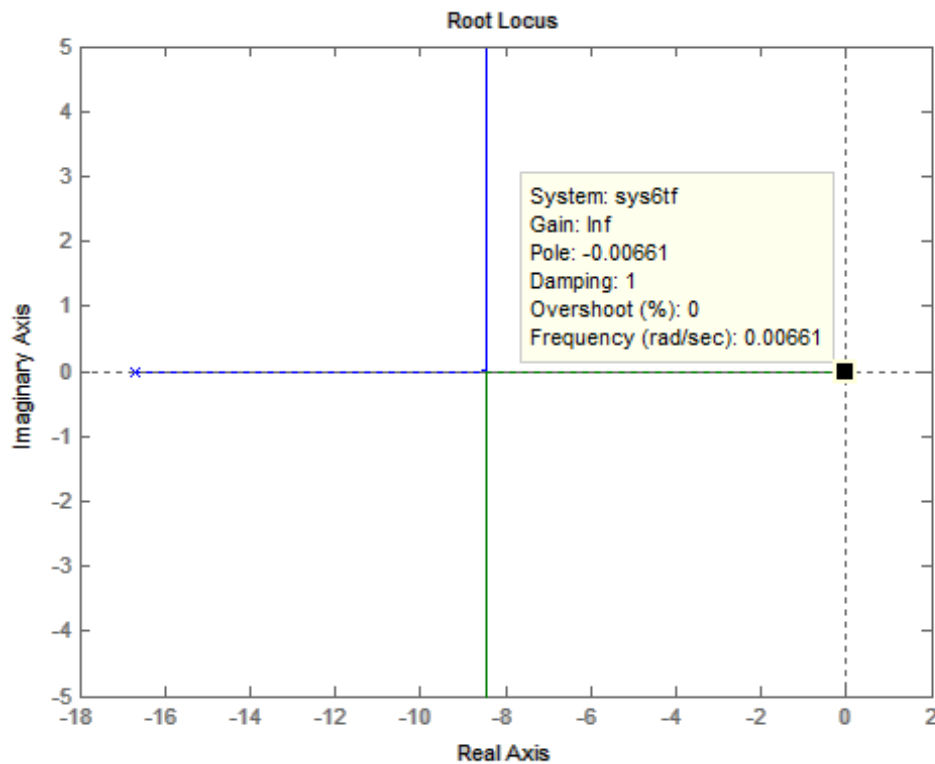
Fig. 3.16 Root locus of the Hypersonic wind tunnel system

5. Bode plot

Bode plot is a graphical tool to ensure stability of a system and it consists of Magnitude and Phase plot which represents the frequency response of a system. The Bode plot of the tunnel system with transfer function given in eq. (3.14) is obtained. Fig. 3.17 shows the frequency domain analysis of the system using bode plot. From the bode plot, gain and phase margin are calculated and it is clear that the gain margin is infinity and phase margin is positive, which indicates that the system is stable. Thus, the stability of the Hypersonic wind tunnel system is ensured using Kalman's test for controllability and observability, Lyapunov stability theorem, Phase portrait method, Root locus and Bode plot methods.
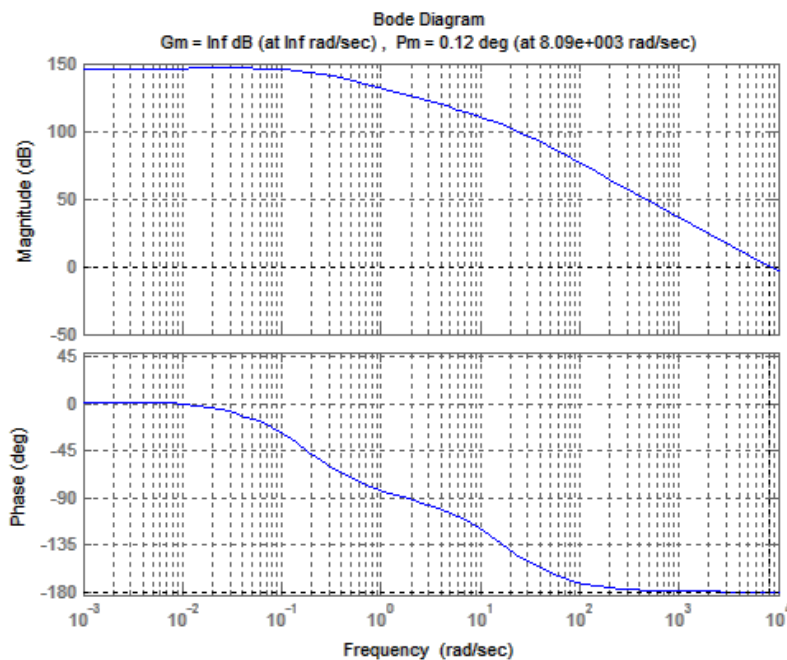
Fig. 3.17 Bode plot of the Hypersonic wind tunnel system

The mode of operation of wind tunnels depends on the power requirements, which in turn depends on the velocity required in the test section. The dependency of power requirement on the flow velocity becomes increasingly non-linear as the testing goes

into the high speed and hypersonic flow regimes. Due to the high power requirements, Hypersonic wind tunnels are usually operated in the intermittent blowdown mode wherein high pressure or vacuum is stored and released within a very short duration in the range of 40 s during a test run. Thus, the crucial factor to be considered while designing any controller for the above purpose is that the regulated pressure in the settling chamber, and thereby uniform hypersonic flow in the test section should be attained within the limited test duration (Savino, 2009; Jones *et al.*, 2011b; Furian *et al.*, 2015). Another vital factor to be considered in the design procedure of specific controllers is the maximum withstandable pressure within the tunnel system. In general, physical specification of the maximum withstandable pressure of a given tunnel system is also very critical in the design procedure of specific controllers (Lee *et al.*, 2014; Jones *et al.*, 2011a; Jacob and Binu, 2009; Jones *et al.*, 2011b). Hence, it becomes very important to conduct theoretical analysis and numerical simulations with various controller designs before venturing into real time experiments for specific applications. Keeping these factors in focus, we design suitable control schemes and carryout a comparative study of their performance with each other as well as, with existing fundamental controllers. This is done to propose the most suitable control schemes to regulate the pressure, which matches the desired performance characteristics like minimum overshoot and short settling time.

This chapter describes in detail the Hypersonic wind tunnel system. The purpose, block diagram description and major elements of Hypersonic wind tunnel are presented with technical details, constraints and relevance. Thus, it provides an overall technical know-how of the system, as such, and suggest a good platform for design of various controllers for pressure regulation inside the settling chamber.

93

Directly applying any controller to a tunnel system would cost long run times and pose danger to the system due to possible instabilities or insufficiencies of the proposed controller. Therefore, to study the effectiveness of any proposed controller, it is advisable to first apply it on tunnel model before implementing on large scale systems. In addition, controller design is very important for maintaining the desired environment in the test section, and also for increasing the consistency and cost effectiveness of the experimental test run (Jacob and Binu, 2009; Jones *et al.*, 2011b).

Several factors like the non-ideal gas behavior, distributed characteristics of storage and settling chambers, uncertainties in the flow characteristics of control valves, makes the system model and control design highly complex and non-linear (Jones *et al.*, 2011a; Jacob and Binu, 2009; Jones *et al.*, 2011b; Hwang and Hsu, 1998; Butler *et al.*, 2010). For these reasons, controllers have to be designed on simplified mathematical models (Jacob and Binu, 2009). However, the control designs are usually complicated so as to overcome model discrepancies for the purpose of practical implementation. For choked flow in the control valve, the related governing equations will depend only on the storage tank pressure (Jones *et al.*, 2011a; Jacob and Binu, 2009; Jones *et al.*, 2011b). For non-choked flow, the flow rate will be decided by coupled non-linear equations between the storage tank pressure and heater pressure (Jones *et al.*, 2011a; Jacob and Binu, 2009).

The performance characteristics of the above system are evaluated for a range of set point values between 1×10^5 Pa to 300×10^5 Pa. It is observed that the general time evolution of the SC pressure has similar characteristics for all the set point values within the chosen range. The representative results for three set points, 100×10^5 Pa,

94

70×10^5 Pa and 50×10^5 Pa are considered and the selected Robust, Hybrid and Adaptive controllers are designed to track the desired system output in the presence of the unknown system uncertainties.

Our aim is to regulate settling chamber pressure constant by pressure regulator valve with variable stem movement facility thereby maintaining a constant hypersonic flow in the test section. This is achieved by properly designing a suitable controller for regulating the valve opening. Chapter 4, 5 and 6 deals with design of various robust, Hybrid and adaptive controller techniques for regulation of settling chamber pressure for the tunnel system.

CHAPTER 4

DESIGN AND ANALYSIS OF ROBUST CONTROLLERS

In Hypersonic wind tunnel system, a constant hypersonic flow in the test section is required to be maintained throughout the test run. However, the storage tank pressure decreases continuously during a test run, which indirectly reduces the settling chamber pressure. Therefore, settling chamber (SC) pressure needs to be controlled by pressure regulator valve (PRV) with variable stem movement facility. The control of the valve opening is very crucial for maintaining the SC pressure in hypersonic flow, which is achieved by properly designing a suitable controller. For high performance pressure regulation requirements including fast response with minimum overshoot, the control of wind tunnel system becomes a challenging problem due to the highly nonlinear structure and variations in parameters with the operating conditions. Controller design is very important for maintaining the desired environment in the test section and also increasing the consistency and cost effectiveness of the experimental test run (Jones *et al.*, 2011a; Jones *et al.*, 2011b; Braun *et al.*, 2008; Bottasso *et al.*, 2014).

Published Research:
- **Rajani S.H, Bindu M. Krishna, Usha Nair (2017)** Pressure regulation inside a hypersonic tunnel using h-infinity optimization control. *Automatic Control and Computer Sciences, Allerton Press, Inc., Springer*, 51(6), 339- 409. (SCOPUS)
- **Rajani S.H, Bindu M. Krishna, Usha Nair**. Design and Analysis of H-infinity controller for a Hypersonic Wind Tunnel. *Proceedings of International Conference on Control Systems and Power Electronics, CSPE, Elsevier*, pp: 513– 518, Dec 2012.
- **Rajani S.H, Usha Nair**. Design and Analysis of a Nonlinear Controller for a Hypersonic Wind Tunnel. *Proceedings of IEEE International Conference on Computational Intelligence and Computing Research*, pp:106-109, Dec 2013.
- **Rajani S.H, Bindu M. Krishna, Usha Nair**. Chattering free Sliding mode controller for Hypersonic wind tunnel. *Proceedings of International Conference on Innovative Mechanisms for Industry Applications (ICIMIA 2017), IEEE Xplore*, pp: 359 – 363, Feb 2017.

Various linear as well as nonlinear controllers have been developed for different wind tunnel systems (Jones *et al.*, 2011a; Jacob and Binu, 2009; Nott *et al.*, 2008; Bhoi and Suryanarayana, 2008; Bottasso *et al.*, 2014; Hwang and Hsu, 1998). A lumped parameter model for Hypersonic wind tunnel system was developed based on the flow rate and the continuity equations for the three pressure vessels viz. HP, H1 and SC (Jones *et al.*, 2011a; Jacob and Binu, 2009; Jones *et al.*, 2011b). The traditional linear controllers like PI and PID controllers are widely used for the control of pressure inside the settling chamber of Hypersonic wind tunnel (Jones *et al.*, 2011a; Jacob and Binu, 2009; Jones *et al.*, 2011b). Though these controllers are easier to design and implement, their settling time and peak overshoot are quite high. In addition, these conventional controllers have major drawback such as performance sensitivity to variations in system's parameters. Also, these controllers need not provide the required speed performance under specific operating conditions and constant gain.

This chapter presents the results of a comparative study of the design methodologies and development of LQR, H-infinity, H-infinity with weight Optimisation, Backstepping and Sliding mode controllers. LQR controller is an optimization-based synthesis problem, used to track the output and follow the changes in set point is designed for the tunnel system. Based on the performance requirements, the optimal state feedback controller gain matrix is designed for the controller (Jacob and Binu, 2009; Jones *et al.*, 2011b; Ogata, 2002; Yin and Zhang, 2006). Robust controller namely, a H-infinity controller is designed based on the selection of weighing functions. To improve the performance characteristics, H-infinity controller with Krill

97

Herd optimization algorithm is designed to regulate pressure inside the settling chamber of a Hypersonic wind tunnel. The Krill Herd algorithm is a novel stochastic algorithm for improving the performance characteristics by optimizing the H-infinity controller parameters. The proposed algorithm minimizes the H-infinity norms by tuning the controller weighing function parameters. The dynamic characteristics of the settling chamber pressure with H-infinity and H-infinity controller with Krill Herd algorithm are studied by numerical simulations. The proposed algorithm is highly efficient and robust in controlling the settling chamber pressure in terms of performance parameters. To further improve the performance characteristics, Backstepping and Sliding mode controllers are designed. Backstepping controller, which is an efficient control algorithm in designing controllers for a large class of nonlinear systems, is designed for regulation of pressure inside the settling chamber of tunnel system. Another class of nonlinear controllers, Sliding mode controller that alters the dynamics of a nonlinear system is designed by properly selecting the sliding surface.

4.1. LQR CONTROLLER

The Linear Quadratic Regulator (LQR) is a control technique that provides optimally controlled feedback gains to enable high performance design of systems. The LQR control law is based on the availability of the complete state vector, which is not fully measurable in all cases. LQR is a well-known control technique that provides practical feedback gains, which helps in minimizing the variation in state trajectories but does not always show acceptable closed loop time domain response and might often include high overshoot and oscillations in the response. In order to achieve

efficient tracking of the set point change, the weighting matrices should be chosen in such a manner that it meets time domain optimality criteria in terms of overshoot, rise time and settling time.

Design

The LQR technique is an iterative controller algorithm in which the design produces optimal controller output by adjusting the weighting functions so as to achieve the desired response. This technique can be applied for multiple input systems. LQR is an optimal control scheme, which provides a systematic way of calculating the state feedback control gain matrix, K. LQR controller design problem deals with optimizing an energy function, J by designing the state feedback controller, K (Ogata, 2002; Yin and Zhang, 2006).

A system in state variable form is represented as,

$$\dot{x} = Ax + Bu$$

$$y = Cx \tag{4.1}$$

with x(t) ε R^n and u(t) ε R^m, where A and B are the state and input system matrices, respectively, x is the state of the system, u is the control input, n and m are integers.

The initial condition is x(0) and states are known. The state space model of the system is obtained from eq. (3.27) and (3.28) of chapter (3). The state-variable feedback (SVFB) control law is given by eq. (4.2).

$$u = -K\,x \tag{4.2}$$

where K is the linear optimal feedback control gain matrix (Ogata, 2002). The closed-loop system using this control becomes

$$\dot{x} = (A - BK)x \qquad (4.3)$$

Where x is the new command input.

The LQR solution relies on the solution of the matrix design equation in which many designs are available for solving the Riccati design equation, thereby obtaining the gain, K (Ogata, 2002; Yin and Zhang, 2006; Huang and Zhou, 2004). Computer-aided designs are common where the LQR control is a formal one and gives a solution to the feedback control problem. The design process involves selection of the weighting matrices Q and R. Once Q is properly selected, the matrix design equation is formally solved for the unique K that guarantees stability.

In LQR controller design, the crucial property is asymptotical stability as long as the system is controllable and observable. It is noted that the output matrices C and D are not used in the design process. The objective is to find the optimal control law that minimizes the following performance index. The performance index (PI) (Ogata, 2002; Yin and Zhang, 2006; Huang and Zhou, 2004) is defined by

$$J = \frac{1}{2}\int_0^\infty (x^T Q X \ + \ u^T R u)\, dt \qquad (4.4)$$

The performance index, J is the energy function which keeps the total energy of the closed-loop system small. The LQR algorithm computes a control law, u such that the performance criterion or cost function is minimized. The design matrices Q and R hold the penalties on the deviations of state variables from their setpoint and the control

actions, respectively. When an element of Q is increased, the cost function increases the penalty associated with any deviations from the desired setpoint of that state variable, resulting in a larger control gain. When the values of the matrix, R is increased, the control gains are decreased uniformly. Thus, the two matrices Q and R are selected such that Q is positive semi-definite and R is positive definite (Ogata, 2002; Yin and Zhang, 2006; Huang and Zhou, 2004; Yadav *et al.*, 2012). The control value u is called the optimal control (Ogata, 2002; Huang and Zhou, 2004) which is given by,

$$u(t) = -R^{-1}B^T Px = -Kx \tag{4.5}$$

where P(t) is the solution of the Riccati equation and is a real symmetric matrix. The matrix Riccati equation is solved by properly selecting the weight matrices, Q and R to obtain the gain, K. Solving eq. (4.5),

$$PA + A^T P - PBR^{-1}BP + Q = 0 \tag{4.6}$$

K is obtained as

$$K = R^{-1}B^T P \tag{4.7}$$

The plant with LQR controller is shown in Fig. 4.1.
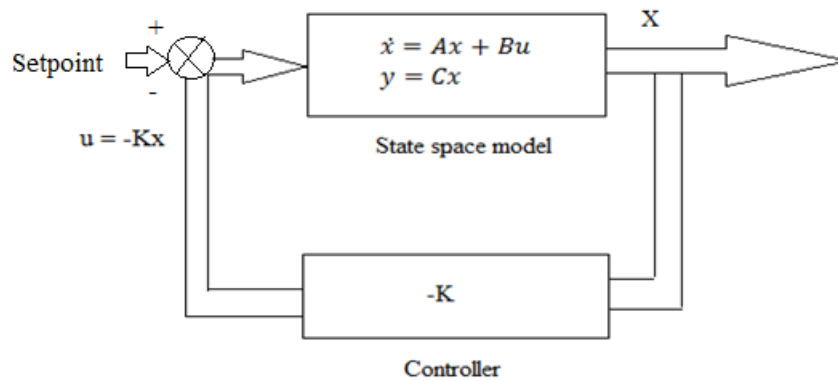
Fig. 4.1 Full state feedback representation of the system

101

In the figure, $\dot{x}, y, u, K, X$ represents input equation, output equation, input, gain and output response. The effect of optimal control using LQR controller depends on proper selection of weight matrices Q and R. The approach used for selecting Q and R is trial and error computer aided design, which helps to find the optimal gain matrix, K.

Results and Discussion

The gain matrix, K satisfying the control law for the LQR controller is estimated by selecting the weight matrices, Q and R as

$$Q = \begin{bmatrix} 1 & 0 & 0 \\ 0 & 1 & 0 \\ 0 & 0 & 1 \end{bmatrix} \qquad (4.8)$$

$$R = 1, \qquad (4.9)$$

The optimal gain matrix, K is obtained as,

$$K = [\text{-}0.9839 \quad 1.1041 \quad 0.3943]. \qquad (4.10)$$

With these values of gain, the system is simulated to get the response of settling chamber pressure in the range from 1×10^5 Pa to 300×10^5 Pa. The response of settling chamber pressure is obtained for three sample set points, 50×10^5 Pa, 70×10^5 Pa, 100×10^5 Pa respectively. Fig. 4.2 (1) (a) (b) (c) respectively from top to bottom show the variation of settling chamber pressure with LQR controller for set points of 50×10^5 Pa, 70×10^5 Pa, 100×10^5 Pa respectively. Correspondingly, its zoomed portion is shown in Fig. 4. 2 (2) (a) (b) (c) to clearly understand the dynamic variation.
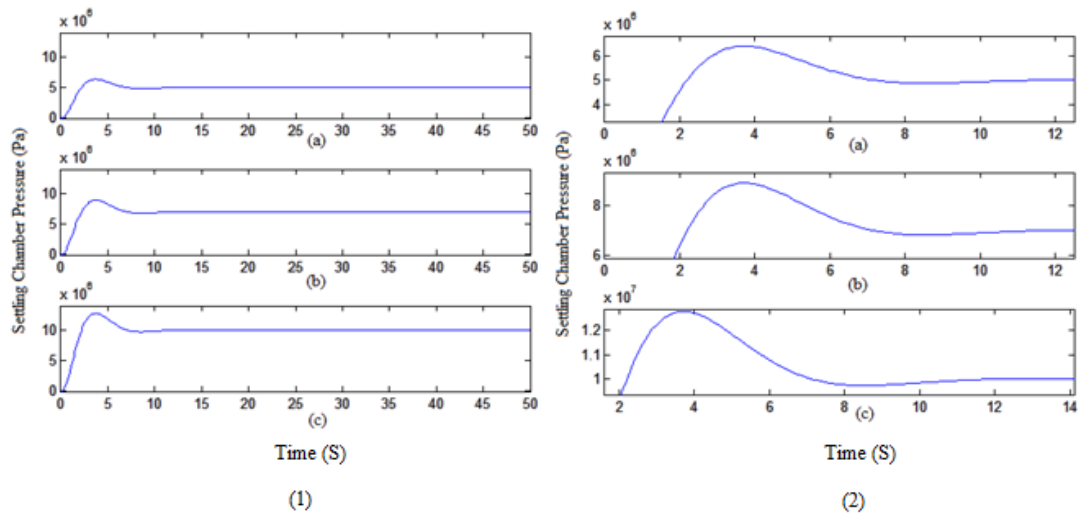
Fig. 4.2   (1) Settling chamber pressure with LQR controller for the set points 50×10^5, 70×10^5, 100×10^5 Pa and Q = (1 0 0; 0 1 0; 0 0 1) (2) Zoomed portion of (1)

The performance parameters and various error indices are also evaluated and the results are tabulated in Table 4.1. From the response, it is observed that the change in set point does not affect the settling time and rise time whereas the percentage overshoot is high for all the set point. Here the settling time is 18, 9.48, 18 s for the three setpoints 50×10^5 Pa, 70×10^5 Pa, 100×10^5 Pa respectively and the rise time is 1.43 s for all the three setpoints. The percentage overshoot values are 32, 27.72 and 76.31 % and the peak time is observed to be, 3.72, 3.69, 3.68 s for the three set points 50×10^5 Pa, 70×10^5 Pa, 100×10^5 Pa respectively. The error indices, Integral of absolute error (IAE), integral of square of errors (ISE), integral of time absolute errors (ITAE) are also computed and show similar trends with increase in set point values.

Table 4.1   Performance parameters of settling chamber pressure using LQR
controller with Q = (1 0 0; 0 1 0; 0 0 1)

PERFORMANCE OF HYPERSONIC WIND TUNNEL WITH LQR CONTROLLER WHEN Q = (1 0 0 0 1 0 0 0 1)			
Parameters	**Set point = 50 × 10^5 Pa**	**Set point = 70 × 10^5 Pa**	**Set point = 100 × 10^5 Pa**
Settling Time (s)	18	9.48	18
Rise Time (s)	1.43	1.43	1.43
Peak Overshoot (%)	32	27.72	76.31
IAE	1.0×10^7	1.6×10^7	2.0×10^7
ISE	5.0×10^{13}	1.28×10^{14}	2.0×10^{14}
ITAE	5.87×10^{13}	1.47×10^4	2.29×10^{14}

From the results tabulated in Table 4.1, it is clear that with the designed values of
matrix, Q, the performance parameters, settling time and overshoot are not
satisfactory. A solution to this problem is to apply the control technique by varying
the matrix, Q to meet the performance criteria (Ogata, 2002; Yin and Zhang, 2006;
Huang and Zhou, 2004; Yadav *et al.*, 2012). The effect of change of weighing matrix,
Q on the performance is evaluated by selecting Q as

$$Q = \begin{bmatrix} 100 & 0 & 0 \\ 0 & 100 & 0 \\ 0 & 0 & 100 \end{bmatrix} \tag{4.11}$$

Corresponding optimal gain matrix, K is

$$K = [\ -10.2745 \quad 11.0853 \quad 3.9464]. \tag{4.12}$$

The system is simulated using these values for the entire range of pressure, and the
response of settling chamber pressure for the three sample set points $50 \times$
10^5 Pa, 70×10^5 Pa, 100×10^5 Pa respectively is plotted. Fig. 4.3 (1) (a) (b) (c)
shows the variation of settling chamber pressure with LQR controller for the
respective three setpoints and the zoomed portion is detailed in Fig. 4.3 (2) (a) (b) (c).
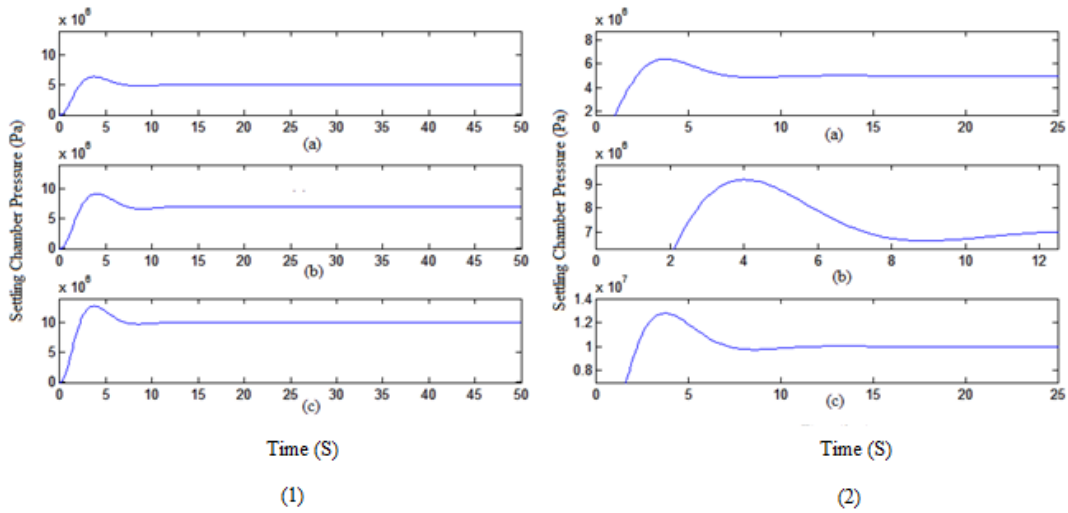
Fig. 4.3　　(1) Settling chamber pressure with LQR controller for the setpoints $50 \times 10^5, 70 \times 10^5, 100 \times 10^5$ Pa and Q = (100 0 0; 0 100 0 0; 0 100) (2) Zoomed portion of (1)

From Fig. 4.3, it is observed that the settling time is 15 s for all the three setpoints and the rise time is 1.43, 1.52 and 1.43 s for the three setpoints 50×10^5 Pa, 70×10^5 Pa, 100×10^5 Pa respectively. It can also be observed that the percentage overshoot is reduced and is 25.38, 31.38 and 29 % and the peak time is observed to be 3.72, 4.00 and 3.68 s for the same corresponding three setpoints.

The various performance parameters and the corresponding error indices are also calculated, and the results are tabulated in Table 4. 2. It is evident from the table that the settling time and rise time do not vary with variation of set point. However, the percentage overshoot values show a slight increase with increase in set points. The error indices corresponding to three set points are also evaluated.

Table 4.2   Performance parameters of settling chamber pressure using LQR controller with Q = (100 0 0; 0 100 0; 0 0 100)

PERFORMANCE OF HYPERSONIC WIND TUNNEL WITH LQR CONTROLLER WHEN Q = (100 0 0 0 100 0 0 0 100)			
Parameters	**Set point = 50 × 10^5 Pa**	**Set point = 70 × 10^5 Pa**	**Set point = 100 × 10^5 Pa**
Settling Time (s)	15	15	15
Rise Time (s)	1.43	1.52	1.43
Peak Overshoot (%)	25.38	31.38	29
IAE	1.0×10^7	1.6×10^7	2.0×10^7
ISE	5.0×10^{13}	1.28×10^{14}	2.0×10^{14}
ITAE	6.09×10^{13}	1.50×10^{14}	2.34×10^{14}

The effect of variation of weighing matrix, Q is clear from this analysis. With increase in value of the weighing matrix, Q to its optimal value, the corresponding gain matrix, K increases resulting in better performance, beyond which the stability of the system gets affected. When the value of Q is changed from (1 0 0; 0 1 0; 0 0 1) to (100 0 0; 0 100 0; 0 0 100) given in eqs. (4.8) and (4.11) respectively, the settling time is reduced from 18 s to 15 s whereas the rise time remains almost the same. The main advantage is the drastic reduction in percentage overshoot. The error indices, IAE and ISE values remain the same for both the values of weighing matrix, Q, whereas the ITAE shows slight increase from 5.87×10^{13} to 2.34×10^{14}. The settling time in the case of open loop response is 450 s which is improved to 18 and 19 s with LQR controller for the Q value (1 0 0 0 1 0 0 0 1) and is 15 s for the Q value (100 0 0 0 100 0 0 0 100).

An LQR based controller is designed for regulating the settling chamber pressure of a Hypersonic wind tunnel system. The stability of the system is ensured using various approaches in chapter 3. The performance of the system is evaluated for increasing values of set points, and the representative results for three setpoints, 50×10^5 Pa, 70

$\times 10^5$ Pa and 100×10^5 Pa are plotted. The effect of variation of weighing matrix on the system performance is also analyzed. It is found that even though the settling time is reduced, there is high overshoot with both designs. Hence to improve the performance further, we propose various Robust controllers.

4.2 ROBUST CONTROLLERS

As the conventional controllers do not perform efficiently in the presence of variation in process dynamics, it is required to design controllers, which can perform under such variations created by perturbations. Robust control is an important field of feedback control theory which ensures stability and performance of systems with uncertainties (Mary *et al.*, 2012; Yilmaz *et al.*, 2012). With the aim of improving the system performance in the presence of disturbances and parametric uncertainties, we design a H-infinity control scheme for regulation of pressure inside the Hypersonic wind tunnel.

4.2.1 H-infinity Controller

H-infinity control technique is one of the advanced techniques, and has applications growing rapidly in varied fields. H-infinity control technique helps in achieving robust performance or stabilization and is readily applicable to problems involving multivariable systems. H-infinity is defined as the space of proper and stable transfer functions in which the control algorithm is well suited for mixture of robustness and performance requirements. This is achieved by properly choosing design parameters called weighting functions. Standard feedback configuration of H-infinity controller with weights (Mary *et al.*, 2012; Yilmaz *et al.*, 2012; Hassibi *et al.*, 2006) is given in Fig. 4.4.
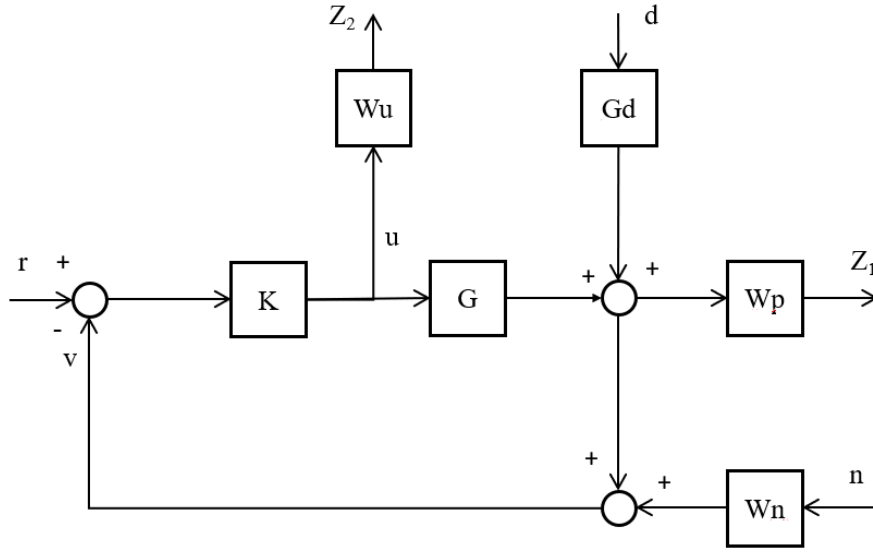
Fig. 4.4 Block diagram of H-infinity controller with weights

The controller is designed by properly selecting the weighing functions given in the above figure (Mary *et al.*, 2012; Yilmaz *et al.*, 2012; Hassibi *et al.*, 2006). From the figure, G is the plant transfer function, G_d represents the transfer function corresponding to input disturbance, r is the set point, u represents the actuator, v is the sensor measurement, K is the controller gain, d is the disturbance, n is measurement noise, Z_1 represents the settling chamber pressure, Z_2 represents the control input. The weight, W_p is the second order transfer function and is selected such that $|S(j\omega)| <$ $\frac{1}{W_p(j\omega)}$, $\forall \omega$ where S is the sensitivity function, weight, W_u indicates control input weight or multiplicative uncertainty weight and sensor noise is represented by W_n (Hassibi *et al.*, 2006).

Design of weighting functions

The main objective of Robust controller design is to regulate the system performance in spite of perturbations. The H-infinity controller is designed based on certain performance criteria. The multiplicative uncertainty weight , W_u shown in Fig. 4.4 is

selected by satisfying the stability conditions (Mary *et al.*, 2012; Yilmaz *et al.*, 2012; Hassibi *et al.*, 2006; Vikalo *et al.*, 2005),

$$|W_u(j\omega)| \geq l_u(\omega), \qquad \forall \omega \tag{4.13}$$

where l_u is the relative error of the plant transfer functions. The bode plot of plant transfer function and weighing function W_u is shown in Fig. 4.5.
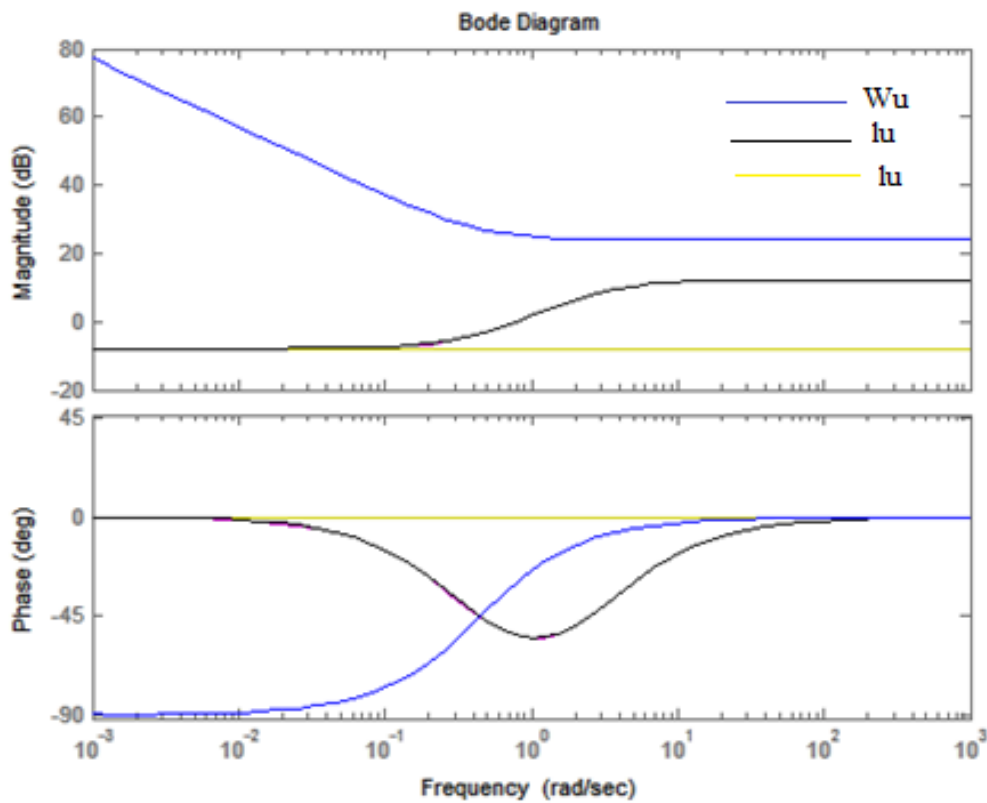
Fig. 4.5 Design of Multiplicative uncertainty weight, W_u

The weight, W_u is selected such that the magnitude of weight transfer function lies above the plant transfer function based on eq. (4.13) as,

$$W_u = \frac{400s + 180}{25s + 0.0002} \tag{4.14}$$

In order to design the weight function, W_p, certain nominal performance requirements based on sensitivity functions need to be met. The sensitivity function S(s) (Mary *et al.*, 2012; Yilmaz *et al.*, 2012; Hassibi *et al.*, 2006; Vikalo *et al.*, 2005) is defined as

$$S(s) = (1 + K(s)H(s))^{-1} \qquad (4.15)$$

Fig. 4.6 represents the magnitude and phase of the sensitivity and complimentary sensitivity function for the above system.
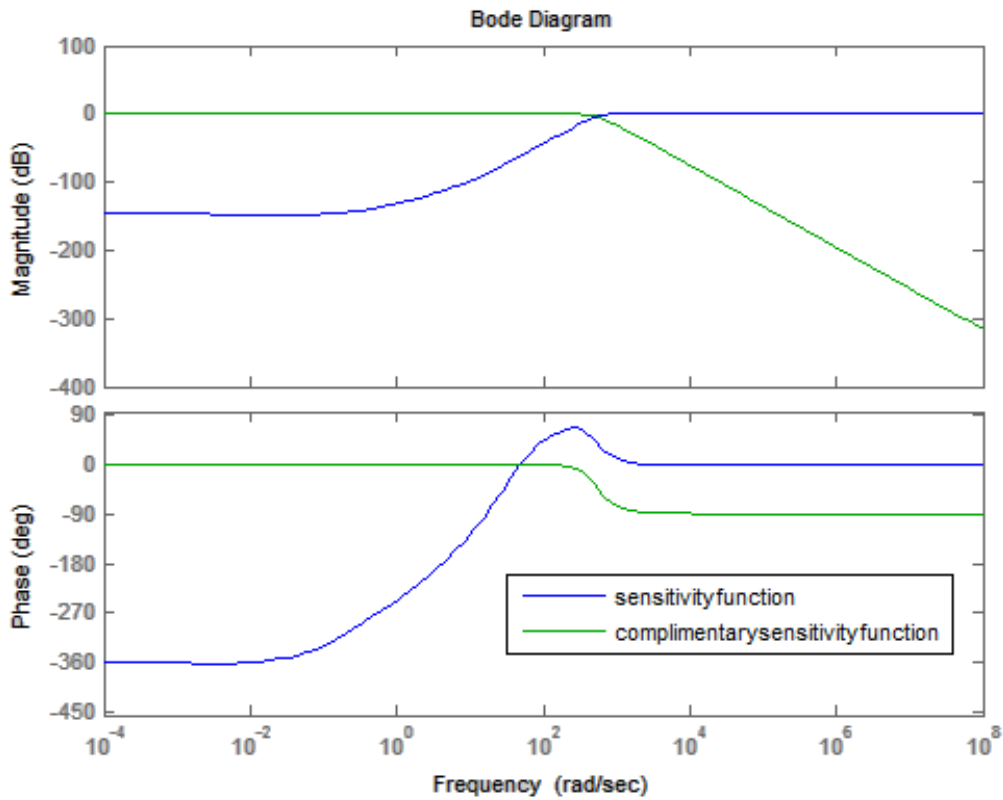
Fig. 4.6 Combined plot of sensitivity and complementary sensitivity function for the tunnel system

The performance requirement for selection of W_p is guaranteed if and only if it satisfies the condition $|S(j\omega)| < \frac{1}{W_p(j\omega)}$, $\forall \omega$ and nominal performance criterion is satisfied.

The nominal performance criterion (Mary *et al.*, 2012; Yilmaz *et al.*, 2012) is given by,

$$|W_p(j\omega)| < |1 + G_m(j\omega)|, \qquad \forall \omega \qquad (4.16)$$

The bode plot of S (jω) and $W_p(j\omega)$ and $|1 + G_m(j\omega)|$ and $W_p(j\omega)$ are shown in Fig. 4.7 and 4.8 respectively. It is observed that $1/|W_p(j\omega)|$ is greater than $|S(j\omega)|$ in Fig. 4. 7 and $|W_p(j\omega)|$ is less than $|1 + G_m(j\omega)|$ in Fig. 4.8.
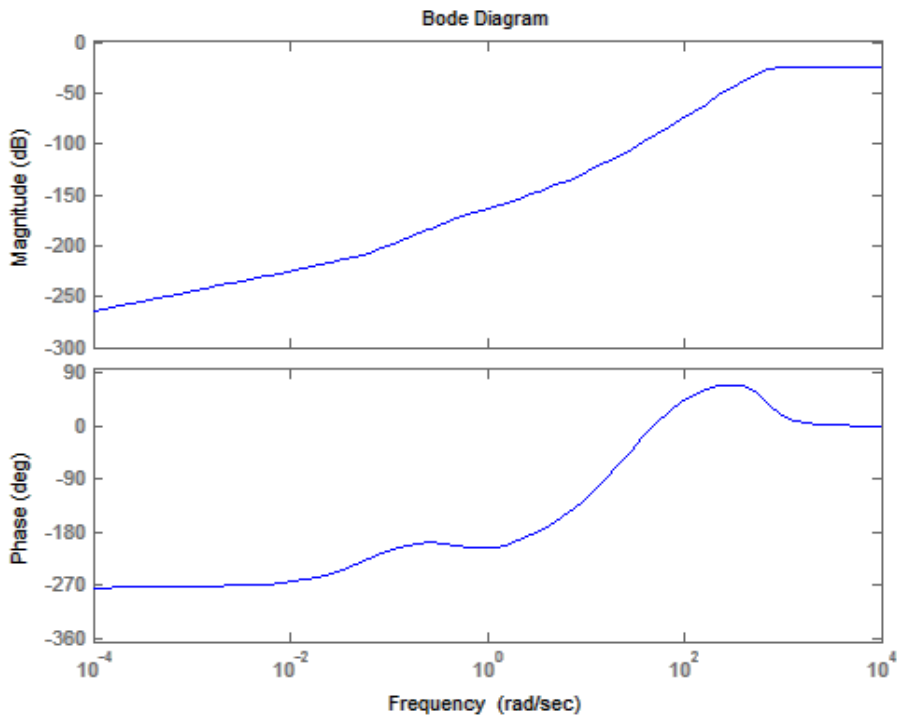
Fig. 4.7 The performance requirement for selection of weight function, W_p
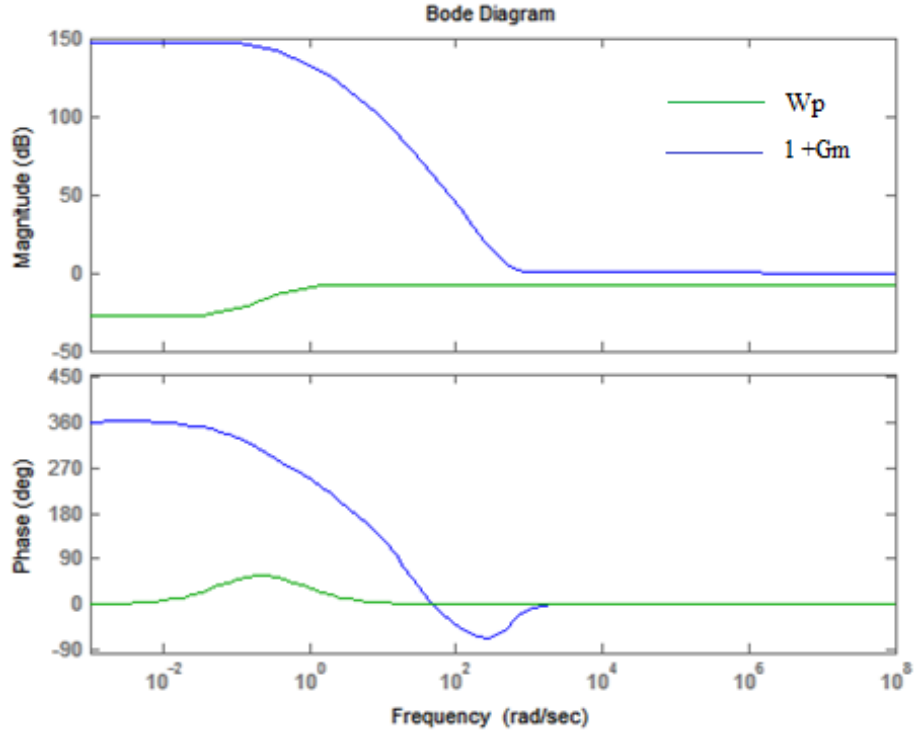
Fig. 4.8 Nominal performance criteria for selection of weight function, W_p.

The weighing function, W_p is selected satisfying the above conditions as,

$$W_p = \frac{35s + 25}{15s + 1}\ .$$

(4.17)

The weighing function, W_n is choosen by trial and error method [16-18] as,

$$W_n = \frac{1}{10}\ .$$

(4.18)

After designing the three weights W_u, W_p and W_n, the H-infinity controller with plant transfer function given in eq. (3.14) is simulated, with the input disturbance transfer function, $G_d = 1$ for the three representative set points 100×10^5 Pa, 70×10^5 Pa and 50×10^5 Pa respectively.

112

Results and Discussion

With the designed weight functions, the effectiveness of H-infinity control scheme for regulation of pressure inside the Hypersonic wind tunnel is investigated. The open loop response of the Hypersonic wind tunnel system is studied using appropriate physical and model parameters in the flow equations obtained from the continuity eqs. (3.1) to (3.14) and (3.27) and (3.28) in chapter (3) (Jacob and Binu, 2009; Echman, 1958; Liptak, 1995). It is observed that the settling chamber pressure gradually stabilizes and the pressure is fully released in 450 s as observed in chapter (3) (Jacob and Binu, 2009; Echman, 1958; Liptak, 1995).

The performance characteristics of the wind tunnel system is evaluated using H-infinity controller for a range of set point values between 1×10^5 Pa to 300×10^5 Pa keeping the temperatures of the three vessels at $T_1 = 300$ K, $T_2 = 700$ K and $T_3 = 539$ K (Jones *et al.*, 2011a; Jacob and Binu, 2009; Jones *et al.*, 2011b; Echman, 1958; Liptak, 1995) respectively. The simulation results for the three set points, 100×10^5 Pa, 70×10^5 Pa and 50×10^5 Pa are shown in Fig. 4.9 (1). The zoomed portion of the settling chamber pressure is shown in Fig. 4.9 (2).
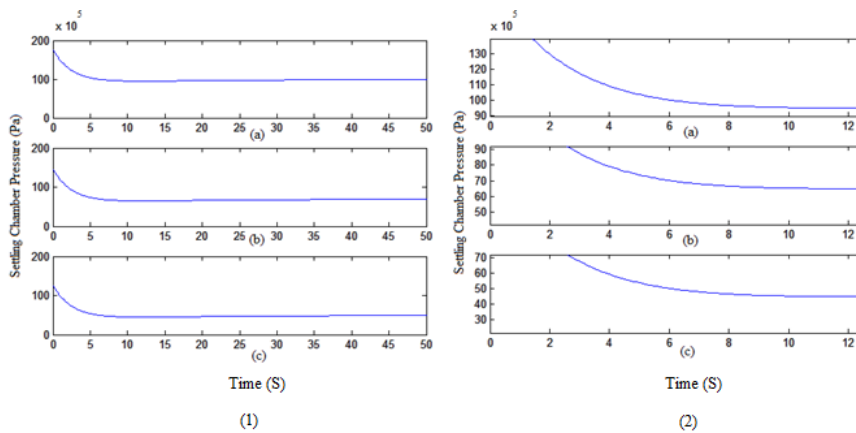
Fig. 4.9   (1) The response of settling chamber pressure with H-infinity controller for the set points of 100×10^5 Pa, 70×10^5 Pa and 50×10^5 Pa (2) Zoomed portion of (1)

From the figure, it is observed that with the designed H-infinity controller, the settling chamber pressure of the system model, y(t) initially overshoots and then settles down to the given set points of 50×10^5 Pa, 70×10^5 Pa and 100×10^5 Pa respectively in 1.2s with Gamma value of the controller as 2.45. The corresponding values of percentage overshoot is found to be 58.33%, 83.33% and 116 % and rise time to be 0.20, 0.85, 0.85 s respectively. The peak time corresponding to the three set points are 50, 70, 100 s respectively.

Thus, an H-infinity controller is designed for the linear model of the high pressure system of the wind tunnel for regulating the settling chamber pressure. The above design is based on the weight functions and tuning sensitivity and complementary sensitivity functions. This controller design is simulated with the input disturbance transfer function, G_d made equal to 1 and the set point equal to 70×10^5 Pa. The controller output performance is compared with the open loop response of the system. It is observed that the pressure in the chamber settles within 2 seconds with 5 % criterion and 12 s with slight disturbances, whereas it takes 450 seconds in open loop. These disturbances in the output response depends on the design of weighing functions. This shows that the system performance is improved to the required speed. However, drawbacks exist with the need for a high level of mathematical understanding, and the presence of overshoot in the output response.

The H-infinity controller is suitably modified to improve the performance characteristics using Krill Herd Optimisation technique. Here, the weight function W_u, the performance index and the fitness function is optimized using Krill Herd optimization algorithm.

4.2.2. Optimized H-infinity Controller

Robust control methods are designed for systems to function correctly so long as tentative parametric variations are within the tolerable limits. After the evolution of optimization technique called genetic algorithm, various techniques have been designed for optimization. Here, we propose an optimal H-infinity controller using Krill Herd optimization technique for regulation of pressure inside the settling chamber of Hypersonic wind tunnel (Wang *et al.*, 2014; Wu *et al.*, 2011; Gandomi and Alavi, 2012). The Krill Herd algorithm (KH) is an intelligent nature inspired algorithm, to solve the complex optimization problems, mimicking the herding behaviour of Krill swarms. In this approach, the objective function used in Krill Herd for krill movement is determined by the least distances from food and the highest herd density and the searching is based on random walks. The position of krill consists of three main components viz: movement affected by other krill, foraging action, physical diffusion (Yang and Gandomi, 2012 ;Alfi; Gandomi and Alavi, 2012; Alfi, 2011; Ali *et al.*, 2010). The main advantage of this technique is that only few variables are required for regulation.

Design

The Krill Herd optimization method is used with the H-infinity controller to tune the parameters and weighing functions of the designed H-infinity controller.

The proposed Krill Herd Algorithm is based on Lagrangian model, which states the objective function as combination of the highest density of the krill and the distance

of food from the krill (Yang a. In n-dimensional space, the fitness function of the algorithm for i^{th} krill individual is defined as:

$$\frac{dX_i}{dt} = N_i + F_i + D_i \tag{4.19}$$

where N_i is the motion induced on i^{th} krill individual due to the other krill individuals, F_i is the Foraging motion and D_i is the Random diffusion. The individual krill motion may depend on the neighboring krill's and their mutual effects.

The krill movement direction, α_i depends upon different swarm densities. Thus, the movement of the ith krill individual, N_i is defined as:

$$N_i{}^{new} = N^{max} \alpha_{i+} \omega_n N_i{}^{old} \tag{4.20}$$

where N^{max} is the maximum induced speed, ω_n is Inertia weight, $N_i{}^{old}$ is previous motion induced. The direction α_i is the sum of local effect provided by the neighboring krill individuals and target effect provided by the best krill individual.

The foraging motion is the motion induced to a krill individual due to the presence of food and its previous locations. The foraging motion value for the ith krill individual is as follows:

$$F_i = V_f \beta_f + \omega_f F_i{}^{old} \tag{4.21}$$

where V_f is foraging speed, ω_f is inertia weight of the foraging motion and $F_i{}^{old}$ is the last foraging motion value. The effect of food on the herding mechanism is defined depending on the food's location and β_f is the sum of effect due to the presence of food and the effect due to the current krill's best fitness value recorded.

116

The random diffusion is based on a maximum diffusion speed and a random directional vector, δ and is given by:

$$D_i = D^{max}\delta \qquad (4.22)$$

where D^{max} is the maximum diffusion speed, δ is the random directional vector and its arrays are random numbers (Yang and Gandomi, 2012; Wang *et al.*, 2014; Wu *et al.*, 2011; Gandomi and Alavi, 2012; Alfi and Modares, 2011). Herein, the position in KH from t to (t + Δt) is formulated as follows:

$$X_i(t + \Delta t) = X_i(t) + \Delta t \frac{dX_i}{dt} \qquad (4.23)$$

Where $X_i(t)$ is the related position for the ith krill at time, t.

Fine tuning of weighting functions

Krill Herd (KH) algorithm is mainly focused on random walks and it cannot converge to the satisfactory function value all the time. KH performs well on unimodal functions and several multimodal functions (Yang and Gandomi, 2012; Wang *et al.*, 2014; Wu *et al.*, 2011; Gandomi and Alavi, 2012; Alfi and Modares, 2011).

Krill Herd optimisation algorithm

The steps involved in the design of Krill Herd optimisation algorithm are as follows:

Step 1: Parameter Initialization: initialization of the population of krill randomly and set the foraging speed, V_f, the maximum diffusion speed, D_{max}, the maximum induced speed N_{max}, and the inertia weights.

Step 2: Fitness evaluation. Evaluate each krill individual according to its position.

Step 3: Sort the krill from best to worst. Update the inertia weights. Perform three motions. Update the krill position. Compute their fitness for all krill.

Step 4: Sort the population and find the current best.

Step 5: Output the best solution.

Step 6: End.

The aim of this algorithm is to arrive at minimum distance of the krill individual from food and highest density of the swarm. Thus, the objective of the optimization algorithm is to design optimal values for the H-infinity weights to minimize the variation in the settling time of the settling chamber pressure (Yang and Gandomi, 2012; Gandomi and Alavi, 2012; Alfi and Modares, 2011; Ali *et al.*, 2010). The constraints of the optimization problem is to define the upper and lower limits for the weight function, W_u of the controller.

The optimization parameters used for KH algorithm is given in Table 4.3.

Table 4.3 Details of parameter values initialized in KH Algorithm

Number of krills	40
Number of Iterations	30
Foraging velocity	0.2 m/s
Maximum diffusion	0.005 m/s
Maximum induced speed	0.01 m/s
Inertia for foraging	0.3
Inertia for movement	0.3
Mutation	0.3

The H-infinity multiplicative uncertainty weight, W_u defined in eq. (4.14) can be rewritten as:

$$W_u = \frac{as+b}{cs+d} \tag{4.24}$$

The optimized values of a, b, c and d in H-infinity multiplicative uncertainty weight, W_u are obtained by properly tuning the parameters and thereby finding the optimal objective function based on the Krill Herd optimization algorithm. Thus, we obtain the optimized values of a, b, c and d for the set points, 50×10^5 Pa, 70×10^5 Pa and 100×10^5 Pa respectively are tabulated in Table 4.4, where fx denotes the objective function of the optimization problem.

Table 4.4 Optimized values of the multiplicative uncertainty weight function, W_u.

Set point	a	B	c	d	Fx
50×10^5 Pa	638.97	182.28	11.39	0.000065	1.0e+006 × 5.0000
70×10^5 Pa	664.7149	135.0019	16.5428	0.000137	1.0e+006 × 7.0000
100×10^5 Pa	581.25	225.98	32.21	0.000034	1.0e+007 × 1.0000

Optimization with H-infinity controller

Here, H-infinity controller is first designed and analyzed using a conventional approach. Depending on the performance of the H-infinity controller, parameters are suitably tuned by using Krill Herd optimization technique to improve its performance.

In order to optimize the multiplicative uncertainty weight, W_u of H-infinity control for the tunnel system, the optimal fitting function is obtained as the iteration process progresses. Once the iterative process is over, the global best values for the controller

parameters is obtained from Krill Herd optimization algorithm as in Table 4.4, and is given by eqs. (4.25), (4.26), (4.27) for the representative set points 100×10^5 Pa, 70×10^5 Pa and 50×10^5 Pa respectively.

$$W_u = \frac{638.97s + 182.28}{11.39s + 0.000065} \tag{4.25}$$

$$W_u = \frac{664.71s + 135}{16.54s + 0.00014} \tag{4.26}$$

$$W_u = \frac{581.25s + 225.98}{32.21s + 0.000034} \tag{4.27}$$

Thus, the multiplicative uncertainty weight, W_u selected based on the above equations is in such a way that the magnitude of weight transfer function lies above the plant transfer function and is shown in Fig. (4.10), (4.11) and (4.12) for the same set points respectively.
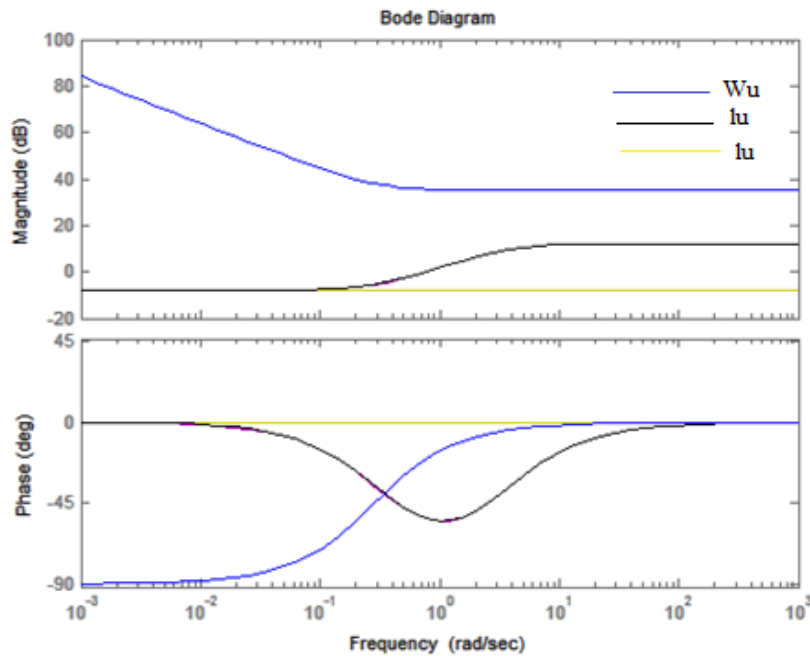
Fig. 4.10   Selection of Multiplicative uncertainty weight, W_u for the set point of 50×10^5 Pa

120
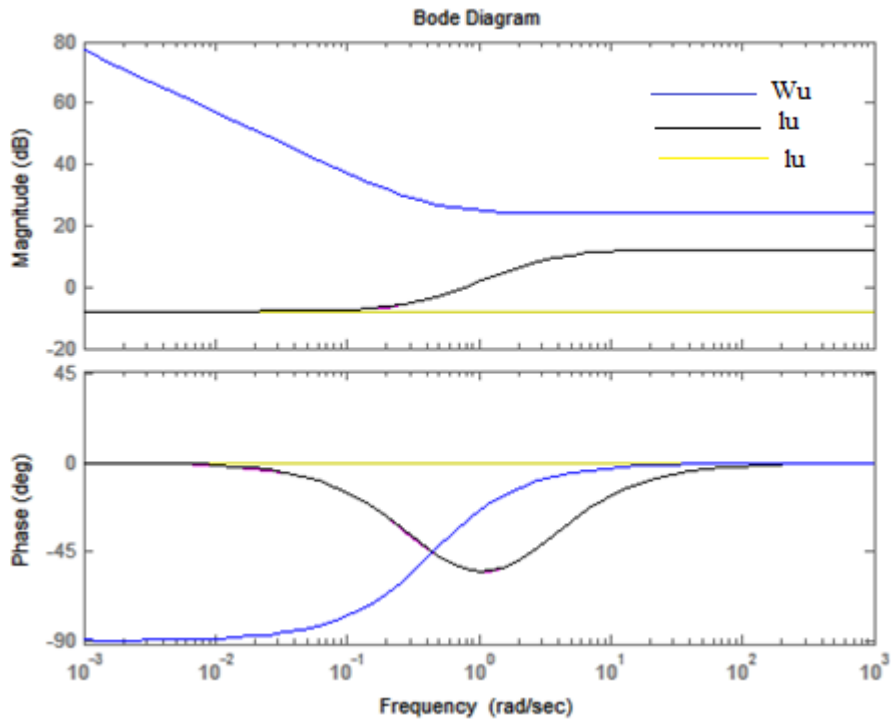
Fig. 4.11   Selection of Multiplicative uncertainty weight, W_u for the set point
of 70×10^5 Pa
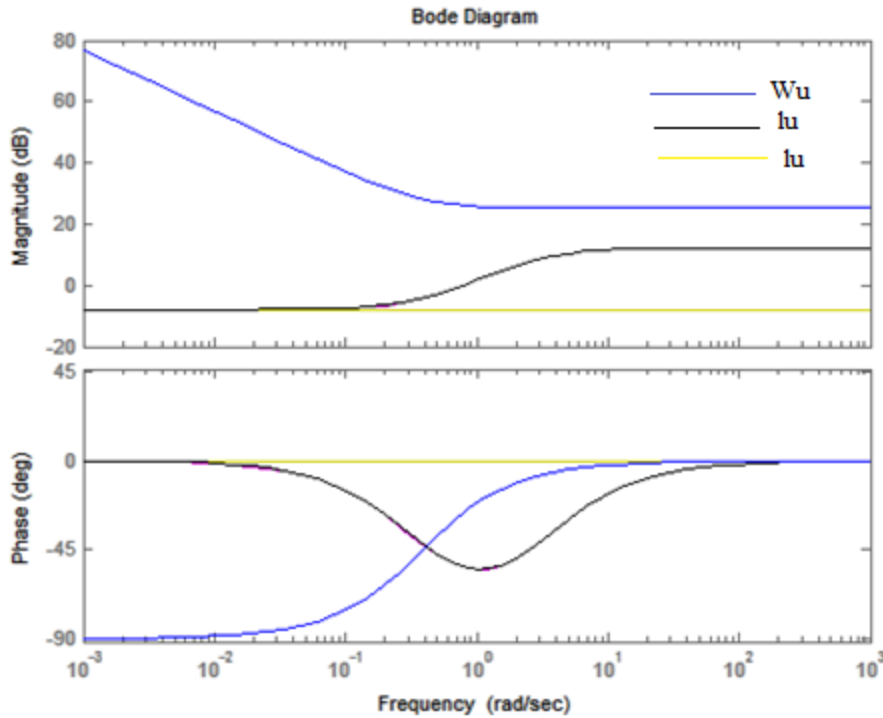
Fig. 4.12   Selection of Multiplicative uncertainty weight, W_u for the set point
of 100×10^5 Pa

Based on the above optimized weights, the response of the settling chamber pressure, P_3 of the tunnel system with H-infinity controller for the set point of 50×10^5 Pa is obtained in Fig. 4.13 (1). Fig. 4.13 (2) shows the zoomed portion of the settling chamber pressure. From the figure, it is observed that the settling chamber pressure of the system initially overshoots and settles down to the set points of 50×10^5 Pa in 1.2 s. The corresponding percentage overshoot is found to be 75 %, rise time is 0.29 s, peak time is 46.17 s and the Gamma value achieved is 1.96.
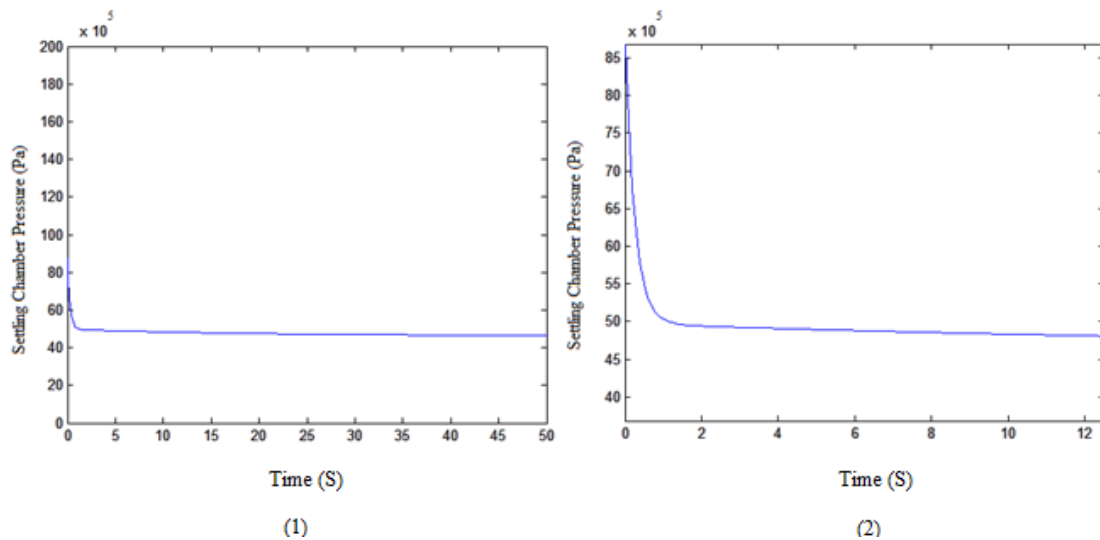
Fig. 4.13 (1) Settling chamber pressure with Optimised H-infinity controller for the set point of 50×10^5 Pa (2) Zoomed portion of (1)

Similarly, the response of the settling chamber pressure, P_3 of the tunnel system with H-infinity controller for the set point of 70×10^5 Pa and 100×10^5 Pa is obtained in Fig. 4.14 and 4.15 respectively.
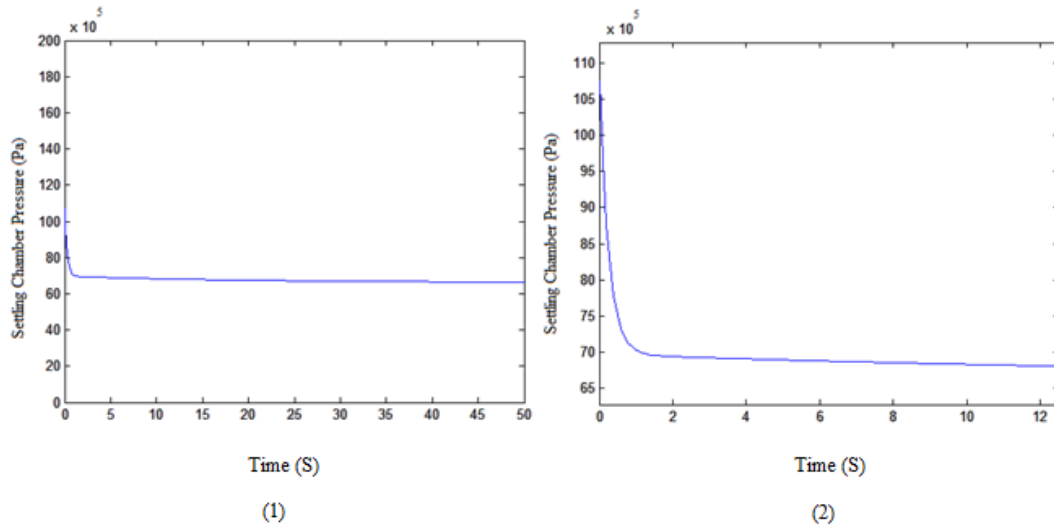
Fig. 4.14   (1) Settling chamber pressure with Optimised H-infinity controller for the set point of 70×10^5 Pa (2) Zoomed portion of (1)
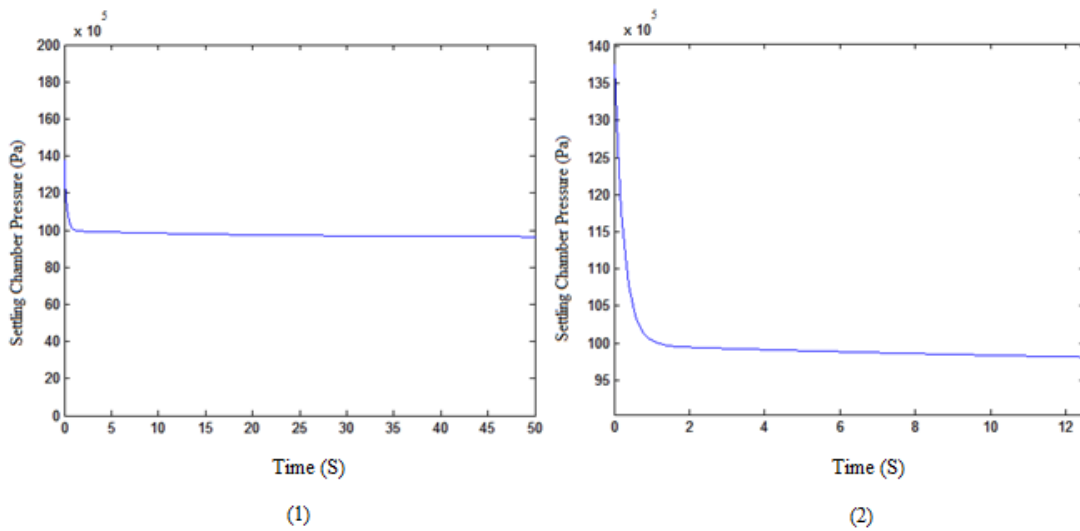
Fig. 4.15   (1) Settling chamber pressure with Optimised H-infinity controller for the set point of 100×10^5 Pa (2) Zoomed portion of (1)

From the Fig. 4.15, it is observed that here also, the settling chamber pressure of the system model initially overshoots and settles down to the set points of 70×10^5 Pa in 1.2 s with rise time of 0.28 s and peak time of 66.17 s. The corresponding percentage overshoot is found to be 53.57 % with the Gamma value 1.96.

123

The response of settling chamber pressure for a set point of 100×10^5 Pa is shown in Fig. 4.15 (1). The zoomed portion is clearly shown in Fig. 4.15 (2). From the figure, it can be observed that the settling chamber pressure settles down in 1.2 s with the rise time, 0.29 s and peak time, 96.17s. However, here also the pressure of the system model initially overshoots the reference model output and is observed to be 37.5 %.

Similar dynamical behavior is observed for other set points in the chosen range. The performance comparison of settling chamber pressure with H-infinity controller and optimized H-infinity controller for the wind tunnel system is shown in Table. 4.5. In the table, ST represents the settling time and PO represents percentage overshoot and RT represents rise time.

Table 4.5   Performance Comparison of H-infinity controller and optimized H-infinity control Technique for Hypersonic wind tunnel

SETPOINT (P_a)	H-INFINITY CONTROLLER			H-INFINITY CONTROLLER WITH WEIGHT OPTIMIZATION		
	ST (s)	PO (%)	RT (s)	ST (s)	PO (%)	RT (s)
50×10^5	1.2	116	0.20	1.2	75	0.29
70×10^5	1.2	83.33	0.85	1.2	53.57	0.28
100×10^5	1.2	58.33	0.85	1.2	37.5	0.29

From the above table, it is clearly evident that the settling time of the above system is same for all the three set points in both H-infinity and its optimized technique. But the percentage overshoot is higher for all the set points using H-infinity controller design. The results show that the optimized design for H-infinity controller is efficient in controlling the settling chamber pressure within a considerably small time range with drastic reduction in overshoot. However, with the optimized design for multiplicative uncertainty weight, W_u, the system is adversely affected by percentage overshoot

which can be further reduced by optimizing other weights of H-infinity controller. The observed percentage overshoot of the settling chamber pressure will drastically affect the safety and performance conditions. Improvement in performance characteristics is possible by suitably optimizing other weight functions with the same technique. From the results, it is clear that with optimized H-infinity control scheme, the chamber pressure of the Hypersonic wind tunnel system stabilises within 1.2 s.

For Hypersonic wind tunnel systems, as the test duration is very short, the settling time is a crucial parameter. The new scheme effectively controls the settling chamber pressure within a very short time. Moreover, with the new scheme even though the percentage overshoot is drastically reduced when compared with conventional H-infinity controller, it is still much more than the desired value. The system performance can further be improved by optimizing other weighing functions of H-infinity controllers and by designing other control schemes.

4.2.3 Backstepping Controller

Backstepping controller is a systematic, nonlinear, recursive design methodology for nonlinear feedback control based on Lyapunov stability theorem. Backstepping is a technique developed in 1990 by Petar V. Kokotovic for designing stabilizing controls for a special class of nonlinear dynamical systems. These systems are built from subsystems that radiate out from an irreducible subsystem that can be stabilized using Lyapunov stability method. The main advantage includes design flexibility due to the recursive use of Lyapunov functions. Because of this recursive structure, the designer can start the design process from stable system and stabilize other subsystems. The process terminates

when the final external control law is reached and hence, the name, Backstepping control (Cooper, 2005; Skjetne and Fossen, 2004; Madani and Benallegue, 2006; Joseph, 2007; Peng, 2008; Farrell *et al.*, 2009). When compared to other control techniques, this approach offers a choice of design tools for accommodation of nonlinearities, and can avoid unwanted cancellations.

Design

Backstepping control is a nonlinear control technique based on Lyapunov stability theory (Cooper, 2005; Skjetne and Fossen, 2004; Madani and Benallegue, 2006; Joseph, 2007; Peng, 2008; Farrell *et al.*, 2009; Rudra and Barai, 2012; Sonneveldt *et al.*, 2007; Yang *et al.*, 2013). These systems are built from subsystems that radiate out from an irreducible subsystem that can be stabilized using Lyapunov technique (Yang *et al.*, 2013). The design process starts from a known-stable system and stabilizes every subsystem by a backout process till final external control is reached (Cooper, 2005; Skjetne and Fossen, 2004; Madani and Benallegue, 2006; Joseph, 2007; Peng, 2008; Farrell *et al.*, 2009; Rudra and Barai, 2012; Sonneveldt *et al.*, 2007; Yang *et al.*, 2013). The Backstepping design involves selecting recursively, some appropriate state variables as virtual inputs for lower dimension subsystems of the overall system and the Lyapunov functions are designed for each stable virtual controller (Cooper, 2005; Skjetne and Fossen, 2004; Madani and Benallegue, 2006; Joseph, 2007; Peng, 2008; Farrell *et al.*, 2009; Rudra and Barai, 2012; Sonneveldt *et al.*, 2007; Yang *et al.*, 2013). Thus, the final control law can guarantee the stability of the entire system.

A. Lyapunov Theory

It is a systematic method for nonlinear control design, which aims to develop a control law that brings the system to the desired state. Here a state vector x(t) is condensed into a scalar function V(x), which is a positive definite function and it satisfies the condition, $\dot{V}(x) \leq 0$. The state, x=0 is the stable equilibrium for such a Lyapunov function. $\dot{V}(x) < 0$ gives the stronger condition of asymptotic stability (Rudra and Barai, 2012; Sonneveldt *et al.*, 2007; Yang *et al.*, 2013).

B. Condition for Backstepping

Backstepping is a technique for designing and stabilizing a special class of nonlinear dynamical systems. The Backstepping approach provides a recursive method for stabilizing the origin of a system in strict-feedback form or lower triangular form as given below.

$$\dot{x_1} = f_1(x_1, x_2)$$

$$\dot{x_{n-1}} = f_{n-1}(x_1, \dots \dots x_{n-1}, x_n)$$

$$\dot{x_n} = f_n(x_1, \dots \dots, x_n, u) \tag{4.28}$$

where $x_1, x_2, \dots, x_n$ are the state variables and u is the controller input. For systems that cannot be written in a lower triangular form, some physical properties are neglected to get the required form. Our aim is to construct a control law based on Lyapunov stability

theory that brings the system to or at least near, some desired state (Farrell *et al.*, 2009; Rudra and Barai, 2012; Sonneveldt *et al.*, 2007; Yang *et al.*, 2013).

C. Controller Design

The state equations of the tunnel system (Jones *et al.*, 2011a; Jacob and Binu, 2009; Jones *et al.*, 2011b; Echman, 1958; Liptak, 1995), in chapter (3), eq. (3.27) and (3.28) are brought to strict feedback form as detailed in Appendix 2 and is represented as,

$$\dot{X}_1 = 22.67X_2 - 24.92X_1 \tag{4.29}$$

$$\dot{X}_2 = 0.08X_3 - 4.36X_2 + 4.36X_1 + 6366996.94 \tag{4.30}$$

$$\dot{X}_3 = -0.005X_3 - 628484.36u \tag{4.31}$$

Now Backstepping is applied (D'souza *et al.*, 2015; Libii, 2011; Jones *et al., 2011a*) to the subsystem in eq. (4.29) and the first control Lyapunov function is selected as

$$V_1(x) = \frac{1}{2} X_1^{\,2} \tag{4.32}$$

The desired value of X_2 to make $\dot{V}_1$ negative definite is given by

$$X_2(des) = -c_1 X_1 \tag{4.33}$$

Now introduce a variable Z_1, which is deviation of X_2 from its desired value and Z_2 is the error variable corresponding to X_2. The augmented Lyapunov function for the above sub-system is given by

$$V_2(x) = \frac{1}{2}X_1{}^2 + \frac{1}{2}Z_1{}^2 \qquad (4.34)$$

The desired value of X_3 to make $\dot{V}_2$ negative definite is given by

$$X_3(des) = \frac{1}{0.08}\left(\frac{-c_2Z_1 - 22.67X_1Z_1 + 24.92X_1{}^2}{Z_1} - 6366996.94 + 4.36Z_1 + \right.$$
$$\left. 20.57c_1X_1 - 4.36X_1 - 22.67c_1Z_1 + 22.67c_1{}^2X_1\right) \qquad (4.35)$$

The second error variable is Z_2 and the system is represented in terms of Z_1 and Z_2 instead of X_2 and X_3. Thus, the third Lyapunov function is

$$V_3(x) = \frac{1}{2}X_1{}^2 + \frac{1}{2}Z_1{}^2 + \frac{1}{2}Z_2{}^2 \qquad (4.36)$$

The desired value of u to make $\dot{V}_3(x)$ negative definite is given by

$$u(des) = \frac{1}{628484.36}\left(-0.005(Z_2 + X_3(des)) - \dot{Z}_2 - c_3Z_2\right) \qquad (4.37)$$

Results and Discussion

This section describes the results for the designed Backstepping controller of the Hypersonic wind tunnel. Fig. 4.16 (1) shows the settling chamber pressure with Backstepping controller for three different set points, 50×10^5, 70×10^5 and 100×10^5 Pa respectively with the operating temperature, $T_1 = 300$ K, $T_2 = 700$ K and $T_3 = 539$ K (Jones *et al.*, 2011a; Jacob and Binu, 2009; Jones *et al.*, 2011b) where the zoomed portion is shown in Fig. 4.16 (2). It is observed that there is no overshoot for all the three set points. The settling time is 7.5, 7 and 6.5 s, the rise time is observed to be 3.44, 3.59, 3.59 s and peak time 19.21, 19.88, 19.88 s for the same three setpoints.
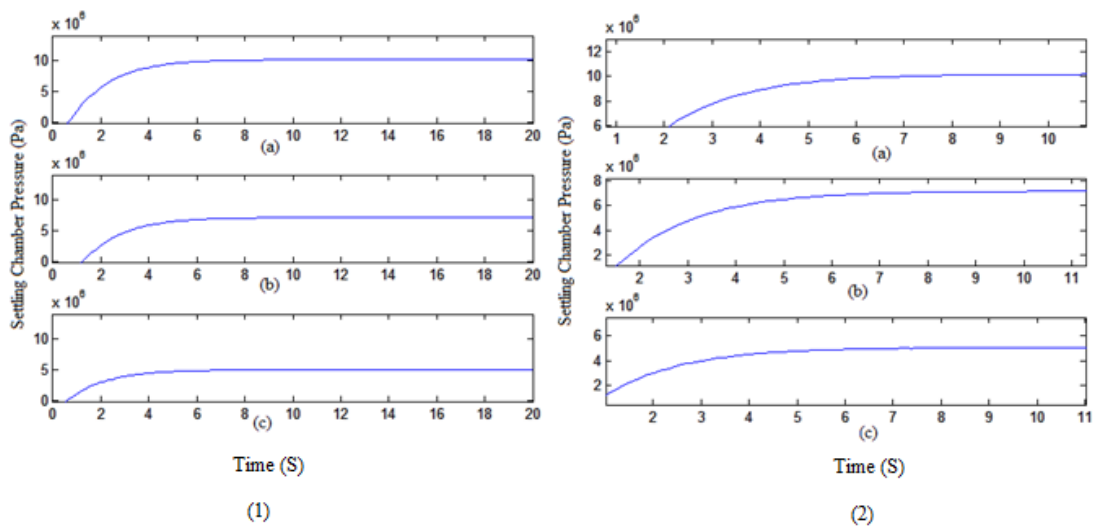
Fig. 4.16   Settling chamber pressure with Backstepping controller for the set point 100×10^5, 70×10^5 and 50×10^5Pa

Fig. 4.17 shows the Backstepping controller output for a sample setpoint of 100×10^5 Pa. It takes 9 s to completely release the valve, which corresponds to the stem movement of 0.23 mm.
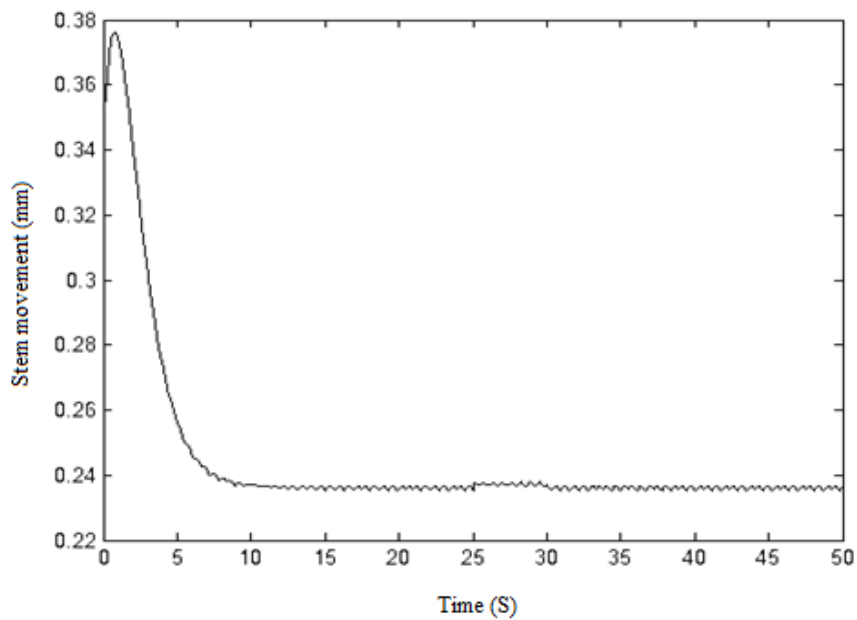
Fig. 4.17 Backstepping controller output, u

In order to study the effect of temperature on the performance of the designed Backstepping controller, a small step change is made in temperature T_3 from 539 K to 508 K at time equals 25 s with a set point of 70×10^5 Pa. Fig. 4.18 (a) shows the variation in temperature corresponding to the above conditions and Fig. 4.18 (b) shows the corresponding variation in settling chamber pressure.
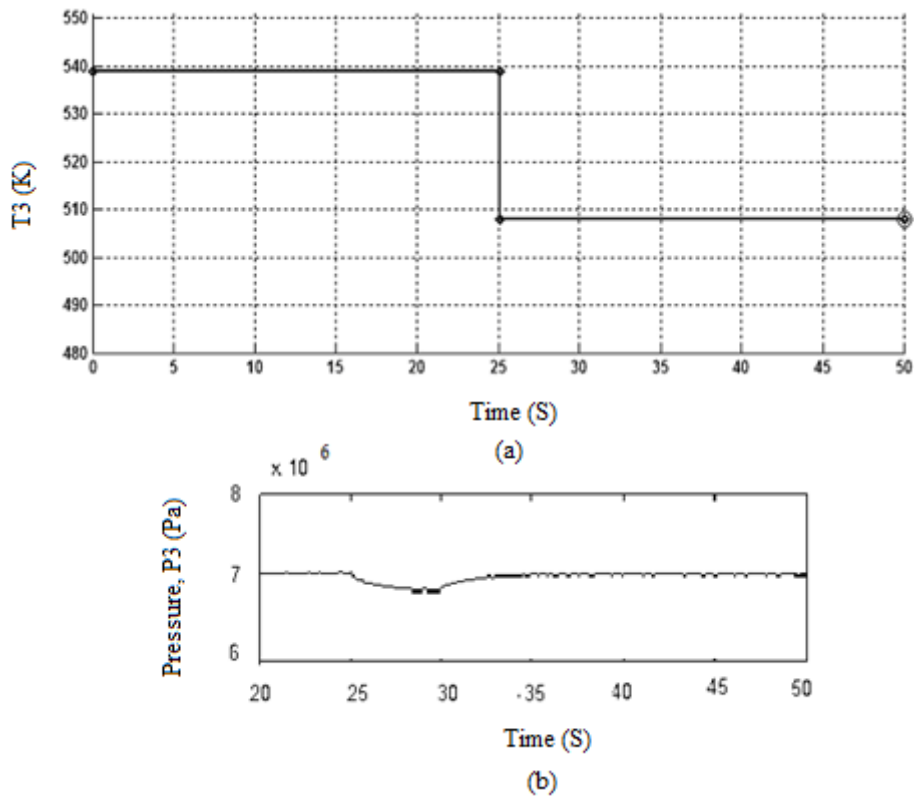
Fig. 4.18   Settling chamber pressure using Backstepping controller with disturbance in temperature, T_3 for a set point of 70×10^5 Pa

From the Fig. 4.18 (b), it is observed that the settling chamber pressure drops slightly from 70×10^5 Pa to 68×10^5 Pa for a duration of 10 s and it settles back at 70×10^5 Pa at time equals to 35 s. The variation in settling chamber pressure corresponding to this change in temperature is quite negligible.

Thus, with the designed Backstepping algorithm, the response of settling chamber pressure has less settling time without any overshoot. However, considering the complexity in design and the difficulty in measuring all the variables, we suggest Sliding mode approach to the tunnel system.

4.2.4 Sliding mode controller

Sliding mode controller is a nonlinear, discontinuous control technique suitable for a large number of industrial applications because of it is varied properties, viz: robustness, invariance, and order reduction (Saravanakumar *et al.*, 2009; Musmade *et al.*, 2011). It is a systematic approach to transform higher order systems to lower order systems. The design of Sliding mode control involves construction of switching surface and development of a switching control law. The system, which is completely insensitive to parametric uncertainties and external disturbances utilizes a high speed switching control law to drive the non-linear plants state trajectory onto a specified and user chosen surface in the state space (Saravanakumar *et al.*, 2009; Musmade *et al.*, 2011; Utkin, 1977; Tan *et al.*, 2005; Utkin, 1993; Shyu and Shieh, 1996; Li *et al.*, 2012). This helps to maintain the plant state trajectory on this surface throughout the operating time. If the state trajectory of the plant is above the surface, the control path has one gain and it has a different gain if the trajectory drops below the surface. The state variables of the plant dynamics are constrained to satisfy another set of equations, which defines the switching surface. After reaching the switching surface, our system depends on the slope of the switching line, based on which the equivalent control law is derived (Terra-Moura *et al.*, 2007; Mondal and Chitralekha, 2013; Ding *et al.*, 2013; Hong *et al.*, 2005; Young *et al.*, 1999). The control law should satisfy a set of sufficient

conditions for the existence and reachability of a sliding mode (Shyu and Shieh, 1996; Li *et al.*, 2012; Terra-Moura *et al.*, 2007; Mondal and Chitralekha, 2013; Ding *et al.*, 2013; Hong *et al.*, 2005; Iggidr *et al.*, 1996; Young *et al.*, 1999).

Design

In the method of equivalent control, we determine the system motion restricted to the switching surface S = 0 (Shyu and Shieh, 1996; Li *et al.*, 2012; Terra-Moura *et al.*, 2007; Mondal and Chitralekha, 2013; Ding *et al.*, 2013; Hong *et al.*, 2005; Iggidr *et al.*, 1996; Young *et al.*, 1999). The sliding surface is selected in such a manner that the state variables converge to it for the development of the equivalent controller. The most important step in the design of sliding mode controllers is to introduce a proper sliding surface so that the errors and output deviations are reduced to a satisfactory level in practical applications. However, this method introduces some drawbacks such as chattering effect and limited flexibility for the designer with a sliding function. The chattering is due to the inclusion of the sign function in the switching term and it can cause the control input to start oscillating around the zero sliding surface, resulting in unwanted disturbances in the output. The sliding mode control based on a PI sliding surface improves performance of control systems and address issues related to the control and demonstrates applicability of the proposed control as an alternative method to traditional sliding mode and PID control in real time applications. The sliding surface, S is a function of state variables X_1, X_2, X_3 and is designed in such a manner that X_3 converges to it for developing the control law as,

$$S = C_3 X_3 + X_2 + X_1 \tag{4.38}$$

133

where C_3 is a constant gain. For the development of control law, the state equations are determined from the state model given in eq. (3.14), (3.27) & (3.28) of chapter (3). The state equations for the system given in eq. (4.29) to (4.31) is,

$$\dot{X}_1 = 22.67\,X_2 - 24.92\,X_1$$

$$\dot{X}_2 = 0.0776X_3 + 636696.94 - 4.355\,X_2 + 4.355X_1$$

$$\dot{X}_3 = -0.004597\,X_3 - 628484.36\,u$$

Using the sliding surface in eq. (4.38), the Lyapunov function is chosen (Saravanakumar *et al.*, 2009; Musmade *et al.*, 2011; Utkin, 1977; Tan *et al.*, 2005; Utkin, 1993; Shyu and Shieh, 1996; Li *et al.*, 2012; Terra-Moura *et al.*, 2007; Mondal and Chitralekha, 2013) as

$$V = \frac{1}{2}S^2 \tag{4.39}$$

The derivative of this function is given by,

$$\dot{V} = S\dot{S} \tag{4.40}$$

$\dot{V}$ is negative definite if,

$$S\dot{S} = \begin{cases} < 0 \; if \; S > 0 \\ = 0 \; if \; S = 0 \\ > 0 \; if \; S < 0 \end{cases} \tag{4.41}$$

The equivalent controller can be found using the above equations (Saravanakumar *et al.*, 2009; Musmade *et al.*, 2011; Utkin, 1977; Tan *et al.*, 2005). The control law is given by,

$$U_{eq} = \beta - k\,sign(s) \tag{4.42}$$

where the gain k is chosen as 1 and equivalent control law, β is obtained from eqs. (4.38) to (4.42) and is detailed in Appendix 3 and is given by,

$$\beta = \frac{1}{628484.36}\begin{pmatrix} -0.0045X_3C_3 \ + \ 0.077X_3 \ + \ 636696.94 - 4.35X_2 \ + \\ 4.35X_1 + 22.67X_2 - \ 24.92 \ X_1 \end{pmatrix} \quad (4.43)$$

Results and Discussion

The Sliding mode controller for regulating the pressure inside a Hypersonic wind tunnel is designed and simulated. The tunnel system is simulated for three sample set points, 50×10^5Pa, 70×10^5Pa and 100×10^5 Pa. The operating condition is maintained at temperatures, $T_1 = 300$ K, $T_2 = 700$ K and $T_3 = 539$ K (Jones *et al.*, 2011a; Jacob and Binu, 2009; Jones *et al.*, 2011b) where T_1, T_2, T_3 are temperatures in three pressure vessels respectively.

Fig. 4.19 (1) show the pressure in the three vessels, P_1, P_2 and P_3 with sliding mode controller for the set point, 50×10^5 Pa where its zoomed portion is shown in Fig. 4.19 (2). Fig. 4.19 (a) shows the pressure P_1 inside the air storage tank which is regulated at 300×10^5 Pa. Fig. 4.19 (b) and (c) shows the pressure P_2 from heater and P_3 from settling chamber respectively. Fig. 4.19 (b) indicates that P_2 settles to the given set point with a settling time of 8 s without any overshoot and from Fig. 4.19 (c), it is clear that the pressure P_3 also settles to the set point of 50×10^5 Pa with settling time of 7 s without any overshoot and chatter effect.
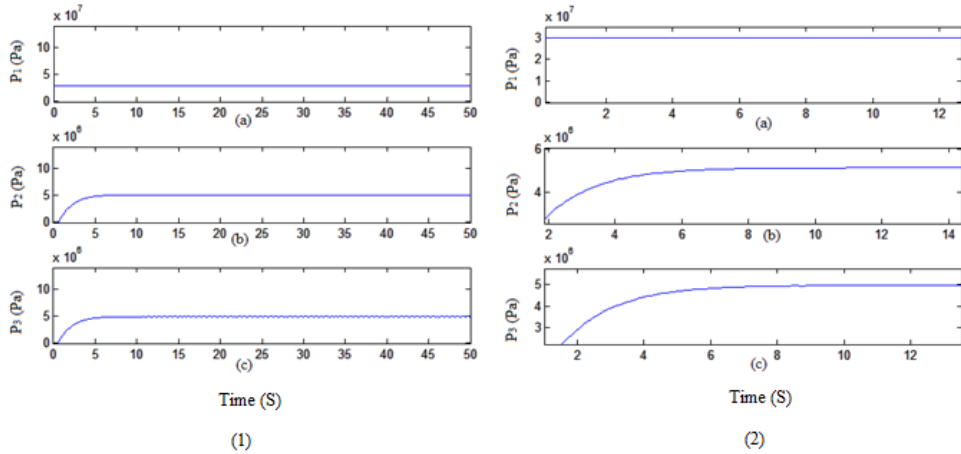
Fig. 4.19   (1) Pressures in the three vessels, P_1, P_2 and P_3 with Sliding mode
controller for the set point 50×10^5 Pa (2) Zoomed portion of (1)

Fig. 4.20 (1), (2) (a), (b) and (c) shows the pressure in the three vessels, P_1, P_2 and P_3 with Sliding mode controller for set points of 70×10^5 Pa where its zoomed portion is shown in Fig. 4.20 (2). Fig. 4.20 (a) shows the pressure, P_1 inside the air storage tank and is regulated to 300×10^5 Pa. Fig. 4.20 (b) and (c) shows the pressure, P_2 from heater and P_3 from settling chamber respectively. Fig. 4.20 (b) indicates that P_2 settles to the given set point with a settling time of 8 s without any overshoot and from Fig. 4.20 (c), it is clear that the pressure P_3 also settles to the set point of 70×10^5 Pa with settling time of 8 s without any overshoot and chatter effect.
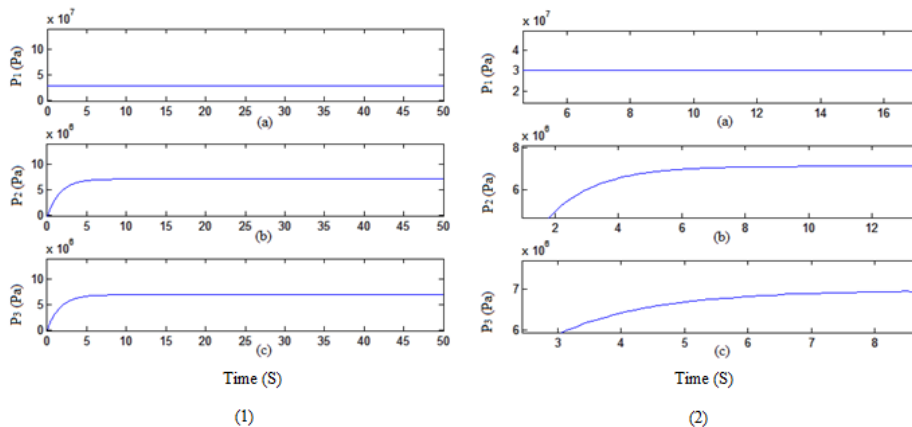
Fig. 4.20   (1) Pressures in the three vessels, P_1, P_2 and P_3 with Sliding mode
controller for the set point 70×10^5 Pa (2) Zoomed portion of (1)

136

Fig. 4. 21 (1) (a), (b) and (c) show the pressures in the three vessels, P_1, P_2 and P_3 with set points of 100×10^5 Pa and its zoomed portion is shown in Fig. 4.21 (2). Fig. 4.21 (a), shows that the pressure in vessel 1 is regulated at 300×10^5 Pa and Fig. 4.21 (b) shows that the pressure from heater settles at 100×10^5 Pa with a settling time of 8 seconds without any overshoot. From Fig. 4.21 (c), it is observed that the settling chamber pressure, P_3 settles to the given set point of 100×10^5 Pa with a settling time of 7.5 s without any overshoot and chatter effect. The rise time is observed to be 3.46 s and peak time is 44.89 s for all the three setpoints, 50×10^5 Pa, 70×10^5 Pa, 100×10^5 Pa respectively.
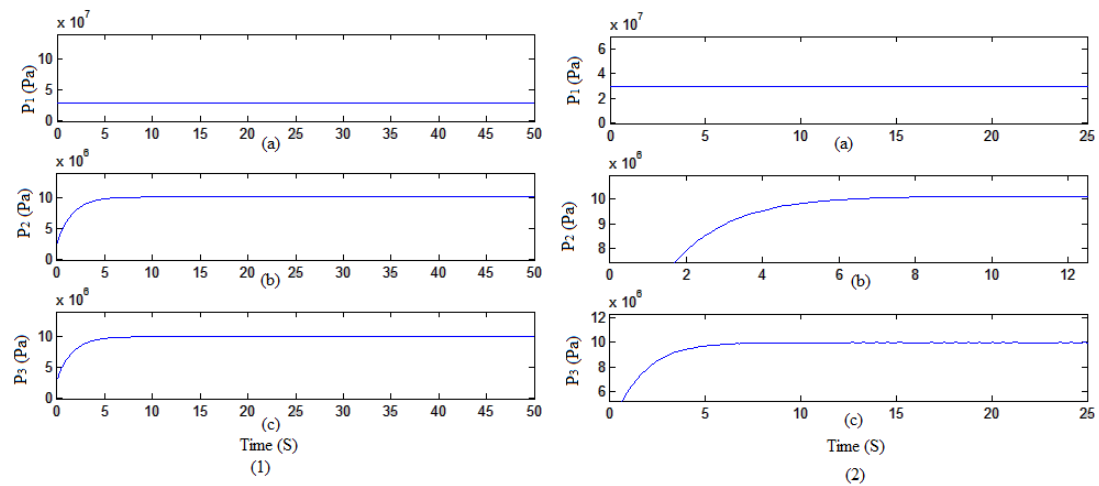
Fig. 4. 21   (1) Pressures in the three vessels, P_1, P_2 and P_3 with Sliding mode controller for the set point of 100×10^5 Pa (2) Zoomed portion of (1)

Fig. 4.22 shows the Sliding mode controller output, u in terms of the stem movement in millimeters for a sample setpoint of 100×10^5 Pa.
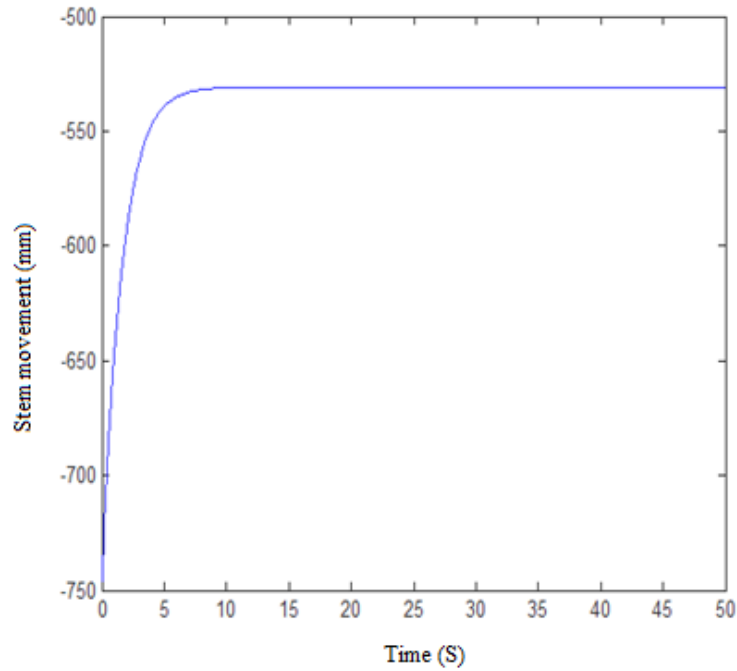
Fig. 4.22 Sliding mode controller output, u for a sample set point of 100×10^5 Pa

From this figure, it is clear that the stem movement is regulated for both the set points and it remains constant at the point where the chamber pressure settles in 7.5 s without chattering effect.

The proper choice of signum function for the development of control law results in improved performance of the Sliding mode controller with reduction in chatter effect.

4.3 Performance Analysis

This section emphasizes on the effectiveness of various controllers for regulation of settling chamber pressure inside the Hypersonic wind tunnel. The stability for the tunnel system is ensured using Lyapunov stability theorem and controllability and observability are confirmed using Kalman's test in chapter 3. The control law is developed for regulating the settling chamber pressure using LQR and other Robust

controllers, viz: H-infinity (HI), H-infinity optimization (HIO), Backstepping (BS) and Sliding mode controllers (SMC). The system is simulated and the performance is evaluated for the range of set points from 1×10^5 Pa to 300×10^5 Pa, from which representative results of sample 3 setpoints, 50×10^5 Pa, 70×10^5 Pa and 100×10^5 Pa are analyzed and their performance are compared. The performance comparison of the designed controllers are given in Table. 4. 6.

Table. 4.6 Performance comparison of the designed controllers.

Set point	Settling Time (s)				Peak Overshoot (%)					Rise Time (s)			
	LQR	HI	HIO	BS	SMC	LQR	HI	HIO	BS	SMC	LQR	HI	HIO	BS	SMC
50×10^5 Pa	15	1.2	1.2	7.5	8	25.38	116	75	NIL	NIL	1.43	0.20	0.29	3.44	3.46
70×10^5 Pa	15	1.2	1.2	7	8	26.25	83.33	53.57	NIL	NIL	1.52	0.85	0.28	3.59	3.46
100×10^5 Pa	15	1.2	1.2	6.5	8	29	58.33	37.5	NIL	NIL	1.43	0.85	0.29	3.59	3.46

From Table 4.6, it is clear that with LQR controller, the settling time is 15 s and rise time is less than 2 s for the three setpoints, whereas the percentage overshoot increases drastically with increase in set point. In order to meet the performance requirement with reduction in overshoot, the weighing functions of LQR controller are increased and the performance is evaluated. To reduce the overshoot further and to improve the settling time, we designed various robust controllers. Initially we design H-infinity controller and from the results it is observed that settling time is less and is 1.2 s for a given setpoint. However, the percentage overshoot is higher for all the set points using the above H-infinity control design. Thus, the H-infinity controller weights are optimized using Krill Herd optimization algorithm. The KH control algorithm is found to be efficient in reducing the overshoot related to selecting weighing functions of H-infinity controller for the Hypersonic tunnel system and is found to be in the range 37 to 75 %. The observed percentage overshoot of the settling chamber pressure will drastically affect the safety and performance conditions. Improvement in performance characteristics is possible by suitably optimizing other weight functions also using the same technique. However, both the control technique couldn't reduce the overshoot to tolerable limit. With the increased values of weighing functions, it is observed that overshoot reduces and is in the range of 25 to 29 % for a given set point with a settling time of 1.2 s. Therefore, we designed Backstepping and Sliding mode controllers for the regulation of settling chamber pressure.

The Backstepping control design focuses on systematic and recursive design methodology for nonlinear feedback control. Thus, we applied Backstepping controller to the tunnel system and from the results, it is found that overshoot is

141

completely eliminated for all set points and the settling time is less than 8 s. But it is noticed that the settling time is not stable for all the set points. From the results, it is clear that even though the Backstepping controller has the advantages of faster response with no overshoot and chatter effect, it has certain drawbacks in terms of sensitivity to parametric variations. Thus, we designed Sliding mode controller to overcome the complexity in design and to stabilize the settling time for a given set point. Sliding mode controller when used independently gives satisfactory performance in terms of settling time and overshoot but has its own limitations with respect to inherent chattering. The Sliding mode controller has the chances of generating chatter in the controlled variable whereas Backstepping controller is sensitive to parametric variations.

Controller design is very important for maintaining the desired environment in the test section and also increasing the consistency and cost effectiveness of the experimental test run (Jones *et al.*, 2011a; Jones *et al.*, 2011b; Bhoi and Suryanarayana, 2008). To study the effectiveness of any proposed controller, it is advisable first to apply it on mathematical model before implementing on large-scale systems. This chapter presents the design of Linear Quadratic Regulator (LQR) controller and Robust controllers viz: H-infinity controllers, Backstepping Controller (BC), Sliding mode controller (SMC) (Jacob and Binu, 2009; Nott *et al.*, 2008; Bhoi and Suryanarayana, 2008; Bottasso *et al.*, 2014; Hwang and Hsu, 1998; Yin and Zhang, 2006). Results of numerical simulation of the designed controllers and their performance evaluation is presented in this chapter.

These popular techniques are not efficient enough to meet the desired transient performance of the system. Considering the limitations with Backstepping and Sliding mode controller, suitable Hybrid control schemes are proposed in chapter 5. This chapter deals with design and numerical analysis of combination of different controllers, Viz: Backstepping Sliding mode controller (BSMC) and Sliding mode Fuzzy controller (SFC). Appropriate combination of these controllers can guarantee stability and robustness to parametric uncertainties with minimal chatter effect. The performance characteristics of the proposed Hybrid controllers are compared with those of existing LQR and Robust controllers (Ogata, 2002; Yin and Zhang, 2006; Huang and Zhou, 2004; Yadav *et al.*, 2012). The combination approach is proposed to overcome the limitations of these controllers when used individually.

CHAPTER 5

DESIGN AND ANALYSIS OF HYBRID CONTROLLERS

This chapter proposes the design of two new controllers, Backstepping sliding mode controller (BSMC) and Sliding mode fuzzy controller (SFC), by combining Sliding mode controller (SMC) with Backstepping (BC) as well as Fuzzy controllers, for the regulation of pressure inside the settling chamber of a Hypersonic wind tunnel. Backstepping controller is a systematic non-linear control based on Lyapunov stability of different subsystems of the main system that ensures appropriate control design for a stable system which can also accommodate non-linearities. Sliding mode controller (SMC) transforms a relatively higher order system to a lower order system. Appropriate combination of these two controllers guarantees stability and robustness to parametric uncertainties with minimal chatter effect. Fuzzy controller is an intelligent controller based on Fuzzy logic rules which is simple to design. On suitable combination with Sliding mode control, these techniques will improve the stability of the system meeting the required performance parameters.

The combination approach is proposed to overcome the limitations of the above controllers when used individually. Sliding mode controller is an efficient control technique to solve higher order non-linear, uncertain, complex problems maintaining stability & consistent performance in the face of modeling imprecision (Musmade *et al.*, 2011; Utkin, 1977; Utkin, 1993; Shyu and Shieh, 1996). This controller has an inherent property of robustness to parametric uncertainties which avoids the requirement of accurate system model. But the Sliding mode controller has the

inherent disadvantage of generating chatter in the controlled variable, which means the state variable is continuously crossing the surface rather than remaining constant on it (He and Luo, 2004; Ackermann and Utkin, 1998; Tan *et al.*, 2008). Backstepping controller design is a flexible non-linear technique, which does not require cancellation of useful non-linearities. The algorithm is a systematic way of constructing the Lyapunov function along with the control input design. The major steps involved in the design is to break the entire system into smaller subsystems thus designing intermediate control laws (Farrell *et al.*, 2009; Rudra and Barai, 2012; Sonneveldt *et al.*, 2007). The limitation with Backstepping controller is that it is sensitive to parametric variations, which finds it difficult for such applications when used alone. Suitable combination of these controllers can provide robustness to parametric uncertainties with chatter free response and minimum overshoot (Ackermann and Utkin, 1998; Tan *et al.*, 2008). Also, as both control technique involve decoupling of overall system into partial components of lower dimensions, complexity of feedback design is reduced. Fuzzy controllers have an important property of decision making based on IF - THEN rules, which have the ability to deal with uncertainty (Mankad *et al.*, 2011; Liu and Tong, 2014; Srinivasan and Raajarajan, 2017). Intelligence of the Fuzzy logic when combined with Sliding mode control technique, ensures a stable controller which gives faster, chatter free response with minimum overshoot (Palmi, 1994; Lin *et al.*, 1997; Wong *et al.*, 2001; Tong *et al.*, 2014; King and Mamdani, 1977). Performance comparisons show that the proposed Backstepping Sliding mode controller outperforms the Sliding mode Fuzzy controller as well as other existing and designed controllers in terms of the performance parameters viz: settling time, overshoot and chatter effect.

Fuzzy controller is an intelligent controller based on Fuzzy logic where the analog inputs are processed using logical rules. Fuzzy control technique has the drawback associated with stability, which can be overcome by suitable combination with other control techniques. Sliding mode control when used in combination with Fuzzy logic will improve stability of the system, as well as robustness to parametric variations. The inherent drawback of chattering of Sliding mode control can be reduced by properly selecting fuzzy rules based on its membership functions (MF).

For each of the proposed Hybrid controllers, the characteristics of the tunnel system is simulated for the set points ranging from 1 x 10^5 Pa to 300×10^5 Pa, keeping the temperatures in the three vessels at $T_1 = 300\,K$, $T_2 = 700\,K$ and $T_3 = 539\,K$ respectively. The performance of the proposed controllers are evaluated based on $\pm\,5\%$ tolerance band of settling time. Here we present the design and analysis of Backstepping Sliding mode and Sliding mode Fuzzy controller for regulation of pressure inside the settling chamber of Hypersonic wind tunnel.

5.1. BACKSTEPPING SLIDING MODE CONTROLLER (BSMC)

In order to improve the performance in terms of settling time and overshoot, here we propose to suitably combine the Sliding mode controller with Backstepping controller. Backstepping controller technique developed by Petar V. Kokotovic and others aimed at designing stabilizing controls for a special class of nonlinear systems. Backstepping control technique is a recursive procedure, which breaks the full system into a sequence of multiple lower order systems. This involves construction of Lyapunov function along with the control input design. This ensures appropriate control design for a stable system, which can accommodate system nonlinearities that are usually cancelled or

146

reduced in other approaches (Farrell *et al.*, 2009; Rudra and Barai, 2012; Sonneveldt *et al.*, 2007). However, Backstepping controller has a general drawback of being sensitive to parametric variations, and that it requires all measurable variables for its design. Sliding mode controller (SMC) is a reliable and robust approach, which transforms a relatively higher order system to a lower order system (Musmade *et al.*, 2011, Utkin, 1977, Utkin, 1993, Shyu and Shieh, 1996; He and Luo, 2004; Ackermann and Utkin, 1998; Tan *et al.*, 2008). The main advantage of Sliding mode controller is that it can handle all system non-linearities, robustness and has properties of the desired dynamics, Lyapunov stability, finite-time convergence. However, it has the drawback that the above control scheme generates chattering in the output response. Thus, combining Backstepping with Sliding mode controller known as Backstepping Sliding mode controller merges the advantages of both Backstepping and Sliding mode controller thereby ensures robustness to parametric uncertainties, tracking trajectory and stability with minimal chatter effect and overshoot (Musmade *et al.*, 2011; He and Luo, 2004; Xia et al., 2013; Ma *et al.*, 2005).

5.1.1 Design

Backstepping is a nonlinear control technique, which initially breaks the entire system into multiple subsystems and designing control law for each subsystem. This technique aims at designing stabilizing control by constructing appropriate Lyapunov function for each subsystem, resulting in a virtual control for the next step. This is accomplished by determining the virtual control satisfying the Lyapunov function in such a way as to guarantee stability for each subsystem. Before designing the Backstepping controller, the system is brought to strict feedback form (Rudra and Barai, 2012; Sonneveldt *et al.*, 2007) as discussed in Chapter 4.

Sliding mode controller is an influential non-linear control technique, first proposed in early 1950 by Emelyanov, whose design includes constructing a switching surface and thereby developing respective switching control law. Thus, the system motion restricted to the switching surface S = 0 is found, and thereby the control law satisfying the sufficient conditions for the existence and reachability of a Sliding mode is determined. A Sliding mode controller is designed by properly selecting the sliding surface whereas for Backstepping control, new update functions are obtained by properly choosing the Lyapunov functions.

The block diagram describing the design procedure for BSMC (Xia et al., 2013; Ma et al., 2005) is shown in Fig. 5.1. For designing BSMC, it should be ensured that the system is in strict feedback form (Farrell et al., 2009; Rudra and Barai, 2012). Therefore, it is ensured that at each step of Backstepping control (Xia et al., 2013; Ma et al., 2005), the new update tuning function and the defined error variables leads to equilibrium position. The equivalent control law for BSMC is obtained by selecting three sliding surfaces for use with each steps of Backstepping control thereby defining new states. Further, the control law for a Backstepping controller in eq. (4.29) to (4.37) in chapter (4) is coupled to the above BSMC control law to obtain a final stable control law. This completes the design scheme for BSMC with coupling.
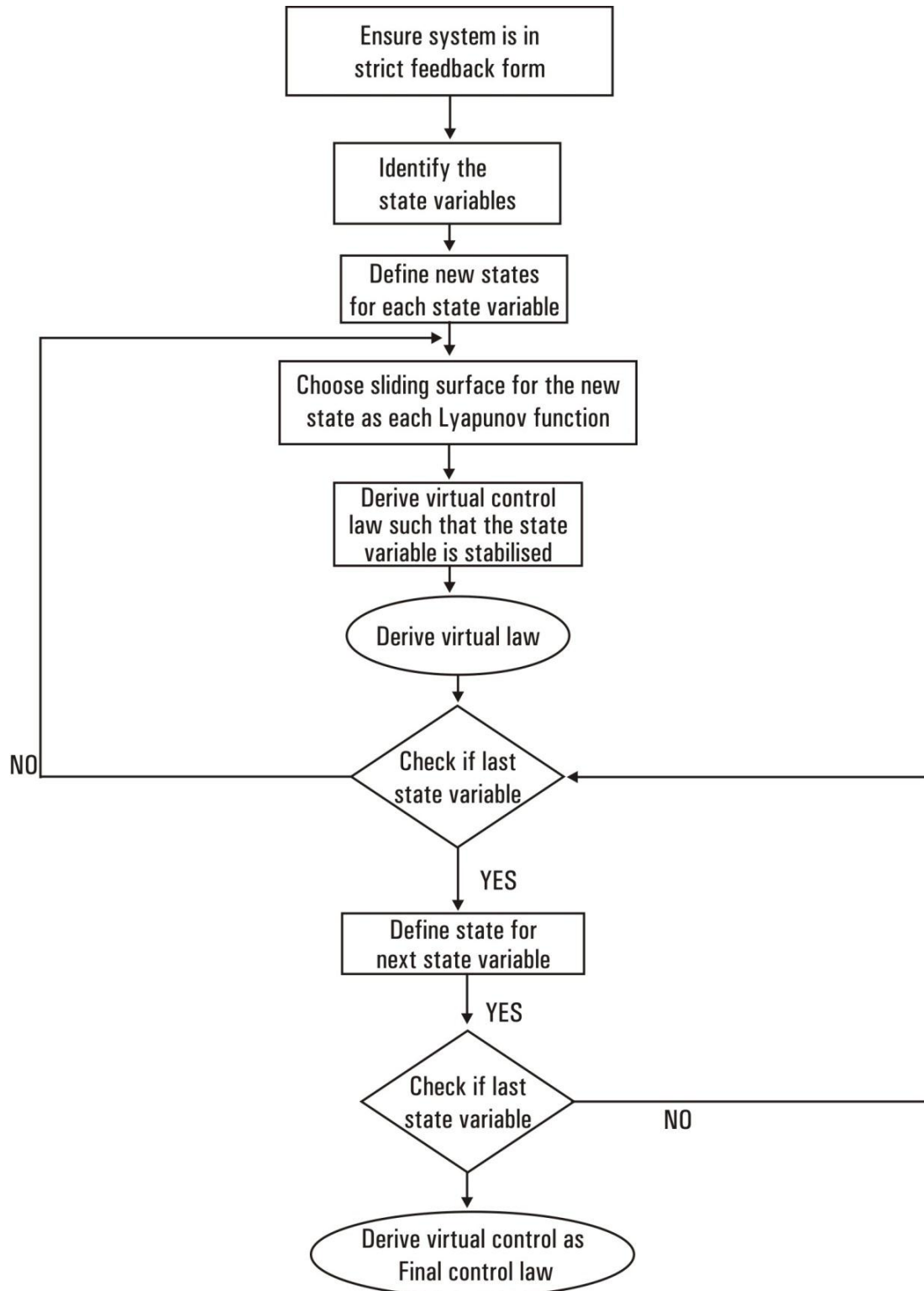
Fig. 5.1 Block Diagram for Backstepping Sliding mode controller.

In order to design BSMC for pressure regulation inside the Hypersonic tunnel system, the state space equation in chapter (3), eq. (3.27) and (3.28) and eq. (4.29) to (4.31) in chapter (4) is modified so as to adhere to the condition for the system to be in strict feedback form which can be represented as,

$$\dot{X}_1 = 22.67\,X_2 - 24.92\,X_1 \tag{5.1}$$

$$\dot{X}_2 = 0.0776X_3 - 4.355X_2 + 4.355X_1 + 6366996.94 \tag{5.2}$$

$$\dot{X}_3 = -0.004597X_3 - 628484.36u \tag{5.3}$$

Based on the design law for BSMC, the new states, Z_{s1} and Z_{s2} are introduced (Ma et al., 2005) which are defined as,

$$Z_{s1} = X_1 \tag{5.4}$$

$$Z_{s2} = X_2 - \propto_{s1} \tag{5.5}$$

where $\propto_{s1}$ is the virtual control. The derivative of Z_{s1} is obtained by substituting eq. (3.1) in (3.4) in chapter (3) and is given by,

$$\dot{Z}_{s1} = \dot{X}_1 = 22.67X_2 - 24.92\,X_1 \tag{5.6}$$

To decide the virtual control $\propto_{s1}$ which stabilizes X_1, the first sliding surface S_1 is chosen as:

$$S_1 = Z_{s1} + \int_0^t Z_{s1}\,dt \tag{5.7}$$

The dynamics that satisfies the reaching condition of sliding motion ($\dot{S}_1 = 0$) can be written as follows (Pinheiro *et al.*, 1994).

150

$$\dot{S}_1 = (Z_{s2} + \propto_{s1})22.67 - 24.92\,X_1 + Z_{s1} \qquad (5.8)$$

To guarantee the sliding motion and satisfy the reaching condition, virtual control $\propto_{s1}$ is selected from eqs. (5.5) and (5.6) as:

$$\propto_{s1} = \frac{1}{22.67}\left[-Z_{s1} + 24.92X_1 - D_1S_1 - K_1 sgn(S_1)\right] \qquad (5.9)$$

The derivative of the new state, Z_{s2} is obtained as,

$$\dot{Z}_{s2} = 0.0776X_3 - 4.355X_2 + 4.355X_1 + 6366996.94 - \dot{\propto}_{s1} \qquad (5.10)$$

and consequently, defining the third state, Z_{s3} as (Ma et al., 2005)

$$Z_{s3} = X_3 - \propto_{s2} \qquad (5.11)$$

The derivative of the new state, Z_{s2} can be rewritten as,

$$\dot{Z}_{s2} = 0.0776(Z_{s3} + \propto_{s2}) - 4.355X_2 + 4.355X_1 + 6366996.94 - \dot{\propto}_{s1} \quad (5.12)$$

Now the second sliding surface is also selected as,

$$S_2 = S_1 + Z_{s2} \qquad (5.13)$$

and

$$\dot{S}_2 = \dot{S}_1 + \dot{Z}_{s2} \qquad (5.14)$$

From eq. (5.14), the second virtual control law, $\propto_{s2}$ can be selected to satisfy the reaching condition of sliding mode control system ($\dot{S}_2 = 0$) as,

$$\propto_{s2} = \frac{1}{0.0776} \left[-22.67 Z_{s2} + D_1 S_1 + K_1 sgn(S_1) - 0.0776(D_2 S_2 + K_2 sgn(S_2)) - \right.$$

$$\left. 6366996.94 + 4.355 X_2 - 4.355 X_1 + \dot{\propto}_{s1} \right] \qquad (5.15)$$

Now for the third state, Z_{s3}, the third sliding surface is selected as:

$$S_3 = S_2 + Z_{s3} \qquad (5.16)$$

Fig. 5.2 (a), (b), (c) shows the three sliding surface selected according to eqs. (5.7), (5.13), (5.16).
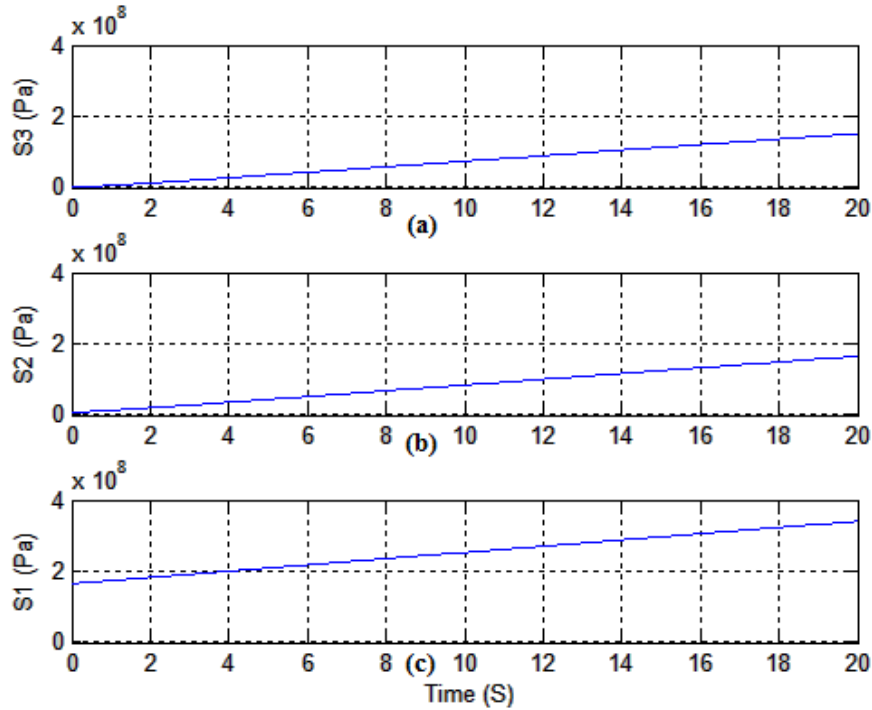
Fig. 5.2 Sliding surfaces, S_1, S_2, S_3

From eq. (5.7), (5.13) and (5.16), the reaching condition of third sliding surface ($\dot{S}_3 = 0$), which gives the control law for BSMC, is given by

152

$$U(des) = 0.0776Z_{s3} - 0.0776\big(D_2 S_2 + K_2 sgn(S_2)\big) - D_3(S_2 + Z_{s3}) -$$

$$K_3 sgn(S_3) + 0.004597 X_3 \tag{5.17}$$

where D_1, D_2 are constants depending on the chosen sliding surface (Palmi, 1994; Wong *et al.*, 2001).

In order to couple the above controller with the Backstepping control scheme, the control law of Backstepping controller obtained from eq. (4.29) to (4.37) in chapter (4) is designed as follows. For a Backstepping controller design of the system given by eqs. (5.1), (5.2) and (5.3), a new state is introduced as,

$$Z_1 = X_2 - X_2(des) \tag{5.18}$$

and the corresponding first Lyapunov function is chosen as,

$$V_1 = \frac{1}{2} X_1^2 \tag{5.19}$$

Now we find $X_2(des) = -C_1 X_1$ from eqs. (5.18) and (5.19) in such a way that $\dot{V}_1$ is negative definite. Thus,

$$\dot{Z}_1 = \dot{X}_2 + C_1 \dot{X}_1 \tag{5.20}$$

$\dot{Z}_1$ is obtained by substituting $\dot{X}_2$ and $\dot{X}_1$ from eqs. (5.14) and (5.15) respectively. Similarly, a second state is introduced as,

$$Z_2 = X_3 - X_3(des) \tag{5.21}$$

The second Lyapunov function is chosen as

$$V_2 = \frac{1}{2} X_1{}^2 + \frac{1}{2} Z_1{}^2 \qquad (5.22)$$

Thus $X_3(des)$ is obtained in such a way that $\dot{V}_2$ is negative definite. The third Lyapunov function is chosen as

$$V_3 = \frac{1}{2} X_1{}^2 + \frac{1}{2} Z_1{}^2 + \frac{1}{2} Z_2{}^2 \qquad (5.23)$$

By substituting values for X_1, Z_1, Z_2, in such a way that $\dot{V}_3$ is negative definite, the final control law for the Backstepping controller (He and Luo, 2004) is obtained as

$$u(des) = \frac{1}{628484.36}\left(-0.005\big(Z_2 + X_3(des)\big) - \dot{Z}_2 - c_3 Z_2\right) \qquad (5.24)$$

where c_3 is a constant, Z_2 is the second error variable and $X_3(des)$ is the desired value of the third state variable (Tan *et al.*, 2008; Liu and Tong, 2014; Tong et al., 2014).

The final control law for BSMC with coupling for the above system can be obtained by combining eqs. (5.17) and (5.24) as follows,

$$U = U(des) + u(des) \qquad (5.25)$$

The above equations from (5.1) to (5.25) is simulated to evaluate the response of settling chamber pressure.

154

5.1.2 Results and Discussion

To analyze the performance of BSMC, eq. (5.1) to (5.25) are simulated numerically with temperature in the three vessels at $T_1 = 300\,K$, $T_2 = 700\,K$ and $T_3 = 539\,K$ respectively. The dynamics of the wind tunnel system with the applied BSMC controller is analyzed using the time evolution of the pressure inside the three pressure vessels, HP, H1 and SC. The efficiency of BSMC in controlling the settling chamber pressure can be clearly inferred from the time evolution of settling chamber pressure. Fig. 5.3 (a), (b), (c) shows the evolution of settling chamber pressure for three representative setpoint values, 50×10^5 Pa, 70×10^5 Pa and 100×10^5 Pa respectively.
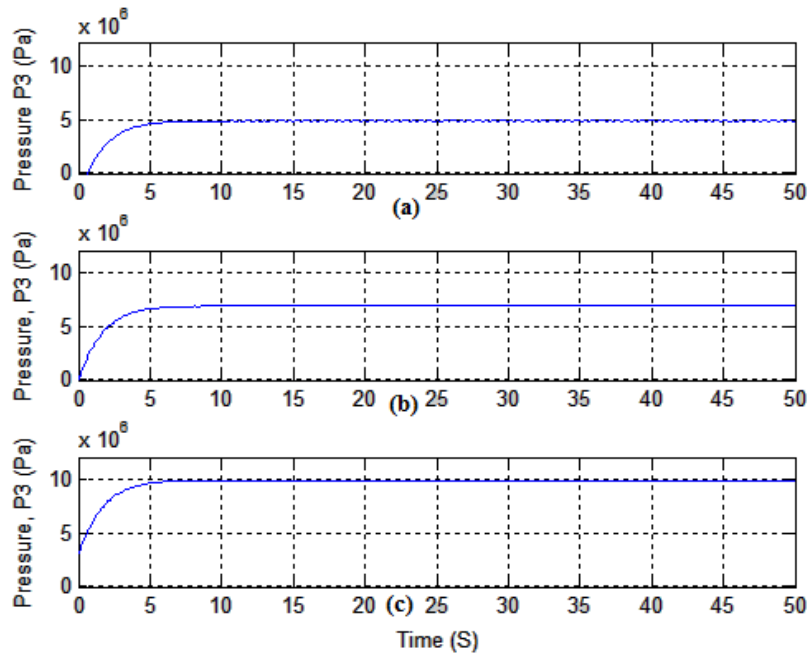
Fig. 5.3   Pressure in the settling chamber, P_3 with BSMC for the set points (a) 50×10^5 Pa, (b) 70×10^5 Pa and (c) 100×10^5 Pa respectively

The zoomed portion of the settling chamber pressure is shown in Fig. 5.4 (a), (b), (c).
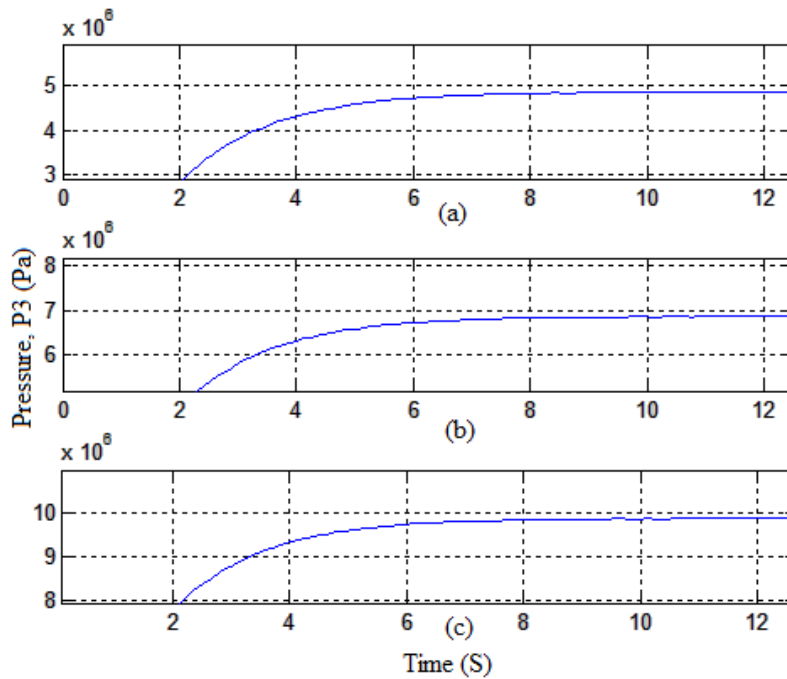
Fig. 5.4   Zoomed portion of Pressure in the settling chamber, P_3 with BSMC for the set points (a) 50×10^5 Pa, (b) 70×10^5 Pa and (c) 100×10^5 Pa respectively

From these figures, it can be inferred that the settling time for the three set points of 50×10^5 Pa, 70×10^5 Pa and 100×10^5 Pa are 8 s. It can also be observed that the settling chamber pressure is approaching the setpoint value in a continuous and smooth manner. It is also observed that the rise time is 3.45 s for all the three setpoints and the peak time is 49.66, 49.40 and 48.51 s for the setpoints 50×10^5 Pa, 70×10^5 Pa and 100×10^5 Pa respectively. Once the settling chamber pressure attains the setpoint value it is retained throughout the experiment time. It is also observed that there is no overshoot for all the three setpoints. The results of simulation studies for all the set points in the range 1×10^5 Pa to 300×10^5 Pa are evaluated, and the results are found to be of similar nature with settling time in the range of 7.5 to 8.5 s.

Thus, it is observed that BSMC is highly efficient in controlling the settling chamber pressure to the specified set point within a very short time around 8 s. In addition, the BSMC scheme has the advantage of controlling the settling chamber pressure with no overshoot and chatter effect.

To cross verify the above results, the evolution of the equivalent controller input of BSMC which is the error between the controlled variable and the set point is analyzed. Fig. 5.5 shows the evolution of the controller input for a sample setpoint of 100×10^5 Pa used in Fig. 5.3 (c). From these results it can be inferred that the error between the setpoint value and the control variable is decreasing with respect to time. This indicates that the controlled variable, which is the settling chamber pressure is approaching the set point as time exceeds.
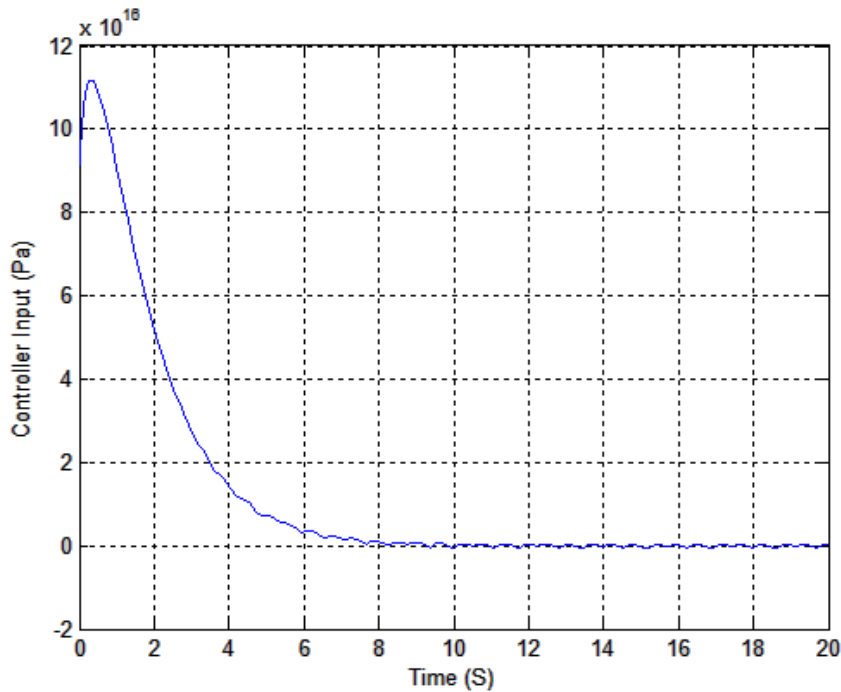
Fig. 5.5 Equivalent Controller input for the set points 100×10^5 Pa

Thus, it can be inferred that BSMC is highly efficient in controlling the settling chamber pressure to the specified set point within a very short time of 8 s. In addition, the BSMC scheme has the advantage of controlling the settling chamber pressure without overshoot and chatter effect.

5.2 SLIDING MODE FUZZY CONTROLLER (SFC)

In the 1970s, King and Mamdani (Mankad *et al.*, 2011; Liu and Tong, 2014; Srinivasan and Raajarajan, 2017; Tong *et al.*, 2014; King and Mamdani;1977) studied the application of FLCs to the control of non-linear industrial processes that typically can only be controlled successfully by a human operator. The intelligent controlling approaches like Fuzzy logic (FL) will provide the required scope for wind tunnels to be more efficient, safe, and economic. The approaches will help to enable a level of performance that far exceeds that of today's wind tunnel in terms of reduction of harmful emissions, maximization of run time, and minimization of noise, while improving system affordability and safety. Fuzzy controller is an intelligent controller based on Fuzzy logic where the analog inputs are processed using logical rules (Mankad *et al.*, 2011; Liu and Tong, 2014; Srinivasan and Raajarajan, 2017). Sliding mode controller is a robust non-linear controller which is capable of rejecting uncertainties and perturbations. The chattering phenomenon present in Sliding mode controller oscillates in the response. Sliding Mode Fuzzy Controller (SFC) is a Sliding mode controller which is combined with Fuzzy Logic to reduce or eliminate the high frequency oscillation, known as chattering thereby compensating the unknown parametric uncertainties. This technique helps in maintaining the stability which is lacking with Fuzzy controller. This algorithm focuses to reduce the fuzzy rules thereby refining the stability of close loop system. As the system state can hit the sliding surface faster, SFC guarantees the system stability and performance.

158

Moreover, tuning with an SFC is much easier when compared with the Sliding mode controller and Fuzzy logic controller. Another feature is that desired transient response is achieved with SFC under varying operating conditions, with no chattering which makes it superior to both these controllers when used individually. Here, we present the design procedure of Sliding mode Fuzzy control for regulation of settling chamber pressure inside the tunnel system.

5.2.1 Design

Fuzzy controller consists of an input stage, processing stage, and an output stage (Mankad *et al.*, 2011; Liu and Tong, 2014). The input stage converts the real inputs to corresponding fuzzy values using appropriate membership functions (MF). Membership function is a set of values defined by Fuzzy rules by assigning each element, a corresponding membership value. The processing stage combines each input with an appropriate rule and produces corresponding fuzzy output. The output stage converts the Fuzzy output back into a specific control output using appropriate membership functions (Mankad *et al.*, 2011; Liu and Tong, 2014; Srinivasan and Raajarajan, 2017). The property of Sliding mode controller is that when the system state reaches the sliding surface, the system state is insensitive to parametric uncertainties of the system. A Sliding mode Fuzzy controller incorporates the robustness property of Sliding mode control and interpolation property of Fuzzy logic control, in such a way that the robustness can be maintained approximating the switching surface (Palmi, 1994; Lin and Chen, 1997; Wong *et al.*, 2001; Tong et al., 2014, King and Mamdani, 1977). Sliding mode Fuzzy controller is designed by incorporating a suitable sliding surface in the output of Fuzzy control logic (Palmi, 1994; Lin and Chen, 1997; Wong *et al.*, 2001).

For controlling the settling chamber pressure inside the Hypersonic wind tunnel system, the error between the set point and settling chamber pressure is taken as the first input, and the error rate is chosen as second input to the fuzzy controller (Mankad *et al.*, 2011; Liu and Tong, 2014; Srinivasan and Raajarajan, 2017). Fuzziness in a fuzzy set is determined by its MF. Different shapes like triangular, trapezoidal, Gaussian etc can be used based on problem size and problem type where a MF must really satisfy the condition that it must vary between 0 and 1. The choice of the type and number of MFs depends on knowledge obtained from experts in the field and Knowledge extracted from trends in empirical data. Triangular and trapezoidal membership functions are simple and facilitate easy computation and they provide a linear mapping of the universe of discourse. Smooth nonlinear membership functions like Gaussian, Bell etc are difficult to compute due to their nonlinear mapping. For triangular membership functions, the membership value can be easily computed and hence from the input range, the corresponding linear range is identified for each input and solved to obtain the membership value. Five triangular MF as shown in Fig. 5.6 and Fig. 5.7 are assigned to each of the inputs. Correspondingly, five output MFs are generated as shown in Fig. 5.8. The x-axis represents the degree of membership corresponding to the error, error rate and fuzzy output in Fig. 5.6, 5.7 and 5.8 respectively.
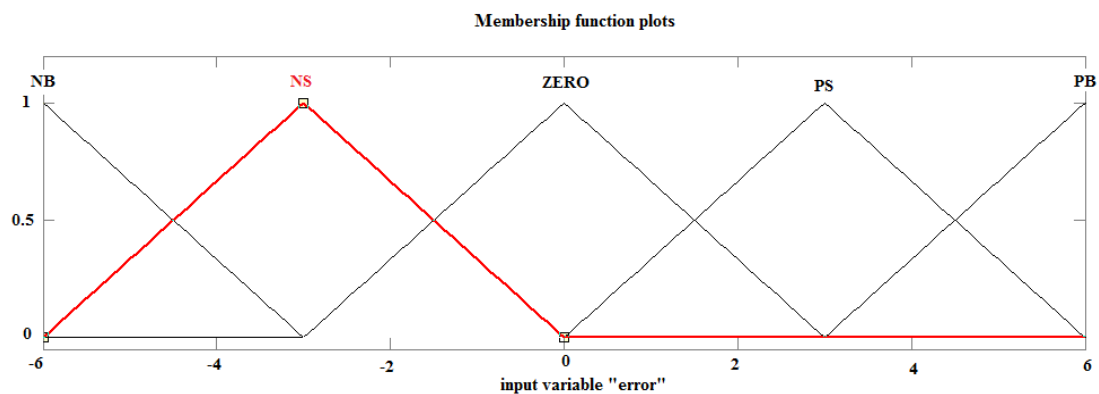
Fig. 5.6 Input membership functions "error"

160
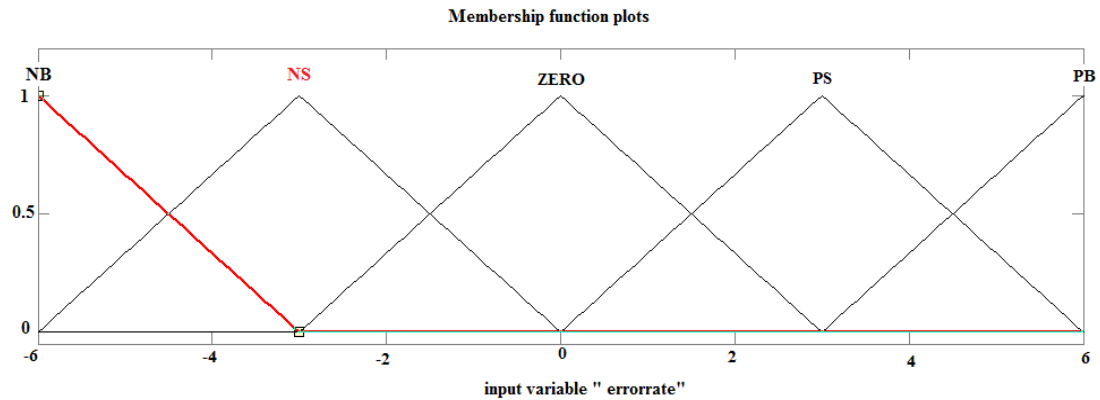
Fig. 5.7 Input membership functions "error rate"
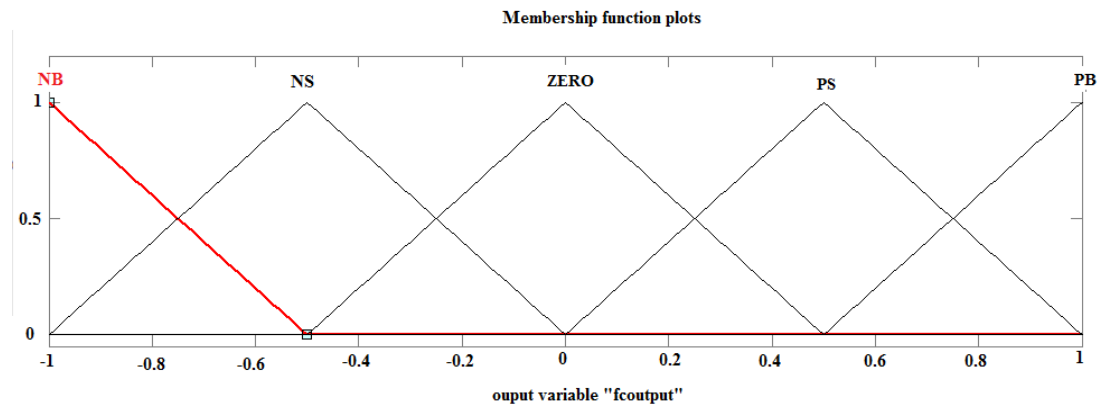
Fig. 5.8 Output membership functions

Fuzzy associative memory is integrated by 25 rules, which are decision making rules that contain input-output relationships that define the control strategy. Generally Fuzzy sets (FS) are named from there relevant position as compared to the error. For any system the desired error is always 0, hence FS associated with 0 error is named as "z" (zero). FS associated with positive error are named as; "PS" (positive small), "PM" (positive medium) and "PB" (positive big). FSs associated with negative error are named as: "NS" (negative small), "NM" (negative medium) and "NB" (negative big). The Fuzzy rules used in the processing stage is given in Table. 5.1 (Srinivasan and Raajarajan, 2017; Tong et al., 2014), where NB denotes negative big, NS denotes

negative small, N is negative, Z is zero, P denotes positive, PB is positive big and PS denotes positive small. The fuzzy inference system used is Mamdani, which is a commonly used fuzzy methodology. The fuzzy rules are selected based on the error and error rate. For example, if the error is chosen as negative big with error rate negative big, then the fuzzy output is also negative big. In another case, for a zero error and positive small error rate, the fuzzy output is zero. In this way the 25 set of fuzzy rules are defined in Table 5.1. Fig. 5.9 shows the surface view of the fuzzy system which is a three dimensional graph between the two inputs and the output.

Table. 5.1 Fuzzy Rules

Error Error rate	NB	NS	Z	PS	PB
NB	NB	NS	NS	Z	Z
NS	NB	NS	Z	Z	PS
Z	NB	Z	Z	Z	PB
PS	NS	Z	Z	PS	PB
PB	Z	Z	PS	PS	PB
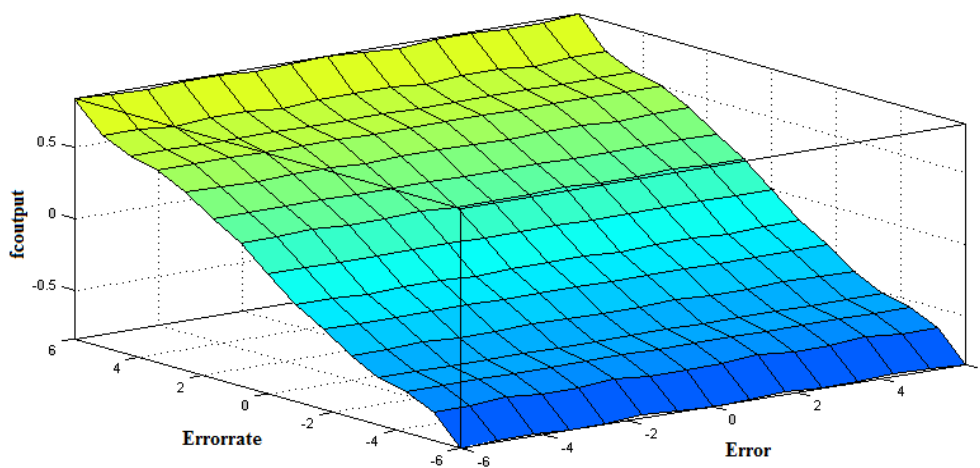
Fig. 5.9 Surface view of the Fuzzy system

162

Sliding mode controller when used independently gives satisfactory performance in terms of settling time and overshoot but has its own limitations with respect to inherent chattering. Fuzzy controller, when used independently has limitation with respect to consistency in selection of fuzzy rules and in ensuring stability. Sliding mode fuzzy controller combines the intelligence of fuzzy logic with the sliding mode technique thereby ensuring stability and elimination of chatter effect. It also has the advantage of minimizing the overshoot and improvement of the settling time. The block diagram of design procedure of SFC is shown in Fig. 5.10.
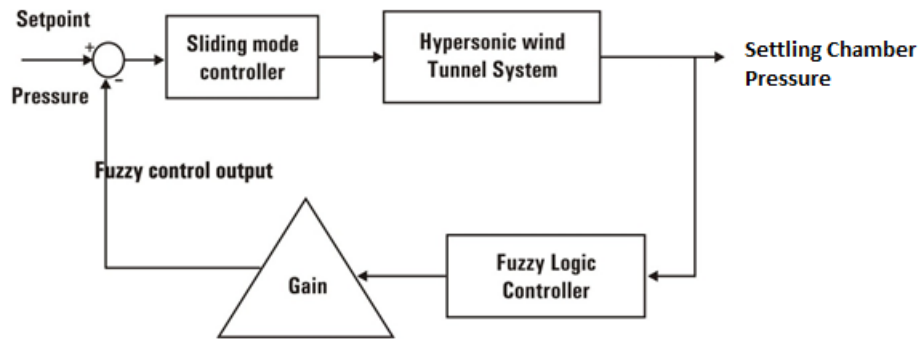
Fig. 5.10 Block diagram of Sliding mode Fuzzy controller

Sliding mode Fuzzy controller involves construction of a set of membership functions corresponding to the Lyapunov functions. For designing the Sliding mode Fuzzy controller, an equivalent control law of Sliding mode is designed, which is appropriately incorporated in the output stage of the above Fuzzy control logic. The equivalent control for Sliding mode is determined by restricting the system dynamics to the switching surface, $S = 0$ (Musmade *et al.*, 2011; He and Luo, 2004; Ackermann and Utkin, 1998). The control law is developed by designing the sliding surface, S as a function of state variables, X_1, X_2, X_3 such that X_3 converges to the sliding surface,

$$S = C_3 X_3 + X_2 + X_1 \tag{5.26}$$

where C_3 is a constant gain chosen as unity. Choosing the Lyapunov function as

$$V = \frac{1}{2}S^2 \tag{5.27}$$

Its derivative is obtained as,

$$\dot{V} = S\dot{S} \tag{5.28}$$

Stability of the system is ensured by selecting S such that $\dot{V}$ has to be negative definite,

$$S\dot{S} = \begin{cases} < 0 \ if \ S > 0 \\ = 0 \ if \ S = 0 \\ > 0 \ if \ S < 0 \end{cases} \tag{5.29}$$

Accordingly, the equivalent controller of SFC is obtained as,

$$U_{eq} = \beta - k \ sign(s) \tag{5.30}$$

Where, β is the obtained Fuzzy controller output and k is a control gain whose value is chosen as 4. The above equations from (5.26) to (5.30) are simulated to evaluate the response of settling chamber pressure with SFC.

5.2.2. Results and Discussion

Results of numerical simulations of the dynamics of Hypersonic wind tunnel with SFC given by eqs. (3.1) to (3.14), (3.27 and 3.28) of chapter (3), (5.26) to (5.30) are shown in Fig. 5.11 (a), (b) and (c). The zoomed portion of the above figure is represented in Fig. 5. 12.
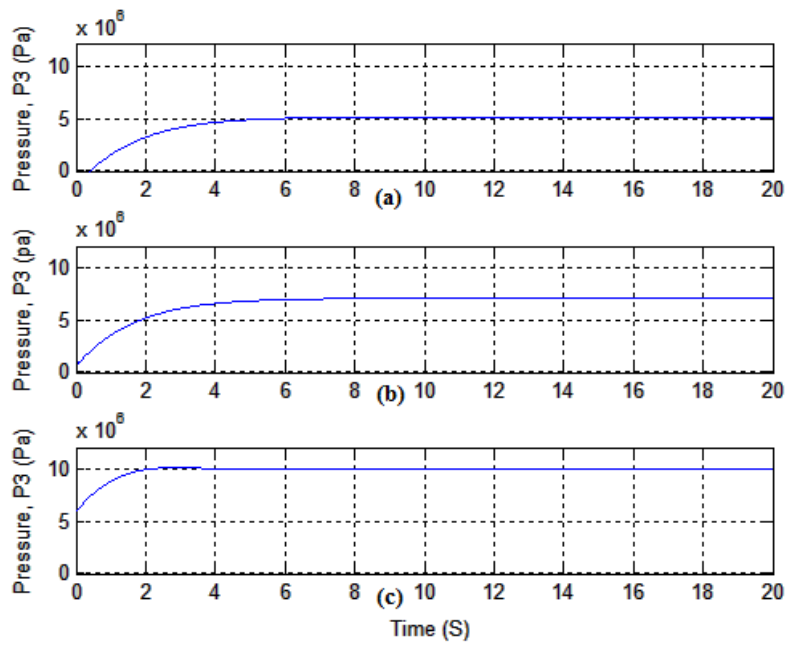
Fig. 5.11 Pressure in the settling chamber, P_3 with SFC for the set points 50×10^5 Pa, 70×10^5 Pa and 100×10^5 Pa respectively
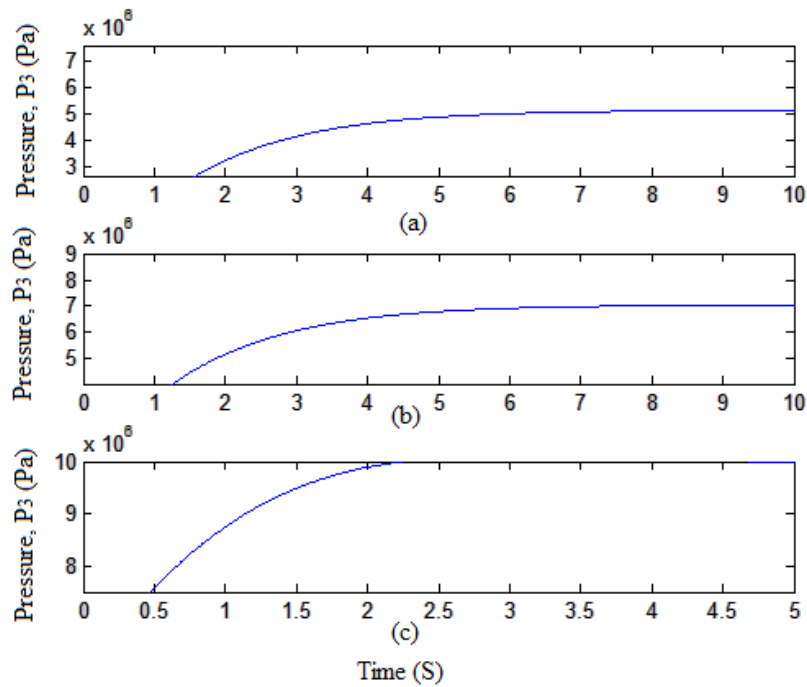
Fig. 5.12 Zoomed portion of the settling chamber Pressure, P_3 with SFC for the set points 50×10^5 Pa, 70×10^5 Pa and 100×10^5 Pa respectively

From these figures, it can be inferred that the settling time for the three set points, 50 $\times$ 10^5 Pa, 70 $\times10^5$ Pa and 100 $\times$ 10^5 Pa are 10.3, 12 and 7 s respectively. It can also be observed that eventhough there is 0.87 % overshoot for 100 $\times$ 10^5 Pa, the settling time is minimum. However for the other two set points, 50 $\times$ 10^5 Pa and 70 $\times$ 10^5 Pa, the responses are achieved within comparable settling times with no overshoot. The rise time for the setpoints, 50 $\times$ 10^5 Pa, 70 $\times10^5$ Pa is 3.45 s and for the setpoint, 100 $\times$ 10^5 Pa is 1.44 s. The peak time corresponding to the setpoints, 50 $\times$ 10^5 Pa and 70 $\times$ 10^5 Pa is 20 s and for the setpoint 100 $\times$ 10^5 Pa is 2.7 s. It is also observed that chatter free response is obtained for all the above cases. Similar results are obtained for all the set points between 1 x 10^5 Pa to 300 $\times$ 10^5 Pa, where the corresponding settling time is obtained in the range of 7-12 s and the overshoot is in the range of 0-1 %. Thus it can be observed that controlling the pressure inside the SC of Hypersonic wind tunnel with SFC is efficient in terms of settling time, overshoot and chatter effect.

5.3 PERFORMANCE ANALYSIS OF THE HYBRID CONTROLLERS

The performance of the proposed BSMC and SFC controllers for regulation of pressure inside Hypersonic wind tunnel for a range of set points values, 1 x 10^5 Pa to 300 $\times$ 10^5 Pa are analyzed. The performance efficiency of the proposed Hybrid controllers are analyzed in terms of the settling time, overshoot and rise time. The results are consolidated in tabular form and is given in Table. 5.2.

Table. 5.2 Performance Comparison of Hybrid Controllers

Sl.No	Set point	Settling Time (S)		Overshoot (%)		Rise Time (S)	
		BSMC	SFC	B S M C	SFC	B S M C	SFC
1	100×10^5 Pa	8	7	NIL	1	3.45	1.44
2	70×10^5 Pa	8	12	NIL	NIL	3.45	3.45
3	50×10^5 Pa	8	10.3	NIL	NIL	3.45	3.45

From the above table, it can be observed that the BSMC has no overshoot, settling time is only 8 s and rise time is 3.45 s for all the set points. In the case of SFC, settling time varies between 7-12 s, the overshoot varies between $0 - 1$ % and the rise time varies between 1.44 and 3.45 s. In addition, from Fig. 5.3, 5.4 and 5.11, 5.12, it is also evident that the chattering, which is inherent in sliding mode controller is completely eliminated in both BSMC and SFC approaches.

From these results, it is clear that among these controllers, BSMC is the most efficient controller with a minimum and steady settling time without overshoot and chatter effect for any given set point. In the case of SFC, even though the settling time is 7 s for the set point of 100×10^5 Pa, which is slightly shorter compared to that of BSMC, it has an overshoot of 1 %. For the other two set points, the settling time is more than that of BSMC but has no overshoot and chatter effect.

From the above observations, it can be clearly inferred that BSMC is a good choice of controller for the regulation of pressure in Hypersonic wind tunnel. The effect of Backstepping on the sliding surface is the reduction in settling time which is very important in the case of Hypersonic wind tunnel testing. BSMC has the advantages of achieving the objectives of stabilization and also of being flexible to allow the non-linearities in the model, which in turn contributes to enhancement of its efficiency. For a Hypersonic wind tunnel system, the settling time is a very important performance

parameter as the test duration is very short. Similarly, achievement of required setpoint without any overshoot is also a very advantageous feature for Hypersonic wind tunnel application due to the high pressures involved in the testing process. The present results clearly evidence the efficiency of BSMC in comparison with SFC controller and that it is a good choice of controller for Hypersonic wind tunnel applications.

This chapter presents the design of suitable Hybrid controllers for regulation of pressure inside the test section of a Hypersonic wind tunnel by designing suitable controllers. In Hypersonic wind tunnel system, the test duration is very short and the pressure levels are very high which demands highly efficient systems for the regulation of pressure. Here, Hybrid controllers, viz: Backstepping Sliding mode and Sliding mode Fuzzy controllers are designed for the regulation of settling chamber pressure. The combination approach is proposed for overcoming limitations of these controllers in terms of settling time, overshoot and chatter effect. Sliding mode controller when used independently gives satisfactory performance in terms of settling time and overshoot but has its own limitations with respect to inherent chattering. Even though the Backstepping controller has the advantages of faster response with no overshoot and chatter effect, it has certain drawbacks in terms of sensitivity to parametric variations. Combination of Sliding mode with Backstepping control approach makes the system robust to parametric uncertainties and also helps to overcome the limitation of chatter effect. In addition, it improves the settling time without any overshoot in the controlled variable. In the proposed BSMC design, a suitable sliding surface is properly designed to eliminate the unwanted chattering resulting from the discontinuous control of Sliding mode approach and the stability is ensured by choosing suitable Lyapunov functions in Backstepping controller.

Fuzzy controller, when used independently has limitations with respect to consistency in selection of fuzzy rules and stability. Sliding mode Fuzzy controller combines the intelligence of Fuzzy logic with the Sliding mode technique thereby ensuring stability and elimination of chatter effect. It also has the advantage of minimizing the overshoot and reduction in settling time.

The performance characteristics of the designed Backstepping Sliding mode controller is compared with Sliding mode Fuzzy controller. The simulation results show that the settling chamber pressure settles faster without any overshoot with the proposed BSMC design. Thus, it is evident that the proposed controller design performs efficiently in terms of settling time, which is very crucial during the test run. Though the design of BSMC is complex, it gives better performance compared to other control techniques, which makes it suitable for regulation of pressure inside the settling chamber of the hypersonic wind tunnel system. Indeed, classical controllers are more easy to design and implement for large tunnel systems. Design of Hybrid controllers are more complex and their implementation is computationally expensive and time consuming.

Considering the complexity in design of BSMC and the presence of overshoot in the response with SFC design, Adaptive controllers are proposed in chapter 6. This chapter deals with design and numerical analysis of Adaptive controllers, viz: Model Reference Adaptive controller (MRAC) and Modified Adaptive control (MAC). The proposed MAC approach is verified by validated model of INCAS Supersonic wind tunnel and is proved to be best suited for pressure regulation inside the tunnel system.

CHAPTER 6

DESIGN AND ANALYSIS OF ADAPTIVE CONTROLLERS

Conventional controllers do not perform efficiently in the presence of variation in process dynamics. For this reason, it must be possible to design controllers which can perform under such variations created by perturbations. With the aim of improving the system performance in the presence of disturbances and parametric uncertainties, we design a Model Reference Adaptive control (MRAC) scheme for regulation of pressure inside Hypersonic wind tunnel. A modified version of this scheme viz: Modified Adaptive control (MAC) is also designed incorporating suitable modifications to the cost function thereby modifying the update law.

LQR based controller designed in chapter 4 for regulating the settling chamber pressure has the advantage of less settling time in spite of various set points, whereas the percentage overshoot increases with increase in set point. The settling time as well as the percentage overshoot are improved by increasing the weighing matrix of LQR controller, which results in increased gain leading to reduced stability (Purnawan *et al.*, 2017; Mauricio *et al.*, 2012). To improve the performance further, a Robust H-infinity controller is designed, which is highly efficient in regulating the variations in system dynamics. With the designed H-infinity controller, even though settling time is reduced, there is substantially high overshoot, which does not satisfy the performance requirements (Mary *et al.*, 2012; Yilmaz *et al.*, 2012; Hassibi *et al.*, 2006). Thus, the problem in selecting the parameters of H-infinity controller to achieve the desired performance and robustness characteristics is overcome by tuning

the weighing function using Krill Herd optimization control technique (Wang *et al.*, 2014). Even though this control algorithm drastically reduces the percentage overshoot, it cannot eliminate this performance index completely. Considering the limitations of LQR and optimised H-infinity controller, other control schemes using Backstepping and Sliding mode techniques are considered. Backstepping controller, a systematic non-linear control based on Lyapunov stability theorem ensures appropriate control design for a stable system which can also accommodate nonlinearities (Rudra and Barai, 2012; Sonneveldt *et al.*, 2007). However, Backstepping controller is sensitive to parametric variations and requires all variables to be measurable which in most cases is not practical. Even though the settling time and overshoot are reduced, the design becomes complex. For the above reason, Sliding mode controller (SMC) is proposed wthat transforms a relatively higher order system to a lower order system. Even though SMC is reliable and robust, it produces chatter in the output response, which is highly undesirable (Musmade *et al.*, 2011; Pinheiro *et al.*, 1994; Chang, 2013).

An appropriate combination of Backstepping with Sliding mode controller and Sliding mode with Fuzzy controllers are suggested in Chapter 5 to evaluate the performance in terms of settling time and overshoot (Lin *et al.*, 2007; Chen *et al.*, 2012; Tong *et al.*, 2009). Even though Fuzzy control based on Fuzzy logic is an intelligent technique, when used independently it has the limitation of stability issues which can be overcome by suitable combination with Sliding mode control. This combination improves stability of the system as well as robustness to parametric variations. Even though the inherent drawback of chattering in Sliding mode control is reduced by using suitable membership functions (MF) of Fuzzy logic, this

171

combination has the drawback that the settling time is not constant throughout its operation and has overshoot in certain values of set points. Similarly, though BSMC is capable of regulating the settling chamber pressure with desirable performance indices, its design is complex. Thus, we propose a Model Reference Adaptive control and Modified Adaptive Control techniques that provide consistent performance in the presence of large and unknown parametric uncertainties.

Adaptive control scheme is highly efficient in regulating the variations in system dynamics (Makoudi and Radouane, 1999; Hovakimyan *et al.*, 2001) and hence it has been widely applied in the control process of various systems (Makoudi and Radouane, 1999; Maity *et al.*, 2015; Hovakimyan *et al.*, 2001; Mehran and Soheili, 2011; Nguyen *et al.*, 2013; Jain and Nigam, 2013). These control schemes are supervisory controls capable of handling long response times and process disturbances than other controller schemes (Jacob and Binu, 2009). The study of Model reference adaptive control systems, which is one of the main approaches of Adaptive control is also extended to non-linear systems extensively, to carry forward the robustness of the Adaptive controllers to variable systems affected by disturbances. This fact makes Adaptive control suitable for a wide range of applications in aerospace and process control where the system performance in the presence of parametric uncertainties and robustness are very significant. (Jacob and Binu, 2009; Imaduddin *et al.*, 2011). Model reference adaptive control (MRAC) is designed based on MIT rule and is capable of compensating for variations in process dynamics in order to optimise the system performance. Here, we investigate the efficiency of a Model reference adaptive control scheme in regulation of settling chamber pressure inside Hypersonic wind tunnel system. Based on the performance

of MRAC, we propose suitable modifications for overcoming its limitations in terms of overshoot and chatter effect for this application. Hence a new Modified adaptive control (MAC) scheme, developed by redefining the control law of MRAC by incorporating suitable modifications to its cost function and update law, is proposed. In this scheme, the cost function is suitably adjusted to overcome the chatter effect while the update law is modified to reduce the overshoot in the response of the system. The proposed scheme of Modified adaptive control is highly efficient in overcoming the limitations of MRAC for regulating the pressure inside the settling chamber of the Hypersonic tunnel system. As MAC is an Adaptive controller, it has the characteristic property that this controller is robust in the presence of disturbances which makes it suitable for any perturbation analysis application.

6.1 MODEL REFERENCE ADAPTIVE CONTROLLER (MRAC)

Model Reference Adaptive Control is a direct control technique (Makoudi and Radouane, 1999; Hovakimyan *et al.*, 2001), which uses a reference model for closed loop systems based on the MIT rule. MIT rule was first developed in 1960 by the researchers of Massachusetts Institute of Technology (MIT) used to design the autopilot system for aircrafts. MIT rule is very sensitive to change in amplitude of reference input and can become unstable for large values of reference input. Here, the error variable, $e(t)$, which is the difference between the plant output and output of the reference model, an adjustable parameter, θ and a cost function, $J(\theta)$ are suitably adjusted to achieve the desired output. The aim is to minimize the cost function $J(\theta)$ by adjusting the parameter, θ and therefore it is reasonable to change the parameters in the direction of negative gradient of $J(\theta)$. An adaptation mechanism adjusts the

control parameters so as to make the system response identical to the response of the reference model (Makoudi and Radouane, 1999, Maity *et al.*, 2015, Hovakimyan *et al.*, 2011; Mehran and Soheili, 2011; Nguyen *et al.*, 2013; Jain and Nigam, 2013).

6.1.1 Design

The block schematic of MRAC based on MIT rule is given in Fig. 6.1 (Jacob and Binu, 2009; Makoudi and Radouane, 1999; Maity *et al.*, 2015; Imaduddin *et al.*, 2011; Karray and Feki, 2014; Tuan *et al.*, 2013; Chen *et al.*, 2016; Mozaffari and Azad, 2017). The plant is the representation of the Hypersonic wind tunnel system under consideration and the reference model is a suitably chosen form of the system, which provides the output expected from the actual plant. Here, $y_m(t)$ is the output of the reference model and $y(t)$ is the plant output, U_C represents the set point to the system. The difference between the plant output and output of reference model is the error variable, $e(t)$. This error is reduced by properly choosing an adjustment parameter, θ.
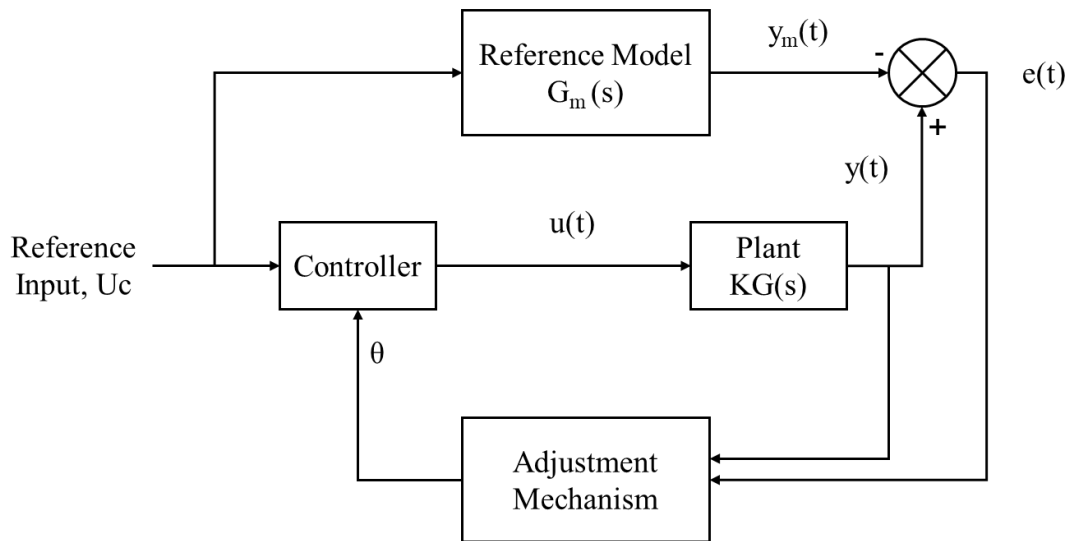
Fig. 6.1 Block diagram of MRAC system

174

The main aim of MRAC design is to minimize the cost function by adjusting this parameter. The controller output, $u(t)$ is fed to the plant for achieving the desired setpoint.

The error signal, $e(t)$ is represented as,

$$e(t) = y(t) - y_m(t) \tag{6.1}$$

In MIT rule, a cost function based on the adjustment parameter, θ is chosen as,

$$J(\theta) = \frac{e^2(\theta)}{2} \tag{6.2}$$

θ is varied in such a way that the cost function is minimized to zero (Maity *et al.*, 2015; Imaduddin *et al.*, 2011; Tuan *et al.*, 2013; Karray and Feki, 2014). For this purpose, θ is varied in the direction of negative gradient of J as,

$$\frac{d\theta}{dt} = -\gamma \frac{\partial J}{\partial \theta} \tag{6.3}$$

where γ represents the adaptation gain of the controller. Substituting for $J(\theta)$ from eq (6.2) we get,

$$\frac{d\theta}{dt} = -\gamma e \frac{\partial e}{\partial \theta} \tag{6.4}$$

where $\frac{\partial e}{\partial \theta}$ represents the sensitivity derivative of the system and (Makoudi and Radouane, 1999, Maity *et al.*, 2015, Hovakimyan *et al.*, 2011; Mehran and Soheili, 2011; Nguyen *et al.*, 2013; Jain and Nigam, 2013).

The control law is defined as,

$$u(t) = \theta U_C \tag{6.5}$$

where U_C is the reference input. Therefore, the error can be redefined in terms of transfer function as,

$$E(s) = KG(s)U(s) - K_0G(s)U_C(s) = KG(s)\theta U_C(s) - K_0G(s)U_C(s) \tag{6.6}$$

where $U(s)$ and $G(s)$ represents the reference input and plant transfer functions, K and K_0 are constants and $E(s)$ is the Laplace transform of the error $e(t)$. The sensitivity derivative can be restated in terms of the model output as,

$$\frac{\partial E(s)}{\partial \theta} = KG(s)U(s) = \frac{K}{K_0}Y_m(s) \tag{6.7}$$

The update law for θ in eq (6.4) is redefined based on this sensitivity derivative as,

$$\frac{d\theta}{dt} = -\gamma e \frac{K}{K_0} Y_m = -\gamma' e Y_m \tag{6.8}$$

where

$$\gamma' = \gamma \frac{K}{K_0} \tag{6.9}$$

Eq. (6.8) represents the adjustment law for θ.

The Adaptive controller for the Hypersonic wind tunnel system given in eq. (3.11), (3.14), (3.27 and (3.28) in chapter (3) is designed based on a suitable reference model. MRAC is designed with a reference model chosen based on the MIT rule. The reference model for the tunnel system is selected based on the literature discussed in Chapter 2 (Jones *et al.*, 2014; Jones *et al.*, 2011a; Jacob and Binu, 2009; Jones *et al.*, 2011b). The appropriate choice of reference model for this system is obtained as,

$$G_m(s) = \frac{e^{-9}s+1}{0.05s+1} \tag{6.10}$$

With this reference model, an Adaptive controller is designed for the tunnel system $G(s)$ given in eq. (3.11) and (3.14) of chapter (3). Here, the reference model is chosen based on empirical analysis and it does not have direct influence to the system. The reference model is incorporated to reduce the error in comparison with the plant output.

6.1.2. Results and Discussion

The performance characteristics of the above system are evaluated for a range of set point values between 1×10^5 Pa to 300×10^5 Pa keeping the temperatures of the three pressure vessels at T_1 =300 K, T_2 = 700 K and T_3 = 539 K (Nott *et al.*, 2008; Enbiya *et al.*, 2011) respectively. From the above range of setpoints, results with three sample setpoints of 100×10^5 Pa, 70×10^5 Pa and 50×10^5 Pa are represented.

Initially the behavior of the system is identified by investigating the error signal, which is the difference between the system output and setpoint for all ranges of setpoints from 1×10^5 Pa to 300×10^5 Pa. A study on the characteristics of the error

signal without applying the control law is carried out and the error signal for a sample setpoint of 100×10^5 Pa is considered. Fig. 6.2 shows the evolution of error in pressure between the system model and the chosen reference model for the set point of 100×10^5 Pa. To minimize this error, the cost function and control law of MRAC are suitably designed using eq. (6.2) and (6.5). The dynamic behavior is studied by simulating eqs. (3.11) of chapter (3) and eq. (6.1) to (6.10) for the tunnel system with the suitably designed MRAC.
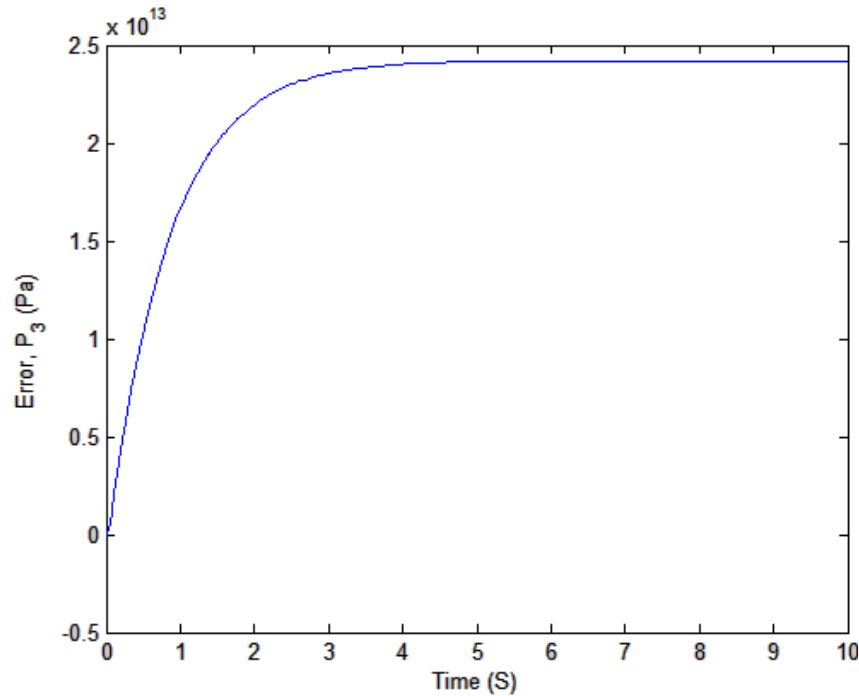
Fig. 6.2 The error signal, e(t) without control for the set point of 100×10^5 Pa

Applying MRAC, the behavior of the system for the given range of setpoints are studied and are presented. It is observed that the general time evolution of the settling chamber pressure has similar characteristics for all the set point values within the chosen range. The representative results for three set points, 100×10^5 Pa, 70×10^5 Pa and 50×10^5 Pa are shown in Figs. 6.3 to 6. 5 (Duarte *et al.*, 1996).

Fig. 6.3 (a) represents the response of the settling chamber pressure, P_3 of the tunnel system with MRAC for the set point of 100×10^5 Pa. From the figure, it is observed that the settling chamber pressure of the system model, $y(t)$ initially overshoots the reference model output $y_m(t)$ and settles down to the set points of 100×10^5 Pa in 1.37 s. The corresponding percentage overshoot is found to be 330.34 %. It is also observed that in this case, the system response is adversely affected by chattering effect and the chattering ranges between 100×10^5 Pa to 114.40×10^5 Pa.
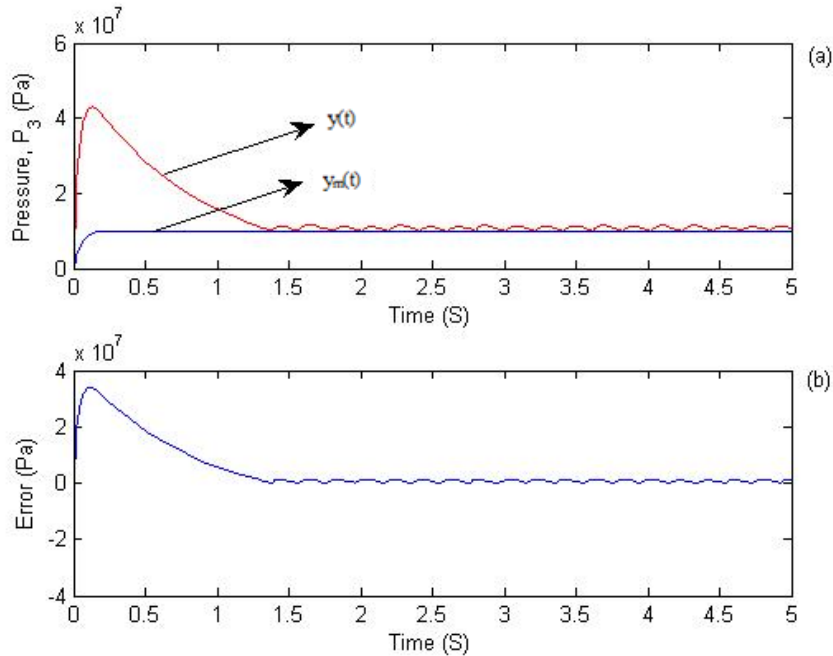
Fig. 6.3 (a) Settling chamber pressure, P_3 ($y(t)$) and reference model output, $y_m(t)$ with MRAC for set point of 100×10^5 Pa (b) The corresponding error signal, $e(t)$

The evolution of error, $e(t)$ for the tunnel system with MRAC is shown in Fig. 6.3 (b). From this figure it is clearly observed that with the chosen design of MRAC, the error between the system model and reference model can be reduced to 0.2×10^7 Pa. The efficiency of the chosen design of MRAC can be clearly understood by comparing this result with the error, before applying controller, shown in Fig. 6. 2.

From Fig. 6. 2 and 6. 3 (b), it is clear that the error which was in the range of 2×10^{13} Pa to 2.5×10^{13} Pa before applying the controller, is minimized to the range of 0.2×10^{7} Pa with the chosen design of MRAC. However, due to the chattering effect, this error varies between -0.22×10^{7} Pa to 0.23×10^{7} Pa.

Similar dynamical behavior is observed for the entire range of set points selected for the study. Fig. 6.4 and 6.5 shows the response of settling chamber pressure for a set point of 70×10^{5} Pa and 50×10^{5} Pa respectively.
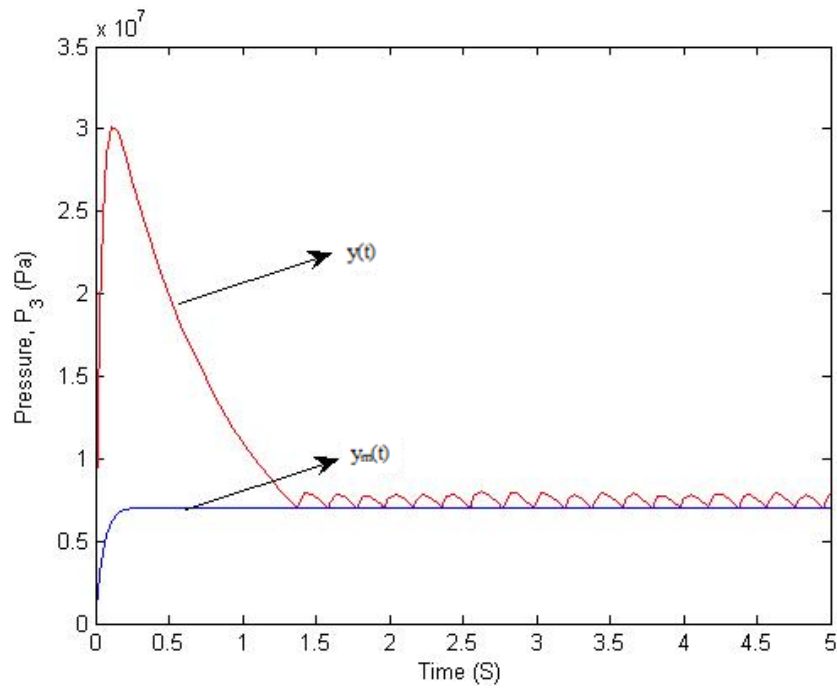
Fig. 6.4   Pressures in the settling chamber P_3, $(y(t))$ and reference model output, $y_m(t)$ with MRAC for the set point 70×10^{5} Pa
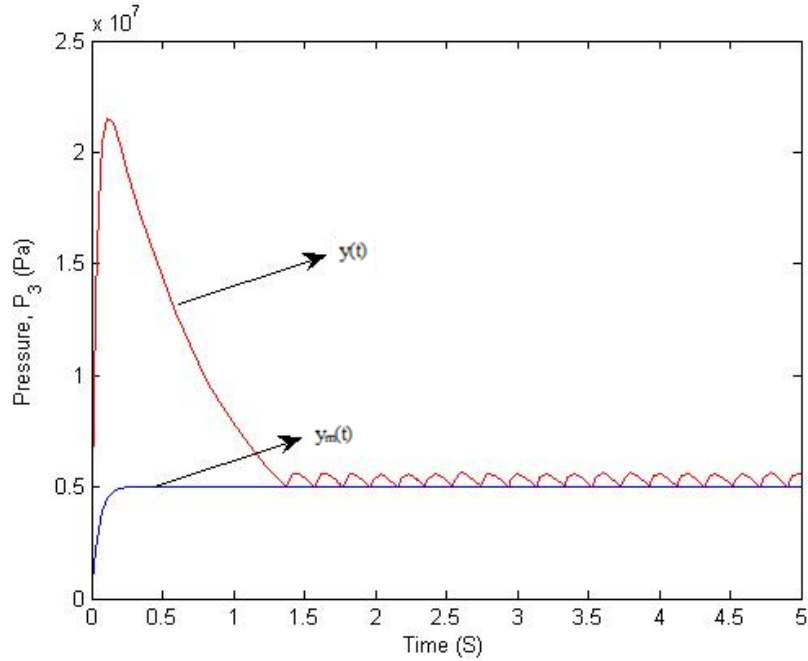
Fig. 6.5 Pressures in the settling chamber $P_{3,}$ $(y(t))$ and reference model output, $y_m(t)$ with MRAC for the set point 50×10^5 Pa

From the response of settling chamber pressure for a set point of 70×10^5 Pa shown in Fig. 6.4, it can be observed that the settling chamber pressure settles down in 1.37 s. However, here also the pressure of the system model initially overshoots the reference model output and the percentage overshoot is observed to be 330.42 %. In this case also the pressure response is adversely affected by chattering effect and the range of chattering is between 70×10^5 Pa to 83.50×10^5 Pa. For a set point of 50×10^5 Pa shown in Fig. 6.5, the percentage overshoot and settling time are observed to be 330.50 % and 1.37 s respectively. In this case, the chattering of settling chamber pressure is found to be in the range from 50×10^5 Pa to 59.16×10^5 Pa. Similar variations in the settling chamber pressure are observed for all other setpoints considered for the study. From Figs. 6.3, 6.4 and 6.5, it is observed that the rise time is 0.007 s for all setpoints and peak time is 0.11, 0.11, 0.13 s for the setpoints, 50×10^5 Pa, 70×10^5 Pa and 100×10^5 Pa respectively.

181

The settling time, percentage overshoot and chatter fall in the same range for all the set points in the chosen range. These results show that the MRAC designed for the Hypersonic wind tunnel system is efficient in controlling the settling chamber pressure within a considerably small time range. However, with this design, the system is adversely affected by very high values of percentage overshoot, which is several times higher than the allowable range. The observed percentage overshoot of the settling chamber pressure will drastically affect the safety and performance conditions. From the above results, it can be concluded that with MRAC even though appreciably small settling time could be obtained, the percentage overshoot and chatter effects are not reduced effectively. Hence, for improvement in performance characteristic and reduction in chatter, we propose a Modified adaptive controller.

Results of MRAC indicates that even though the control scheme has the advantage of achieving a settling time of less than 2 s, it induces an overshoot of approximately 330 % for all the set points, which crosses the limit of the pressure vessels. In addition, it also has the disadvantage of chatter in the output response. To overcome this, we propose a Modified adaptive controller which is capable of compensating for the overshoot, eliminating chatter effect and at the same time maintaining short settling time.

6.2 MODIFIED ADAPTIVE CONTROLLER (MAC)

With the aim of improving the performance of MRAC for Hypersonic wind tunnel system, a Modified adaptive control scheme is designed (Maity *et al.*, 2015; Hovakimyan *et al.*, 2011). The block schematic of MAC is also based on MIT rule

and is same as that of MRAC given in Fig. 6.1 (Jacob and Binu, 2009; Tong *et al.*, 2009; Jain and Nigam, 2013; Imaduddin *et al.*, 2011; Karray and Feki, 2014; Tuan *et al.*, 2013). For improving the performance of MRAC in terms of performance parameters especially the percentage overshoot, chatter effect and short settling time appropriate modifications are incorporated into MRAC thereby redesigning the cost function suitably as a Modified adaptive control scheme. Performance improvement is observed with modified design to maintain the same stability and robustness properties (Duarte and Kumpati, 1996).

6.2.1. Design

In order to improve the transient performance as reducing percentage overshoot and chatter effect, the error has to be reduced thereby minimizing the cost function. For this purpose, the adjustment parameter, θ is properly chosen with respect to the error in terms of signum function. Thus, the Modified adaptive controller is designed by redefining the cost function (Duarte and Kumpati, 1996) as,

$$J\left(\theta\right) = |e(\theta)| \tag{6.11}$$

Hence the update law will be modified as,

$$\frac{d\theta}{dt} = -\gamma \frac{\partial e(s)}{\partial \theta} \, sgn(e) \tag{6.12}$$

With the modified design in update law, the percentage overshoot could be nullified. For effective control of percentage overshoot, the signum function in the adjustment parameter is replaced by saturation function and the update law is redefined as,

$$\frac{d\theta}{dt} = -\gamma' sat(eY_m)$$ (6.13)

where,

$$sat(eY_m) = \begin{cases} eY_m & if\ eY_m > 0.5 \\ sgn(eY_m) & if -0.5 < eY_m\ > 0.5 \\ eY_m & if\ eY_m < -0.5 \end{cases}$$ (6.14)

The reference model chosen in the design of MAC for Hypersonic wind tunnel is same as that chosen for MRAC given in eq. (6.10). Finally, the control law is redefined as,

$$u(t) = \frac{d\theta}{dt}\ u_C$$ (6.15)

6.2.2. Results and Discussion

The dynamic behaviour of the tunnel system with the MAC is studied by simulating eqs. (3.1) to (3.11) of chapter (3) and eq. (6.1) to (6.11). The results with Modified control law help to attain the transient performance while maintaining the stability. As discussed in section 6.1, the cost function of MRAC is modified as in eq. (6.11) and the update law is suitably modified by incorporating the signum function as in eq. (6.12). The settling chamber pressure with the modified update law is studied for the range of setpoints from 1×10^5 Pa to 300×10^5 Pa and representative results of the response of settling chamber pressure incorporating the above modifications in the controller design is given in Fig. 6.6 (a-c). Fig. 6. 6(a-c) represents the response of settling chamber pressure using the modified update law of MRAC for the same set points of 100×10^5 Pa, 70×10^5 Pa and 50×10^5 Pa respectively.
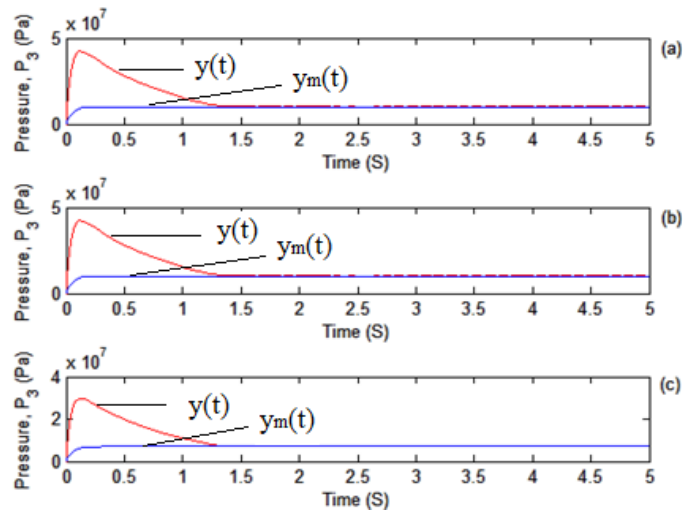
Fig. 6.6   Settling chamber Pressure, P_3 incorporating modification in the cost function of MRAC (a) for the set point 100×10^5 Pa (b) for the set point 70×10^5 Pa (c) for the set point 50×10^5 Pa

Comparing the response of settling chamber pressure in Fig. 6. 6 (a-c) with the results of MRAC shown in Fig. 6.3 to 6.5, it can be observed that with the proposed modification of cost function, the chatter effect could be slightly reduced. Fig. 6.7 (1) and (2) represents the zoomed portion of the settling chamber pressure showing the chatter effect and percentage overshoot of Fig. 6.6 (a), (b) and (c) for the setpoints 100×10^5 Pa, 70×10^5 Pa and 50×10^5 Pa respectively.
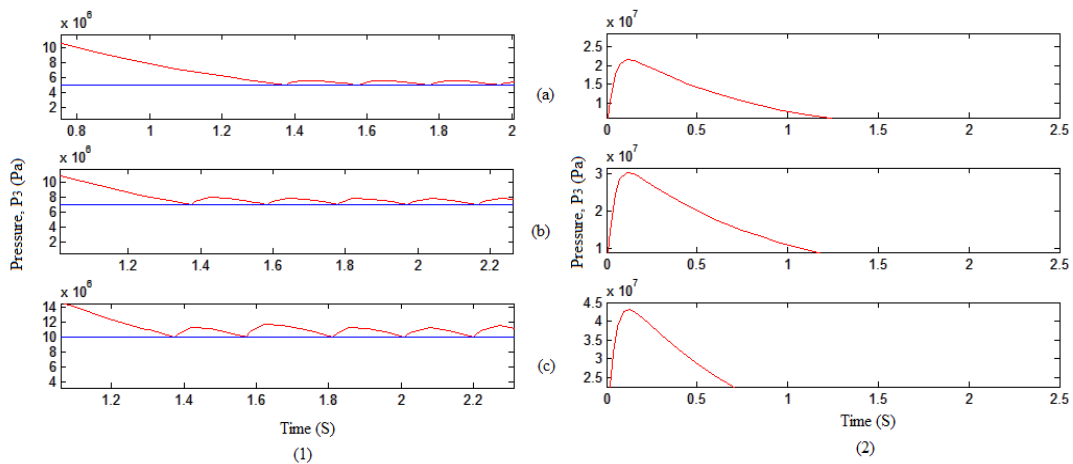
Fig. 6.7   Zoomed portion of Fig. (6.6) (1) chatter effect (2) Percentage Overshoot (a) for the set point 100×10^5 Pa (b) for the set point 70×10^5 Pa (c) for the set point 50×10^5 Pa

185

From Fig. 6.7, it is clear that though the settling time is short and is 1.37 s for the three setpoints respectively, the chatter ranges from 50×10^5 Pa to 56.1×10^5 Pa for setpoint of 50×10^5 Pa, 70×10^5 Pa to 78.42×10^5 Pa for setpoint of 70×10^5 Pa and 100×10^5 Pa to 117.1×10^5 Pa for a setpoint of 100×10^5 Pa. The rise time for the three setpoints are 0.007 s. However, the percentage overshoot remains in the same range as in MRAC and is 291.85, 309.29 and 306.24 % and the peak time is observed to be 0.11, 0.11, 0.13 s for the three setpoints, 50×10^5 Pa, 70×10^5 Pa and 100×10^5 Pa respectively. Hence to reduce the percentage overshoot and to reduce the chatter effect further, the control law is suitably modified as in eq. (6.15). In order to further improve the chatter effect, the update law is further modified replacing the signum function with saturation function.

Fig. 6.8 to 6.10 shows the response of the settling chamber pressure of the tunnel system with the MAC for three set points, 100×10^5 Pa, 70×10^5 Pa and 50×10^5 Pa respectively. Fig. 6. 8 (a) (1) represents the response of settling chamber pressure, P_3 for the set point of 100×10^5 Pa, Fig. 6. 8 (b) represents its reference model output and Fig. 6.8 (2) (a) (b) represents the corresponding zoomed portion of settling chamber pressure and reference output with MAC.
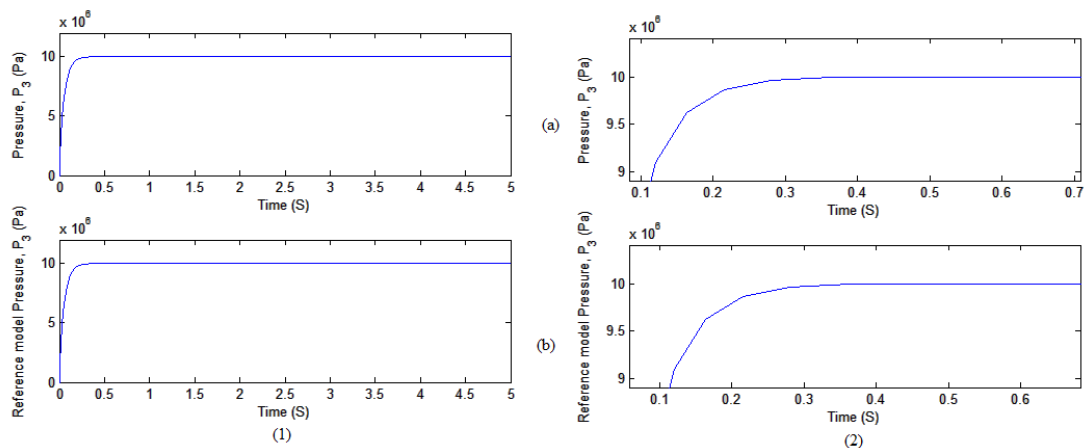
Fig. 6.8   Settling chamber pressure for set point of 100×10^5 Pa with MAC (a) Settling chamber pressure, P_3 $(y(t))$ (b) Reference model Pressure, P_3 $(y_m(t))$

From the figure, it can be observed that with the newly designed MAC, the percentage overshoot is completely suppressed and that error between the system model and reference model is eliminated. The corresponding settling time is observed to be 0.56 s which is considerably lesser than that of MRAC for the same set points. It is also noteworthy that the set point is achieved without any chatter effect. The rise time is observed to be 0.11 s. From the above figure, it can be observed that the settling chamber pressure is controlled and maintained exactly at the desired set point. Also, it is observed that the peak time is 1.96 s.

Fig. 6.9 (1) shows the settling chamber pressure and the reference model output for a setpoint of 70×10^5 Pa and its zoomed portion is shown in Fig. 6.9 (2). From the figure, it is clear that the settling chamber pressure matches with the reference model output. This is achieved with a rise time of 0.11 s with a peak time of 1.96 s and settling time of 0.56 s without any percentage overshoot and chatter effect.
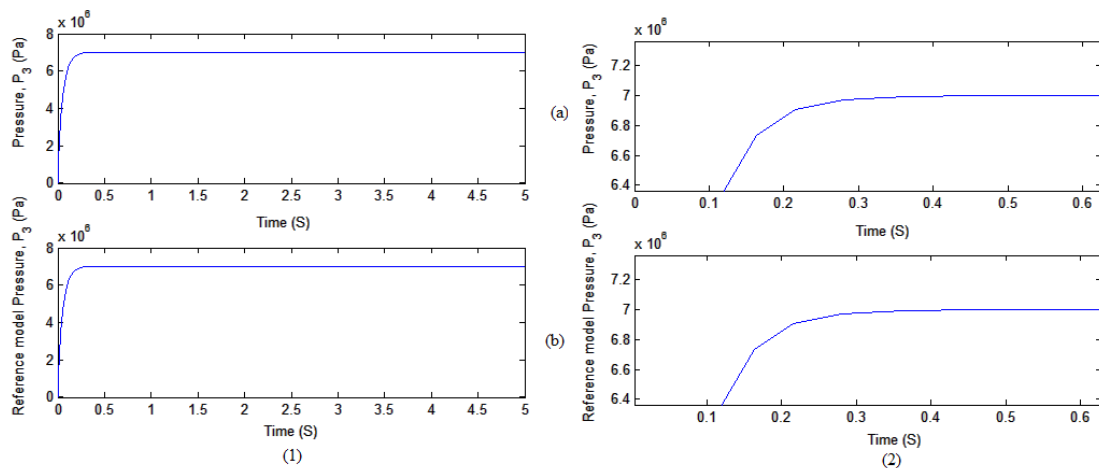
Fig. 6.9   Settling chamber pressure for set point of 70×10^5 Pa with MAC (a) Settling chamber pressure, P_3 ($y(t)$) (b) Reference model Pressure, P_3 ($y_m(t)$)

Fig. 6.10 shows the settling chamber pressure for a set points of 50×10^5 Pa. It is evident from the figures that the settling time is 0.56 s, there is no overshoot and chatter effect. The rise time with this setpoint is observed to be 0.11 s and peak time as 1.96 s. For the entire range of set points from 1×10^5 Pa to 300×10^5 Pa, short settling time without any chatter effect and percentage overshoot are obtained with the Modified adaptive control.
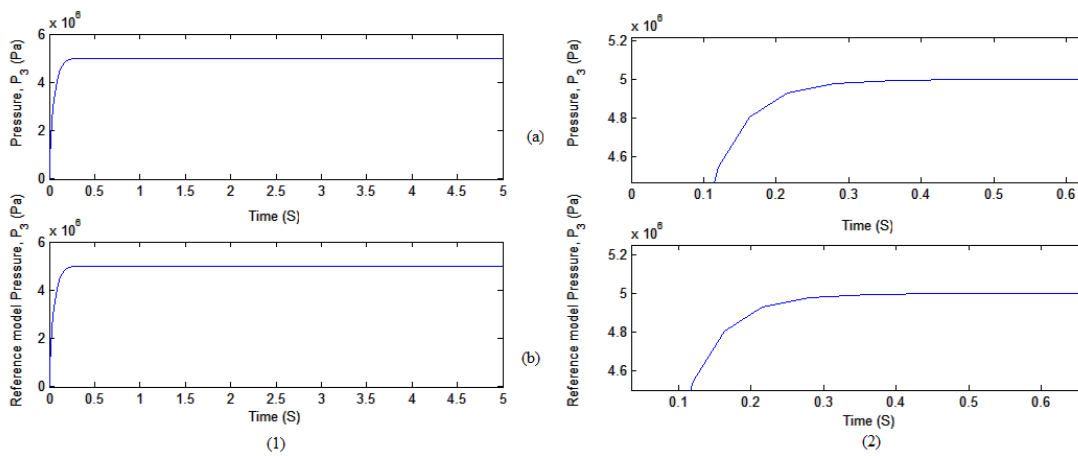
Fig. 6.10   Settling chamber pressure for set point of 50×10^5 Pa with MAC (a) Settling chamber pressure, P_3 $(y(t))$ (b) Reference model Pressure, $P_3(y_m(t))$

Fig. 6.11 (1) (a), (b), (c) shows the response of settling chamber pressure with MRAC and MAC controllers for the set points of 100×10^5 Pa, 70×10^5 Pa and 50×10^5 Pa respectively. The zoomed portion of the settling chamber pressure for the given three setpoints is represented in Fig. 6.11 (2). The figure clearly indicates the effectiveness of the proposed MAC scheme in suppressing the overshoot and providing drastic improvement in the settling time. It can also be observed with the modifications proposed, the newly designed MAC efficiently reduces the chatter effect in the output response.
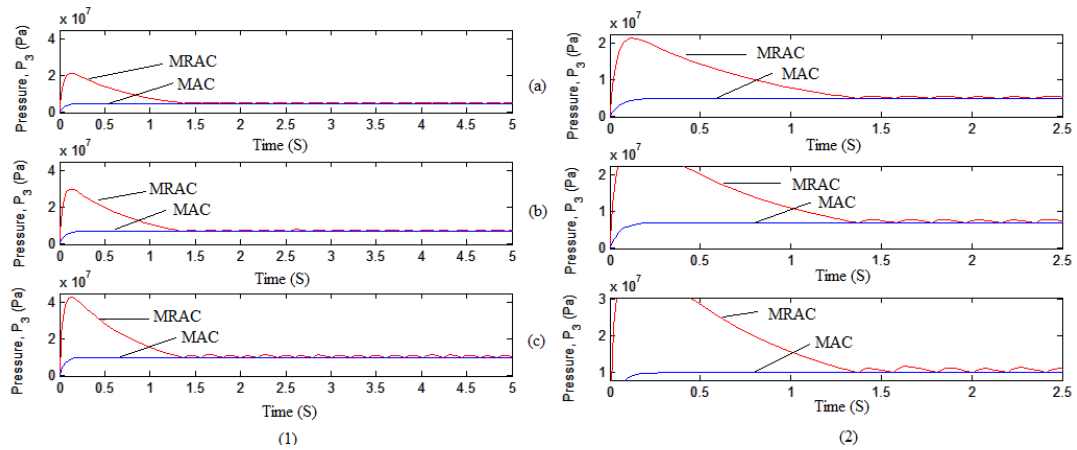
Fig. 6.11   Settling chamber Pressure, P_3 with MRAC and MAC (a) for the set point 100×10^5 Pa (b) for the set point 70×10^5 Pa (c) for the set point 50×10^5 Pa

The performance results of MRAC and MAC for regulation of pressure inside Hypersonic wind tunnel is analyzed and compared (Duarte and Kumpati, 1996). Table 6.1 shows the comparison of MRAC and MAC in terms of their performance indices.

Table 6.1 Performance Comparison of MRAC and MAC

Sl. No	Set point	Settling Time (S)		Overshoot (%)		Rise Time (S)	
		MRAC	MAC	MRAC	MAC	MRAC	MAC
1	100×10^5 Pa	1.37	0.56	330.34	NIL	0.007	0.11
2	70×10^5 Pa	1.37	0.56	330.34	NIL	0.007	0.11
3	50×10^5 Pa	1.37	0.56	330.34	NIL	0.007	0.11

From the results it is clear that with MAC scheme, the chamber pressure of the Hypersonic wind tunnel system stabilises within 0.56 s (Yilmaz *et al.*, 2012; Lin *et al.*, 2007; Chen *et al.*, 2012). Percentage overshoot and settling time for MAC proposed here is much lower than other control techniques applied to the system.

189

From the above results it is observed that the Modified adaptive control scheme is highly efficient in controlling the settling chamber pressure to the specified set point within a very short time of 0.56 s as compared to that of 1.37 s with MRAC. It is also observed that the rise time is 0.11 s for all setpoints.

In addition, the MAC scheme has the advantage of controlling the settling chamber pressure with zero percentage overshoot. Moreover, with the proposed modifications, the chattering effect observed with MRAC is also nullified by MAC that makes it more suitable for pressure regulation in the Tunnel systems. It could also be observed that the system is stable as the pressure attains 0.56 s to settle and remains for a infinitely longer time with the same transient performances achieved. This is maintained during the entire range of closed loop condition of the system.

Verification of the proposed controller is based on the theoretical and simulation studies. From the results of the performance comparison analysis, it is observed that Modified adaptive control is the most suitable scheme for regulation of pressure in the settling chamber of Hypersonic wind tunnel. The usual procedure for validation of controllers is performed in real time experimental setup. The MAC thus proposed is applied to a Supersonic wind tunnel model for verification (Sonneveldt *et al.*, 2007). Due to the constraints in implementing the controller in Hypersonic wind tunnel, we adopt a verification process of the proposed MAC scheme in the INCAS Supersonic wind tunnel model validated on real time with Adaptive fuzzy PI controller (Sonneveldt *et al.*, 2007).

6.3. VERIFICATION OF MODIFIED ADAPTIVE CONTROLLER

Verification and validation are processes to quantify and build credibility for the solutions of the respective design problems thereby ensuring closeness of the simulations to the real world representations. Verification is a process wherein we assure that the proposed algorithm is correct and efficient enough to solve for the particular application. Here, we ensure the effectiveness of the proposed Modified Adaptive control (MAC) for the Hypersonic wind tunnel by verifying on different wind tunnel models which are already experimentally validated. For this purpose, we considered the INCAS Supersonic blowdown tunnel, whose plenum pressure is controlled by PI and Adaptive Fuzzy PI controllers and is validated using experimental data collected from real test cases (Corneliu, 2013). The proposed controller is applied to this validated model and found to be efficient in regulating the plenum chamber pressure of blowdown type Supersonic wind tunnel.

Wind tunnels operating in the Mach number range 1 to 5 are called as supersonic tunnels whereas the tunnels used for higher Mach numbers (> 5) are called as hypersonic tunnels. For high speed tunnels, more focus is given to simulating flow Reynolds number and the Mach numbers in the test section of the tunnel. In addition to these parameters, the total energy content of the flow also becomes important at hypersonic speeds. Static stability analysis conducted for hypersonic and supersonic tunnels are similar. Considering the practical difficulty in availing the validated Hypersonic wind tunnel models, a readily available validated Supersonic model with similar performance characteristics is selected for verification of the proposed MAC.

Review of Adaptive Fuzzy PI Controller for INCAS Supersonic Wind Tunnel

The INCAS Supersonic Blowdown Wind Tunnel developed is a pressurized aerodynamic tunnel based on two geometrically variable transversal sections, capable of operating both at Subsonic and Supersonic speeds with Mach numbers, 0.1 to 3.5, with high Reynolds number of 100 mil/m in transonic regimes. In a Supersonic flow, decreasing the cross-sectional area causes the flow to decrease in velocity and increase in pressure and vice versa. These properties exhibited are exactly the opposite to that of Subsonic wind tunnels (Busa, 2010; Corneliu, 2013; Butler *et al.*, 2010; Shahrbabaki *et al.*, 2014a; Shahrbabaki *et al.*, 2014b; Ilic *et al.*, 2016; Sunny *et al.*, 2017). An experimental facility using Supersonic wind tunnel was developed by INCAS (Corneliu, 2013) in order to deliver constant plenum pressure for the test run. The main objective is to maintain constant plenum chamber pressure throughout the test which is achieved by regulating the pressure regulator valve. For the experiment conducted by INCAS which completes in 15 to 100 seconds, depending on the required flow regime, many techniques from manual operation of control valves to automatic control using various modern controllers were designed and developed (Bhoi and Suryanarayana, 2008; Corneliu, 2013).

The schematic used by INCAS for the Supersonic Blowdown Wind Tunnel is shown in Fig. 6.12 below (Corneliu, 2013).

192
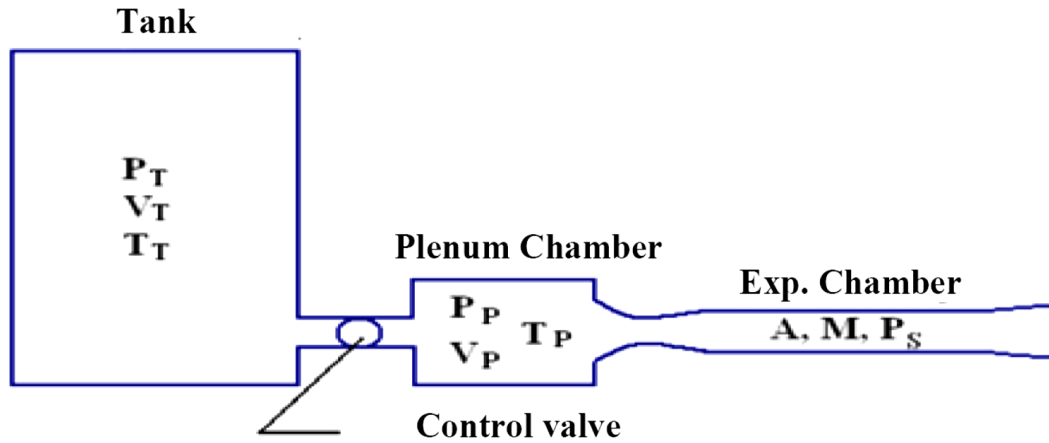
Fig. 6.12   General layout for a Blowdown Supersonic Wind Tunnel (Hollis and Griffith, 1991).

The principle of operation is similar to the Hypersonic wind tunnel system. The Supersonic tunnel system consists of 3 vessels, viz: Storage tank, Plenum chamber and experimentation chamber. The air from the high pressure tank is released to the plenum chamber through a pressure regulating valve. The basic principle involves controlling the airflow using regulator valve while ensuring stabilized flow parameters, viz: pressure, speed, temperature and perturbations in the experimentation chamber. The operation of control valve is very critical during a test in order to ensure proper parameters in the plenum chamber depending on the airflow available in the storage tank. The operation of valve is such that the difference in pressure between the two faces of the valve can be maximum of 20 Bar and at high speeds of up to 10 seconds for full opening of the valve. With these specifications, the transfer function of the validated tunnel system is obtained from (Bhoi and Suryanarayana, 2008; Corneliu, 2013) as follows:

$$H(S) = \frac{2.54\times 10^7 \times s + 5.321 \times 10^5}{s^3 + 16.68 \times s^2 + 3.367 \times s + 0.01937} \qquad (6.16)$$

Experimental Validation of INCAS Supersonic wind tunnel system

The Supersonic wind tunnel system validated with PI and Adaptive Fuzzy PI controllers (Corneliu, 2013) using INCAS system's real time data for a setpoint of 250 Bar is reviewed. The PI controller is designed based on pole-zero allocation method with K_p value as 3.26×10^{-6} and K_i value as 5.6013×10^{-7}. The results are simulated in LabVIEW environment (Bhoi and Suryanarayana, 2008; Corneliu, 2013). The results show that the plenum chamber pressure quickly follows the reference output. From the results, it is observed that the designed PI controller is capable of controlling the plenum chamber pressure within 2 s for a given setpoint of 250 Bar but the overshoot is high and is 18.08 %.

To improve the performance of the tunnel system especially in terms of percentage overshoot, an Adaptive Fuzzy PI controller was designed by INCAS (Corneliu, 2013) with a reference model chosen as:

$$M(s) = \frac{1}{0.05s+1} \tag{6.17}$$

The Fuzzy rules are selected with 7 membership triangular functions for both input and output. With the improved design using Adaptive Fuzzy PI controller, it is observed that the settling time is 1.75 s, overshoot is drastically reduced and is 9.41% and the rise time is close to 1.5 s. Thus, it is noted that there is considerable improvement in the performance with Adaptive Fuzzy PI controller (Corneliu, 2013).

In order to verify our design of Modified adaptive controller in Section 6.2, we apply the control algorithm to the modelled INCAS Supersonic wind tunnel system.

6.3.1. Modified Adaptive Controller Design for INCAS Supersonic Wind Tunnel

The proposed MAC algorithm in section 6.2.1 is applied to validated model of INCAS blowdown Supersonic wind tunnel (Bhoi and Suryanarayana, 2008; Corneliu, 2013) given in eq. (6.16). For this purpose, an adjustment parameter, θ is properly chosen with respect to the error in terms of signum function. The cost function for this model is chosen (Duarte and Kumpati, 1996; Maity *et al.*, 2015) as,

$$J(\theta) = |e(\theta)| \tag{6.18}$$

Thus, the update law is,

$$\frac{d\theta}{dt} = -\gamma' \, sat(eY_m) \tag{6.19}$$

where,

$$sat(eY_m) = \begin{cases} eY_m & if \ eY_m > 0.5 \\ sgn(eY_m) & if -0.5 < eY_m > 0.5 \\ eY_m & if \ eY_m < -0.5 \end{cases} \tag{6.20}$$

The model is simulated with this update law. For effective control of plenum chamber pressure, the signum function in the adjustment parameter is replaced by saturation function of Model reference adaptive controller.

The reference model chosen in the design of MAC is same as that chosen for MRAC of INCAS given in eq. (6.17). Finally, the control law is defined as,

$$u(t) = \frac{d\theta}{dt} \, u_C \tag{6.21}$$

6.3.3. Verification of Results

Verification is a technique to assure solutions to various Engineering problems are quantified to maintain a high level of confidence in performance, safety and reliability. Now a days, the government and Industries demand for validated models with solutions to improve efficiency, reduce cost, risk for testing, time management etc. This objective motivates the need of highly accurate validated or verified results to predict desired performance.

The behaviour of the Supersonic wind tunnel system is studied by simulating eq. (6.16) to (6.21). The response of the plenum chamber pressure with the designed Modified adaptive controller for a sample setpoint of 250 Bar is shown in Fig. 6.13. From the results, it is observed that the settling time is 0.5 s, rise time is 0.11 s and peak time is 1.90 s for the given setpoint. However, it is observed that there is no peak overshoot with the proposed design.
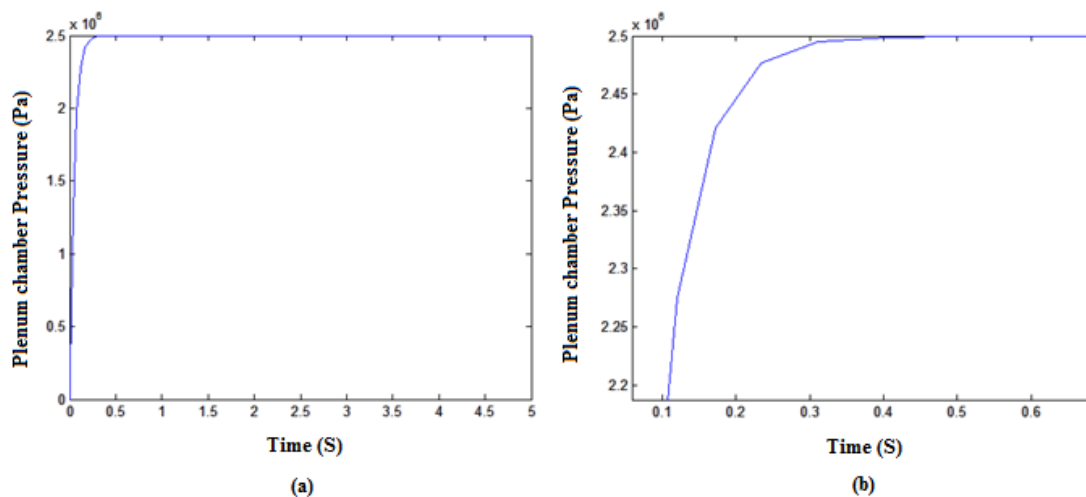
Fig. 6.13   Plenum chamber pressure of INCAS Supersonic wind tunnel with Modified adaptive control for a setpoint of 250 Bar

Table 6. 2 gives the performance comparison of our simulated results with that of simulated and validated Adaptive Fuzzy PI controller for INCAS Supersonic wind tunnel (Corneliu, 2013).

Table 6.2   Performance Comparison of Modified Adaptive Controller (MAC) with Adaptive Fuzzy PI (AFPI) Controller for a set point of 250 Bar

	Settling Time (S)		Overshoot (%)		Rise Time (S)	
Set point	MAC	AFPI	MAC	AFPI	MAC	AFPI
250 Bar	0.5	1.75	NIL	9.41	0.11	1.5

Table 6. 2 gives the performance comparison of our simulated results with that of simulated Adaptive Fuzzy PI controller for INCAS Supersonic wind tunnel. From the results of our design, it is observed that the settling time which is required to be less is in the same range as that of validated Adaptive Fuzzy PI design. However, the percentage overshoot in real time was 9 % which is nullified with the Modified adaptive control approach. Similarly, the rise time is also found to be less than 2 s in both designs. Thus, it is clear from our results that all the transient parameters performs well and are in the same range as that of validated Adaptive Fuzzy PI design and hence we could verify the Modified Adaptive control (MAC) design (Corneliu, 2013). Hence, the proposed Modified adaptive control design for the selected Hypersonic wind tunnel model is verified.

The regulation of pressure inside the test section is very significant for Hypersonic wind tunnel system, which is achieved by controlling the settling chamber pressure. Here, we propose a Modified adaptive control scheme by incorporating suitable modifications to the cost function and the control law of MRAC. For developing MRAC, a reference model based on MIT rule is selected and an adjustment parameter

is designed so as to minimize the cost function. An equivalent control law is designed based on the selected adaptation gain. The proposed MAC scheme is designed by suitably modifying the cost function and the update law of MRAC. The dynamics of the tunnel system with both MRAC and the newly proposed MAC schemes are simulated and the performance characteristics are evaluated.

MRAC has the inherent advantage of fast settling time and robustness towards parametric uncertainties. Results of MRAC indicate that even though this control scheme has the advantage of achieving a settling time of less than 2 s, it produces an overshoot around 330 % for all the set points. The extremely high overshoot which crosses the safe limit of the pressure vessels makes it unsuitable for this model. In addition, it also has the disadvantage of chatter in the output response. This necessitates suitable modifications in the design of MRAC which can eliminate or reduce the overshoot to the tolerable limits without affecting the other performance parameters. For this purpose, suitable modifications in the cost function is incorporated and the performance is evaluated. It is observed that modification in cost function alone will results in elimination of only the chatter effect. For eliminating the overshoot, further modifications are incorporated in the update law. The combined modifications are found to be efficient in nullifying the extremely high overshoot of 330 % and have the added advantage of eliminating the chatter effect and the settling time is reduced to 0.56 s which is found to be half of 1.37 s obtained with MRAC.

For Hypersonic wind tunnel systems, as the test duration is very short, the settling time is a crucial parameter. The results of our investigations show that the newly proposed MAC scheme effectively controls the settling chamber pressure within a

very short time. Moreover, with the new scheme the percentage overshoot observed with MRAC is completely eliminated. In addition, the newly designed MAC has the ability to eliminate the unwanted chattering resulting from discontinuous control of MRAC. The above advantages make the proposed MAC scheme highly suitable for regulating the pressure inside the settling chamber of the Hypersonic wind tunnel system. However, the economic aspects of the proposed schemes are to be evaluated. Such studies can contribute to the effective implementation of the proposed scheme in real time applications.

The design of Modified Adaptive control schemes for pressure regulation in the settling chamber of Hypersonic wind tunnel, based on its simulation in Section 6.2 is verified. For this purpose, initially a survey on plenum pressure regulation inside the validated model of INCAS Supersonic wind tunnel (Bhoi and Suryanarayana, 2008; Corneliu, 2013; Vincent *et al.*, 1999) is considered and analyzed the preliminary results of simulation. In the Supersonic wind tunnel developed by INCAS, the method of controlling plenum chamber pressure using PI and Adaptive Fuzzy PI controller is simulated and experimentally validated with real time test results (Corneliu, 2013). Here, we designed the proposed Modified adaptive control schemes for the regulation of plenum chamber pressure for INCAS Supersonic wind tunnel model. The simulation results of the above control schemes were analyzed and compared with validated INCAS model for Adaptive Fuzzy PI controllers. From the comparison, it is observed the results with the newly designed control scheme is matching and in the tolerable range with that of INCAS control schemes. Thus, the proposed Modified adaptive control scheme designed is verified for the INCAS model and Hypersonic wind tunnel model.

Chapter 7 presents a comparison of the designed controllers and proposes the suitable controller design for regulation of settling chamber pressure based on the verification carried out with INCAS Supersonic wind tunnel.

CHAPTER 7

PERFORMANCE COMPARISON OF

NONLINEAR CONTROLLERS

This work focusses on identifying the best suitable controller for the regulation of pressure inside the settling chamber of Hypersonic wind tunnel. For this purpose, the tunnel system is modelled incorporating the important nonlinearities of transport delay and valve saturation function and is represented in transfer function as well as state space forms. Analysis of the modelled system is carried out to ensure stability using Lyapunov Stability Theorem, Phase Portrait method, Bode plot, Root locus and Kalman's test for controllability and observability. The negative definiteness of Lyapunov function, convergence of phase portrait to origin, positive values of gain margin and phase margin from bode plot, root locus on the left half of the s-plane and nonsingular values of controllability and observability matrix confirm the stability of the system. Sensitivity analysis is also carried out to find out the variation in pressure with variation in stem movement. It is observed that the system exhibits nonlinear behaviour as the sensitivity varies continuously and has infinite values at infinite regions.

The pressure regulating valve that maintains constant air flow in the Hypersonic flow regime in the settling chamber is precisely controlled during the test run thereby maintaining constant pressure in the test section where the specimen is placed. For this purpose, various controllers are designed and the most suitable controller is

proposed after comparing their transient performance characteristics for the regulation of settling chamber pressure in the Hypersonic wind tunnel. From the open loop response of the system, it is observed that it takes 450 s to release the air from the storage tank to the settling chamber. However, this value is quite high and is to be reduced so as to achieve the minimum settling time possible keeping the other parameters in the desired range. This, necessitates the development of suitable control law capable of maintaining the air flow through the settling chamber constant and thereby meeting the desired characteristics like minimum overshoot, short settling time and fast rise time without any chatter effect. In this work, various linear, Robust, Hybrid and Adaptive controllers are designed and their performance indices are compared and the best controller for this application is proposed.

A basic LQR controller is designed which provides feedback gain to reduce the variation in the output variable from the setpoint. In order to reduce this variation in the output variable, weighing matrices, Q and R are properly selected thereby achieving the optimal gain and the dynamic behaviour is analyzed. H-infinity controller that is robust to parametric variations is then designed to evaluate the performance. The development of this control algorithm includes designing suitable weighing functions that meets the nominal performance of the system. To further optimise the values of weighing functions, Krill Herd optimisation algorithm is used to tune the parameters of the weight function for the H-infinity controller. Other two nonlinear approaches applied for the pressure regulation application includes Backstepping and Sliding mode controllers. Backstepping is a Lyapunov based nonlinear technique in which the control algorithm starts from a stable system and

back out to stabilize each subsystem until the final control law is reached. Sliding mode controller is a robust, nonlinear, systematic control technique in which the design includes the development of switching law. The switching law is built from the switching surface that is selected based on a Lyapunov function. Based on the performance evaluation of conventional controllers, Hybrid controllers, viz: Backstepping Sliding mode and Sliding mode Fuzzy controllers are designed for the tunnel system. In the design of Backstepping Sliding mode controller, the switching surface is selected as a function of the new states in Backstepping approach. In Sliding mode Fuzzy controller design, the sliding surface selection is based on the fuzzy rules thereby ensuring stability and elimination of chatter effect in the response.

Adaptive controllers, viz: Model Reference Adaptive controller and Modified Adaptive controllers are also designed for the modelled system. Model reference adaptive controller is a popular adaptive control technique based on MIT rule. Here, a reference model which suits with the desired transient characteristics is chosen for the controller deign. A cost function based on adjustment parameter is selected to develop the control law. To improve the performance indices with MRAC design for the tunnel system, the cost function is redefined to design a Modified Adaptive controller. In this approach, the redefined cost function is used to develop the control law which depends on the signum function of the error signal and the output of reference model. A comparison of various performance indices of all the above controllers are discussed in detail to propose the Modified Adaptive controller as the most suitable one to meet the purpose. The Modified adaptive control design is verified by applying to the validated model of INCAS Supersonic wind tunnel (Bhoi

and Suryanarayana, 2008; Corneliu, 2013). By comparing the test results of Modified Adaptive control with that of existing Adaptive fuzzy PI of INCAS Supersonic wind tunnel plenum pressure regulation, it is found that the performance parameters are in the comparable and tolerable range.

7.1. RESULT AND DISCUSSION

LQR, HI, HIO, BS, SMC, BSC, SFC, MRAC, MAC controllers are designed for the efficient and accurate control of pressure in the settling chamber of a Hypersonic wind tunnel system and their performance are evaluated for a range of setpoints from 1×10^5 Pa to 300×10^5 Pa. The performance indices corresponding to representative setpoints 50×10^5 Pa, 70×10^5 Pa and 100×10^5 Pa are tabulated in Table 7.1 and comparison of settling time, percentage overshoot and rise time for these controllers are shown in Fig. 7.1 (a) (b) and (c) respectively.

Table. 7.1 Performance comparison of Different Controllers

SET POINTS CONTROLLERS	Settling Time (S)			% overshoot			Rise Time (S)		
	50×10^5Pa	70×10^5Pa	100×10^5Pa	50×10^5Pa	70×10^5Pa	100×10^5Pa	50×10^5Pa	70×10^5Pa	100×10^5Pa
LQR	15	15	15	25.38	31.38	29	1.43	1.52	1.43
HI	1.2	1.2	1.2	116	83.33	58.33	0.2	0.85	0.85
HIO	1.2	1.2	1.2	75	53.57	37.5	0.29	0.28	0.29
BS	7.5	7	6.5	NIL	NIL	NIL	3.44	3.59	3.59
SMC	8	8	8	NIL	NIL	NIL	3.46	3.46	3.46
BSMC	8	8	8	NIL	NIL	NIL	3.45	3.45	3.45
SFC	10.3	12	7	NIL	NIL	1	3.45	3.45	1.44
MRAC	1.37	1.37	1.37	330.34	330.34	330.34	0.007	0.007	0.007
MAC	0.56	0.56	0.56	NIL	NIL	NIL	0.11	0.11	0.11
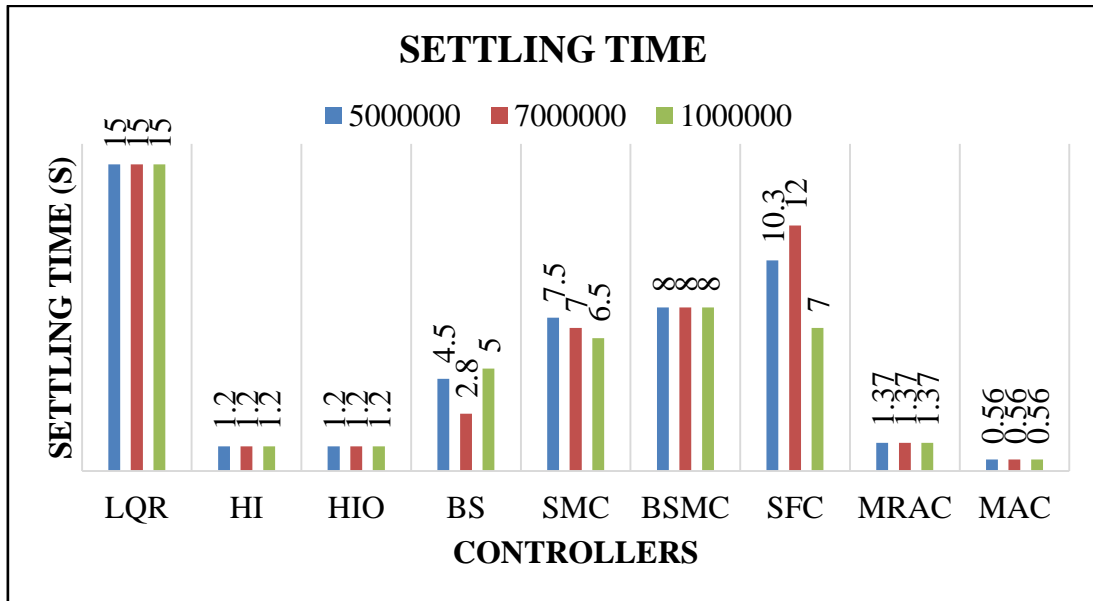
(a)
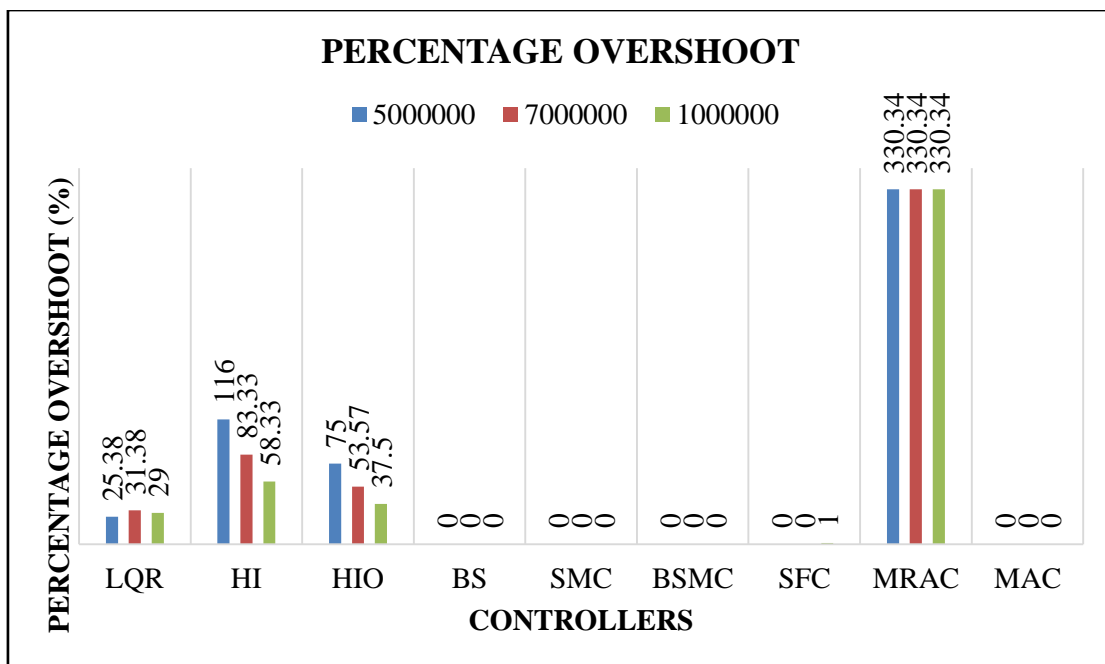
(b)

Fig. 7. 1 (a) Comparison of Settling Time for the setpoints, 50×10^5, 70×10^5 and 100×10^5 Pa. (b) Comparison of Percentage Overshoot for the setpoints, 50×10^5, 70×10^5 and 100×10^5 Pa (c) Comparison of Rise Time for the setpoints, 50×10^5, 70×10^5 and 100×10^5 Pa

205
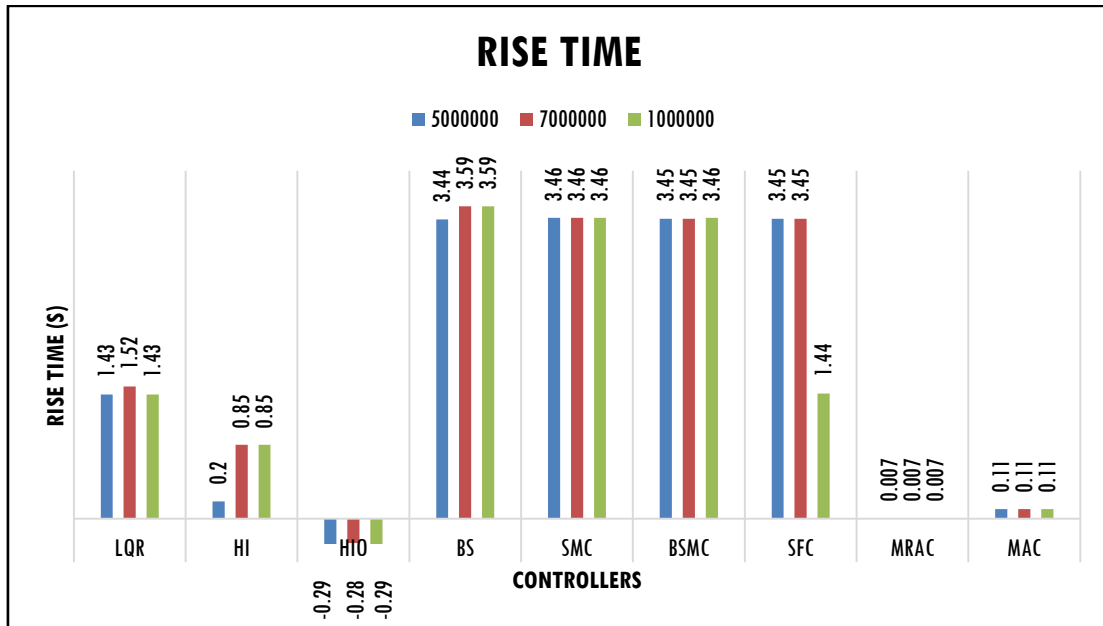
(c)

Fig. 7. 1 (**Contd.**)

The performance of LQR controller is decided by the matrices, R and Q whose values cannot be increased beyond an optimum limit. Higher values of Q cause increase in gain, K leading to instability. It is observed from Fig. 7.1 (a) that optimum value of matrix, Q gives consistent settling time for all three setpoints and is 15 s. However, as indicated in Fig. 7.1 (b), the percentage overshoot of LQR controller corresponding to the above three setpoints are 25.38, 31.38 and 29 % respectively and does not remain consistent for all three setpoints. The corresponding values of rise time from Fig. 7. 1 (c) are 1.43 s, 1.52 s and 1.43 s for three setpoints which are again not consistent for all the setpoints. Due to these limitations, an H-infinity controller with weighing matrices, W_u and W_p are selected so as to meet the stability and performance requirements respectively. Even though the settling time remains constant at 1.2 s with all the setpoints, percentage overshoot as well as rise time varies according to the setpoints. The corresponding values of percentage overshoot are 116, 83.33 and

206

58.33 % for the three setpoints respectively and the rise time is 0.2 s for the setpoint, 50×10^5 Pa and 0.85 s for the setpoints, 70×10^5 and 100×10^5 Pa and hence not consistent for all the setpoints. This high value of overshoot is due to the chosen values of weighing matrices, W_u and W_p. For reduction in overshoot, we found the optimal value of the weight function, W_u using Krill Herd Optimisation algorithm. With the optimised weighing function, it is observed that, settling time remains same and is 1.2 s for all the setpoints whereas the value of percentage overshoot is improved. With the optimized H-infinity controller, it is observed that overshoot is reduced but not nullified and is 75, 53.57 and 37.5 % corresponding to each value of setpoints and rise time 0.29 s for the setpoints, 50×10^5 and 100×10^5 Pa and 0.28 s for the setpoint, 70×10^5 Pa. However, these values of overshoot are not tolerable and hence we designed two nonlinear techniques for pressure regulation, viz: Backstepping and Sliding mode controllers. It is observed that with the Backstepping controller design, settling time of the chamber pressure is 7.5, 7 and 6.5 s for the three set points, 50×10^5 Pa, 70×10^5 Pa and 100×10^5 Pa respectively. However, the percentage overshoot is zero and rise time is 3.44 s for the setpoint of 50×10^5 Pa and 3.59 s for the setpoints, 70×10^5 and 100×10^5 Pa. Even though, the settling time and rise time are less, it is found that these values are not consistent for all the setpoints. This variation is due to the selection of Lyapunov function for each of the sub-systems which depends on the respective error variable. This drawback can be overcome by suitably selecting the Lyapunov function. Thus, to avoid this limitation, Sliding mode controller is suggested and proposed wherein the time duration for settling is 8 s which is short and consistent for any given set point. It could also be observed that the rise time for the Sliding mode controller design is 3.46 s for all the

three setpoints and there is no overshoot for any setpoint values. However, there are chances of occurrence of chattering in the output response under variations in operating conditions using this approach.

Due to the difficulty in meeting the performance requirements with the previous controllers, the response using combination approaches, Backstepping Sliding mode and Sliding mode Fuzzy controllers are also analyzed. In Backstepping Sliding mode controller design, the time required to settle is less and is 8 s which is same as that with Sliding mode controller. It is also noted that the consistency problem with Backstepping controller is nullified by combining it with Sliding mode controller. In this design technique, each sliding surface is defined in terms of the respective error variable ensuring stability criterion. With Backstepping Sliding mode controller, it is observed that the rise time is 3.45 s for the setpoints, 50×10^5 and 70×10^5 Pa and 3.46 s for the setpoint, 100×10^5 Pa without any overshoot in the output response. In the proposed BSMC design, a suitable sliding surface is properly designed to eliminate the unwanted chattering resulting from the discontinuous control of Sliding mode controller. But due to design complexity, we tried the second approach, Sliding mode Fuzzy controller for the tunnel system. It is observed that the settling time is 10.3, 12 and 7 s for the respective three setpoints and is not consistent for all the setpoints. However, this control scheme has no overshoot for the setpoints, 50×10^5 and 70×10^5 and has 1 % overshoot for the setpoint, 100×10^5 Pa. it is also noted that the rise time is 3.45 s for the setpoints, 50×10^5 and 70×10^5 Pa and 1.44 s for the setpoint, 100×10^5 Pa. Thus, it is observed that even though the settling time and rise time are quite less, the values are not consistent with respect to the set points. Moreover, overshoot could not be completely eliminated. This is due to the fact that sliding surface selection depends on the fuzzy rules and that it changes accordingly.

Considering the complexity in design with BSMC and the overshoot and consistency issues in SFC, we designed Adaptive controllers, viz: Model Reference Adaptive controller and Modified Adaptive controller for our pressure regulation application. With the MRAC design, it is observed that the settling time is less and is 1.37 s and the rise time is equal for all the three setpoints and is 0.007 s. As the update law has direct relation with the error and output of the reference model, the MRAC control design generates high overshoot and chatter in the output. It is also observed that the percentage overshoot is very high and is 330.34 % for all the setpoints and it is beyond the tolerable limit. Thus, the above design is modified as Modified Adaptive controller incorporating signum function in the update law and is found that the settling time is further reduced to 0.56 s. The proposed approach of Modified Adaptive controller does not have overshoot and chatter in the output response for any given setpoints and it is also found that the rise time is 0.11 s for all the three setpoints. Thus, we could conclude that the shortcomings of MRAC approach associated with high overshoot and chatter is nullified with the proposed control algorithm of MAC.

7.2. PERFORMANCE ANALYSIS

The response of the control strategies, LQR controller, H- infinity, H-infinity with Krill Herd Optimisation, Backstepping, Sliding mode, Backstepping Sliding mode, Sliding mode Fuzzy, Model Reference Adaptive and Modified Adaptive controllers used to operate the control valve for the regulation of settling chamber pressure inside the Hypersonic wind tunnel are analyzed. The settling time (2% criterion), rise time and percentage overshoot are evaluated for each of these controllers and are tabulated in Table 7.1.

209

In Hypersonic wind tunnel system, the pressure levels are very high and the test duration is to be maintained as low as possible even though the maximum allowable test duration is 40 seconds for various other applications (Jones *et al.*, 2011a; Jacob and Binu, 2009; Jones *et al.*, 2011b; Vargese and Binu, 2009). This demands highly efficient control techniques for the regulation of pressure in the settling chamber. LQR controller for the regulation of settling chamber pressure is designed and its results are evaluated in detail in chapter 4. It is observed that the settling time is less whereas the percentage overshoot increases with increase in set point in the response. To reduce the overshoot and to improve the settling time, a robust H-infinity controller is designed. It is observed that the conventional H-infinity controller with the designed weights reduces the settling time. However, the percentage overshoot for these weights are quite high. Hence, the weight optimisation is done using Krill Herd Optimisation technique and the optimised H-infinity controller gives reduced percentage overshoot with the same settling time as that of conventional one. To reduce the overshoot further, Backstepping control algorithm is proposed based on recursive design methodology for nonlinear feedback control. From the results, it is clear that even though the Backstepping controller has the advantages of faster response with no overshoot and chatter effect, the settling time does not remain consistent for all the set points. To overcome this drawback and to reduce the design complexity, a Sliding mode controller is designed. Sliding mode controller when used independently gives satisfactory performance in terms of settling time and overshoot but it has chances of occurrence of chattering in the output response under variations in operating conditions. Thus, with the aim of making the system robust to parametric uncertainties with chatter free response, a Hybrid controller, which is the combination

210

of Backstepping and Sliding mode control technique is suggested in chapter 5. From the results, it is observed that Backstepping Sliding mode controller is able to regulate the settling chamber pressure in a very short duration without percentage overshoot and chatter effect. However, considering the design complexity, a Sliding mode Fuzzy controller is designed. The intelligence of Fuzzy logic is effectively used for selecting the sliding surface of the controller. It is clear from the result that even though the settling time is less, the overshoot varies with setpoints. Each of the above controllers under consideration, has its own advantages and disadvantages in their performance and this led to the design of more accurate Adaptive control strategies, viz: Model Reference Adaptive and Modified Adaptive controller for the pressure regulation in Hypersonic wind tunnel.

A Model Reference Adaptive controller based on MIT rule is designed and it results in high percentage overshoot and chattering in the response in spite of its short settling time. Thus, Modified Adaptive Control scheme is designed by suitably modifying the cost function and the update law of MRAC for the tunnel system. The dynamics of the system is evaluated with the new MAC design and found that the pressure settles in a very short time without any overshoot and chattering in the output response. The new scheme thus outperforms all other controllers in terms of the performance indices, viz: settling time, percentage overshoot, rise time and chattering. This also provides consistent performance in the presence of modeling uncertainties, large, unknown parameter variations as well as variations in the selected range of setpoints.

7.3. VERIFICATION OF MODIFIED ADAPTIVE CONTROLLER

From the analysis of various controllers under consideration, it is proposed to regulate the settling chamber pressure of the Hypersonic wind tunnel system using a Modified Adaptive controller. The verification of this control scheme is carried out by applying it to the validated model of INCAS Supersonic wind tunnel (Bhoi and Suryanarayana, 2008; Corneliu, 2013). Fig. 7. 2 shows the performance comparison of Modified Adaptive controller with existing Adaptive Fuzzy PI controller of INCAS Supersonic Wind Tunnel.
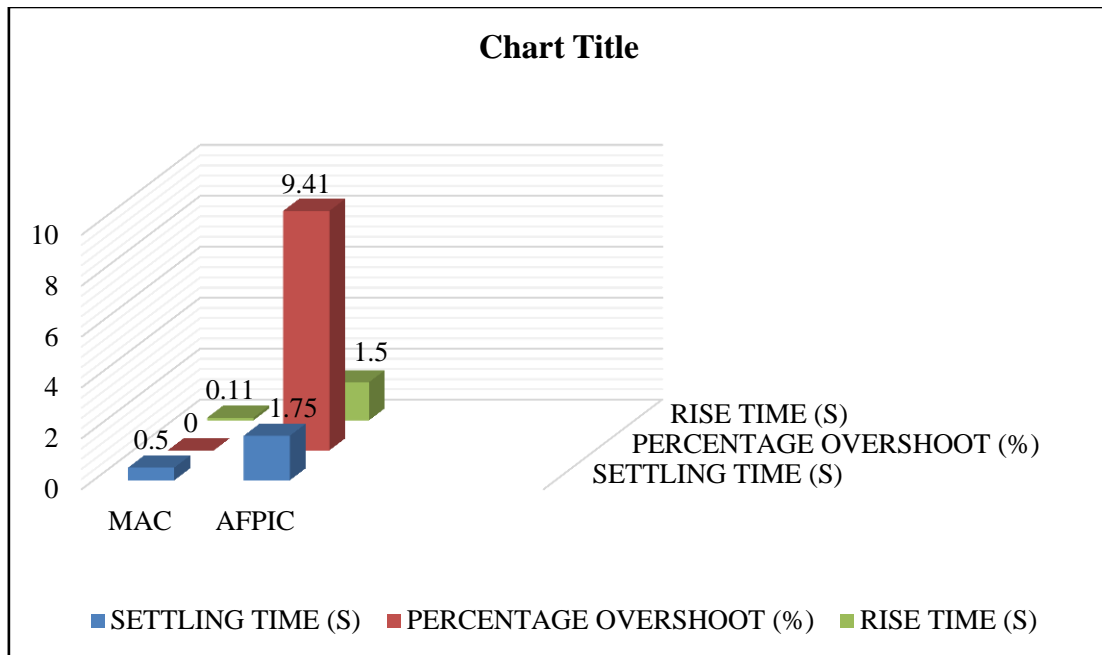
Fig. 7.2   Performance comparison of Modified Adaptive controller with existing Adaptive Fuzzy PI controller of INCAS Supersonic Wind Tunnel

The results of analysis show that the settling time of MAC for regulating the plenum pressure in the INCAS Supersonic wind tunnel is 0.5 s, rise time is 0.11 s without any overshoot. The reduction in settling time without overshoot and chatter effect is due to the selection of adjustment parameter that reduces the cost function of MAC. The

results of existing Adaptive Fuzzy PI controller for the validated model of INCAS Supersonic wind tunnel (Bhoi and Suryanarayana, 2008; Corneliu, 2013) has a settling time of 1.75 s, a rise time of 1.5 s and percentage overshoot of 9.41 %. By comparing these two results, it is observed that the percentage overshoot is eliminated with proposed Modified adaptive control scheme whereas it is 9.41 % for the existing controller, keeping other parameters in the same range. Thus, the design of Modified adaptive control is verified using the results of existing Adaptive Fuzzy PI control on INCAS Supersonic wind tunnel system. From these observations, it can be concluded that the proposed Modified adaptive controller is equally efficient in pressure regulation of other wind tunnel systems also.

This chapter gives a detailed discussion on the implications of various control algorithms based on their settling time, rise time, percentage overshoot, chatter effect and parametric uncertainties. Based on this analysis, the best suited control scheme is proposed for the regulation of pressure in the Hypersonic wind tunnel system. The proposed Modified adaptive control scheme is verified with the validated model of INCAS Supersonic wind tunnel. The thesis is effectively concluded in the next chapter.

CHAPTER 8

CONCLUSION AND FURTHER SCOPE

Hypersonic wind tunnel systems are ground-based test facilities for simulating the real time flight conditions with high Mach numbers (> 5) suitable for hypersonic regime under the desired conditions of air velocity, pressure and temperature. These are usually operated in the intermittent blowdown mode where high pressure or vacuum is stored and released within a very short duration of time that matches with the real time system during its test run. For the purpose of regulating the pressure in the settling chamber and thereby maintaining the uniform hypersonic flow in the test section within the withstandable pressure limit, a suitable controller is carefully designed and analyzed. Hence it becomes very important to conduct theoretical analysis and numerical simulations with various controller designs before venturing into real time experiments for specific applications. Thus, we designed various control schemes for this purpose and a comparative study of their performance with each other as well as with existing fundamental controllers is done to propose the most suitable one to regulate the pressure which matches the desired performance characteristics like minimum overshoot and short settling time for the selected model of Hypersonic wind tunnel system.

8.1 CONCLUSION

Mathematical model using state space approach of the Hypersonic wind tunnel system is selected by considering the transport delay and valve transfer function into account (Jacob and Binu, 2009; Jones *et al.*, 2011b). The nonlinear behaviour of this model is verified by sensitivity analysis. The stability of the system is ensured using

Lyapunov Stability Theorem, phase portrait method, Bode plot, Root locus, Kalman's test for controllability and observability. It is observed from the open loop response of the system that the pressure in the settling chamber is released in 450 s in the absence of any controller. For the purpose of controlling the settling chamber pressure within a short duration without exceeding the tolerable limit of the chamber, various control schemes are designed and their performance are evaluated for a range of set points from 1×10^5 Pa to 300×10^5 Pa in terms of the performance indices rise time, percentage overshoot and settling time.

Linear Quadratic Regulator controller, Optimised H-infinity, Backstepping, Sliding mode, Hybrid controllers like Backstepping with Sliding mode, Sliding mode with Fuzzy and Adaptive controllers, viz: Model reference adaptive and Modified Adaptive controllers are designed for the system. The performance of these controllers are evaluated based on the transient response and compared with each other to identify the best suitable choice among them.

- Linear Quadratic Regulator (LQR) controller: LQR controller is designed by choosing suitable weighing matrices, Q and R. An optimal state feedback controller gain matrix based on these weighing matrices is designed and simulated over the selected range of setpoints. The overshoot is further reduced by increasing the value of Q to the maximum limit beyond which it results in high gain leading to instability. Even though LQR controller has reasonably good values of rise time and settling time, the pressure overshoots above the tolerable limits of the settling chamber. To overcome the limitations and to improve the performance further, Robust controllers are designed.

215

- H-Infinity Controller: Robust H-infinity controllers are capable of handling perturbations within short durations of time. Results of H-infinity controller with selected values of weighing functions reveal that the percentage overshoot in this case also exceeds beyond the acceptable limits. To improve the performance further, the weights of H-infinity controller are optimized by Krill Herd optimization algorithm. This algorithm is found to be efficient in designing the weighing functions, thereby regulating the settling chamber pressure faster with better rise time. However, even though the percentage overshoot is drastically reduced, it couldn't be brought to the acceptable limit. To overcome the limitation of H-infinity controller, Backstepping as well as Sliding mode controller techniques are selected.

- Backstepping Controller: Backstepping control technique is a nonlinear control based on Lyapunov stability theorem. This design results in improved rise time as well as settling time without any overshoot. But from the result, it is clear that the performance is not consistent throughout the selected range of setpoints. Due to this limitation, we considered Sliding mode controller for further improvement in performance.

- Sliding Mode Controller: The system which is completely insensitive to parametric uncertainties and external disturbances utilizes a high speed switching control law to drive the nonlinear plants state trajectory onto a specified and user chosen surface in the state space. Thus, the sliding surface of the Sliding mode controller is selected so that the state variables converge to it. The controller thus designed produces better rise time, settling time as

216

well as percentage overshoot. However, Sliding mode controller when used independently, has chances of occurring of chattering in its response. Hence a combination of Sliding mode with Fuzzy logic as well as Backstepping with Sliding mode controllers are investigated.

- Sliding Mode Fuzzy Controller (SFC): Fuzzy logic when used for converging the sliding surface of Sliding mode control, results in stable and chatter free response. From the results, it is also observed that the output response has less settling time, but has slight overshoot for certain setpoints. Thus, with the aim of further improvement, a combination of Backstepping with Sliding mode control technique is proposed.

- Backstepping Sliding Mode Controller (BSMC): Backstepping Sliding mode controller can provide robustness to parametric uncertainties with chatter free response and minimum overshoot. The results show that BSMC is highly efficient in controlling the settling chamber pressure to the specified set point within a very short time with no overshoot and chatter effect. However, the design procedure with BSMC is highly complex and computationally expensive. In order to have a simple design with desired output response, Adaptive controllers, viz: Model Reference Adaptive Control (MRAC) and Modified Adaptive control (MAC) are designed and investigated.

- Model Reference Adaptive controller (MRAC): MRAC are supervisory controls capable of handling large response times and process disturbances when compared with other controller schemes. Model reference adaptive control

217

(MRAC) is designed based on MIT rule, capable of compensating parameter variations. From the results, it is clear that MRAC is efficient in regulating the settling chamber pressure within a short acceptable duration. However, it has the drawback of high overshoot and chatter effect in the output response. In order to improve the performance further, MRAC is modified by redefining its control law to obtain the Modified adaptive controller (MAC).

- Modified adaptive controller (MAC): The control law of MAC is obtained by suitably modifying the cost function in terms of adjustment parameter and incorporating saturation function in the update law of MRAC. It is observed from the results of our analysis that the settling time is very short without overshoot and chattering. It can also provide consistent performance in the presence of modeling uncertainties as well as large and unknown parametric variations throughout the range of setpoints.

The available literature focuses on developing conventional PI, Adaptive fuzzy, PID, Fuzzy assisted PI, Backstepping tracking with Fuzzy inference and Model reference fuzzy cascade controllers (MRFC). From the results of literature, it is observed that even though Backstepping tracking with fuzzy inference gives better settling time, it has high overshoot and design complexities where as MRFC has comparatively less settling time and overshoot, but it cannot be minimized beyond its limits due to the inclusion of Fuzzy logic. The crucial factor to be considered while designing any controller is to regulate the pressure in the settling chamber to maintain uniform hypersonic flow in the TS within the limited test duration. Hence, in this work, appropriate controllers are designed to regulate the flow through the pressure

regulator valve meeting all the transient performance indices. Controller design is very important for maintaining the desired environment in the test section and also increasing the consistency and cost effectiveness of the experimental test run. Thus, we designed and compared the performances of LQR, H-infinity, H-infinity with weight optimization, Backstepping, Sliding mode controllers, Hybrid controllers like Backstepping Sliding mode and Sliding mode Fuzzy controllers and Adaptive controllers like Model reference adaptive controller and Modified adaptive controllers to decide the most suitable one for the purpose of pressure regulation in the TS. With the use of these appropriate controllers, stability and robustness to parametric uncertainties with minimal chatter effect is guaranteed.

Finally, a concluding remark of various control schemes is presented, which proposes **Modified Adaptive control (MAC)** to be the best suited based on various performance indices for the regulation of pressure inside the settling chamber of Hypersonic wind tunnel.

- In order to verify the performance of our proposed Modified Adaptive controller, we applied it in the validated model of INCAS Supersonic wind tunnel. It is observed that the MAC exhibits a similar performance with that of the existing Adaptive Fuzzy PI controller. Hence it can be concluded that the proposed MAC is very effective for other Wind tunnel pressure regulation applications.

219

8.2 FUTURE SCOPE

Numerical simulations are highly important for studying the performance of a particular control design in situations where real time experiments are expensive or dangerous considering all the input and output variables as well as possible disturbances to the system. However, the economic aspect of the proposed schemes is to be evaluated. Such studies can contribute to the effective implementation of this scheme in future pressure regulation applications. The system performance can further be improved by following other combination techniques whose design is simple as well as economical.

- Neural Network based control

- Genetic Algorithm based control

- Adaptive Backstepping control

- Optimisation of weighing functions of various controller schemes.

It is worthwhile to note that before implementing any control scheme it is desirable to evaluate the economic aspects also, and then finalize the most suitable combination which is effective in all respects. It is also important that the performance of the proposed controller has to be verified and validated in real time environment.

APPENDICES

APPENDIX -1

A1. DERIVATION OF TRANSFER FUNCTION AND STATE SPACE MODEL

The flow rate through the three vessels, F_1 , F_2, F_3 and the gas capacitances through the three vessels, C_1 , C_2, C_3 are given in eqs. (3.1) to (3.10).

For choked flow ($F_1 = f(P_1, m)$), the total differential for the flow rate, F_1 is,

$$dF_1 = \frac{\partial F_1}{\partial P_{1m}} dP_1 + \frac{\partial F_1}{\partial mP_1} dP_1 dm \qquad (A1.1)$$

Where,

$$F_1 = 2.39 \times 10^{-5} m \ (P_1 - 0.5P_2) \qquad (A1.2)$$

$$dF_1 = 2.39 \times 10^{-5} m dP_1 (2.39 \times 10^{-5} P_1 - 2.39 \times 10^{-5} \times 0.5 \ P_2) dm \qquad (A1.3)$$

Substituting m=0.3, $P_1 = 250 \times 10^6 \ Pa$ and $P_2 = 70 \times 10^6 \ Pa$, we obtain

$$F_1 = 0.717 \times 10^{-5} P_1 + 418.25m \qquad (A.1.4)$$

Similarly, F_2 can be written as,

$$dF_2 = \frac{\partial F_2}{\partial P_{2P_3}} dP_2 + \frac{\partial F_2}{\partial P_{3P_2}} dP_3 \qquad (A1.5)$$

Where,

$$dF_2 = 1.569 \times 10^{-5} dP_2 - 0.7845 \times 10^{-5} dP_3 \qquad (A1.6)$$

Thus,

$$F_2 = 1.569 \times 10^{-5} P_2 - 0.7845 \times 10^{-5} P_3 \qquad \text{(A1.7)}$$

Similarly,

$$F_3 = 2.26 \times 10^{-4} P_3 \qquad \text{(A1.8)}$$

Thus, equations, (A1.4), (A1.7), (A1.8) are the general equations of flow through the three vessels with parameter constants given in Table.3.5 in chapter 3. Thus, the state space model is obtained as,

$$\begin{bmatrix} \dot{P}_1 \\ \dot{P}_2 \\ \dot{P}_3 \end{bmatrix} = \begin{bmatrix} -K_1/C_1 & 0 & 0 \\ K_1/C_1 & -K_3/C_2 & -K_4/C_2 \\ 0 & K_3/C_3 & K_4 - K_n/C_3 \end{bmatrix} \begin{bmatrix} P_1 \\ P_2 \\ P_3 \end{bmatrix} + \begin{bmatrix} -K_2/C_1 \\ K_2/C_2 \\ 0 \end{bmatrix} m. \quad \text{(A1.9)}$$

$$Y_1 = \begin{bmatrix} 0 & 0 & 1 \end{bmatrix} \begin{bmatrix} P_1 \\ P_2 \\ P_3 \end{bmatrix}. \qquad \text{(A1.10)}$$

Substituting the values of parameters from Table 3.5, the state space model becomes,

$$\begin{bmatrix} \dot{P}_1 \\ \dot{P}_2 \\ \dot{P}_3 \end{bmatrix} = \begin{bmatrix} -0.0045 & 0 & 0 \\ 0.0045 & 2.51 & 2.51 \\ 0 & 12.85 & -14.14 \end{bmatrix} \begin{bmatrix} P_1 \\ P_2 \\ P_3 \end{bmatrix} + \begin{bmatrix} 617679.68 \\ 6133259.91 \\ 0 \end{bmatrix} m. \quad \text{(A1.11)}$$

$$Y_1 = \begin{bmatrix} 0 & 0 & 1 \end{bmatrix} \begin{bmatrix} P_1 \\ P_2 \\ P_3 \end{bmatrix}. \qquad \text{(A1.12)}$$

Converting the state space model to transfer function form, we obtain the transfer function as,

$$\frac{P_3(s)}{m(s)} = \frac{7.898e007s + 4.21e005}{S^3 + 16.68S^2 + 3.367S + 0.01937} \qquad \text{(A1.13)}$$

Hence, we use Pade's approximation for the delay based on empirical analysis and analyzed the resulting system. Considering the transport delay in eq. (3.12) and valve transfer function (Lee *et al.*, 2014; Savino *et al.*, 2009; Jacob and Binu, 2009; Jones *et al.*, 2011b; Pope and Goin, 1965) in eq. (3.13), the system transfer function is given in eq. (3.14).

$$Transport\ delay\ transfer\ function = \frac{-0.03S+1}{0.03S+1} \qquad (A1.14)$$

$$Valve\ transfer\ function = \frac{1}{0.5S+1} \qquad (A1.15)$$

A transport delay of about 30 milliseconds is added and time constant for PRV is taken as 0.5 seconds. First order valve transfer function is also incorporated into the process. Thus, the final plant transfer function from $G_p(s)$ is obtained by multiplying eq.(A1.13) with (A1.14) and (A1.15) (Jacob and Binu, 2009; Jones *et al.*, 2011b; Pope and Goin, 1965) and is given by,

$$G_p(s)$$
$$= \frac{-2.369e006s^2 + 7.897e007s + 4.21e005}{0.015s^5 + 0.7802s^4 + 9.89s^3 + 18.46s^2 + 3.377s + 0.01937} \qquad (A1.16)$$

APPENDIX -2

A2. BACKSTEPPING CONTROLLER DESIGN

The state equations of the tunnel system (Jones *et al.*, 2011a; Jacob and Binu, 2009; Jones *et al.*, 2011b; Echman, 1958; Liptak, 1995), in chapter (3), eq. (3.27) and (3.28) are brought to strict feedback form given in eq. (4.28).

For this purpose, the pressure equations obtained from eqs. (3.7) to (3.9) can be written as,

$$\dot{P}_1 = \frac{-F_1}{C_1} \tag{A2.1}$$

$$\dot{P}_2 = \frac{F_1 - F_2}{C_2} \tag{A2.2}$$

$$\dot{P}_3 = \frac{F_2 - F_3}{C_3} \tag{A2.3}$$

Substituting the values of parameters given in Table. 3.5, the flow through the three vessels in eqs. (3.1), (3.5) and (3.6) becomes,

$$F_1 = 40.74 \times 10^{-7} \times P_1 + 556.9\,m \tag{A2.4}$$

$$F_2 = 22.86 \times 10^{-5} \times P_2 - 22.86 \times 10^{-5}P_3 \tag{A2.5}$$

$$F_3 = 2.26 \times 10^{-5} \times P_3 \tag{A2.6}$$

Substituting eqs. (A2.4) to (A2.6), eqs. (A2.1) to (A2.3) becomes,

$$\dot{P}_1 = -0.0045 \times P_1 + 628484.36\,m \tag{A2.7}$$

$$\dot{P}_2 = 0.0776 \times P_1 + 10611661.58\, m - 4.355 \times P_2 + 4.355 \times P_3 \quad \text{(A2.8)}$$

$$\dot{P}_3 = 22.67 \times P_2 - 24.92 \times P_3 \quad \text{(A2.9)}$$

Considering the state variables, $X_1 = P_3, X_2 = P_2, X_3 = P_1$ and u=m=0.6, we obtain the state equation for Backstepping controller as,

$$\dot{X}_1 = 22.67X_2 - 24.92X_1 \quad \text{(A2.10)}$$

$$\dot{X}_2 = 0.08X_3 - 4.36X_2 + 4.36X_1 + 6366996.94 \quad \text{(A2.11)}$$

$$\dot{X}_3 = -0.005X_3 - 628484.36u \quad \text{(A2.12)}$$

Appendix -3

A3. SLIDING MODE CONTROLLER DESIGN

The state equations for the system given in eq. (A2.10) to (A2.12) is,

$$\dot{X}_1 = 22.67\ X_2 - 24.92\ X_1$$

$$\dot{X}_2 = 0.0776X_3 + 636696.94 - 4.355\ X_2 + 4.355X_1$$

$$\dot{X}_3 = -0.004597\ X_3 - 628484.36\ u$$

The sliding surface chosen is,

$$S =\ C_1X_1 + C_2X_2 +\ C_3X_3 \qquad\qquad (A3.1)$$

the Lyapunov function is chosen (Saravanakumar *et al.*, 2009; Musmade *et al.*, 2011; Utkin, 1977; Tan *et al.*, 2005; Utkin, 1993; Shyu and Shieh, 1996; Li *et al.*, 2012; Terra-Moura *et al.*, 2007; Mondal and Chitralekha, 2013) as

$$V = \tfrac{1}{2}S^2 \qquad\qquad (A3.2)$$

The derivative of this function is given by,

$$\dot{V} = S\dot{S} \qquad\qquad (A3.3)$$

$\dot{V}$ is negative definite if,

$$S\dot{S} = \begin{cases} < 0\ if\ S > 0 \\ = 0\ if\ S = 0 \\ > 0\ if\ S < 0 \end{cases} \qquad\qquad (A3.4)$$

For $\dot{V}$ to be negative definite, $S\dot{S} < 0$. Thus, the value of u/m for $S\dot{S} = 0$ is given by,

$$u = \beta = \frac{1}{628484.36}\begin{pmatrix} -0.0045X_3C_3 + 0.077X_3 + 636696.94 - 4.35X_2 + \\ 4.35X_1 + 22.67X_2 - 24.92\ X_1 \end{pmatrix}$$

$$\text{(A3.5)}$$

Thus,

$$U_{eq} = \beta - k\ sign(s) \tag{A3.6}$$

Where K is the controller gain and its value is taken as 1.

REFERENCES

1.   **Lee, Y.J., Sang Hun Kang, Soo Seok Yang, and   Se Jin Kwon**   (2014) Starting characteristics of the hypersonic wind tunnel with the Mach number variation. *Journal of Mechanical Science and Technology*, **28(6)**, 2197-2204.

2.   **Savino, R., R. Monti, A. Esposito, Daniel R. Lewis, and Keith Williams** (2009) Behaviour of hypersonic wind tunnels diffusers at low Reynolds numbers. *Aerospace Science and Technology*, Elsevier, **3(1)**, 11-19.

3.   **Jones, Rini S.B., P. Poongodi, and A. Immanuel Selvakumar** (2014) Performane Evaluation of various control strategies for Hypersonic wind tunnel, Thesis Report, *Karunya University*, 12-42.

4.   **Baals, D.D., and William R. Corliss** *Wind Tunnels of NASA*, National Aeronautics and Space Administration, Washington D. C., 1981 [https://www.grc.nasa.gov/www/k-12/WindTunnel/history.html]

5.   **D'Souza, Alister Gleason., Joel I. Concessao, Jaimon Quadros, Keith Williams** (2015) Study of Aerofoil Design Parameters for Low Speed Wind Tunnel. *Journal of Mechanical Engineering and Automation*, **5**, 47-54.

6.   **Josué Njock Libii** *Wind Tunnels in Engineering Education.* pp: 235-260. *In .* **Josué Njock Libii** (eds.) *Wind Tunnels and Experimental Fluid Dynamics Research,* Intech Open Science, 2011.

7.   **John Lohan** (2002) Design and application of low speed wind tunnels. *John Lohan, Galway-Mayo Institute of Technology, Galway, Ireland , 1-7*

8.   **Flay, R.G.J.** (2015) Model tests of wind turbines in wind tunnels. *Technical Transactions*, *CZASOPISMO TECHNICZNE*, 63-81

9.   **Jones, Rini S.B., P. Poongodi, and Binu L.S** (2011a) Fuzzy Assisted PI Controller with Anti-reset wind up for Regulating Pressure in a Hypersonic Wind Tunnel, *IJCA Special Issue on Artificial Intelligence Techniques - Novel Approaches & Practical Applications*, 29-33

10.   **Jacob, V., and L.S. Binu** (2009) Adaptive fuzzy PI controller for hypersonic wind tunnel pressure regulation, Proceedings of *10th National Conference on Technological Trends (NCTT)*, 184–187.

11.   **Jones, Rini S.B., P. Poongodi, and Binu, L.S** (2011b) Fuzzy assisted PI controller for pressure regulation in a hypersonic wind tunnel. *International Journal Hybrid Information Technology*, **4(1)**, 13–24.

12. *Supersonic Wind Tunnel.* Wikimedia, 2016.
[https://upload.wikimedia.org/wikipedia/commons/f/f0/Supersonic-en.svg]

13. **Nott, Cameron R., Semih M. Ölçmen, Daniel R. Lewis, and Keith Williams** (2008) Supersonic, variable-throat, blow-down wind tunnel control using genetic algorithms, neural networks, and gain scheduled PID. *Appl Intell, Springer*, **29**, 79-89.

14. **Braun, Eric M., Frank K. Lu, Philip K. Panicker, Richard R. Mitchell, and Donald R. Wilson** (2008), Supersonic Blowdown Wind Tunnel Control Using LabVIEW. Proceedings of *46th AIAA Aerospace Sciences Meeting and Exhibit*, American Institute of Aeronautics and Astronautics, Reno, Nevada.

15. **Gayon, Jio Ross, Godfrey S. Oarde, Kevin Victor L. Zaide, and Chester A. John** (2013) Wind Tunnel. *LinkedIn Slideshare*, Slide 14.

16. **Bhoi, S.R. and Suryanarayana, G.K.** (2008) Prediction of total pressure characteristics in the settling chamber of a supersonic blowdown wind tunnel. Proceedings of the *International Conference on Aerospace Science and Technology*, 26–28.

17. **Pope, A., and K. L. Goin** (1965) High speed wind tunnel theory. *High-speed wind tunnel testing*, Wiley & Sons, Inc.

18. **Arbuckle, Alex Q.** (2016) NASA Wind Tunnels 1927-1992. Mashable.
[https://mashable.com/2016/05/09/nasa-wind-tunnels/]

19. **Kegelman, Jerome T., Paul M. Danehy and Richard J. Schwartz** (2014) Advanced Capabilities for Wind Tunnel Testing in the 21 st Century. *American Institute of Aeronautics and Astronautics*, **2(3)**, 1-17.

20. **Arnaiz, Henry H., John B. Peterson, James C Daugherty** (1980) Wind Tunnel/ Flight correlation study of Aerodynamic characteristics of a large flexible Supersonic cruise Airplane (XB-70-1). *NASA Technical Paper*, 1-57

21. **Kakate, V.L., D S Chavan, P.B Karandikar, Niraj Mahulkar** (2014) Study of Measurement and Control Aspects of Wind Tunnel, *International journal of Innovative Research in Electrical, Electronics, Instrumentation and Control engineering*, **2(3)**, 1291–1294.

22. **Bruce Ralphin, Rose J, Jinu G.R., and Brindha C.J.** (2015) A numerical optimization of high altitude testing facility for wind tunnel experiments. *Chinese Journal of Aeronautics*, **28(3)**, 636–648.

23. **Bottasso, C.L., Campagnolo, F. and Petrovic, V.** (2014) Wind tunnel testing of scaled wind turbine models: beyond aerodynamics. *Journal of Wind Engineering and Industrial Aerodynamics*, Elsevier, **127**, 11–28.

24. **Hwang, D.S. and Hsu, P.L.** (1998) A robust controller design for supersonic intermittent blow down type wind tunnels. *Aeronaut. J. R. Aeronaut. Soc.*, **102(1013)**, 161–169.

25. https://nasasearch.nasa.gov/search?query=wind+tunnels&affiliate=nasa&utf8 =%E2%9C%93

26. http://www.vssc.gov.in/VSSC_V4/index.php/retired-employee-portal/58-infrastructure/1179-hypersonic-wind-tunnel-facility-2

27. **Singh, Chaturi and K. Poddar** (2006) PXI-based High-Performance Versatile Instrumentation and Motion Control System for Wind Tunnel Applications. Proceedings of the *IEEE International Conference on Industrial Technology*, DOI: 10.1109/ICICT.2006.372266, 704-709

28. **Reddy, K.P.J.** (2007) Hypersonic Flight and Ground Testing Activities in India. Proceedings of the *16th Australasian Fluid Mechanics Conference*, 32-37.

29. **Stepanek, S. A Chip** (1995) Non-Intrusive Flow Diagnostic Applications in High-Enthalpy Flow Facilities. Proceedings of the *IEEE International Congress on Instrumentation in Aerospace Simulation Facilities*, DOI:10.1109/ICIASF.1995.519115, 9.1-9.10.

30. **Yang Zhao, Shuyang Cao, Yukio Tamura, Zhongdong Duan and S. Ozono** (2009) Simulation of Downburst in a Multiple Fan Wind Tunnel and Research on Its Load on High-Rise Structure by Wind Tunnel Experiment. Proceedings of the *2009 IEEE International Conference on Mechatronics and Automation*, China, 4506-4511.

31. **Owen, A.K., and F.K. Owen** (2007) Hypersonic Free Flight Measurement Techniques. *IEEE Instrumentation in Aerospace Simulation Facilities*, Proceedings of the *22nd International Congress on Instrumentation in Aerospace Simulation Facilities*, USA, DOI:10.1109/ICIASF.2007. 4380898, 1-11.

32. **Smith, A.J.D., and D.R.J. Baxter** (1989) Liquid Crystal Thermography For Aerodynamic Heating Measurements In Short Duration Hypersonic Facilities. Proceedings of the *IEEE International Congress on Instrumentation in Aerospace Simulation Facilities*, DOI:10.1109/ICIASF.1989.77663, 104-112.

33. **Cristofolini, A., Carlo A. Borghi, Mario R. Carraro, Gabriele Neretti, Andrea Passaro, Gabriele Fantoni, and Leonardo Biagioni** (2008) Hypersonic MHD Interaction on Conical Test Body With a Hall Electrical Connection. *IEEE Transactions On Plasma Science*, **36(2)**, 530-541.

34. **Hollis, Brian R., and Wayland C. Griffith** (1991) A Fine Wire Thermocouple Probe For Measurement Of Stagnation Temperatures In Real Gas Hypersonic Flows Of Nitrogen. Proceedings of the *IEEE International Congress on Instrumentation in Aerospace Simulation Facilities*, DOI:10.1109/ICIASF.1991.186234, 136-145.

35. **Daikert, C., A. Danckert, G. Gundlach, K. Lehmkiister** (1995) Measurement of Rotational Temperatures near Surfaces in Hypersonic Flow. Proceedings of the *IEEE International Congress on Instrumentation in Aerospace Simulation Facilities*, DOI:10.1109/ ICIASF. 1995.519469, 38.1-38.7.

36. **Lin, C.L., and T.L. Wang** (2008), Fuzzy side force control for missile against hypersonic target, *IET Control Theory Applications*, **1(1)**, 33-43.

37. **Alfyorov, V.I., G.I. Shcherbakov, A.P. Rudakova, I.V.Yegorov, V. N. Skirda, A.S. Bushmin, L.M. Dmitriyev, B.V. Yegorov, Yu Ye. Markachev, A.N. Morozov, and A.A. Orlov** (1995) Investigation Of Relaxation Processes In Flow About models In Hypersonic Wind Tunnels of Different Types. Proceedings of the *IEEE International Congress on Instrumentation in Aerospace Simulation Facilities*, DOI:10.1109/ICIASF.1995. 519479, 48.1-48.11.

38. **Vargese, Jacob and Binu L.S.** (2009) High Pressure System Modeling of Hypersonic wind tunnel. Proceedings of the *International Conference on Modeling and Simulation*, College of Engineering, Trivandrum, India.

39. **Imraan M, Sharma and R.N., Flay, R.G.J. (2011)** Wind tunnel testing of a wind turbine with telescopic blades. *Proc. 13th International Conference on Wind Engineering, Amsterdam, The Netherlands*.

40. **Keisuke, Asai., Hiroshi Kanda, Corey T. Cunninghamt, Rick Erausquinii, and John P. Sulliva** Surface Pressure Measurement in a Cryogenic Wind Tunnel By Using Luminescent Coating, *National Aerospace Laboratory*, Tokyo, 0-7803-41 67-8.

41. **Yamaguchi, Yutaka., Masashi Kashitani, Kenji Kaibara and Teruo Saito** (1999) Feasibility Of Airfoil Tests With A Small High Subsonic Cryogenic Wind Tunnel. *IEEE* 0-7803-57.

42. **Klfyorov, V.I., L.M. Dmitriyev, B.V. Yegorov, Yu.Ye. Markachev and A.P. Rudakova** Background and Prediction of correct full-scale reproduction in Wind Tunnels as concerns Gas Dynamic Parameters of hypervelocity atmospheric flights and Scramjet Combustion Chamber conditions. *IEEE Xplore*, 0-7803-4167-8

43. **Kotwani, Kailash., S K Sane, and Hemendra Arya** (2003) Wind tunnel performance analysis, Practical training report. *Center for Aerospace system and Design Engineering*, 1-20.

44. **Debecker, I., A. K. Mohamed, and D. Romanini** (2005) Speed Cavity Ringdown Spectroscopy by Simultaneous Laser and Cavity Tuning: Towards 02 Sensing in Blow-Down Wind Tunnels, *IEEE Xplore*, Proceedings of *CTuY2 2005 Conference on Lasers Electro-Optics (CLEO)*.

45. **Boudreau, Harold Sherwood III.** (2009) Design, Construction, And Testing Of An Open Atmospheric Boundary Layer Wind Tunnel. A dissertation presented at *the University Of Florida*.

46. **Butler, Kelly., David Cancel, Brian Earley, Stacey Morin, Evan Morrison, and Michael Sangenario** (2010) Design and Construction of a Supersonic Wind Tunnel. A major qualifying Project at *Worcester Polytechnic Institute*.

47. **Dolan, Dale S., Danny Zepeda, and Taufik Taufik** Development of Wind Tunnel for Laboratory Wind Turbine Testing. *Electrical Engineering Department California Polytechnic State University San Luis Obispo*, California, USA.

48. **Wei, Liu., Ma Xin, Li Xiao, Chen Ling, Zhang Yang, Li Xiaodong, Shang Zhiliang and Jia Zhenyuan** (2015) High-precision pose measurement method in wind tunnels based on laser-aided vision technology. *Chinese Journal of Aeronautics*, **28(4)**, 1121-1130.

49. **Jones T.W., Lunsford C.B.** (2005) Design and development of a real-time model attitude measurement system for Hypersonic facilities. Proceedings of the *43rd AIAA aerospace sciences meeting and exhibit*, USA, *Reston: AIAA*; 1-10.

50. **Bharath, Bhavin K.** (2015) Design and fabrication of a supersonic wind tunnel. *International journal of Engineering and Applied Sciences*, **2(5)**.

51. **Wegener, Peter P., R. Kenneth Lobb** (1953), An Experimental study of a Hypersonic wind tunnel Diffuser. *Journal of the Aeronautical Sciences*, **20(2)**, 105-110.

52. **Owen, F., Complere Inc., Paio Alto** (1990) Transition and Turbulence Measurements in Hypersonic Flows. *AIAA Second International Aerospace Planes Conference.*

53. **McKenzie, Robert L., and Douglas G. Fletcher** (1992) Spectroscopic Measurement Techniques for Hypersonic, Turbulent Wind Tunnel Flows. *National Aeronautics and Space Administration.*

54. **Le Sant, Y., and J.L. Edy** (1993) Phosphor Thermography Technique in Hypersonic Wind Tunnels: First Results. *IEEE Xplore*, *Office National d'Etudes et de Recherches ACrospatiales* BP n"72, 92322 Chatillon Cedex, France.

55. **Mohamed, Ajmal Khan., Thierry Pot and Bruno Chanetz** (1995) Diagnostics by Electron Bani Fluorescence in Hypersonics. *IEEE Xplore*, CH34827-9510000.

56. **Tirres, Carlos** (1999) The future of Hypersonic wind tunnels. 37th *AIAA Aerospace Sciences meeting and exhibit*, AIAA 99-0819, 1-11.

57. **Simeonides, G., J.P. Vermeulen, H.L. Boerrigter and J.F. Wendt** (1991) Quantitative Heat Transfer Measurements in Hypersonic Wind Tunnels by means of Infrared Thermography. Proceedings of the *IEEE International Congress on Instrumentation in Aerospace Simulation Facilities*, DOI:10.1109/ICIASF. 1991.186238, 178-189.

58. **Pandian, S., P.G. Raveendran, K. Srinivasan, S. Subramanian and A.N. Subash** Instrumentation Technique for Mixed Hypersonic Flow in Short Duration Facility. *IEEE Xplore*, Vikram Sarabhai Space Centre (VSSC), Indian Space Research Organisation, Thiruvananthapuram.

59. **Alfyorov, V.I.**, Current State And Potentialities Of Hypersonic MHD-Gas Acceleration Wind Tunnels. *IEEE Xplore*, TsAGI, Russia, 0-7803-4167-8.

60. **Buck, Melvin L., Alfred C. Draper**, Non-Isentropic Effects On The WRDC 20 Inch HypersonicWind Tunnel Calibration. *IEEE Xplore*, Aeromechanics Division, Wright Research Development Center Wright-Patterson AFB OH 45433-6553.

61. **Salas, Manuel D.** A Review of Hypersonics Aerodynamics, Aerothermodynamics and Plasmadynamics Activities within NASA's Fundamental Aeronautics Program. *NASA Langley Research Center*, Hampton, AIAA 2007-4264.

62. **Ogunnaike B.A., and W.H. Ray** (1994) Process dynamics modeling and control. *Oxford University Press*, New York.

63. **Aslam, Farhad., and Gagandeep Kaur** (2011) Comparative Analysis of Conventional, P, PI, PID and Fuzzy Logic Controllers for the Efficient Control of Concentration in CSTR. *International Journal of Computer Applications*, **17(6)**, 12-16.

64. **Jeng, Jyh-Cheng., and Ming-Wei Lee** (2012) Identification and Controller Tuning of Cascade Control Systems Based on Closed-Loop Step Responses. Proceedings of the *8th IFAC Symposium on Advanced Control of Chemical Processes*, *The International Federation of Automatic Control*, Singapore, 415-419.

65. **Ang, Kiam Heong., Gregory Chong Yun Li** (2005) PID control system analysis, design, and technology. *IEEE Trans. Control Systems*, **13(4)**.

66. **Roy, D., R. Goswami, S. Sanyal and A.N. Sanyal** (2013) Pitch Attitude Control of a Booster rocket. *International Journal of Engineering and Science*, **2**, 8-12.

67. **Ogata, Katsuhiko** (2002) Modern Control Engineering. *PHI learning Private Limited*, New Delhi, 897-909

68. **Purnawan, Heri., Mardlijah and Eko Budi Purwanto** (2017), Design of linear quadratic regulator (LQR) control system for flight stability of LSU-05. *Journal of Physics: Conference Series*: 890- 012056.

69. **Mohammad A., Joga D.S., and Ismoyo H** (2013) Journal Rotasi **15**, 16-27.

70. **Mauricio V.P.G., Edilberto C.V.G., and Carol I.R.F.** (2012) Simulation of The Quadrator Controlled with LQR with Integral Effect. *ABCM Symposium Series in Mechatronics*, **5**, 390.

71. **Yin, Y-Z., H-S. Zhang** (2006) Linear Quadratic Regulation for discrete-time systems with single input delay. *International Proceedings of the China Control Conference*, Harbin, China, 672-677.

72. **Huang, Dan., Shaowu Zhou** (2004) Inverted Pendulum Control system based on LQR optimal regulator. *J. Micro Computer Information*, **20(2)**, 37-39.

73. **Yadav, Sandeep Kumar., Sachin Sharma, Narinder Singh** (2012) Optimal Control of double inverted pendulum using LQR controller. *International Journal of Advanced Research in Computer Science and Software Engineering*, **2(2)**, 189-192.

74. **Mary, Dolly A., Abraham T. Mathew, Jeevamma Jacob** (2012) Robust H-infinity (H∞) Stabilization of Uncertain Wheeled Mobile Robots. *Global Journal of Researches in Engineering Electrical and Electronics Engineering*, **12(1)**.

75. **Yilmaz, Muhittin., Salman Mujeeb, Naren Reddy Dhansri** (2012) A H-infinity Control Approach for Oil Drilling Processes. *Procedia Computer Science*, Elsevier, **20**, 134-139.

76. **Hassibi, B., A.T. Erdogan and T. Kailath** (2006) MIMO linear equalization with an H-infinity criterion. *IEEE Transactions on Signal Processing*, **54(9)**, 499-511.

77. **Vikalo H., B. Hassibi, A.T. Erdogan and T. Kailath** (2005) On H-infinity design techniques for robust signal reconstruction in noisy filter banks. *EURASIP Signal Processing*, **85(1)**, 1-14.

78. **Doyle J.C., K. Glover, P.P. Khargonekar, and B.A. Francis** (1989) State-space solutions to standard H/sub 2/ and H/sub infinity / control problems. *IEEE Transactions on Automatic Control*, **34(8)**, 831-847.

79. **K. Lenz (1995)** Properties of optimal weighted sensitivity designs. *IEEE Transactions on Automatic Control*, **40**, 298–301.

80. **Yang X.S., and A.H. Gandomi** (2012), Bat algorithm: a novel approach for global engineering optimization. *Eng. Comput.*, **29(5)**, 464–483.

81. **Gümüşsoy, Suat** (2004) Optimal H-Infinity Controller Design and Strong Stabilization for Time-delay and MIMO Systems. Ph.D. Dissertation.

82. **Walvekar A.G., and Lambert B.K.** (1970) An application of geometric programming to machining variable selection. *Int. J. Production Research*, **8(3)**, 241-245.

83. **Swisher, J.R., P.D. Hyden, S.H. Jacobson, and L.W. Schruben** (2002) A survey of simulation optimization techniques and procedures. Proceedings of the *Simulation Conference*, *IEEE Explore*, Winter.

84. **Kwakernaaak, Huibert** (1993) Robust control and H-Infinity Optimisation – Tutorial Paper. *Automatica*, **29(2)**, 255-273.

85. **Prempain, Emmanuel., and Ian Postlethwaite** (2005) Static H∞ loop shaping control of a fly-by-wire helicopter, *Automatica*, **41(9)**, 1517-1528.

86. **Wang, Gai-Ge., Amir H. Gandomi, and Amir H. Alavi** (2014) An effective krill herd algorithm with migration operator in biogeography-based optimization. *Applied Mathematical Modelling*, Elsevier, **38**, 2454–2462.

87. **Wu, P., L. Gao, and D. Zou** (2011) An improved particle swarm optimization algorithm for reliability problems. *ISA Trans.*, **50(1)**, 71–81.

88. **Gandomi, A.H., A.H. Alavi** (2012) Krill herd: a new bio-inspired optimization algorithm. *Commun. Nonlinear Sci. Numer. Simulat.*, **17(12)**, 4831–4845.

89. **Alfi, A., H. Modares** (2011) System identification and control using adaptive particle swarm optimization. *Applied Mathematical Modeling*, **35(3)**, 1210–1221.

90. **Ali H.I., S.B. Mohd. Noor, S.M. Bashi, M.H. Marhaban** (2010) Design of H-infinity based robust control algorithms using particle swarm optimization method. *The Mediterranean Journal of Measurement and Control*, **6(2)**.

91. **Gu, D-W., P.Hr. Petkov, M.M. Konstantinov** (2005) Robust control design with Matlab. *British Library*.

92. **Cooper, David Maurice** (2005) Nonlinear Tracking by Trajectory Regulation Control Using Backstepping Method. Thesis submitted, *Department of Electrical Engineering and Computer Science, Ohio University*, 1-93.

93. **Skjetne, Roger., and Thor I. Fossen** (2004) On Integral Control in Backstepping: Analysis of Different Techniques. Proceedings of *American Control Conference*, Bosten, Massachusetts.

94. **Madani, Tarek., and Abdelaziz Benallegue** (2006) Backstepping Control for a Quadrotor Helicopter. Proceedings of the *2006 IEEE/RSJ International Conference on Intelligent Robots and Systems*.

95. **Joseph, A., S. Geetha** (2007) Application of Backstepping for the Control of Launch Vehicle. Proceedings of *IE(I) Journal*, **88**.

96. **Peng, Wu., Ming Yang** (2008) Design of Missile Attitude Controller Based on Backstepping Method. Proceedings of the *7th World Congress on Intelligent Control and Automation*.

97. **Farrell, Jay A., Marios Polycarpou, Manu Sharma, and Wenjie Dong** (2009) Command Filtered Backstepping. *IEEE Transactions On Automatic Control*, **54(6)**.

98.   **Rudra S., Barai R.K.** (2012) Robust Adaptive Backstepping Control of Inverted Pendulum on Cart System. *International Journal of Control and Automation*, **5(1)**, 13-26.

99.   **Sonneveldt L., Chu Q.P., Mulder J.A.** (2007) Nonlinear flight control design using constrained adaptive backstepping [J]. *Journal of Guidance, Control, and Dynamics*, **30(2)**, 322–336.

100. **Yang C., J. Sun, Q. Zhang, X. Ma** (2013) Lyapunov Stability and Strong Passivity Analysis for Nonlinear Descriptor Systems. *IEEE Transactions on Circuits and Systems*, **60(4)**, 1003-1012.

101. **Kim J., and Y. Kim** (2003) Robust backstepping control for slew maneuver using nonlinear tracking function. *IEEE Trans. Control Syst. Technol.*, **11(6)**, 822-829

102. **Krstic, M., P. Tsiotras** (1999) Inverse optimal stabilization of a rigid spacecraft. *IEEE Trans. Automatic Contr.*, **44(5)**, 1042-1050.

103. **Frazzoli, Emilio., Munther A. Dahleh, Eric Feron** (2000) Trajectory tracking control design for autonomous helicopters using a backstepping algorithm. Proceedings of the *American Control Conference*, Chicago, Illinois.

104. **HarkegArd, Ola., S. Torkel Glad** (2000) A Backstepping Design for Flight Path Angle Control, *IEEE* 0-7803-6638-7.

105. **Beji, Lotfi., Azgal Abichou, Yasmina Bestaoui** (2002) Stabilization of a Nonlinear Underactuated Autonomous Airship-A Combined Averaging and Backstepping Approach. *Third International Workshop on Robot Motion and Control*, November.

106. **Benaskeur, A.R., and A. Desbiens** (2002) Backstepping-based adaptive PID control. *IEEE*. Proceedings Online no. 20020100.

107. **Zhou, Jing., Changyun Wen, and Ying Zhang** (2004) Adaptive Backstepping Control of a Class of Uncertain Nonlinear Systems With Unknown Backlash-Like Hysteresis. *IEEE Transactions On Automatic Control*, **49(10)**, October.

108. **Abdulgalil, Farag., Houria Siguerdidjane** (2005) Backstepping Design for Controlling Rotary Drilling System. Proceedings of the *2005 IEEE Conference on Control Applications*, Toronto, Canada, August.

109. **Ebrahim, Arbin., Gregory V. Murphy** (2005) Adaptive Backstepping Controller Design of an Inverted Pendulum. *IEEE*, 0-7803 8808.

110. **Ghommam, Jawhar., Faïçal Mnif, Abderraouf Benali, and Nabil Derbel** (2006) Asymptotic Backstepping Stabilization of an Underactuated Surface Vessel. *IEEE Transactions On Control Systems Technology*, **14(6)**, November.

111. **Wang, Qingwei., Zhenghua Liu, and Lianjie Er** (2006) Adaptive Backstepping Control for Flight Simulator. Proceedings of the *First International Conference on Innovative Computing, Information and Control* (ICICIC'06), *IEEE*.

112. **Madani, Tarek., and Abdelaziz Benallegue** (2006) Backstepping Control for a Quadrotor Helicopter. Proceedings of the *2006 IEEE/RSJ International Conference on Intelligent Robots and Systems*, Beijing, China, October.

113. **Shieh, Hsin-Jang., and Chia-Hsiang Hsu** (2007) Trajectory Tracking of a Piezoactuator-Driven Stage Using an Adaptive Backstepping Control Scheme. *IEEE Transactions on Ultrasonics, Ferroelectrics, and Frequency Control*, **54(4)**, April.

114. **Zhang, Y., S. Li and Q. Zhu** (2007) Backstepping-enhanced decentralised PID control for MIMO processes with an experimental study. *IET Control Theory Appl.*, **1(3)**, 704-712.

115. **Ju, Hann-Shing., and Ching-Chih Tsai** (2007) Longitudinal Axis Flight Control Law Design by Adaptive Backstepping. *IEEE*, 0018-9251,2007.

116. **Semsar-Kazerooni, E., M. J. Yazdanpanah, and Caro Lucas** (2008) Nonlinear Control and Disturbance Decoupling of HVAC Systems Using Feedback Linearization and Backstepping with Load Estimation. *IEEE Transactions On Control Systems Technology*, **16(5)**, September.

117. **Sheng Bi, Haibo Ji, and Shanjie Chen** (2009) Robust Attitude Control of Aircraft Based on Partitioned Backstepping. *IEEE International Conference on Control and Automation Christchurch*, New Zealand, December.

118. **Hua, Changchun., Peter X. Liu, and Xinping Guan** (2009) Backstepping Control for Nonlinear Systems With Time Delays and Applications to Chemical Reactor Systems. *IEEE Transactions on Industrial Electronics*, **56(9)**, September.

119. **Farivar, Faezeh., Mahdi Aliyari Shoorehdeli, Mohammad Ali Nekoui, and Mohammad Teshnehlab** (2012) Chaos control and modified projective synchronization of unknown heavy symmetric chaotic gyroscope systems via Gaussian radial basis adaptive backstepping control. *Nonlinear Dynamics*, Springer, **67**, 1913-1941.

120. **SaravanaKumar, R., K. Vinoth Kumar, and Dr. K.K. Ray** (2009) Sliding Mode Control of Induction Motor using Simulation Approach. *International Journal of Computer Science and Network Security* (IJCSNS), October, **9(10)**.

121. **Musmade B.B., R.K. Munje, and B.M. Patre** (2011) Design of Sliding Mode Controller to Chemical Processes for Improved Performance. *International Journal of Control and Automation*, **4(1)**, March, 15-31.

122. **Utkin, Vadim I.** (1977) Variable Structure Systems with Sliding Modes. *IEEE Transactions on Automatic Control*, **22(2)**, April, 212-222.

123. **S. C. Tan, Y. M. Lai, C. K. Tse and M. K. H. Cheung (2005)** A fixed frequency pulse width modulation based quasi-sliding-mode controller for buck converters. *IEEE Trans. Power Electronics*, **20(6)**, 1379-1392.

124. **Utkin, V.I** (1993) Sliding mode control design principles and applications to electric drives. *IEEE Transactions on Industrial Electronics*, **40(1)**, February, 23-36.

125. **Shyu, Kuo-Kai., and Hsin-Jang Shieh** (1996) A new switching surface sliding mode speed control for induction motor drive systems. *IEEE Transactions on Power Electronics*, **11(4)**, July, 660-667.

126. **Li, Chunlai., Kalin Su, and Lei Wu** (2012) Adaptive Sliding Mode Control for Synchronization of a Fractional-Order Chaotic System. *Journal of Computational and Nonlinear Dynamics*, 8(3).

127. **Terra Moura, Jairo., Hakan Elmali, and Nejat Olgac** (2007) Sliding Mode Control with Sliding Perturbation. *Observer Journal of Dynamic Systems, Measurement, and Control*, **119(4)**, 657-665.

128. **Mondal, Sanjoy., and Chitralekha Mahanta** (2013) Adaptive integral higher order sliding mode controller for uncertain systems. *Journal of Control Theory and Applications*, **11(1)**, 61-68.

129. **Ding, Shihong., Shihua Li , and Wei Xing Zheng** (2013) Brief paper: new approach to second-order sliding mode control design. *IEEE Journal on Control Theory & Applications*, IET, **7(18)**, 2188 – 2196.

130. **Hong, Yiguang., Guowu Yang, Daizhan Cheng, and Sarah Spurgeon** (2005) A new approach to terminal sliding mode control design. *Asian Journal of Control*, **7(2)**, 77-81.

131. **Iggidr, A., B. Kalitine, and R. Outbib** (1996) Semidefinite lyapunov functions stability and stabilization. *Mathematics of Control, Signals and Systems*, **9(2)**, 95-106.

132. **Kachroo, Pushkin., and Masayoshi Tomizuka** (1996) Chattering Reduction and Error Convergence in the Sliding-Mode Control of a Class of Nonlinear Systems. *IEEE Transactions on Automatic Control*, **41(7)**, 1063-1068.

133. **Young, David K., Vadim I. Utkin, and Umit. O. Zguner** (1999) A Control Engineer's Guide to Sliding Mode Control. *IEEE Transactions on Control Systems Technology*, **7(3)**, 328-342.

134. **Rodic, Miran., and Karel Jezernik** (2002) Speed-Sensorless Sliding-Mode Torque Control of an Induction Motor. *IEEE Transactions On Industrial Electronics*, **49(1)**.

135. **Xu, Huangsheng., Zheng Zhang, and Layne Heilman** (2005) Sensorless Direct Field Oriented Control of Threephase Induction Motors Based on ¸ Sliding Mode˘T for Washing Machine Drive Applications. *IEEE 0-7803-9208-6*.

136. **Cortes, Domingo., Jaime Alvarez, and Andres Bautista** (2006) A dynamical sliding-mode control boost converter: Implementation Details. *IEEE 1-4244-0545-9/06*.

137. **Franco-Gonzalez, A., R. Marquez and H. Sira-Ramirez** (2007) On the Generalized-Proportional-Integral Sliding mode Control of the Boost-Boost Converter. *4th International Conference on Electrical and Electronics Engineering* (ICEEE 2007), September.

138. **Ahmed, Mohamed Said Sayed., Ping Zhang, and Yun Jie Wu** (2008) Position control of synchronous motor drive by modified adaptive two-phase sliding mode controller. *International Journal of Automation and Computing*, 5(4), 406 - 412.

139. **Jiao, Yan Ping., and Fang Lin Luo** (2009) An Improved Sliding Mode Controller for Boost Converter in Solar Energy System. *IEEE 978-1-4244-2800-7*.

140. **Alaa, Hijazi., Di Loreto Michael, Bideaux Eric, Venet Pascal, Clerc Guy, and Rojat Gerard** Sliding Mode Control of Boost Converter: Application to energy storage system via supercapacitors. Bât. Omega, Université Lyon I, Villeurbanne, Bât. Saint Exupéry, Insa de Lyon, *Villeurbanne University of Lyon,* France.

141. **Zong, Q., Z.-S. Zhao1, and J. Zhang** (2009) Higher order sliding mode control with self-tuning law based on integral sliding mode. Published in *IET Control Theory and Applications*.

142. **Biel, D., E. Fossas, and R. Ramos** (2010) Sliding Mode Control Multiphase Buck Converter Implementation Issues. *11th International Workshop on Variable Structure Systems,* Mexico City, Mexico, June.

143. **Tingna, Shi., Lu Na, and Li Wenshan** (2010) Sensorless Control for Brushless DC Motors Using Adaptive Sliding Mode Observer. Proceedings of the *29th Chinese Control Conference*, July, Beijing, China.

144. **Tseng, Ming Lei., and Min Shin Chen** (2010) Chattering reduction of sliding mode control by low-pass filtering the control signal. *Asian Journal of Control,* **12(3)**, 392-398.

145. **Lin, Kuo Jung.** (2014) Adaptive sliding mode control design foe a class of uncertain singularly perturbed nonlinear systems. *International Journal of Control*, 87(2), 432-439.

146. **Zhang, Jinhui., and Wei Xing Zheng** (2014) Design of adaptive sliding mode controllers for linear systems via output feedback. *IEEE Transactions on Industrial Electronics*, **61(7)**, 3553-3562.

147. **Tang, Chuansheng., Yuehong Dai, and Yong Xiao** (2014) High precision position control of PMSLM using adaptive sliding mode approach. *J. Electrical systems*, **10(4)**, 456-464.

148. **Shen, Liqun., Chengwei Li, and Mao Wang** (2014) Adaptive sliding mode control and its application in chaos control. *Systems and Control*, Cogent Engineering, 1:942049, 1-13.

149. **Ni, Jiangfan., Pu Yang, Jr., and Xia Li** (2014) Adaptive Robust Sliding mode control for Time-varying delay systems with uncertainties. Proceedings of 2014 *IEEE Chinese guidance, Navigation and Control Conference*, 1312-1316.

150. **Smaoui, Mohamed., Xavier Brun, and Daniel Thomasset** (2006) Control of an Electropneumatic System: Integrator Backstepping and Sliding Mode Control. *IEEE Transactions On Control Systems Technology*, **14(5)**, September.

151. **Bai, Rui., and Shaocheng Tong** (2014) Adaptive Backstepping Sliding mode control of the electronic throttle system in Modern Automobiles. *Mathematical Problems in Engineering*, Hindawi, 1-8, Article ID: 383064.

152. **Miroslav Barić, Ivan Petrović, and Nedjeljko Perić** (2005) Neural network-based sliding mode control of electronic throttle. *Journal Engineering Applications of Artificial Intelligence*, **18(8)**, 951-961.

153. **Mohd Basri, Mohd Ariffanan., Abdul Rashid Husain, and Kumeresan A. Danapalasingam** (2014) Robust Chattering Free Backstepping Sliding Mode Control Strategy for Autonomous Quadrotor Helicopter. *International Journal of Mechanical & Mechatronics Engineering* IJMME-IJENS, **14(3)**, 36-44.

154. **Yager, R. R., and Filer D. P.** (1994) Essentials of Fuzzy Modeling and Control. *John Wiley*.

155. **Mendel, J.M.** (1995) Fuzzy Logic Systems for Engineering: A tutorial, *Proc. IEEE*, **83**, 345-377.

156. **Jäkel, Jens., Ralf Mikut, and Georg Bretthauer** (1990) Fuzzy Control Systems. *Control Systems, Robotics And Automation*, **XVII**, 1-11.

157. **Gowrishankar, K., and Vasanth Elancheralathan** (2005) Adaptive Fuzzy Controller to Control Turbine Speed. *Ubiquitous Computing and Communication Journal*, **3(5)**, 53-59.

158. **Montiel, Oscar., Roberto Sepúlveda, Patricia Melin, Oscar Castillo, Miguel Ángel Porta, and Iliana Marlen Meza** (2007) Performance of a Simple Tuned Fuzzy Controller and a PID Controller on a DC Motor. Proceedings of the *2007 IEEE Symposium on Foundations of Computational Intelligence* (FOCI 2007), 531-537.

159. **Kandiban, R., and R. Arulmozhiyal** (2012) Design of Adaptive Fuzzy PID Controller for Speed control of BLDC Motor. *International Journal of Soft Computing and Engineering* (IJSCE), **2(1)**, 386-391.

160. **Wang, Chonghua** (2015) A Study of Membership Functions on Mamdani-Type Fuzzy Inference System for Industrial Decision-Making. MS Thesis Report, *Lehigh University*, 1-216.

161. **Dahiru, Ahmed Tijjani.** (2015) Fuzzy Logic Inference Applications in Road Traffic and Parking Space Management. *Journal of Software Engineering and Applications*, **8**, 339-345.

162. **Palmi, Rainer** (1994) Robust Control by Fuzzy Sliding Mode. *Automatica*, 30(9), 1429-1437.

163. **Lin, Sinn-Cheng, and Yung-Yaw Chen** (1997) Design of self-learning fuzzy sliding mode controllers based on genetic algorithms. *Fuzzy Sets and Systems*, Elsevier, **86**, 139-153.

164. **Wong, Ching-Chang., Bing-Chyi Huang, and Hung-Ren Lai** (2001) Genetic-based Sliding Mode Fuzzy Controller Design. *Tamkang Journal of Science and Engineering*, **4(3)**, 165-172.

165. **Enbiya, S., F. Mahieddine and A. Hossain** (2011) Model Reference Adaptive Scheme for Multi-drug Infusion for Blood Pressure Control. *Journal of Integrative Bioinformatics*, **8(3, 173)**, 1-14

166. **Mirkin, B., E.L. Mirkin, and P.O. Gutman** (2008) Model reference adaptive control of nonlinear plant with dead time. *47th IEEE Conference on Decision and Control*, DOI:10.1109/ CDC.2008. 4739318, 1920-1924.

167. **Duarte, Manuel A., and Kumpati S. Narendra** (1996) Indirect model reference adaptive control with dynamic adjustment of parameters. *International Journal of Adaptive Control and Signal Processing*, John Wiley & Sons, **10**, 603-621.

168. **Makoudi, M., and L. Radouane** (1999) A robust decentralised model reference adaptive control for non-minimum phase interconnected systems. *Automatica*, **35**, 1499-1508.

169. **Duarte-Mermoud, Manuel A., Franklin A. Rojo, and Ricardon Perez** (2002) Experimental evaluation of combined model reference adaptive controller in a PH regulation process. *International Journal of Adaptive Control and Signal Processing*, John Wiley & sons, **16**, 85-106.

170. **Yassen, M.T.** (2003) Adaptive control and synchronization of a modified chua's circuit system. *Applied Mathematics and Computation*, Elsevier, **135**, 113-128.

171. **Liu, Yang., Jin Zhao, Mingzi Xia, and Hui Luo** (2014) Model Reference Adaptive Control-Based Speed Control of Brushless DC Motors With Low-Resolution Hall-Effect Sensors. *IEEE Transactions on Power Electronics*, **29(3)**, 1514-1520.

172. **Yang, L., S.A. Neild, D.J. Wagg, and D.W. Virden** (2006) Model reference adaptive control of a nonsmooth dynamical system. *Nonlinear Dynamics*, Springer, **46**, 323-335.

173. **Wise, Kevin A., Eugene Lavretsky, and Naira Hovakimyan** (2006) Adaptive control of flight: Theory, applications and open problems. Proceedings of the *2006 American Control Conference*, USA, 5966-5970.

174. **Zhou, Jing., Chengjin Zhang, and Changyun Wen** (2007) Robust Adaptive Output Control of Uncertain Nonlinear Plants With Unknown Backlash Nonlinearity. *IEEE Transactions On Automatic Control*, **52(3)**, March.

175. **Nguyen, Nhan T., and Kalmanje Kishnakumar** (2008) An optimal control modification to model refernce adaptive control for fast adaptation. *AIAA Guidance, Navigation and control conference and exhibit*, Hawaii, AIAA 2008-7283, 1-19.

176. **Adrian, Coman., Axente Corneliu, and Boscoianu Mircea** (2008) Simulation of adaptive systems using the MIT rule. *10th WSEAS Int. Conf. on Mathematical Methods and Computational Techniques in Electrical Engineering* (MMACTEE 08), **4(3)**, 301-305.

177. **Agrawal, S.K., and S. Das** (2013) A modified adaptive control method for synchronization of some fractional chaotic systems with unknown parameters. *Nonlinear Dynamics*, Springer, **73**, 907-919.

178. **Kharisov, Evgency., Naira Hovakimyan, and Karl J. Astrom** (2013) Comparison of architectures and robustness of model reference adaptive controllers and L$_1$ adaptive controllers. *International journal of adaptive control and signal processing*, John Wiley & sons, **28**, 633-663.

179. **Barkana, Itzhak** (2013) Simple adaptive control- a stable direct model reference adaptive control methodology-brief survey. *International Journal of Adaptive Control and Signal Processing*, John Wiley & sons, **28**, 567-603.

180. **Garikayi, Talon., Stephen Matope and Dawie van den Heever** (2014) Development of a model reference adaptive controller of the plantarflexion and dorsiflexion movements within the sagittal plane. *Int'l Conf. on Chemical Engineering and Advanced Computational Technologies* (ICCEACT'2014), South Africa, 60-67.

181. **Black, William S., Poorya Haghi, and Kartik B. Ariyur** (2014) Adaptive systems: history, techniques, problems, and perspectives. *Systems*, **2**, 606-660.

182. **Chetaswi, K., G. Madhu Kumar, Desai Feroz and Nithin Krishna Gupta** (2015) Lyapunov design based MIT Rule for model reference adaptive control systems. *International Journal of Emerging Trends in Science Technology Engineering and Management*, 117-120.

183. **Maity, Arnab., Leonhard Hocht, and Florian Holzapfel** (2015) Higher order direct model reference adaptive control with generic uniform ultimate boundedness. *International Journal of Control*, Taylor and Francis, **88(10)**, 2126-2142.

184. **Zhang, Guijun., Tianyou Chai, and Cheng Shao** (1997) A Synthetic Approach For Control of Intermittent Wind Tunnel, *Proceedings of the American Control Conference*, New Mexico, 203-207.

185. **Ambrosino, G., G. Celentano, and M. Mattei** (2001) A control design oriented mathematical model for the scirocco plasma wind tunnel. *Mathematical and Computer Modelling of Dynamical Systems*, Taylor & Francis, **7(1)**, 109-127.

186. **Rennie, Mark R., and Alan B. Cain** (2012) Management of wind tunnel performance data using neural networks. *50th AIAA Aerospace Sciences Meeting Including the New Horizons Forum and Aerospace Exposition*, Tennessee, AIAA 2012-0321.

187. **Matsumoto, J., F. K. Lu, and D. R. Wilson** (2001) Pre-programmed controller for a supersonic blowdown tunnel. *95th Meeting of the Supersonic Tunnel Association International*, 1-9.

188. **Silva, Mauricio Guimaraes da., and Falcao Joao Batista Pessoa Filho** (2007) Control of high speed wind tunnel mach number. *19th International congress of Mechanical engineering*, Brasilia.

189. **Lu, F.K., D.R. Wilson, and J. Matsumoto** (2008) Rapid valve opening technique for supersonic blowdown tunnel. Elsevier, *Experimental Thermal and Fluid Science*, **33**, 551-554.

190. **Silva, Mauricio G., Victor O. R. Gamarra, and Vitor Koldaev** (2009) Control of Reynolds number in a high speed wind tunnel. *Journal of Aerospace Technology and Management*, **1(1)**, 69-77.

191. **Bakhtian, Noel M., and Michael J. Aftosmis** Analysis of Inviscid Simulations for the Study of Supersonic Retropropulsion. *American Institute of Aeronautics and Astronautics*.

192. **Busa, Kristin M.** (2010) Application of propositional integral derivative control to a supersonic wind tunnel. *48th AIAA Aerospace Sciences Meeting Including the New Horizons Forum and Aerospace Exposition*, Florida, AIAA 2010-187.

193. **Corneliu. Andrei NAE.,** (2013) Blowdown wind tunnel control using an adaptive fuzzy PI controller. *INCAS BULLETIN*, **5(3)**, 89-98.

194. **Butler, Kelly., David Cancel, Brian Earley, Stacey Morin, Evan Morrison, and Michael Sangenario** (2010) Design and Construction of a Supersonic Wind Tunnel. A Major Qualifying Project at *Worcester Polytechnic Institute*, March.

195. **Shahrbabaki, Nazarian A., M. Bazazzadeh, A. Shahriari and M. Dehghan Manshadi**, (2014a) Intelligent controller design for a blowdown supersonic wind tunnel. *International Journal of Control and Automation*, 7(1), 409-426.

196. **Shahrbabaki, Nazarian A., M. Bazazzadeh, A. Shahriari and M. Dehghan Manshadi**, (2014b) Enhancing the supersonic wind tunnel performance based on plenum temperature control. *ISRN Aerospace engineering*, Hindawi, Article id: 317049, 1-6.

197. **Ilić, Biljana., Marko Miloš, Mirko Milosavljević and Jovan Isaković,** (2016) Model-Based Stagnation Pressure Control in a Supersonic Wind Tunnel. *FME Transactions*, **44**, 1-9.

198. **Sunny, Kalakanda Alfred., C. Likith Kumar Reddy, Nallapaneni Manoj Kumar and Harithra M.** (2017) Hybrid Fuzzy-PID Controller for pressure regulation in Supersonic wind tunnel. *International Journal of Earth Sciences and Engineering*, **10(1)**, 24-28.

199. **Owen, A.K., and F.K. Owen** (2007) Hypersonic Free Flight Measurement Techniques. *IEEE Instrumentation in Aerospace Simulation Facilities*. Proceedings of *22nd International Congress on Instrumentation in Aerospace Simulation Facilities*, USA, DOI:10.1109/ICIASF.2007.4380898, 1-11.

200. **Popov, A.V., L. T. Grigorie, R. M. Botez , M. Mamou, and Y.Mebarki** (2010) Controller Optimization in Real Time for a Morphing Wing in a Wind Tunnel. Proceedings of the *15th IEEE Mediterranean Electro-Technical Conference*, DOI:10.1109/MELCON.2010.5476329, 107-112.

201.   **Kabin, S.V., K.A. Kolinko., A. Khrabrov, and P.D Nushtaev** (1995) Test Rig and Test Technique for the Aircraft Models Lr1stea.d;- Aerodynamic Characteristics Measurements, High Subsonic and Transonic Wind Tunnels", IEEE Explore CH34827- 9510000 1995.

202.   **Sorensen, J.N., Wen Zhong Shen and Mikkelsen R. (2006)** Wall correction model for wind tunnels with open test section. *AIAA Journal*, **44(8)**, 1890-1894

203.   **Furian, N., M.O. Sullivan, C. Walker, S. Vössner, and D. Neubacher** (2015) A conceptual modeling framework for discrete event simulation using hierarchical control structures. *Simulation Modelling Practice and Theory*, Elsevier, **56**, 82-96.

204.   **Murray-Smith, David J.** (2015) A Review of Inverse Simulation Methods and Their Application. *Simulation Modelling Practice and Theory*, Taylor and Francis Elsevier, **34(3)**, 120-125.

205.   **Echman, D.P.** Automatic Process Control, *Wiley Eastern Limited*, New Delhi, 1958

206.   **Liptak, B.G.** Instrument Engineers Handbook: Process Control. *Elsevier*, 1995

207.   **Swain, Akshya K., Srikanth Devarakonda, and Udaya K. Madawala** (2014), Modeling, Sensitivity Analysis, and Controller Synthesis of Multipickup Bidirectional Inductive Power Transfer Systems. *IEEE Transactions on Industrial Informatics*, **10(2)**, 1372-1380.

208.   **Delfour, M.C., and S.K. Mitter** (1972) Controllability and Observability for infinite-dimensional systems. *SIAM. Journal of Control*, **10(2)**, 329-333.

209.   **Jacques, J., and E. Slotine** (1991) Applied nonlinear control. *Massachusetts Institute of Technology, Weiping Li. Prentice-Hall Pub.*, 17-39

210.   **Shyu K.K., and Shieh H.J.** (1996) A new switching surface sliding-mode speed control for induction motor drive systems. *IEEE Transactions on Power Electronics*, **11(4)**, 660 – 667.

211.   **He, Yi and F.L., Luo (2004)** Study of sliding mode control for DC-DC converters. *International Conference on Power System Technology-POWERCON 2004, Singapore*, 600-611.

212. **Ackermann J., and Utkin V.** (1998) Sliding mode control design based on Ackermann's formula. *IEEE Transactions on Automatic Control*, **43(2)**, 234 – 237.

213. **S. C, Tan, Y. M, Lai and C. K, Tse (2008)** Indirect sliding mode control of power converters via double integral sliding surface, *IEEE Trans. Power Electronics*, **23(2)**, 600-611.

214. **Xia Y., K. Lu, Z. Zhu, and M. Fu** (2013) Adaptive back-stepping sliding mode attitude control of missile systems. *International Journal of Robust and Nonlinear Control*, **23(15)**, 1699–1717.

215. **Ma L., K. Schilling, and C. Schmid** (2005) Adaptive backstepping sliding mode control with Gaussian networks for a class of nonlinear systems with mismatched uncertainties [C]. 44*th IEEE Conference on Decision and Control, and the European Control Conference*, Seville, Spain.

216. **Mankad K., P.S. Sajja, and R. Akerkar** (2011) Evolving rules using genetic fuzzy approach - an educational case study. *International Journal on Soft Computing (IJSC), 2(1), 35-46.*

217. **Liu Y.J., and S. Tong** (2014) Adaptive Fuzzy Control for a Class of Nonlinear Discrete-Time Systems With Backlash. *IEEE Transactions on Fuzzy Systems, 22(5),* 1359-1365.

218. **Srinivasan, S.P., L. Raajarajan** (2017) Wear rate and surface coating optimization of coconut coir-based polymer using fuzzy logic, *Sadhana, online first article*.

219. **Tong S., S. Sui, Y. Li** (2014) Adaptive Fuzzy Decentralized Output Stabilization for Stochastic Nonlinear Large-Scale Systems With Unknown Control Directions. *IEEE Transactions on Fuzzy Systems, 22(5),* 1365 – 1372

220. **King P.J., and E. H. Mamdani** (1977) The application of fuzzy control systems to industrial processes. *Automatica*, **13(3)**, 235–242.

221. **H. Pinheiro, A. Martins and J. Pinheiro (1994)** A sliding mode controller in single phase voltage source inverters, *International Conference on Industrial Electronics Control and Instrumentation (IECON)*, 394– 398.

222. **Chang J L (2013)** Robust dynamic output feedback second-order sliding mode controller for uncertain systems. *International Journal of Control, Automation and Systems*, 11(5): 878-884.

223. **F. Lin, C. Chang, and P. Huang (2007)** FPGA-based adaptive backstepping sliding-mode control for linear induction motor drive, *IEEE Transactions on Power Electronics*, **22(4)**, 1222–1231.

224. **R. Chen, L.Mi, and W. Tan (2012)** Adaptive fuzzy logic based sliding mode control of electronic throttle, *Journal of Computational Information Systems*, **8**, 3253–3260.

225. **S. Tong, X. He, and H. Zhang (2009)** A combined backstepping and small-gain approach to robust adaptive fuzzy output feedback control," *IEEE Transactions on Fuzzy Systems*, **17(5)**, 1059–1069.

226. **Hovakimyan, N., Kim, N., Calise, A.J., Prasad, J.V.R., and Corban, E.J. (2001)** Adaptive Output Feedback for High-Bandwidth Control of an Unmanned Helicopter, *AIAA Guidance, Navigation and Control Conference, AIAA-2001-4181*.

227. **Mehran Zareh, Sahel Soheili** (2011) A modified model reference adaptive control with application to MEMS gyroscope. *Journal of Mechanical Science and Technology*, **25(8)**, 1-7.

228. **Nguyen, To Hieu., Shogo Odomari, Tomohiro Yoshida, Tomonobu Senjyu, and Atsushi Yona** (2013) Nonlinear Adaptive Control of Ultrasonic Motors Considering Dead-Zone. *IEEE Transactions on Industrial Informatics*, **9(4)**, 1847-1854.

229. **Jain, Priyank., and Dr. M.J. Nigam** (2013) Design of a Model Reference Adaptive Controller Using Modified MIT Rule for a Second Order System. *Advance in Electronic and Electric Engineering*, **3(4)**, 477-484.

230. **Imaduddin, Fitrian., Khisbullah Hudha, Janatul Islah Mohammad, and Hishamuddin Jamaluddin** (2011) Simulation and experimental investigation on adaptive multi-order proportional-integral control for pneumatically actuated active suspension system using knowledge-based fuzzy. *International Journal of Modelling, Identification and Control, Inderscience Publishers*, **14(1/2)**, 73-92.

231. **Karray, Amal., and Moez Feki** (2014) Adaptive and sliding mode control of a mobile manipulator actuated by DC motors. *International Journal of Automation and Control, Inderscience Publishers*, **8(2)**, 173-190.

232. **Tuan, Le Anh., Sang-chan Moon, Won Gu Lee, and Soon-Guel Lee** (2013) Adaptive sliding mode control of overhead cranes with varying cable length. *Journal of Mechanical Science and Technology*, Springer, **27(3)**, 885-893.

233. **Chen, Long., Zhihui Zhang, Hai Wang, Ming Huang, and Xingkun Xu** (2016), Sliding mode adaptive control for DC motors using function approximation form. *International Journal of Modelling, Identification and Control*, Inderscience Publishers, **26-3**, 238-252.

234. **Mozaffari, Ahmad., and Nasser L. Azad** (2017) Empirical investigation and analysis of the computational potentials of bio-inspired nonlinear model predictive controllers: success and challenges. *International Journal of Bio-Inspired Computation*, Inderscience Publishers, **9-1**, 19 – 34.

235. **Karray, Amal., and Moez Feki** (2014) Adaptive and sliding mode control of a mobile manipulator actuated by DC motors. *International Journal of Automation and Control*, Inderscience Publishers, **8-2**, 173-190.

236. **Vincent L. Rausch, Charles R. McClinton, and J. Larry Crawford (1999)** Hyper-X: Flight Validation of Hypersonic Airbreathing Technology, *NASA Hyper-X Program Office*, 1-7.

LIST OF PAPERS

SUBMITTED ON THE BASIS OF THIS THESIS

I. REFEREED JOURNALS

1. **Rajani S.H**, **Bindu M. Krishna, Usha Nair** (2018) Adaptive and modified adaptive control for pressure regulation in a hypersonic wind tunnel. *International Journal of Modelling, Identification and Control, Inderscience Publishers,* **29(1)**, 2018, 78-87. (Scopus (Elsevier))

2. **Rajani S.H**, **Bindu M. Krishna, Usha Nair** (2017) Pressure regulation inside a hypersonic wind tunnel using H-infinity optimization control. *Automatic Control and Computer Sciences, Allerton Press, Inc.,* Springer, 51(6), 339- 409. (SCOPUS)

II. PRESENTATIONS IN CONFERENCES

1. **Rajani S.H**, **Bindu M. Krishna, Usha Nair.** Design and Analysis of H-infinity controller for a Hypersonic Wind Tunnel. *Proceedings of International Conference on Control Systems and Power Electronics, CSPE, Elsevier*, pp: 513– 518, Dec 2012.

2. **Rajani S.H, Bindu M. Krishna, Usha Nair.** Stability Analysis and temperature effect on the settling chamber pressure of a Hypersonic Wind Tunnel, *Proceedings of IEEE International Conference on Computational Intelligence and Computing Research*, pp:1-5, Dec 2012.

3. **Rajani S.H**, **Usha Nair.** Design and Analysis of a Nonlinear Controller for a Hypersonic Wind Tunnel. *Proceedings of IEEE International Conference on Computational Intelligence and Computing Research*, pp:106-109, Dec 2013.

4. **Rajani S.H**, **Bindu M. Krishna, Usha Nair.** Chattering free Sliding mode controller for Hypersonic wind tunnel. *Proceedings of International Conference on Innovative Mechanisms for Industry Applications (ICIMIA 2017), IEEE Xplore,* pp: 359 – 363, Feb 2017.

CURRICULUM VITAE

1. **NAME**   :   RAJANI S H

2. **DATE OF BIRTH**   :   17 AUGUST 1985

3. **EDUCATIONAL QUALIFICATION**

2007 Bachelor of Technology. (B. Tech.)

Institution	:	K.M.E.A Engineering College, Ernakulam
Branch	:	Electronics and Instrumentation

2010 Master of Technology (M. Tech)

Institution	:	College of Engineering, Trivandrum
Branch	:	Electronics and Communication Engineering.
Specialization	:	Applied Electronics and Instrumentation

Doctor of Philosophy (Ph. D)

Institution	:	Cochin University of Science & Technology
Registration date	:	24.11.2011 (Part-time)